HIGH STRAIN RATE CONSTITUTIVE EQUATION FOR METALLIC MATERIALS

BY

A.M.S. HAMOUDA (BSc)

This thesis is submitted as the fulfilment of requirement
for the award of Master of Engineering (M.Eng)
by research to:

DUBLIN CITY UNIVERSITY

September 1991

HIGH STRAIN RATE CONSTITUTIVE EQUATION FOR METALLIC MATERIALS

A.M.S. HAMOUDA (BSc)

M.Eng. 1991

TO MY BROTHER

'MOHAMMED'

DECLARATION

I hereby declare that all the work prepared in this thesis was carried out by me at Dublin City University during the period December 1989 to September 1991.

To the best of my knowledge, the results presented in this thesis originated from the present study except where references have been made. No part of this thesis has been submitted for a degree at any other institution.

SIGNATURE OF CANDIDATE: _____

A.M.S. Hamouda.

TABLE OF CONTENTS

ABSTRACT

HIGH STRAIN RATE CONSTITUTIVE EQUATION FOR METALLIC MATERIAL

by

A.M.S. HAMOUDA

The yield stress and flow stress increase significantly with strain rate. High speed Forming and Machining operation gives rise to strain rates varying from 10 to 10^6 per second. A number of research work have been reported in which various techniques have been described for strain rates sensitivity. One of the reported technique [1] was based on high speed compression of small cylindrical specimens with tool steel projectile. The deformation was recorded with a high speed camera operating at 500,000 frames per second. The equipment is very expensive and the processing of the picture for data is very tedious and subjected to human error.

The present study was aimed at using a similar technique of high speed compression without having to use any high speed photographs. From known initial and final dimension of the specimen together with the mass and the impact speed of the projectile, the deformation is simulated using a finite-difference technique based on an assumed dynamic constitutive equations. By iterative computation the constants of the constitutive equations are established and give close agreement between the experimental and simulated results in terms of the final dimensions of the cylindrical test specimens.

Finally the principal aim of this investigation was to establish high strain rate constitutive equations for commercially pure Copper, Mild steel and Stainless steel, and compare the results with those obtained using more sophisticated and expensive equipment.This principal objective has been achieved and high strain rate constitutive equations have been determined for strain rates ranging between 10^3 to 10^5 per second.

1Reference No. 56

ACKNOWLEDGEMENTS

'If I have seen farther than others, it is because I have stood upon the shoulders of giants.'

Sir Isaac Newton

Of all the words put forth in this thesis, none are more important, or more difficult to write, than are the ones on these few pages. The heart and soul of my education has relatively little to do with the staff of Mechanical and Manufacture Engineering; instead it resides in the kindness and friendship shown to me over the two years by a great many people. Without them, this work would not exist.

I feel privileged to have been a student of Prof. M.S.J.Hashmi, Head of School of Mechanical and Manufacture Engineering. His patience, sense of humor, and tolerance of the perturbations of my spirit, gently allowed me to develop my sense of self-worth. I am deeply grateful to him.

I would like to thank every one in the School for making it a very pleasant place to work in. Particular thanks go to Dr. El-Baradie, M ; Mr Anderson, G; Mrs Lucy, M; Ms Lesle, all the technician in the workshop and all my fellow research students.

The acknowledgements would not be completed without mentioning Mr Martain, F; Mr Soughley, F; Mrs Deirdre, J and Mrs Celine, J For their Help and advice.

A special thank-you to be extended to my Brother Mohammed and his Wife, who opened their home and hearts to me.

I am forever indebted to my loving Mother and Father, they have freely given their love and support to me and the rest of my family. My thanks also goes to all my brothers and sisters for their moral support and advice.

LIST OF TABLES

LIST OF FIGURE

NOMENCLATURE

Δs	Link Length in Lumped Model.
N	Axial Force.
M	Mass of Element.
A '	Cross-section Area of Each Layer.
A1	Cross-section Area of Each Sub-Layer.
u	Displacement.
u	Single Differentiation with Time.
u	Double Differentiation with Time.
V	Impact Speed.
σ	Modified Stress with Inertia Effect.
σ_o	Static Flow Stress.
σ	Dynamic Flow Stress.
ε	Strain.
ε_o	Strain Rate Constant.
ε	Starin Rate.
ρ	Density.
T_o	Test Temperature.
T	Temperature Rise During Deformation.
s	Specific Heat.
G	Temperature Factor in Strain Hardening.
G_1	Temperature Factor in Strength Coefficient.
R	Strain Rate Factor in Strain Hardening.
θ, θ_1	Material Temperature Constant.
β	Strain Rate Constant.
α	Both Temperature and Strain Rate Factor.
m, P	Material Strain Rate Senstivty.

Subscripts

i	Mass Number.
j	Instant of Time.
o	Initial Value.

CHAPTER ONE

INTRODUCTION

1.1 Overview

In the past few years the knowledge of strength of materials at high strain rates has become increasingly important. A considerable number of researches have been focused on the studies of the mechanical properties of metals at high strain rates as shown recently by the growing numbers of international conferences all over the world, in Europe, United States of America, Australia, Japan and China. These intensive studies were carried out to solve many practical problems associated with cleavage fracture, cracking, spalling, explosive, and stress wave propagation.

The behavior of metals under very high strain rate is obviously of very important interest in the mechanical analysis of design problems where dynamic loads are present, specially for the design engineer who would be concerned with a variety of structures. Unfortunately in the past decades much of the engineering designs were based on the static mechanical properties of the materials rather than the dynamic behaviour which is so important as long as aircraft, ships, rockets, vehicles etc., are in service and are subjected to rapid loading which so often brings failure and causes severe damages.

Although it is clearly known that the stress-strain relationship of metals is influenced by the strain, strain rate, strain rate history and temperature, there is very little quantitative information available on the relation between these variables in compression. Therefore it is very important to determine and investigate the mechanical properties of metals at high strain rates.

The determination of the mechanical properties at high strain rates appears to be a difficult experimental task due to the difficulty in measuring stress, strain and strain rate where a dynamic load is applied for a very short duration of time. However, in the recent years many researches were focused on the solution of this problem, and it has been made possible to make progress through the use of the most advance electronic measuring and recording devices [1-4].

It can be concluded that, the mechanical behaviour of materials at high rates of loading is of interest from two points. Firstly, the engineer, who wishes to use the materials under conditions where they may have to withstand sudden impacts, requires to know how their behaviour depends on the rate at which the stress is applied. Secondly, since the variation of stress-strain curves with loading rate is related to relaxation process taking place in a microscopic scale in the material, the results are of interest to the physicist who is studying the relation between physical problems and molecular structure.

1.2 Classification Of Strain Rate

The strain rate can be an important variable in metal forming operations and in some service application.The whole range of strain rate can be classified as follows:

1-Creep (of order 10^{-12}).

2-Static (of order 10^{-4} to 10^{-2}).

3-Rapid (longer than static less than impact).

4-Impact

(a) Plastic wave regime (up to 10^{5}).

(b) Shock wave regime (from 10^{6}).

Table(1.1)

STRAIN RATE FOR MANUFACTURING PROCESS	
Process	**Strain rate of order**
Metal cutting	1000 To 100,000
Wire drawing	up to 200,000
Rolling	up to 2000
Forging	1000
Deep drawing and forming	100
Dynamic blanking	5000
Stand-off explosive, magnetic and capacitor discharge forming	100 to 10,000

This classification is not a rigid one, as considerable overlapping occurs.

Strain rate normally of interest in studies of plastic flow range from static to high strain rate (**Impact**) of the order 10^5 per second, produced by detonation of high explosive or direct impact. Most of the manufacturing processes involve strain rates that fall within impact classification **Table[1]**.

1.3 APPLICATION OF HIGH STRAIN RATE

The main processes and areas which involve high strain rates are as the following :

1) Impact Loading Of Structure.

2) Strain Rate Effect In Manufacturing Processes.

3) Powder Metallurgy.

1.3.1 Impact Loading Of Structure

The design engineer who is concerned with structures that are most likely to be subjected to rapid loading wants to know if the material properties he wishes to use differ significantly from those that are used in static design. If the answer is yes, he then asks how the static properties are altered under dynamic loading condition.

The mechanical properties of materials under dynamic loading has received considerable attention, particularly in recent years [5,6,7] and is discussed in test books [8,9] and [10]. Most of the researches have been directed towards finding the mathematical models for studying the behaviour of structure under dynamic loading, inorder to find the accurate material properties at both static and dynamic loading.

The construction industry in general, and the structural design engineer in particular, require adequate information and data on the behaviour of materials to be available specially in terms of stress and strain characteristic at low and high strain rates. In order to achieve their objectives of resistance to shock, provide adequate protection from collapse or excessive damage, and easy demolition when it is needed, such data are essential

The principal area of interest to design engineer in the design of the structure are as the following

Nuclear Industry:

The nuclear industry has long been at the forefront of development in the field of structural mechanics and dynamics because of the obvious need to design and construct very high integrity plant. Accidental overload has been a major focus of interest within the industry and load cases such as explosion, impact and earthquake command regular attention. The behaviour of material at high rates of strain is therefore an item of special interest to those involved in justifying design and preparing safety cases. This subject was examined in papers [11,12].

Aerospace:

Aerospace usage of structure materials almost always involves exposure to dynamic loading environments. The nature of the response for a given material system depends on both the type and the severity of

loading experienced. The loading type can be periodic, random, or impulsive and the severity varies from low to high amplitude. The high strain rate material response occurs when the loading is of the high amplitude impulsive variety, giving rise to several engineering concerns underlying subdisciplinary focus such as vehicle crashwortiness, penetration mechanics, fracture mechanics, stress wave propagation. A more detailed coverage of this field can be obtained from reviews [13].

Military Industry:

Extensive studies were made during the second world war independently by investigators in (USA, USSR and Uk), and published after the war. these analysis did not include any strain rate dependence in the constitutive equation .

Mean while, in many branches of the modern arms industry a growing need for a better understanding of the mechanical and fracture properties of materials at high strain rate has become evident. A large number of products for military use are susceptible to a wide variety of impact condition including low velocity, high velocity, fragment and rod penetration. All these areas of impact response need high strain rate data for a wide range of temperature and for several types of materials such as alloys, ceramic and composite. These subjects were widely examined in references [14,15].

1.3.2 METAL FORMING

In recent years there has been an unprecedented interest in metal forming technology. The design of metal forming process often needs to estimate the load and energy required for a given forming operation. It is so important that metal processing engineers have to know the influence of the strain rates, friction condition, material properties and tool geometry on of the mechanics process, it is then possible to predict the force required, design the dies and equipment adequately and predict the occurrence of defects.

A compression test is known to be favoured for the determination of materials properties pertinent to metal forming. The axisymmetric compression test has been used at high speed inorder to obtain stress strain data at high strain rates. A considerable effort has been devoted during the past twenty years to a discussion and experimental determination of the effect of strain rate in metal forming [16-20]. It is so essential to know firstly which material are sensitive to high strain rate and to what extent, secondly to estimate reasonably accurately the strain rates involved in any particular metal forming operation.

The metal forming technique could be divided into the following categories:

1) Cold working.

2) Warm working.

3) Hot working.

The production of components by cold forming is becoming an increasingly important process and is still being rapidly developed [21] with the main object of increasing both the range of component and types of materials that can be formed.

The main feature of the hot working is that extremely large strains are applied to materials at high rates of strain at temperature above the recrystallization temperature. Strength and ductility under these condition are markedly dependent on both temperature and strain rate. Hot working is normally carried out at high rates of strain, in dynamic forging, impact, extrusion, rolling and drawing the strain rate is around 10^4 per second and in machining were approximately up to 10^6 per second.

However, in the last few years there has been growing interest in warm-forming with the aim of combining the advantages of both cold and hot working, inorder to make it possible to produce a new range of components, which have some of the shape and complexity of hot forming component and retain a large proportion of the mechanical and physical properties of cold forming.

High-Velocity Forming.

Techniques for forming metals at high velocities or in short times have received a great deal of attention in the past decade **[22-24]**.The important distinguishing characteristics of most of the processes is that the rate of energy transfer to the workpiece, or the power, is high during an unusual short operating cycle. This principle has been applied for both hot working and cold working. **Table[1.2]** gives some of the typical deformation velocities for various energy sources.

Table(1.2)

SYSTEM	VELOCITY ft/sec
Hayraullic press	0.13
Brake press	0.15
Mechanical press	3.00
Drop hammer	1-20
Gas-mechanical	10-250
Explosive gas	30-330
Low explosive	30-330
High explosive	100-700
Electrohydraulic	100-700
Electromagnetic	100-700

The potential of the H.E.R.F processes, have been reported in the various literature and reviews published by machine users, yielding the following comments:

1) The rate of deformation is high and the consequent forging cycle is short enough to accomplish the manufacture of the component without significant drop in stock temperature.

2) The reduced contact time of the billet with die will delay the onset of thermal softening, given a longer die life.

1.3.3 Powder Metallurgy

In the recent years, the process has been highly developed and a large numbers of powder metallurgy products were being made available annually. The concept of making parts from powder metals normally consists of the following three basic steps:

1- Blending.
2- Compacting .
3- Sintering.

Figure[1.1], shows a typical block diagram of the process.

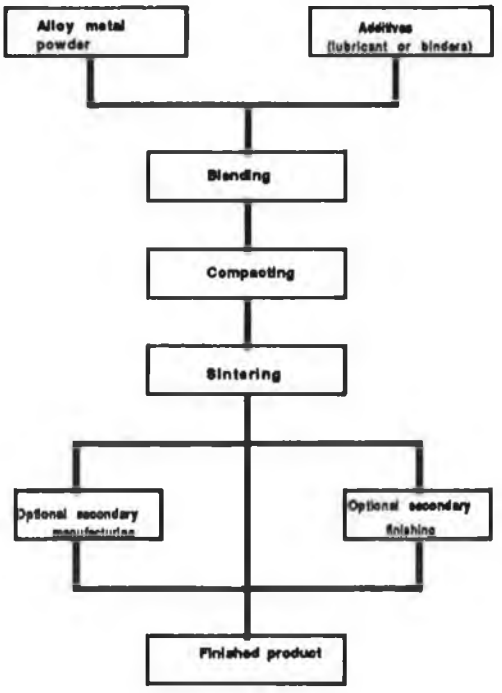

Fig.(1.1) Flow chart of the powder metallurgy process

One of the most critical and controlling steps in powder metallurgy process is compacting. The main problem in compacting is internal friction, as when placed in the dies the pressure are not distributed uniformly through out the compact and when the distance from the punches is decreased both the hardness and the density are increased.

Dynamic compaction has been known to be a much better technique for producing the powder compacts than the static compacting technique [25]. The dynamic compacting has been used since 1950. It has been proved to be the most suitable means for securing the compact properties such as uniform density, improved green strength and increase the production rates. The dynamic compaction of metal powder by means of ballistic and explosive process may involve strain rates of 10^2 and 10^3 per second respectively.

It appears from what have been mentioned above that fundamental information and accurate data about the stress strain properties of metals powders at high strain rates has to be made available in order to secure better compaction system.

In the sintering process, the compact is subjected to elevated temperature in a controlled atmospheric environment. There are many parameters which affect the mechanical properties of sintered parts, such as, particle size and sintering time and temperature. The effect of sintering temperature on the mechanical properties, in general, has been reported in detail in reference [26].

1.4 LITERATURE REVIEW

The first aim of this literature review is to give upto-date information on the mechanical properties of metals at high strain rate, and how these properties vary with strain rate . Another objective is to obtain good back-ground about the subject of impact dynamic in relation to the methods used in determining these properties.

The question of strain rate effect seems to be the central problem of the dynamic plasticity at the present time, as considerable theoretical and experimental work has been conducted in this field. **Kolsky [27]** in (1949) was the first to use the split Hopkinson pressure bar for obtaining the stress strain properties at high strain rates. Subsequently modification of Kolsky's original technique have been described by **Davies and Hunter [28]**. The assessment of these properties remains the important part of the study as it gives a clear picture and better understanding of the mechanical behaviour of metals under high velocity deformation.

Analytical method

Many investigation have been carried out on the analytical method of dynamic impact problems. **Taylor[29]** presented a theoretical analysis and supported his analysis by doing some experiments using flat ended transparent cylinders made from a cast block of paraffin wax.

The cylinders were projected by means of a catapult at rigid anvil. He used momentum equation, ignoring the radial inertia effect, so that the stress can be considered constant over any cross-section.

Since Taylor[29] considerable efforts have been made by a number of investigators **[30,31]**. **Wiffens [32]** followed Taylor's [29] work and conducted his tests using steel, copper and lead. He reported that an increase in dynamic strength of mild steel can be obtained by pre-straining either in tension or compression, and he established equations relating dynamic stress to static strength of steel.

Lee and Tupper [33] examined the elastic wave reflection within the projectile and obtained a stepped profile, which, upon smoothing resembles the Taylor's [29] convex profile. They reported that for high strength alloy steel, impacts of the order 1000 ft/sec can be analyzed on the basis of static stress-strain relation.

Hawkyard et al [34] obtained the mean dynamic strength for copper and mild steel from strain measurement of Mushroomed ends of flat ended projectiles, firing against a rigid anvil. They reported that in the analysis they developed for determining the mean dynamic stress, the kinetic energy at impact was equated with plastic work done. They added that the phenomenon of Double frustum was observed in tests conducted on annealed materials, suggesting that a suitable theory would include strain-hardening from which it might be possible to deduce the actual form of the dynamic stress-strain curves.

Hawkyard [35] used energy equilibrium equation on his analysis to predict the final shape of Mushrooming of flat ended projectile fired on rigid anvil, and he derived equations for providing a mushroomed profile of concave form. He reported that the use of an energy equilibrium equation across the plastic wave gives a better overall approximation to actual condition than does the momentum equation . In his analysis he studied the case of non-strain hardening material for the first part and expanded it for strain hardening materials. In addition, he determined the value of the mean effective strain and mean dynamic yield stress.

Hutching and O'Brien [36] examined the case of normal impact of copper projectiles against a rigid target at low velocities. They reported that, the impact deformation of cylindrical copper projectiles is found to differ significantly from the theoretical prediction of Taylor [29] and Hawkyard [35]. The differences arise because both theories assume rigid plastic behaviour, where as at low velocity account must be taken of elastic strain in the projectile which will be of comparable magnitude with plastic strain.

Balendra and Travis [37] investigated the Double-frustum phenomena in the mushrooming of cylindrical projectiles when impacted at high speed 1100 ft/sec on to a rigid anvil. They reported that the effects of radial inertia and yield behaviour at high strain rate were responsible for the double- frustum phenomenon.

Hashmi and Thomphson [38] suggested a numerical technique which enabled them to predict the final shape of a cylindrical projectile after impact on a rigid anvil and the distribution of strain, taken into account the strain rate and strain hardening effects. They reported that the final shape of the profiles predicted by this technique are found to be made up of both concave and convex regions.

Hashmi [39] incorporated into the technique previously outlined, the effect of material inertia and strain rate sensitivity. The out-come of this work was the ability to establish the strain rate dependent constitutive equation of materials at high strain rate.

Pope and Field [40] developed an analysis for high speed impact and reported that their analysis showed good agreement with those obtained by direct observation using high speed photography.

Effect Of Friction, Inertia and Specimen size

Axial compression of solid cylinders was investigated by many earlier authors, due to its importance and application in diverse material forming, such as, forging, upsetting and a comprehensive review of their work has been given by **Johson [41]**. The shape of the deformed work piece has been repeatedly investigated and reviews have been given in references **[42,43,44]**.

Schey et al [45] presented the shape changes in upsetting of slender cylinders of mild steel and aluminum alloys which were incrementally upset with good lubricant. They developed formulas for calculation of barrelled dimension and these are found to be reasonable accurate also for hot forging. **Dean [46]** studied the influence of billet inertia and die friction in forging process, and he presented analytical work to show the variation of the load due to friction.

Lee and Altan [47] studied the influence of flow stress and friction upon metal flow in upsetting by using an upper bound method. **Venugopal et al [48]** studied the effect of strain rate and temperature on the friction factor of pure titanium. They reported that, as the strain rate increases, the friction factor increase for both the dry and the lubricant condition. The reason for this behavior could be that as the strain rate increase, the adiabtic heating causes a temperature rise which results in lubricant break-down.

Hashmi [49] presented a numerical technique for a study of upsetting of cylindrical billets between a free falling tup and a stationary anvil with unequal end friction. He reported that no significant variation of the load on either the tup or anvil occurs as along as friction at one interface remains negligible. It was, howoever, noted that a marked increase in tup and anvil load occurs when friction at both ends are considerably higher. It was also predicted that unequal end friction affects the instantaneous and final shape of the billet.

Kozo [50] studied a mechanism of lubricant trapping in slow speed compression in metal forming, the principle of this mechanism being the introduction of elastic deformation of the tool. He reported that this mechanism depends on the thickness of the lubricant film, speed of compression and the radius of billet undergoing the test. **Thomson and Myoe [51]** examined the profile of the billets of circular, square and rectangular cross-section under high and low friction.

Male and Cockcraft [52] developed a technique for studying the coefficient of friction between rigid tools and plastically deforming metals at elevated temperature. They indicated that at low strain rate the coefficient of friction increase as the amount of deformation increased. **Sheikh et al [53]** studied the effect of impact speed on lubricant in hot forging and reported that the coefficient of friction decreases with the increase of impact velocity, and the deformation load to upset the ring specimen increases with the inter-face friction.

Narayanasamy et al [54] developed a method to predict the barreling of solid cylindrical specimen and the uniaxial compression load. **Holze and Brown [55]** investigated the behaviour of steel in compression at strain rate between the range 10^{-3} to 10^{4} per second. They reported that there is no significant radial inertia effect, because there is no large separation between the stress-strain curves at high and low strain rates.

Haque[56] ignored the effect of radial inertia and reported that the radial inertia and temperature effects will cancel each other.

Gorham[57] studied the effect of specimen inertia in high strain rate compression .He reported that,even at very high strain rate of up to 10^5 per second inertia error can be reduced to negligible levels by limiting specimen dimension to less than 1 mm. **Dharan and Hauser[58]** used a split Hopkinson bar to determine the stress-strain relationship of aluminium at strain rates of up to 1.2×10^2 per second. They reported that during high impact velocity compression, in addition to the axial particle velocity the radial and tangential particle velocities may achieve high values of compressive stresses in three direction. **Hauser[59]** developed the split Hopkinson technique to measure the stress-strain relations at high strain rates. He reported that , if the test specimen is small enough, the transmission time for elastic wave is too short, so equilibrium throughout the specimen is rapidly established and uniform plastic deformation takes place within the specimen.

Gunasekera et al [60] studied the effect of specimen size on stress-strain behaviour in compression, they reported that large aspect ratio test specimens (height/diameter) are desirable and kept their aspect ratio at 1.5 to avoid buckling and barreling. **Haque[56]** kept the aspect ratio of his test specimen less than unity to avoid buckling and barreling.

Techniques and Equipment

Since the introduction in reference [27], the spilt Hopkinson bar has been used in dynamic compression impact testing of metals, rocks, and various materials [61,62]. Various other different techniques and equipments have been also used to study the dynamic behaviour. **Gorham [63]** used modified Hopkinson bar system in which the projectile bar struck the specimen directly, thus achieving strain rate of up to 10^5 per second. He used a high speed camera incorporating a novel optical system to accurately record the strain distribution along the specimen. **Haque[56]** used the ballistic test with a high speed camera which was capable of recording the event at framing rates of up to 10^6 frames per second, in order to record the deformation time history. **Yokoynama and Kishida [64]** developed a microcomputer-based system for high speed compression test by spilt Hopkinson pressure bar technique, to determine the dynamic behaviour. **Lengyel and Mohitpour [65]** developed an incremental method of determining stress-strain curves for large strain at high strain rates. They used a modified high energy-rate forging machine. **Yew and Ricardson [66]** used a torsional impact machine to find the effect of shearing strain rate and plastic wave in copper specimen. **Mohitpour and Lengyel [67]** developed a novel forging machine to obtain isothermal strain rates of up to $8X10^2$ per second. **Hoge [68]** presented a technique for determining mechanical properties of Aluminium under axial and biaxial tensile loading.

Effect Of Strain Rate In Mechanical Properties

The mechanical properties of the material can vary considerably with the deformation conditions. In other- words, the strength, ductility, and toughness differ with speed,specimen configuration, and applied stress.

In 1950, **Clark and Wood [69]**, performed tensile impact test on several metals and velocities ranging from $2x10^{-3}$ to $2.4x10^{3}$ per second, their data showed that the ultimate strength of metals are appreciably higher at high speeds than at low rates of deformation. Furthermore, they found that in some metals, deformation did not start immediately after application of stress higher than yield stress. This occurs in annealed steels which exhibit a sharp yield point in conventional tests. They measured the delay times of about 0.005 second between the time the stress was applied and the onset of yielding.

Alder and Philips [70] found that the strain rate has a slight but noticeable effect on the flow stress of Aluminium at low temperatures, the effect being considerably more significant at high temperatures. **Venugopal et al [71]** studied the effect of temperature and strain rate on the flow stress while forming commercially pure titanium. They reported that adiabtic heating generated in the specimen reduced the true stress, and this reduction can be noticed at higher strain rates rather than lower rates of strain. Since the work done on the specimen

is greater at higher strain rates due to high stress, the rise in specimen temperature is larger, even at lower strain.

Serenen and Dul'nen [72] examined the effect of strain rate on the mechanical characteristics of steel at increased temperatures. They reported that, strain, modulus of plasticity and plasticity characteristics increases with the increase in strain rate.

Muller [73] studied the effect of high strain rate on the behaviour of Iron and Nickel.He stated that both metals have been found to be strong strain rate sensitive, indicating that the deformation mechanism at high strain rate is different from that in static region.

Tanaka et al [74] examined the effect of high strain rate on the strength of Mild-steel . They reported that yield point and flow stress at a certain amount of strain become higher with an increase in the stricking velocity, and the shape of the stress-strain curves after yielding becomes more horizontal. The yield stress is more sensitive than the flow stress at a certain amount of strain.

Dean and Sturgess [75] obtained the dynamic stress strain curves of Steel over a wide range of strain rates and temperature. They reported that the flow stress of steel is increased either by a reduction in temperature or by an increase in strain rate, and that the strain rate sensitivity increase with increasing test temperature.

Lindholm and Yeakely [76] used the spilt pressure bar method for obtaining the dynamic stress-strain curves of Aluminium up to strain

rates of 10^3 per second . Also they presented some factors which may have affected the accuracy of the result such as friction and inertia effect. **Woodward [77]** obtained the dynamic stress-strain properties of Steel and Brass at high strain rates of up to 10^4 per second. He reported that, Brass is shown to be relatively more sensitive to strain rate, and the upper yield stress of Mild steel is strongly dependent on the strain rate, where as the lower yield stress is not.

1.5 Material Selection

The present study is aimed at investigating the following three types of materials:

1) Mild Steel (En-2)

2) Stainless Steel (304)

3) Copper (Cu)

All the above materials have been selected to be tested at different rates of strain and room temperature. The specific information and the application of these materials are described as follows:

Mild Steel

Without steel the state of technology would be set back considerably, many varieties of steel alloys have been developed in order to meet the specific needs of an advancing civilization. The design and manufacturing engineer have a big responsibility to familiarise themselves with so as to make the best selection from the available alternative materials.

The EN-2 steel has a (0.16-0.24 %) carbon contant, and it can therefore be quenched and tempered by conventional heat treatment method. This feature has resulted in EN-2 steel being used in many applications which requires good strength and wear resistance.

This type of steel is easily available in plate, slab, bar and rods forms. Mild steel is widely used in many applications such as Structural Engineering which is widely used in buildings as such, it has a very important place in the list of materials used in this sector of the industry. It is also used in the Packaging and Transport industry which are probably the most commonly used of steel materials. Its advantages lie in the fact that, it has the excellent strength and ductility characteristics. In addition to that the EN-2 type of steel is quite often used for making components which are subjected directly or indirectly to dynamic loading. It is also widely used for the manufacture of plants, different types of machines and for shafts, connecting rods, axles and crank.

Stainless Steel(304)

The development of stainless steel has been mainly due to their corrosion resistance properties. However, many types of stainless steel could be used at high temperature. The stainless steel (304) is the most common type that has been used in nuclear industry. It is widely used in the manufacture of most nuclear plants and equipment, much of which is used either within the reactor or is very closely associated with highly active materials. It is used in order to sustain minimum damage from the nuclear radiations and due to its corrosion resistance and its good cold and hot ductility properties as well as its reasonably good fabricating characteristics.

Copper

Copper is an important engineering metal and has been used for over six thousand years. Copper is widely used in electrical engineering including cables, motor generators, transformer and telecommunications as well as in the manufacture of hot water cylinder, tubes for water and gas supply and many other general engineering applications. The use of copper is due to its important properties such as high electrical conductivity, high ductility and corrosion resistance.

1.6 Aims of the Study

The aim of this study is to establish high strain rate constitutive equations for commercially pure copper, En-2 mild steel and stainless steel. The steps to determine these properties may be summarized as follows:

1) Using the Universal compression test to find out the static stress- strain curves of the three materials at room temperature.

2) Select the best lubricant , which minimize the effect of friction.

3) To carry out the ballistic test, by firing cylindrical projectile made from tool steel onto small specimen made from previously selected material.

3) To develop computer simulation, of the deformation history of small cylindrical specimens impacted by a tool steel projectile, based on finite difference technique. This technique gives theoretical prediction of the final dimension of the specimen as well as the deformation history for given high strain rate constitutive equation.

4) To establish a new dynamic constitutive equation based on the static properties and assumed strain rate sensitivity.

5) To find the dynamic stress-strain curves at high strain rates.

6) To find the effect of strain rate on the dynamic flow stress of the material at room temperature.

Finally, the principal aim of this investigation is to develop a simple technique to determine new constitutive equations to describe the dynamic properties of the metals, and compare the result with those obtained using more sophisticated and expensive equipment.

CHAPTER TWO

EXPERIMENTAL EQUIPMENT

2.1 Static Compression Test

2.1.1 Introduction

The INSTRON universal testing instrument model [4204] was used in order to find the static properties of the materials used. The advantage of this machine is its accuracy and highly reliable precision for evaluating the mechanical properties. The machine model [4204] frame has a load capacity upto 50 KN.This frame is designed for testing materials in either tension or compression.

The basic operation of the instrument consists of selecting a load cell for a particular testing application, mounting the load cell in the moving cross head within the loading frame, then setting a specimen in position so that the applied load and the displacement can be measured. The specimen is held by grips for tension testing, or is table mounted for compression testing.

2.1.2 Description of the Static Testing machine.

The main component of the machine [4204] model are shown in Plate [2.1] and are identified below:

1- Loading frame

This is the part of the machine where test specimen is mounted and either a tension or compression load is applied.

2- Moving Cross-head

The moving element within the loading frame which applies a load to the test specimen at commanded speed.

3- Load Cell

The calibrated transducer in the moving cross-head which precisely measures the applied load.

4- Upper Grip Coupling

The connection between the upper grip and the compression anvil and the load cell.

5- Lead Screws Cover

Protective curtains that shield the lead screws from debris due to test specimen breakage or from an accidental contact by the operator or fixtures.

6- Fixed Cross-head

The top structure that supports the head screws.

7- Control Panel

The system main power switch and (JOG) the controls for moving cross-head are located on this panel.

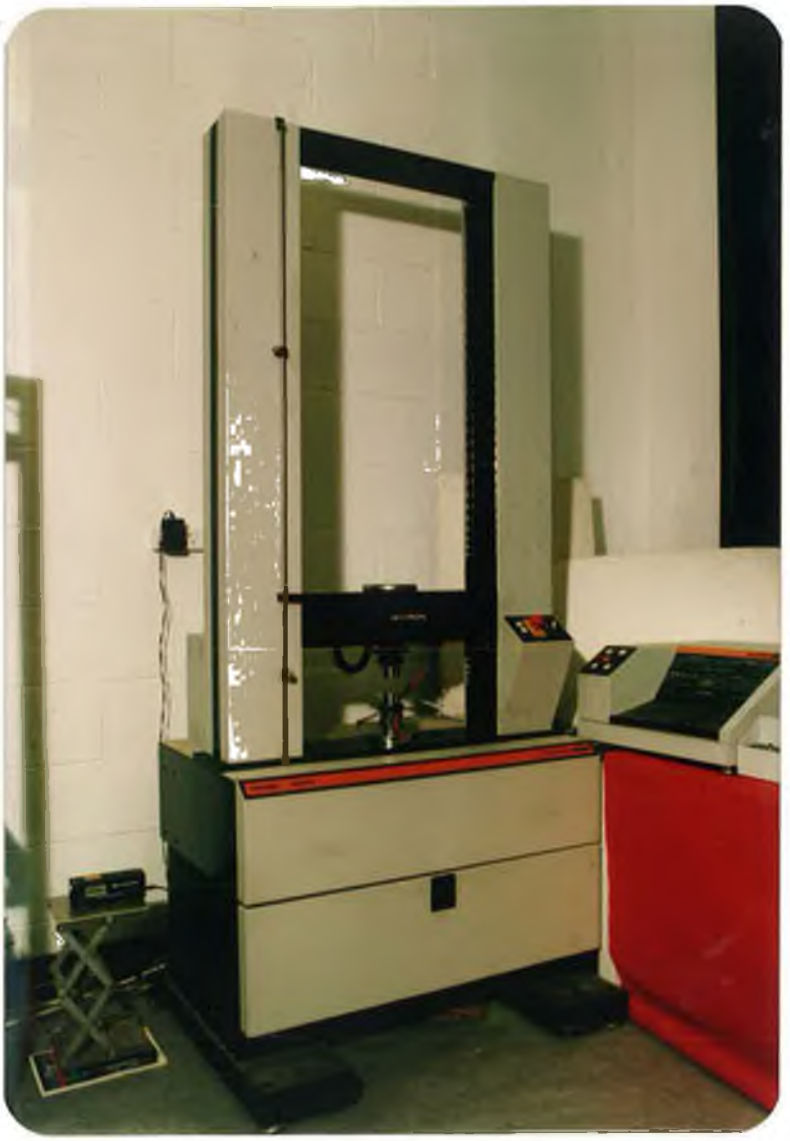

PLATE NO [2.1] UNIVERSAL TESTING MACHINE MODEl [4204].

The accessories attached to the Static Testing Machine are the Following:

A) Plotter

The INSTRON plotter **Plate [2.2]**, has a horizontal flat-bed with single pen and single range **X** and **Y** axes. The plotter accepts any paper of size (29 X 42 cm) or smaller and has an effective writing area of (25 x38 cm).

B) Control System

The control system shown in **Plate [2.2]**, provides an interface between the operator, loading frame and peripheral devices (recorder-printer-computer) by functions contained on a cross-head control panel and the basic panel.

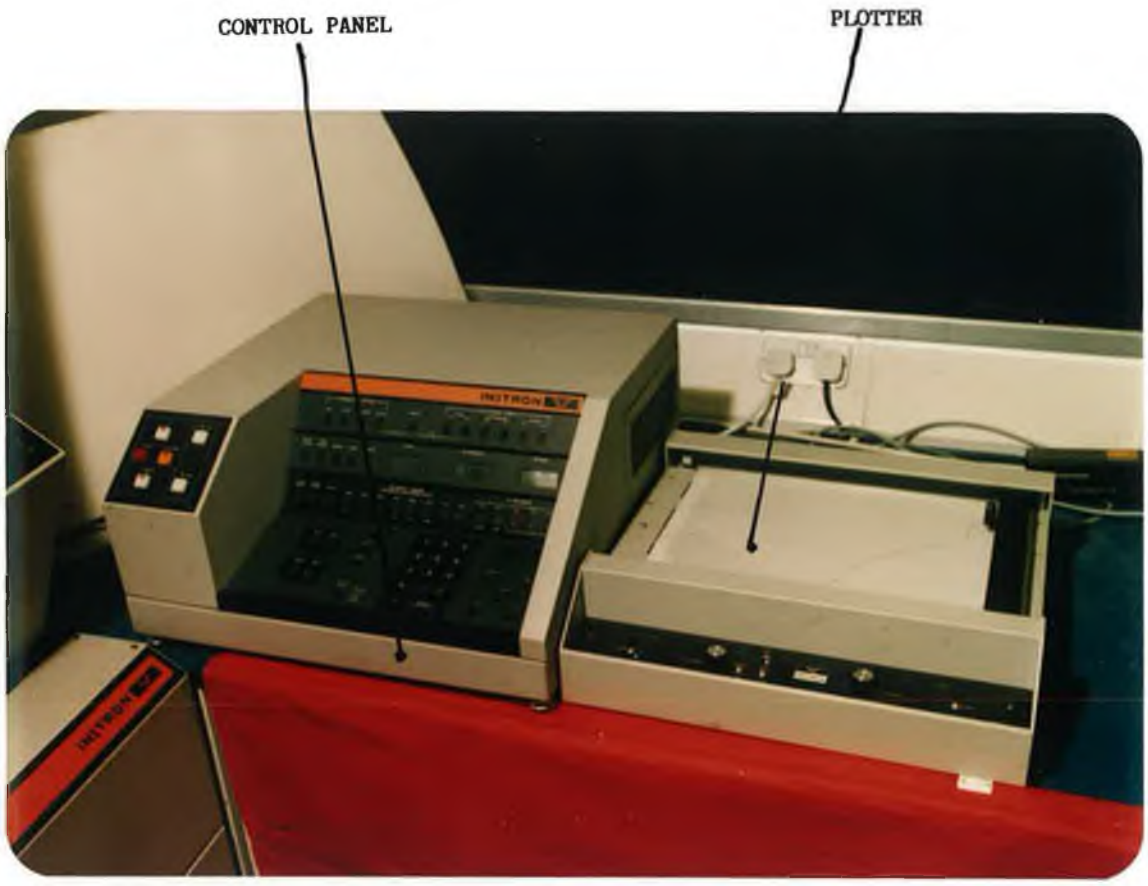

PLATE NO [2.2] CONTROL PANEL AND PLOTTER FOR THE UNIVERSAL STATIC MACHINE TEST

2.2 Dynamic compression Test:

2.2.1 Introduction

The ballistic test apparatus used for this work has been designed, constructed and commissioned by **Hashmi et al [78]**, for firing of cylindrical projectile at speeds varying from 30-1000 m/sec onto small cylindrical or disc shaped test specimen placed upon a rigid anvil. **Haque [56]** used this ballistic test apparatus together with a high speed camera, for determining the behaviour of mild steel at high strain rates and at temperatures ranging from zero to room temperature. In this study ballistic tests were carried out using the same apparatus with some modifications to the valve as well as to the electronic timer for recording of the velocity of the projectile, in order to deform small cylindrical billets at room temperature and at strain rate of up to 10^5 per second.

A schematic diagram of the ballistic rig with its other accessories is shown in **Fig.(2.1)**, while **Plate [2.3]** shows a number of Photograph of the experimental setup.

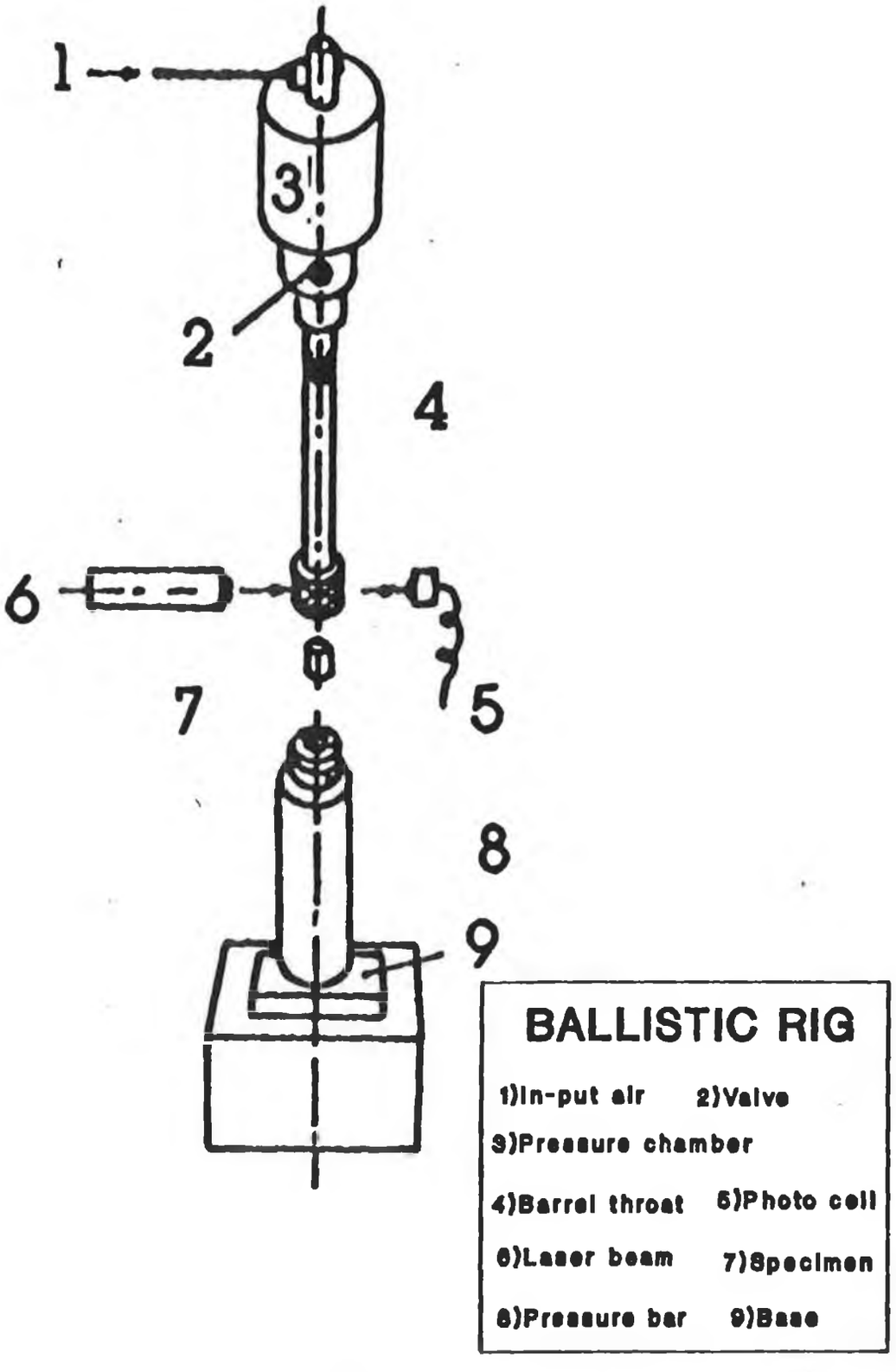

Fig.(2.1) Ballistic Rig

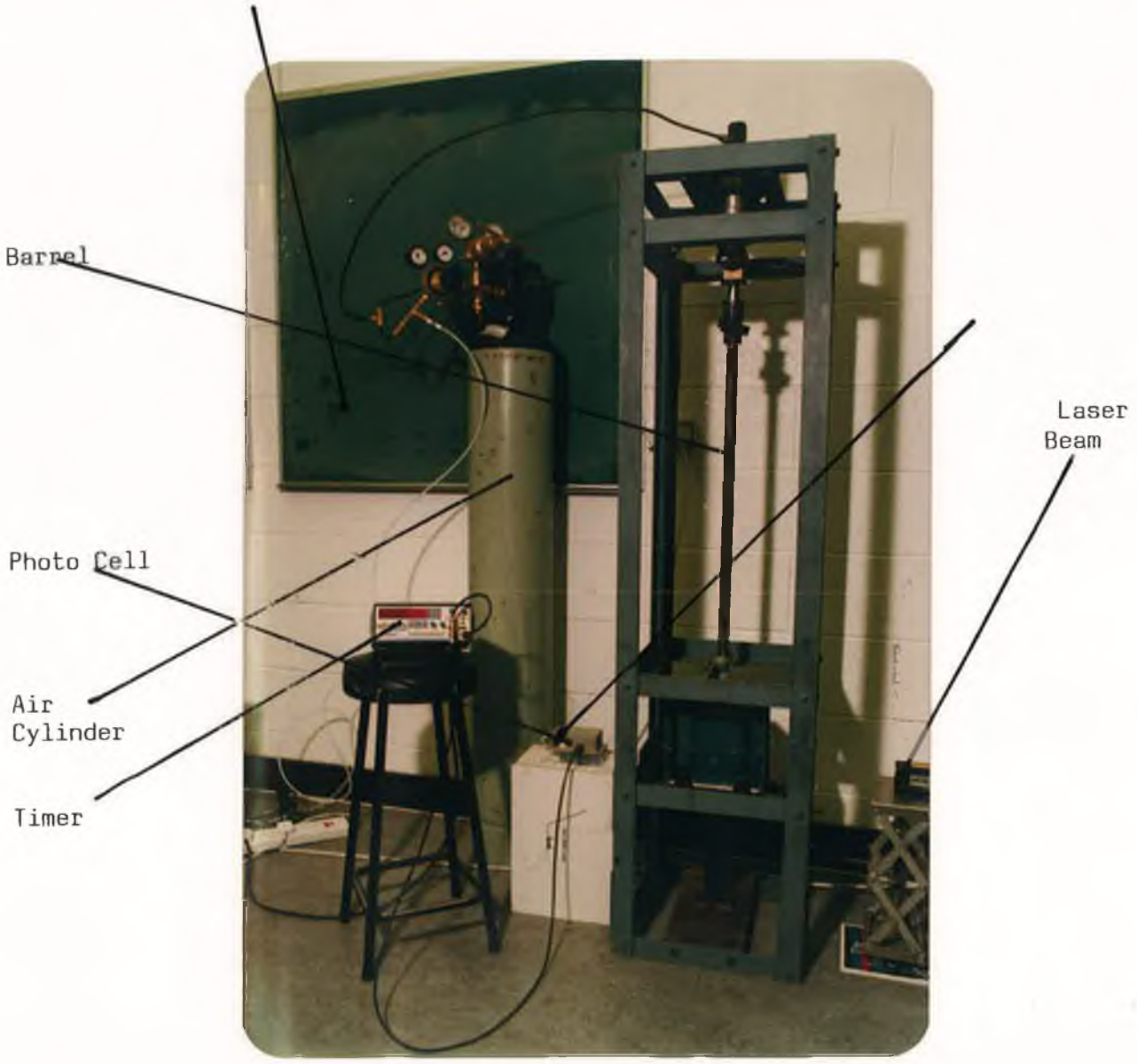

PLATE(2.3) Ballistic Test System.

2.2.2 Description of the ballistic test apparatus

The basic construction of the ballistic test apparatus can be seen by consideration of **Fig.(2.1)** as follows:

A- Pressure chamber and solenoid value.

B- Barrel and loading throat Unit.

C - Rig frame.

D- Anvil Unit.

A- Pressure Chamber and Solenoid Valve

The bottom end of the pressure chamber is firmly fixed to the solenoid valve, series [137], by means of the valve nuts.A copper gasket is used between the two parts to make the assembly leak proof. The solenoid valve is suitable for the operation at pressure range from 0.8 to 40 bar and at temperatures between -10 to 180 °C. The valve is controlled by an electric switch [on & off] which is operated by a 12 V DC power supply.

The top end of the pressure chamber is connected by a flexible reinforced rubber hose to compressed air cylinder which can fill the chamber with a pressure of upto 140 bar. The Compressed air cylinder was fitted with two pressure gauges, one to measure low pressure from 0.8 to 10 bar, and another for high pressure from 10 to 40 bar. **Plate[2.4]** shows the pressure chamber.

A flexible reinforced rubber
hose to compressed air cylinder
which can fill chanber with a pressure
upto 140 bar.

PLATE(2.4) Shows the Pressure Chamber.

B- Barrel and loading Throat

The arrangement of the barrel and loading throat is showing in **Fig.(2.2)**. It includes the following parts:

(i) Extension barrel.	(ii) Surge suppressor cap.
(iii)Coupling Sleeve.	(iv) Loading Unit.
(v) Split Cover.	(vi) Sliding Collar.
(vii)Collar Nut.	(ix) Projectile gripped mechanism.

To minimize the noise, the suppressor cap is attached at one end of the extension barrel which is made from En-16 steel with (0.3-0.4) carbon and it has a good shock resistance properties. There are small slots in the suppressor cap to permit the laser beam to pass through it. The other end of the extension barrel is connected to the loading throat **(primary barrel)** by means of a threaded and coupling sleeve. The loading throat is made of En-32 alloy steel. This kind of steel has high strength, and good wear and shock resistance.

A cut-out segment in the loading throat allows the projectile to be inserted, pushed up and held by the gripping mechanism. A close fitting cover of En-32 steel is used to cover the cut-out segment, and a sliding collar and nut is used to hold the cover in position. The projectile gripping mechanism consists of three grip screws which can be adjusted to hold the projectile in position, and thus prevent it from sliding down the barrel. The coupling sleeve provides two holes in order

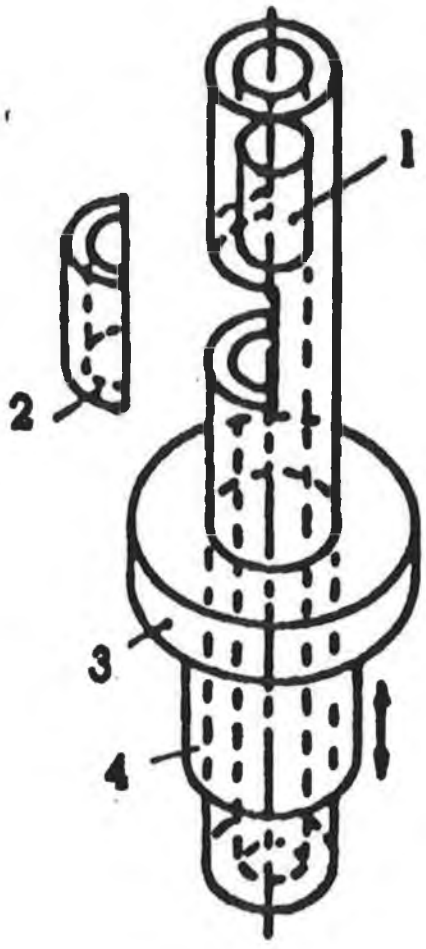

LOADING THROAT

1)Projectile

2)Cut-out segment

3)Split cover

4)Extension barrel

Fig.(2.2) Loading Throat

to fix the stop pins used to prevent the collar nut from sliding down. The position of the barrel is always held perpendicular to the anvil by means of a circular bracket fixed to the frame of the rig.

C- Frame Of The Ballistic Rig

The frame is made of welded and bolted mild steel angles. The height of the frame is about two meter while the width and the depth are about 40 cm each. Two platforms were provided, each on the opposite side of the rig in order to fix the laser beam and the photo cell. A small safety chamber was built using wire mesh and thick perspex sheet to contain the projectile and specimen after impact. Two holes were made in the wire mesh on the opposite sides to allow the laser beam to pass through from the laser unit to the photo cell. The front panel can be easily opened and closed in order to place the specimen onto the anvil as well as to remove the specimen and the projectile after each test.

D- Anvil Unit

The anvil unit **Fig.(2.3)** consists of the following components:

(i)	Base Plate	(ii)	Back- up anvil.
(iii)	Holder Plate	(iv)	Pressure Bar.
(v)	Top anvil	(vi)	Cover Plate.

The top anvil unit is made of tool steel **D2**, while the pressure bar is made from a cylindrical alloy steel En-32 bar, and the rectangular base plate is made of solid En-32 steel plate.

The top anvil and the pressure bar were both heat treated at **970** ^{o}C, oil

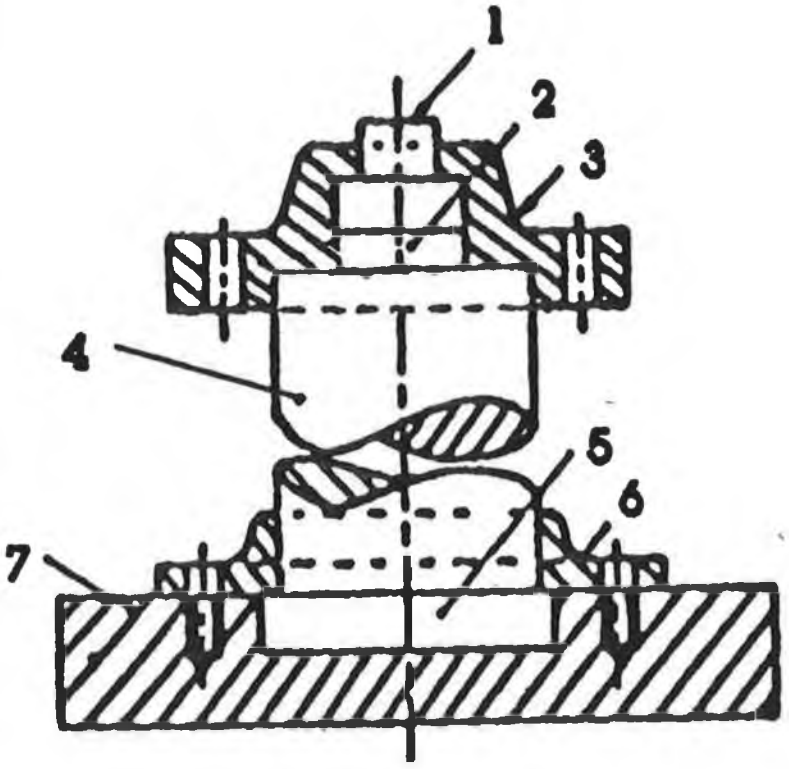

ANVIL UNIT

1)Top-anvil 2)Middle anvil

3)Cover plate 4)Pressure bar

5)Back-up anvil

6)Holder plate 7)Base plate

Fig.(2.3) Anvil Unit

quenched and tempered to 800 Hv. These two parts are held in place by cover plate at the top and holder plate, which is fastened to the base plate at bottom end of the pressure bar.

The accessories of the Dynamic Testing Machine are as following:

Universal Counter-timer

The time recorder model (Apoll 10) made by Black Star Company with size (219x240x98 mm) is shown in **Plate[2.5]**.

One of the many practical application of the counter is the velocity measurement of a travelling object. In this study the timer was used to record the time intervals when the projectile passed through the laser beam *[just before impact]*, and as the length of the projectile is known, therefore the velocity could be calculated.

Laser Unit

The laser unit used (Model 1508-0), is manufactured by the Laser Lines Company . The laser beam and photo cell were fixed at one side of the ballistics rig as shown in **Fig.(2.1)** and in **Plate [2.3]** . The beam passes through the circular holes in the wire mesh and suppressor cap to the photo cell detector. The photo cell detector is connected to the timer. As the projectile passes through the suppressor cap, it cuts the laser beam and the change in voltage at the photo cell detector is recorded by the timer.

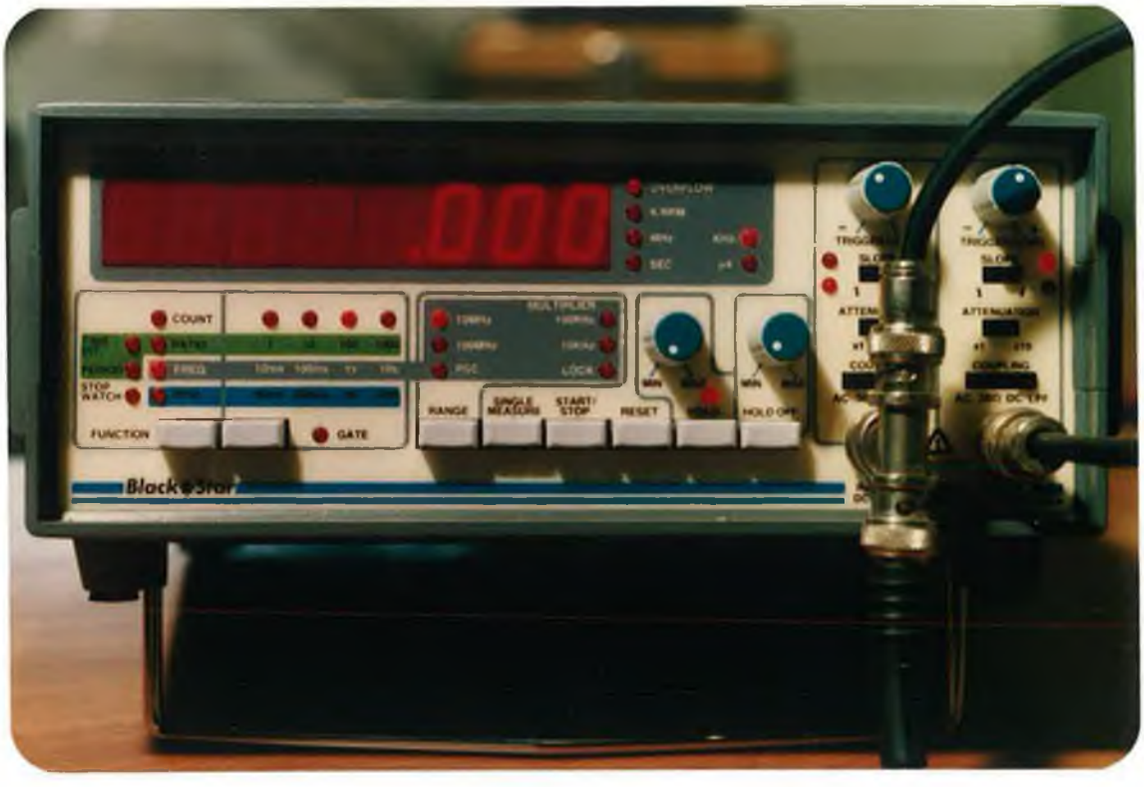

PLATE NO [2.5] **UNIVERSAL COUNTER-TIMER.**

2.3 Hardness Tester

One of the most common tests for assessment of the mechanical properties of metals is the Hardness Test. The hardness of a material is generally defined as its resistance to permanent deformation. Various techniques have been developed to measure the hardness of materials using different indentor material and geometries. The most common standardized hardness tests are, **(Brinell, Rockwell, Vickers and Knoop).** The hardness test is a cheap and simple non- detractive test for determing the yield strength of materials, yield strength is approximately One-Third of the vickers hardness value **[79].**

A micro-hardness tester model [Leize Mimlload 2] **Plate[2.6]** was used to measure the hardness at the specimen surface before and after deformation. By changing the diamond head three kinds of hardness measurement could be done using the micro hardness tester [Vickers, Knoop and Scratch hardness]. This tester is accompanied by the hardness test plate for the calibration and a set of loads ranging from 5 g to 300 g. These loads could be chosen according to the thickness of the test specimen.

In the current study only the Vicker hardness method was used. In order to obtain a good result, the micro hardness tester was installed on a rigid surface isolated from vibration and all the specimens were polished before measuring the hardness inorder to find a clear structure.

PLATE NO [2.6] Shows the Micro-hardness Tester.

2.4 Lubrication

The presence of friction is a major cause of concern to all connected with metal forming operations in general and upsetting of cylindrical billets in particular. The main reason for using a lubricant in a compression test is to eliminate contact between the specimen and the projectile. The influence of friction in an upsetting operation is manifested in two major ways:

1) The deformation of the billet is rendered inhomogenuos and barreling on the sides of billets occurs.

2)The load required for a given deformation is increased as the friction coefficient increases.

However, the choice of lubricant and lack of knowledge of its behaviour under complex and dynamic loading situation makes it difficult to estimate the exact frictional properties which prevail during a particular forming process.

In this study the following lubricants were used at different stages of the test programme;

1-Pure Petroleum Jelly.

2- Polythene sheet.

3-Mixed Graphite and Petroleum Jelly.

CHAPTER THREE

EXPERIMENTAL PROCEDURE AND RESULT

3.1 Static Compression Test

3.1.1) Lubricant

In order to choose the best lubricant, to minimize the effects of friction, specimens of 22 mm diameter with an aspect ratio of unity were prepared from lead bar[1]. All the specimen were deformed at the same strain level, with the following types of lubricant:

1) Pure petroleum Jelly.

2) Mixed Graphite With Petroleum Jelly.

3) Polythene Sheet.

Also, some specimen were deformed without lubricant, and others under high friction using Silicon paper at the two faces of the specimen. For each test, three specimens of the same dimension were used and deformed to the same strain level under the same speed of deformation [5mm/min], and all the dimensions were recorded before and after deformation, as shown on **Table [3-1]**.

[1] Lead was used due to the limitaion of the machine, and also its avilabity for biger sizes at that time.

By applying the following equation on reference [54], the best lubricant can be decided which has eliminating the barreling.

$$X = d/2 - 0.5[(3h_o d_o^2)/h - 2d^2]^{0.5} \qquad (3.1)$$

where

h_o Initial height of specimen.

d_o Initial diameter of specimen.

h Final height of specimen.

d Final diameter of specimen.

The value of (x) in the above equation represents the barreling. shown on Fig.(3.1). Larger (x) means the more barreling and high friction coefficient, but if (x) near to zero, this means no barreling and low friction

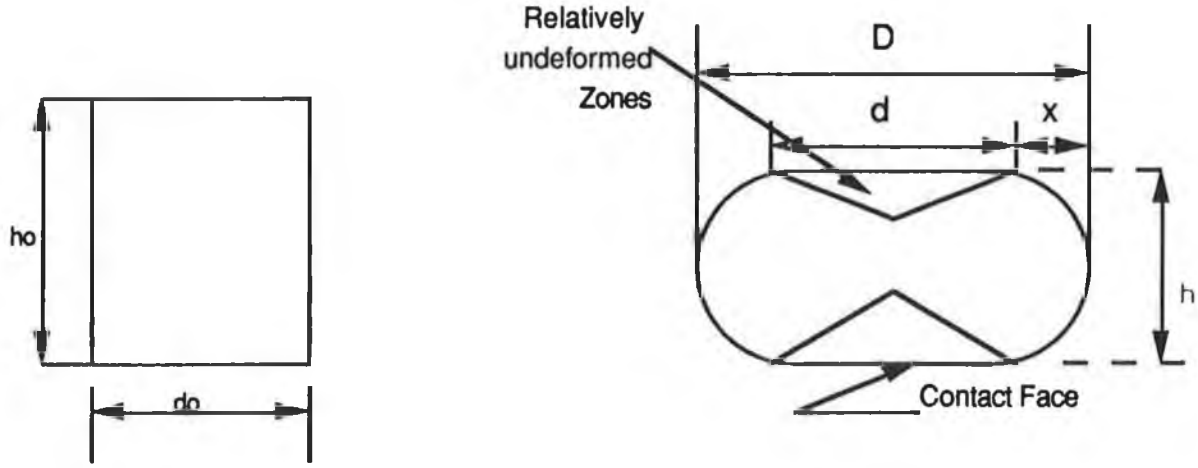

a) Before Deformation b) After Deformation

Fig.(3.1) Compression Test Specimen Before and After Deformation

This method has a particular advantage when applied to study the friction at high strain rate. No direct measurement of force is required,

and no yield strength values are needed, hence the major difficulties of compression test are eliminated. **Plate [3.1]** shows the lead specimens which have been deformed statically using polythene sheet lubricant, without any lubricant and with high friction.

3.1.2 Static Stress-Strain Curve

Specimens of 5 mm diameter with a unit aspect ratio were machined from mild steel and stainless steel bars. Copper specimens were machined from copper bars to 8 mm diameter with unit aspect ratio. These specimens were then tested in simple compression using the "INSTRON 4204" machine between two flat hardened die steel plates, at room temperature, as shown in **Plate[3.2]**. The speed of the cross head movement for every loading or unloading was [5mm/min], each test was limited to 50% deformation with varying load from 20-40 KN. All the tests were conducted with polythene sheet as the lubricant, and some without lubricant.

For each type of the material one specimen was tested continuously, other two were tested in successive stages by interrupting the test at different stages and unloading the specimen for taking different measurements. Before these specimens were reloaded to next stage, the plate was carefully cleaned and relubricated. The initial and final dimension of the specimen were measured before and after deformation, and the average of five reading were taken for each specimen to eliminate the error in reading.

Table (3.1)

NO	CASE	INITIAL (DIAMETER)	INITIAL (HEIGHT)	FINAL (DIAMETER)	FINAL (HEIGHT)
1	Without Lubricant	22.05	21.94	29.74	12.40
2	With H igh Friction	22.04	21.94	29.44	12.95
3	With Petroleum Jelly	22.05	22.07	28.82	13.02
4	With Mixed Petroleum And Graphite	22.00	21.98	28.67	13.04
5	With Polythene	22.00	22.09	28.90	12.84

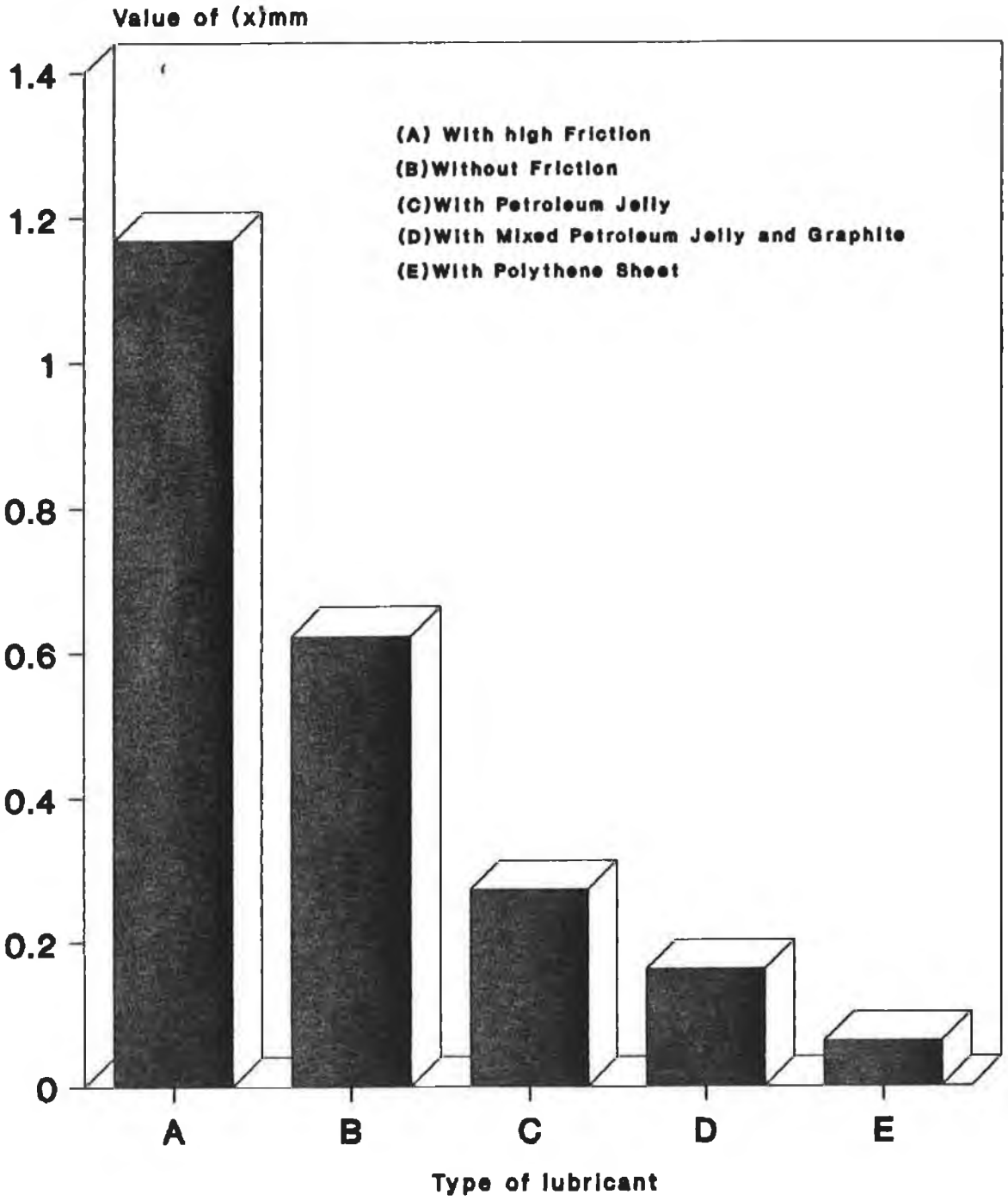
Static Test
Lubricant Selection
Value of (x)mm
1.4
1.2
1
0.8
0.6
0.4
0.2
0
(A) With high Friction
(B)Without Friction
(C)With Petroleum Jelly
(D)With Mixed Petroleum Jelly and Graphite
(E)With Polythene Sheet
A
B
C
D
E
Type of lubricant

Fig.(3.1b)

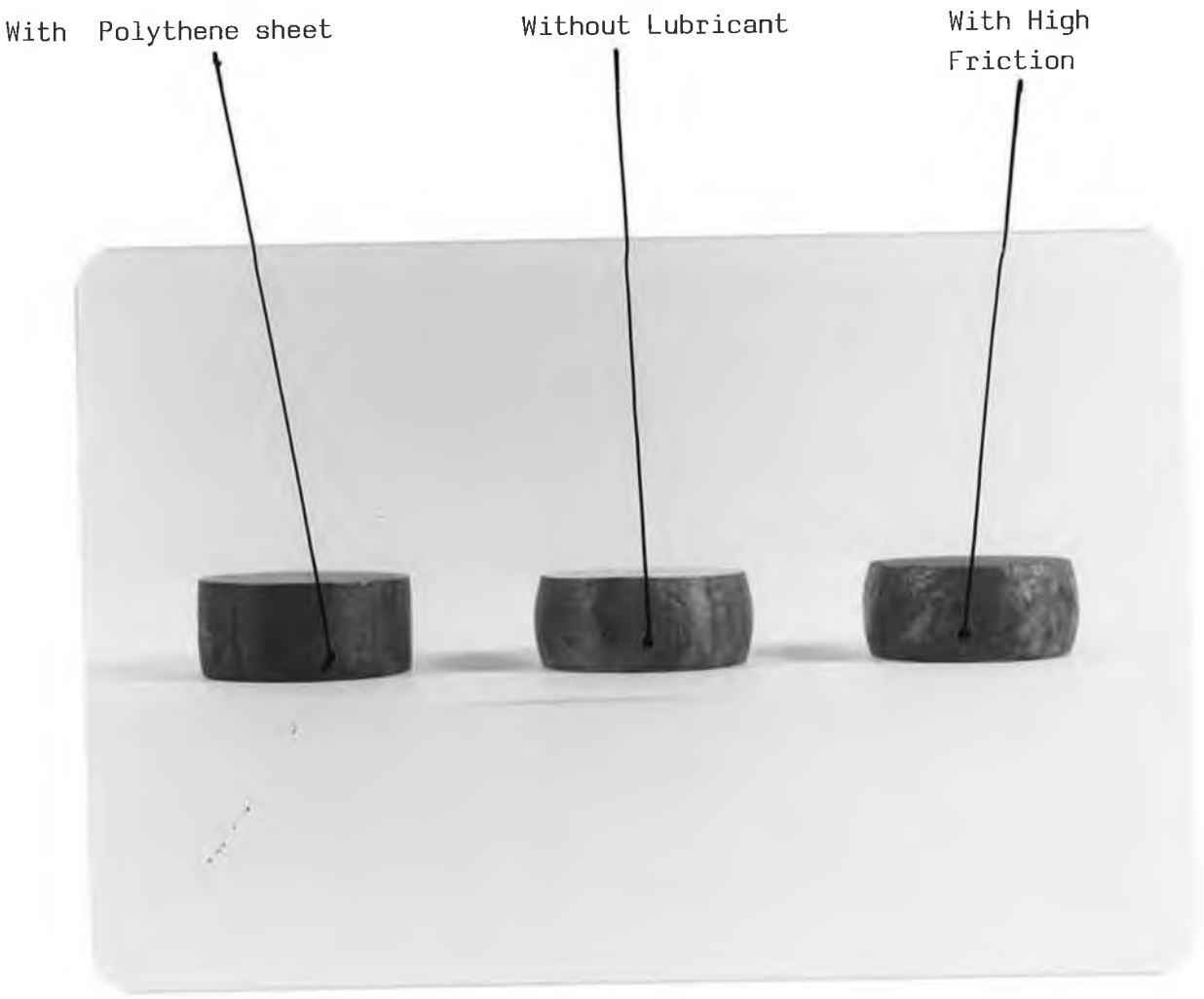

PLATE(3.1) Shows the Final Shape Of the deformed specimen .

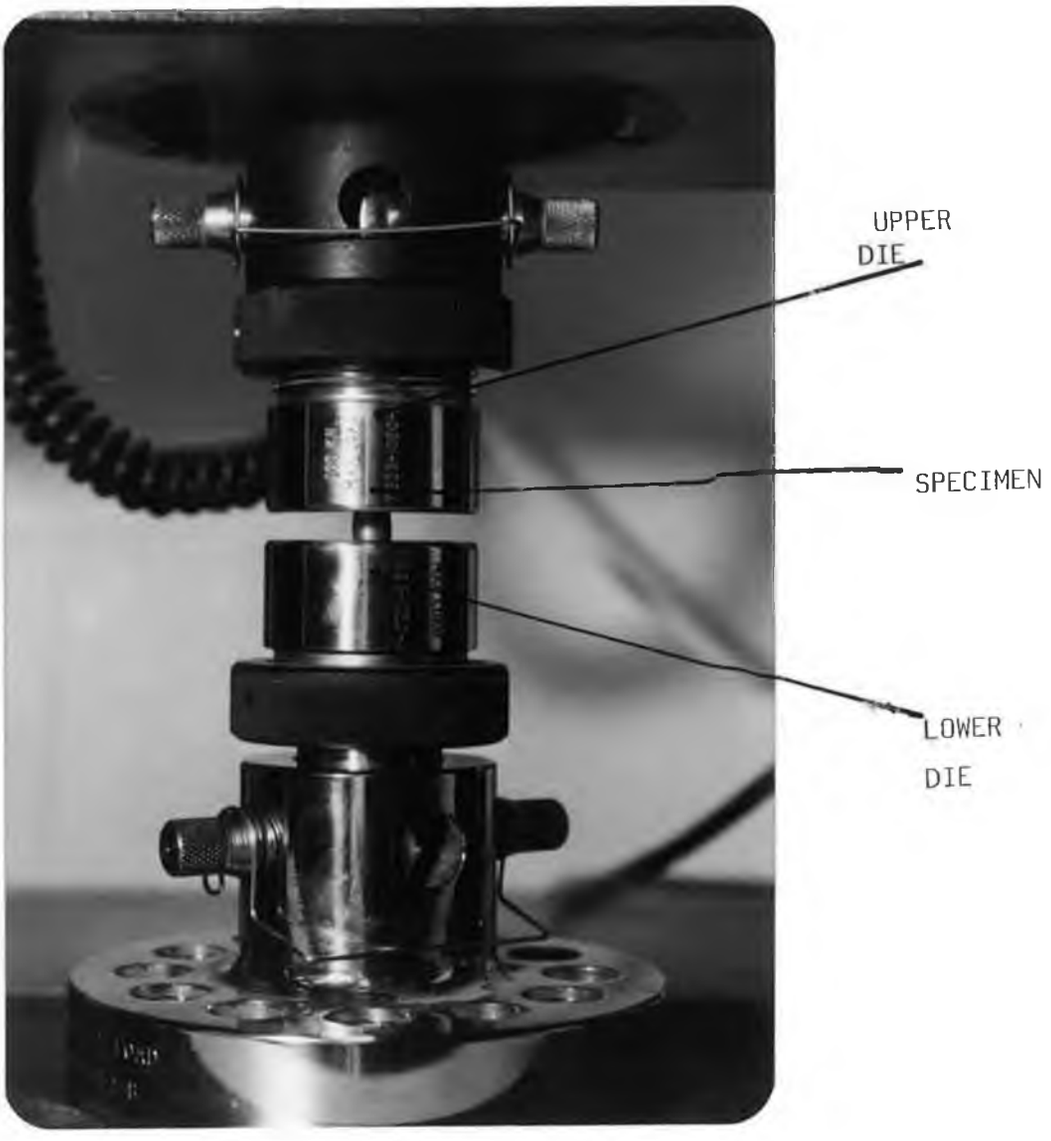

PLATE(3.2) Shows the Static Compression Test.

True stress-strain curves under uniaxial compression were obtained by assuming volume constancy during deformation and barreling. The stress was calculated in each stage using the simple expression.

$$\sigma = F/A$$

where

F Applied force.

A Current area.

The true stress is plotted against the true strain , where the true strain is based on height measurement.

$$\varepsilon = \text{Ln}\,[h_0/\,h]$$

The resulting curves are shown on Fig.[3.2] to Fig.[3.4].

STATIC TEST
True Stress-Strain Curve of Mild-Steel

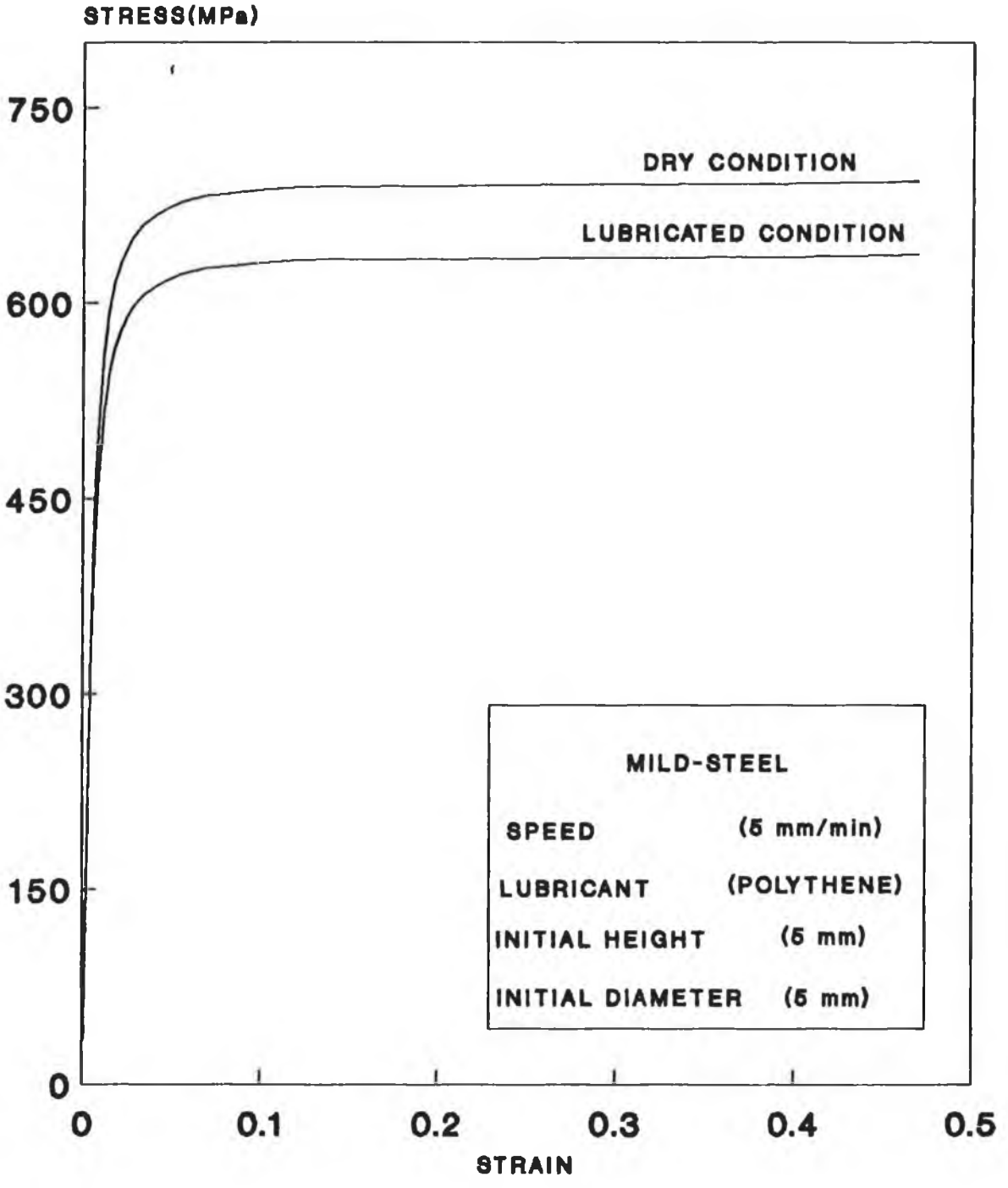

Fig.(3.2)

STATIC TEST
True Stress-Strain Curve of Copper

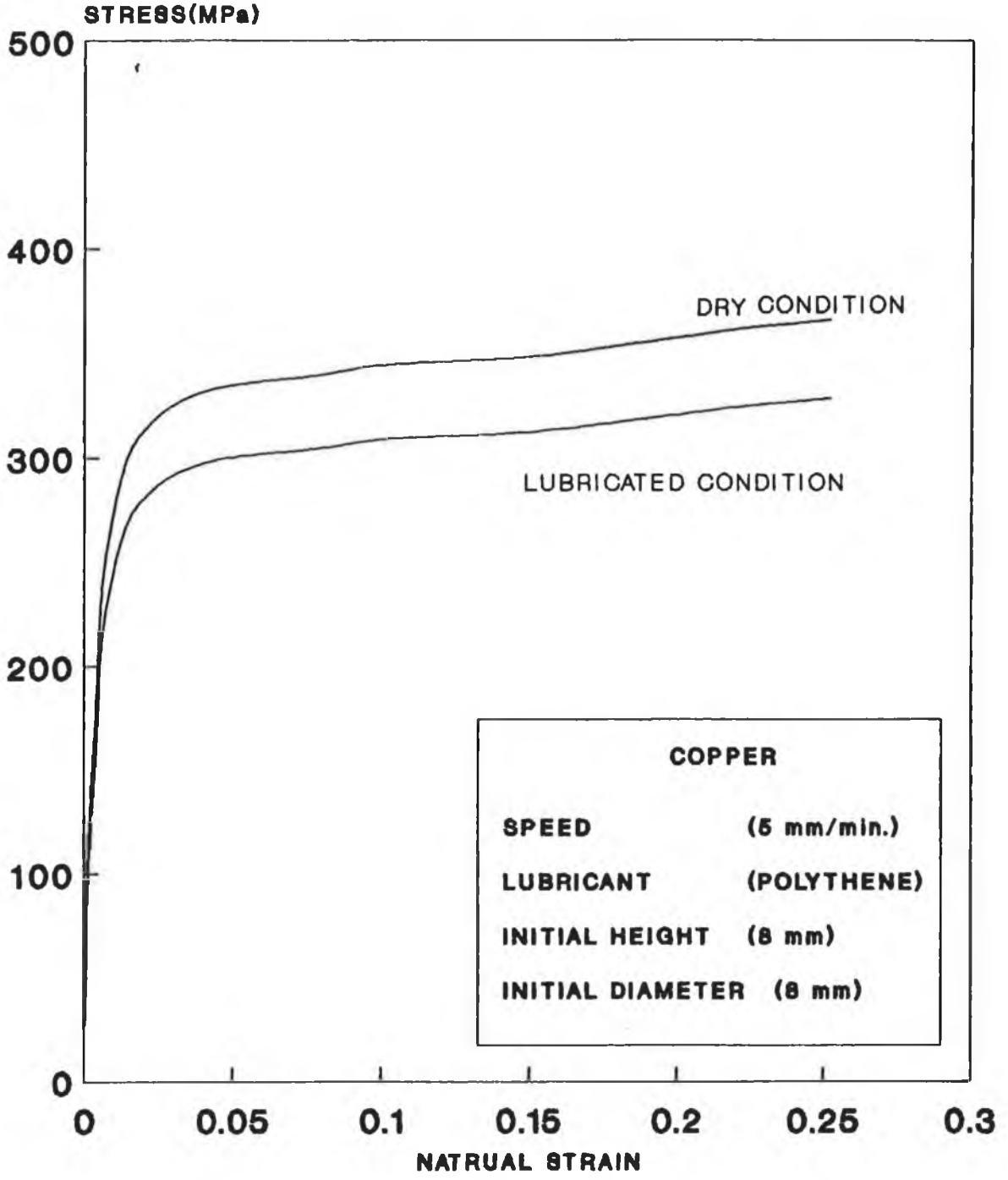

Fig.(3.3)

STATIC TEST
True Strain Stress Curve Of Stainless-Steel (304)

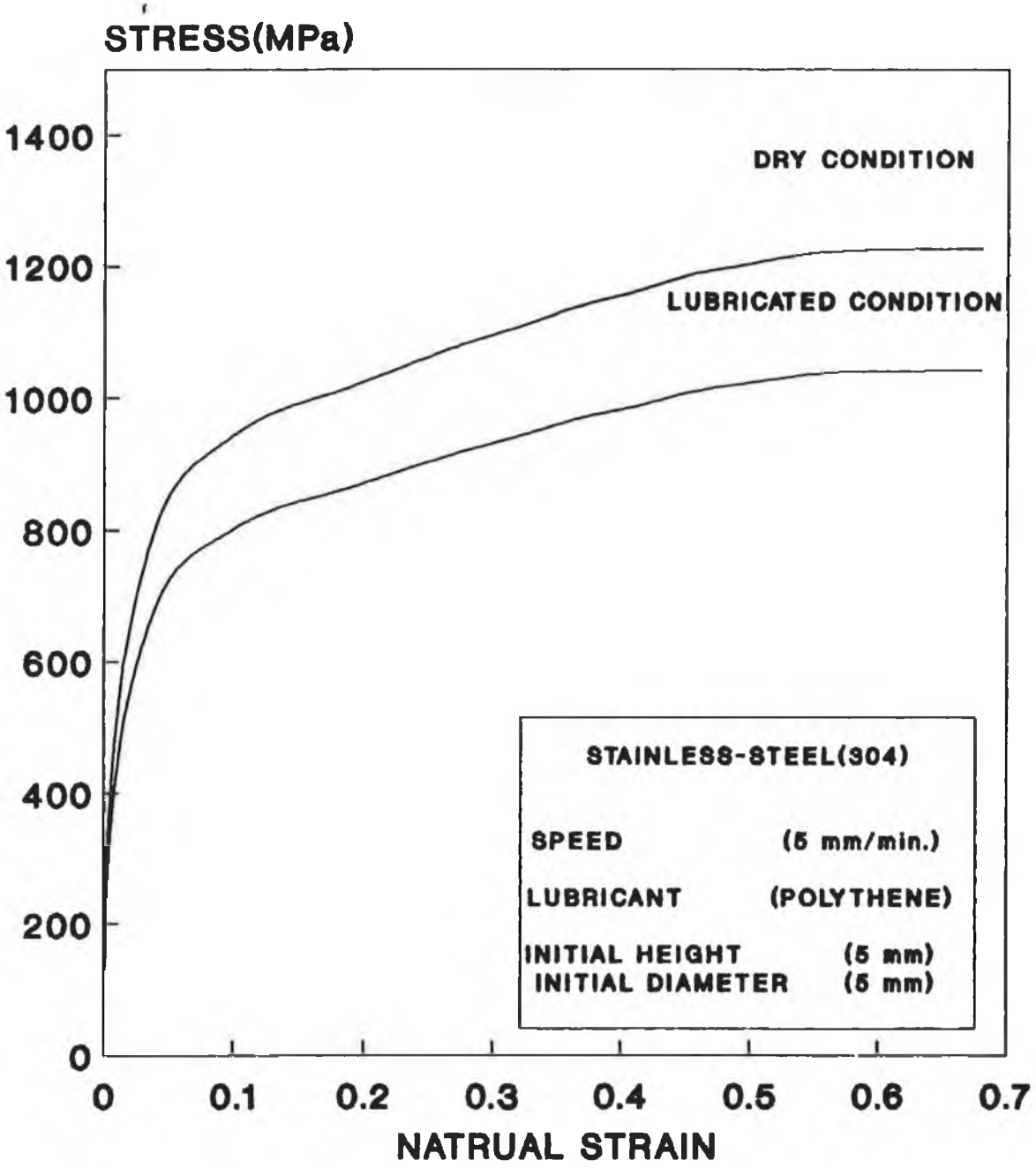

Fig.(3.4)

3.2 Dynamic Compression Test

3.2.1 Preparation of the projectile and test specimen

All the projectiles were made from Tool-steel [D2], with dimension of **19.01mm** in length and **9.05 mm** in diameter. Each projectile was machined into this size to fit closely in the loading throat of the ballistic rig, and the flat surface of the projectile were polished to a mirror finish. The hardness of the projectile was measured to be about **800 Hv** after a series of heat-treatment process (oil quenched at 970 ^{o}C and tempered at temperature of 150 ^{o}C) to increase the strength. This hardness is about eight times higher than that of copper, four times higher than that of mild-steel and two and half times higher than stainless-steel. **Table[3.2]** shows the composition of the material used to make the projectile and of the test specimen, and **Fig.[3.5]** show the configuration of the tool steel projectile.

The test specimens were prepared from as received copper, mild-steel and stainless-steel bars. Each specimen was machined and ground at both surfaces to obtain flat surface inorder to achieve homogeneous deformation. In this investigation the specimen size was 5mm in length and 5mm in diameter inorder to obtain strain rates of upto $6x10^{4}$ per second. Other specimens of 6mm length and 5mm diameter were used inorder to obtain strain rates of upto 10^{3} per second and finally to obtain strain rates above 10^{5} per second, specimens of 3mm length and 5mm diameter were used.

Table (3.2)

Material chemical composition (wt%)			
Mild steel En2 No.3C	Copper C101	Stainless-steel (304)	Tool steel(D2) (AISI)
C 0.16/0.24 Si 0.1/0.4 Mn 0.5/0.9 P 0.05 MaX. S 0.05 Max.	Cu 99.90 Lead 0.005 Impurites (0.03)	C 0.08 Max. Si 1.00 Max. Mn 2.000 Max. Ni 10/14 Cr 16/18 Mo 2./3. Max. P 0.03 Max. S 0.045 Max.	C 1.50 Cr 12.0 Mn 1.00

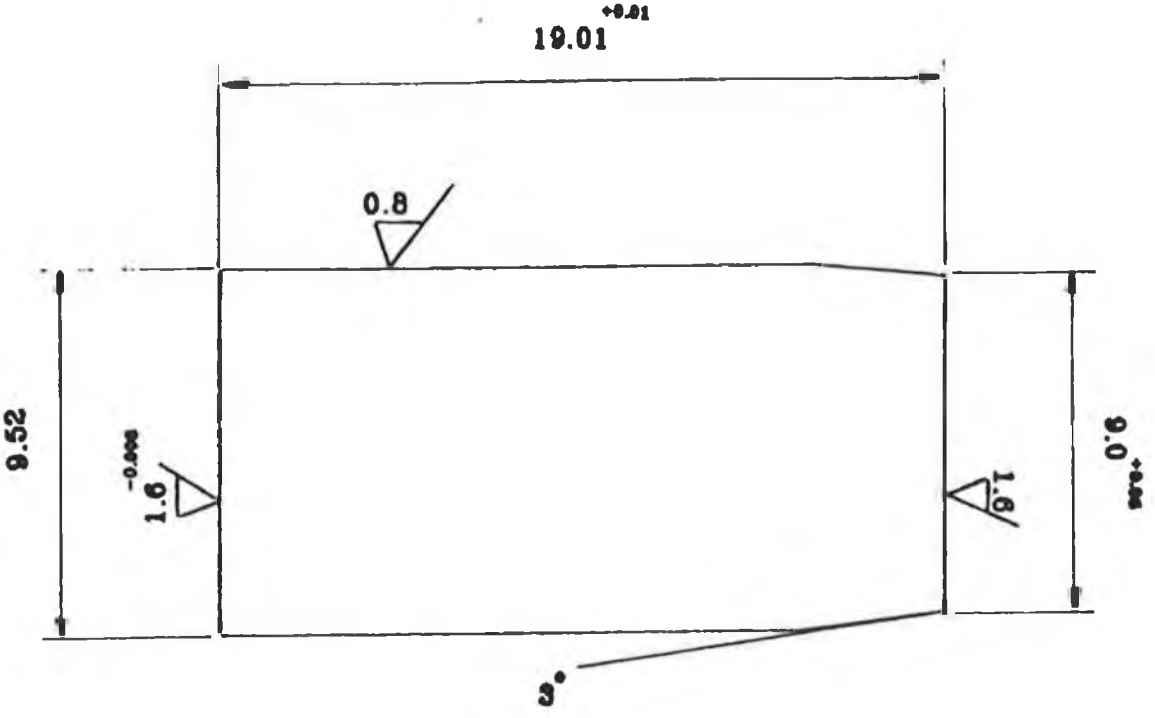

Fig.(3.5) Configuration of the Projectile

3.2.2 Calibration of Air Pressure and Projectile Velocity

The ballistic rig was calibrated to establish the initial relationship between the impact speed and the air pressure for the tool-steel projectile, as shown in Fig.(3.6).The following steps were taken inorder to calibrate the ballistic rig.

1) Adjust the pressure transducer to certain value.

2) Insert the projectile into the slot in the barrel.

3) Put lead specimen on the anvil.

4) Fire the projectile onto the lead specimen.

5) Record the time from the timer.

6) Repeat step [1-5] at the same pressure two times.

7) Take the average of the speed for a certain pressure.

8) Repeat steps [1-7], agaain for different pressures.

From the values of impact speed and pressure, the calibrated chart can be obtained and from this chart, it is easy to select approximate pressure for any intended speed to fire the projectile.

Dynamic Test
Calibration of air-pressure and velocity

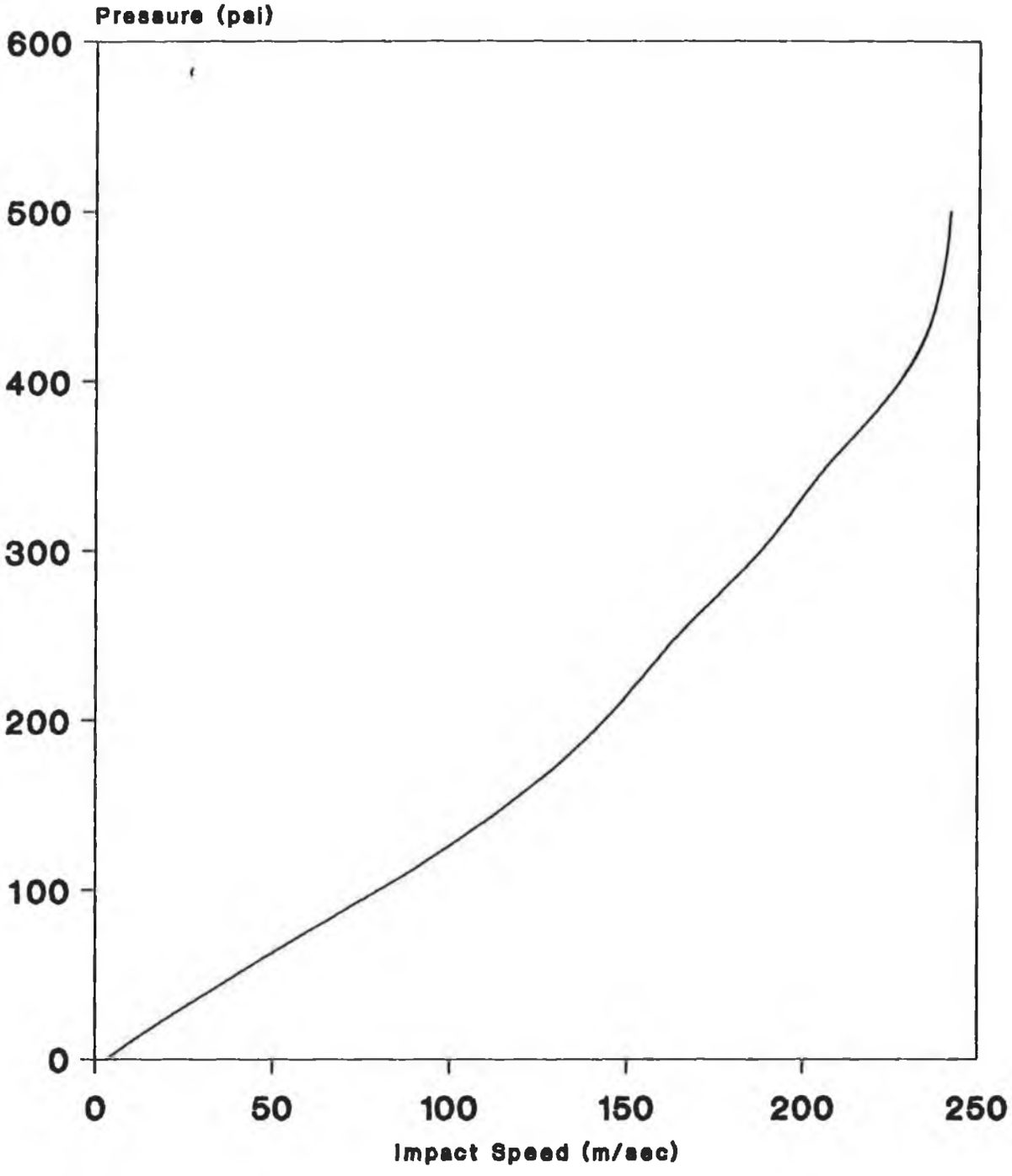

Fig(3.6)

(3) Procedure for the Ballistic Test

After finding the relation between the pressure and the impact speed, a number of preliminary tests were carried out inorder to obtain a suitable speed range for deforming the test-specimen without causing any fracture of the specimen. Before setting the equipment, the whole ballistic rig was checked for horizontal level by means of spirit level inorder to ensuring a perpendicular impact between the projectile and the test specimens. The test procedure may be outlined as follows:

1) Check the laser beam unit to ensure that it is fully operational and that nothing is obstructing the path of the laser, while passing through the suppressor cap to the photo cell.

2) Fill the chamber with air from the air cylinder and record the pressure in the chamber from the pressure transducer.

3) Position the projectile into the slot inside the loading throat, as shown in **Plate [3.3]** and **Plate [3.4]**.

4) Measure the initial height and initial diameter of the test specimen.

5) Put the polythene sheet on the anvil.

6) Lubricate the two faces of the test-specimen with polythene sheet and placed it on the anvil.

7) Fire the projectile by opening the valve, which allows air to escape from the chamber to propel the projectile down the barrel.**Plate [3.5]**.

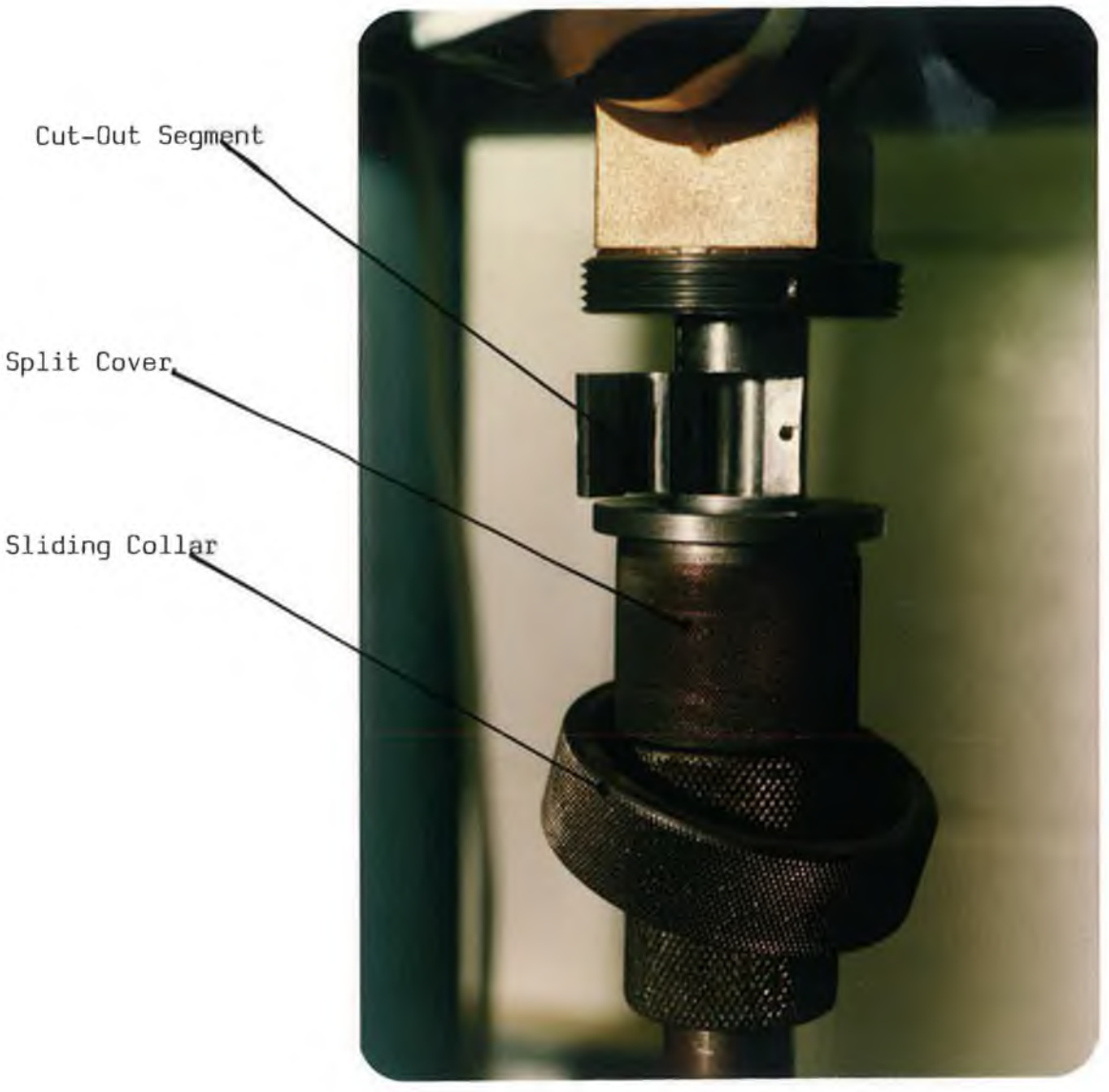

PLATE(3.3) Shows the Position of the Projectile inside the loading throat.

PLATE NO [3.4] Shows the Projectile inside the Slot.

PLATE(3.5) Fire the Projectile aginst the test specimen placed in rigid anvil.

8) Record the time indicated on the timer. When the projectile travels through the barrel at high velocity, it passes through the laser beam, cutting off its path and the resulting signal is recorded in the timer as a travel time, from knowing the length of the projectile and the elapsed time, the impact velocity was calculated.

Impact speed (v)=height of the projectile/time

9) Calculate the initial strain rate from knowing the velocity and initial height of the specimen.

$$\varepsilon = V/h$$

10) Record the final height and final diameter of the specimen as well as the impact speed.

11) Repeat steps [1-10], with two other specimens.

12) Take the average of the impact speeds, strain rate, final height, and final diameter.

13) Repeat steps [1-13], after changing the pressure five times.

During the impact of the tool steel projectile against the test specimen using polythene sheet as the lubricant, (one layer of polythene sheet on each face), it was observed that slight non-homogenuos deformation occurs, as shown in **Plate[3.6]**. This may be due to the fact that the heat rise during deformation is working to brake down the lubricant on the top face. This problem was reduced by **coating** the contact surface of the projectile with Petroleum Jelly and using **two layers of polythene** on

the upper face, and the result of this , is

1) Homogenuos deformation.

and

2) Uniform strain .

Fig.(3.7) and Fig.(3.12) show the variation of the final height and final diameter with impact speed.

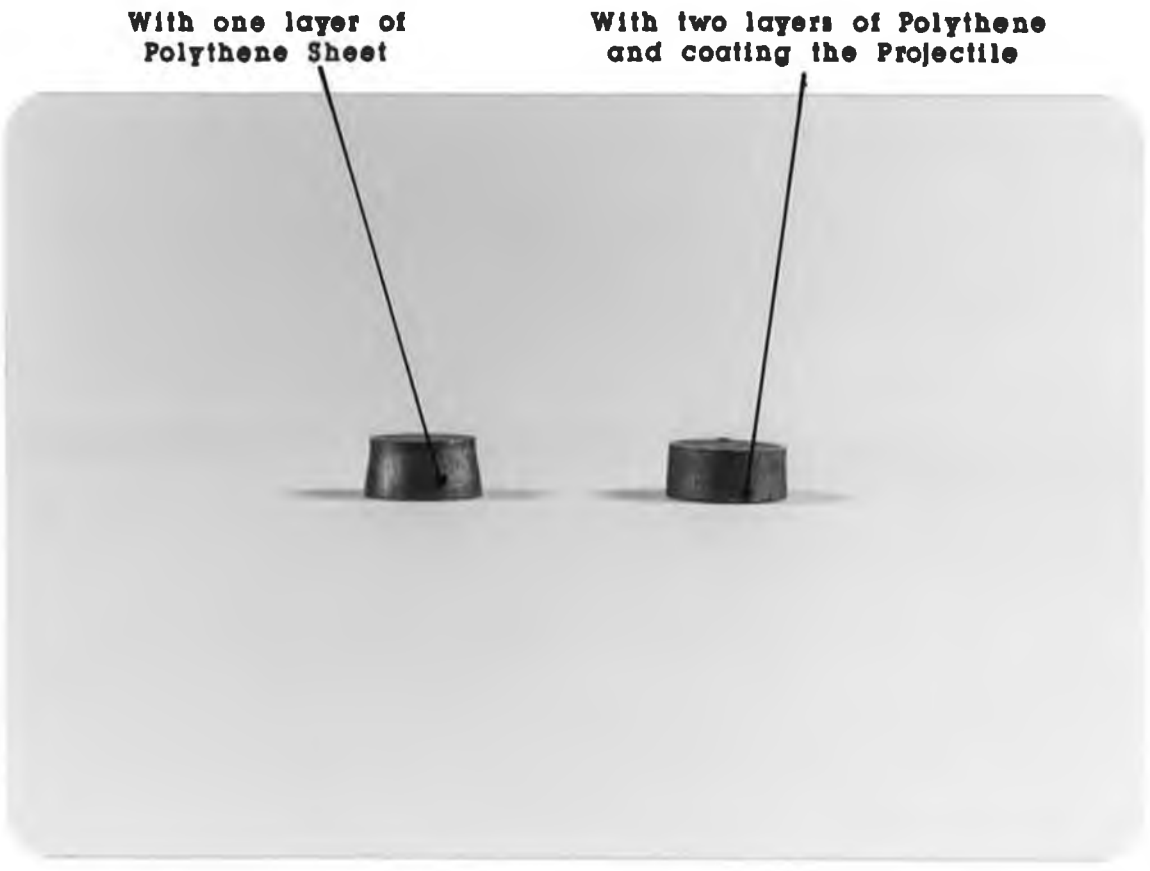

PLATE NO [3.6] EFFECT OF THE FRICTION ON THE FINAL SHAPE OF THE DEFORMED TEST SPECIMEN.

Variations In the Final Height Of Mild-Steel With Impact Speed

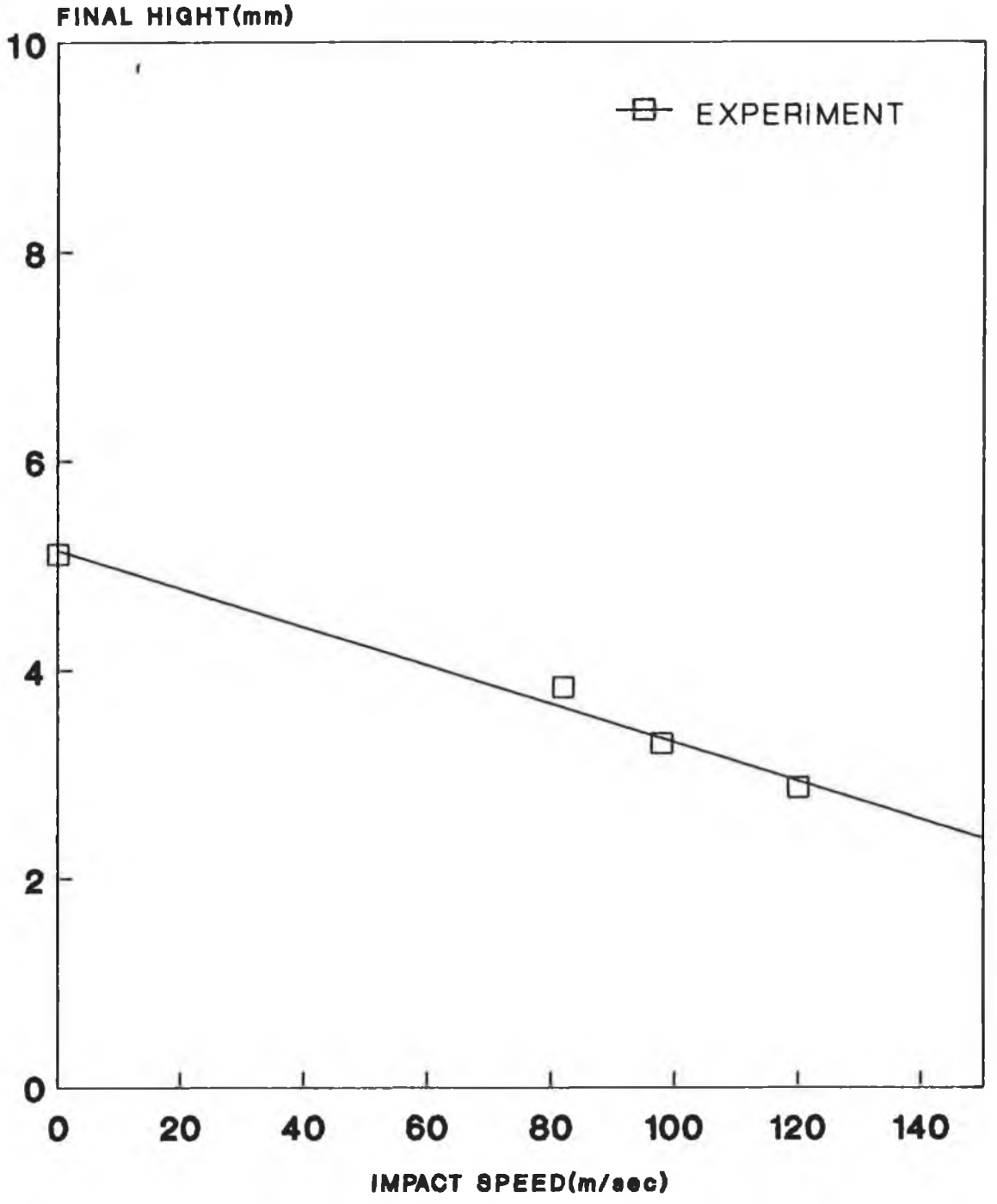

Fig.(3.7)

Variations In the Final Diameter Of Mild-Steel With Impact Speed

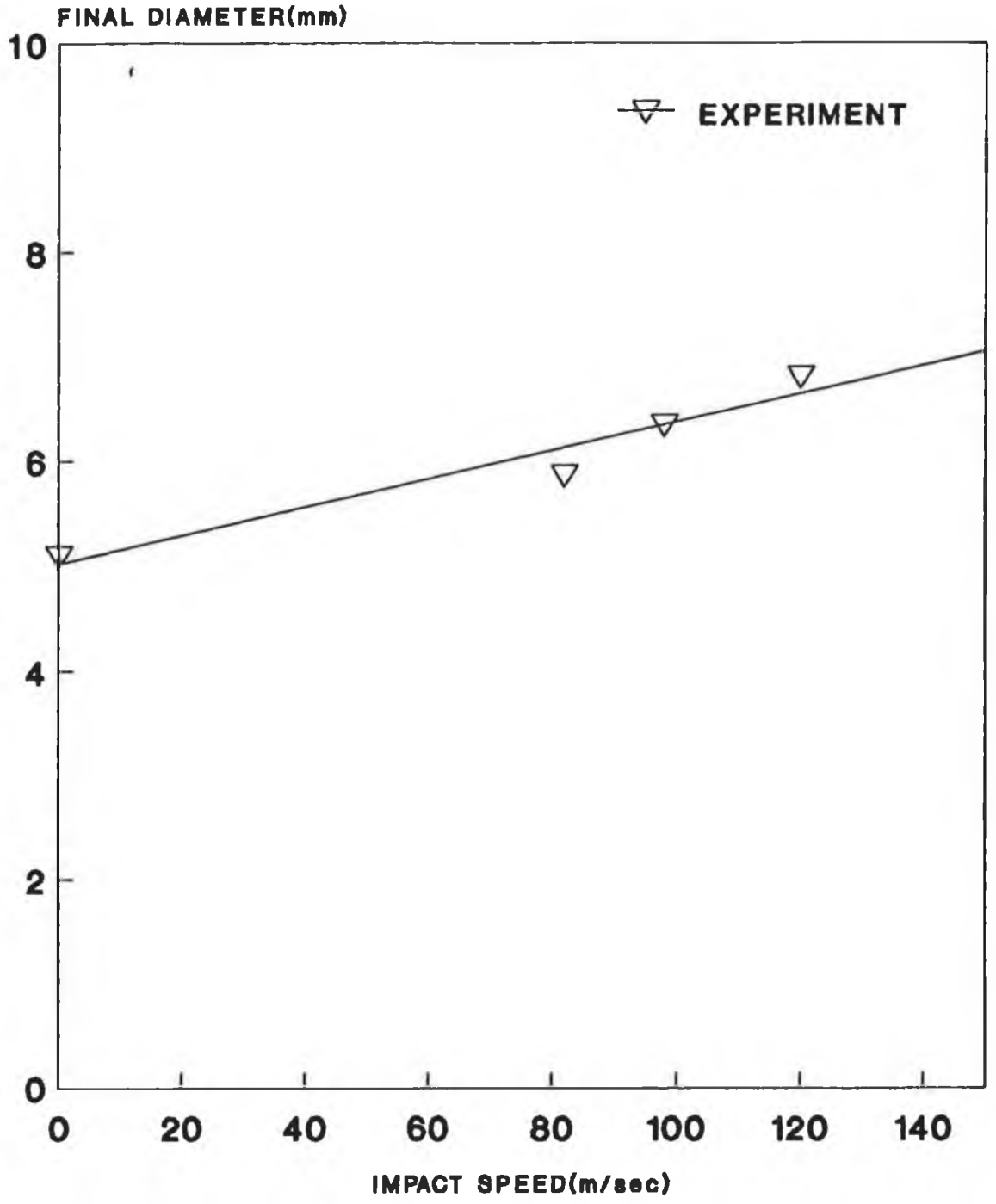

Fig.(3.8)

Variations In the Final Height Of Copper With Impact Speed

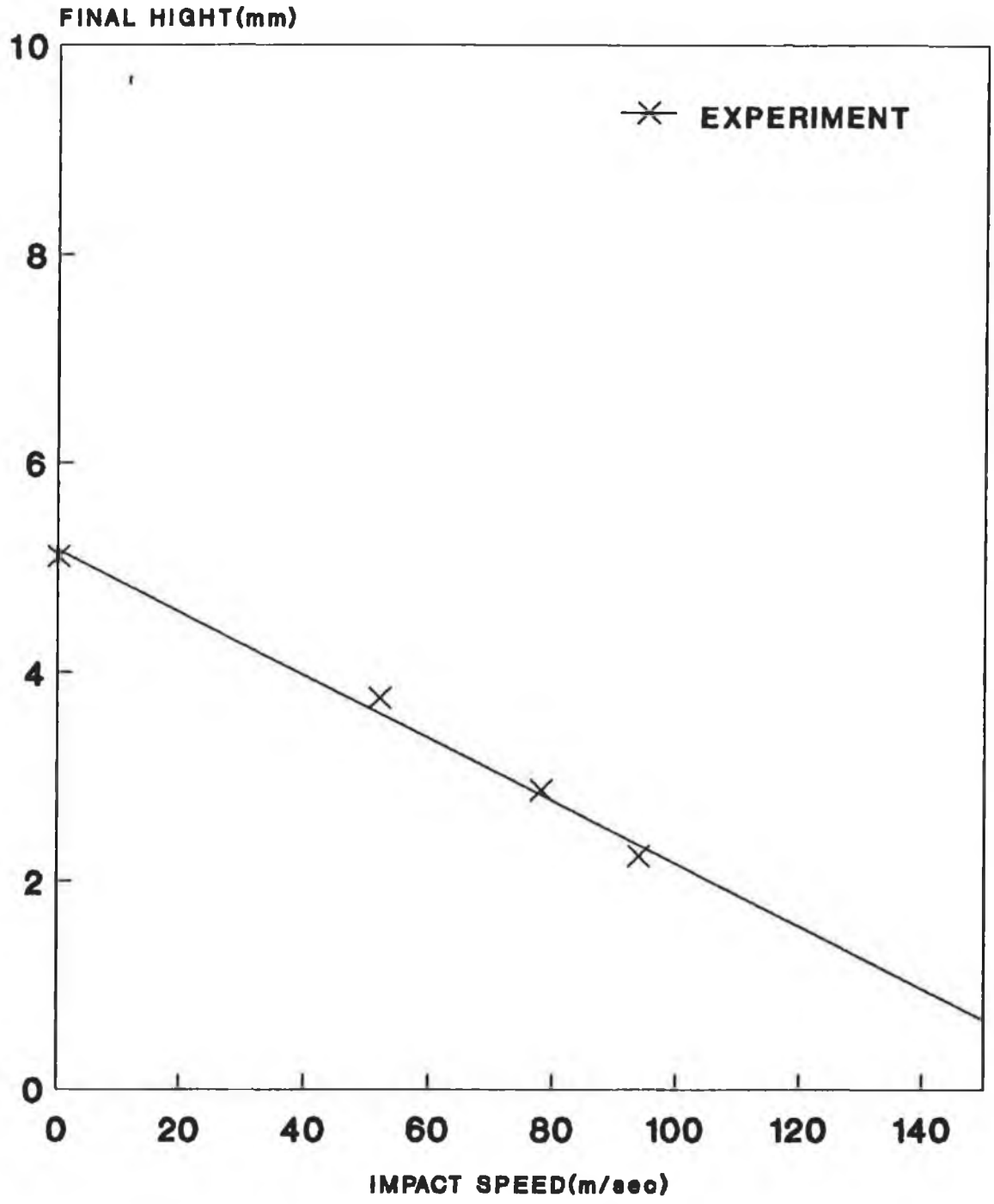

Fig.(3.9)

Variations In the Final Diameter of Copper with Impact Speed

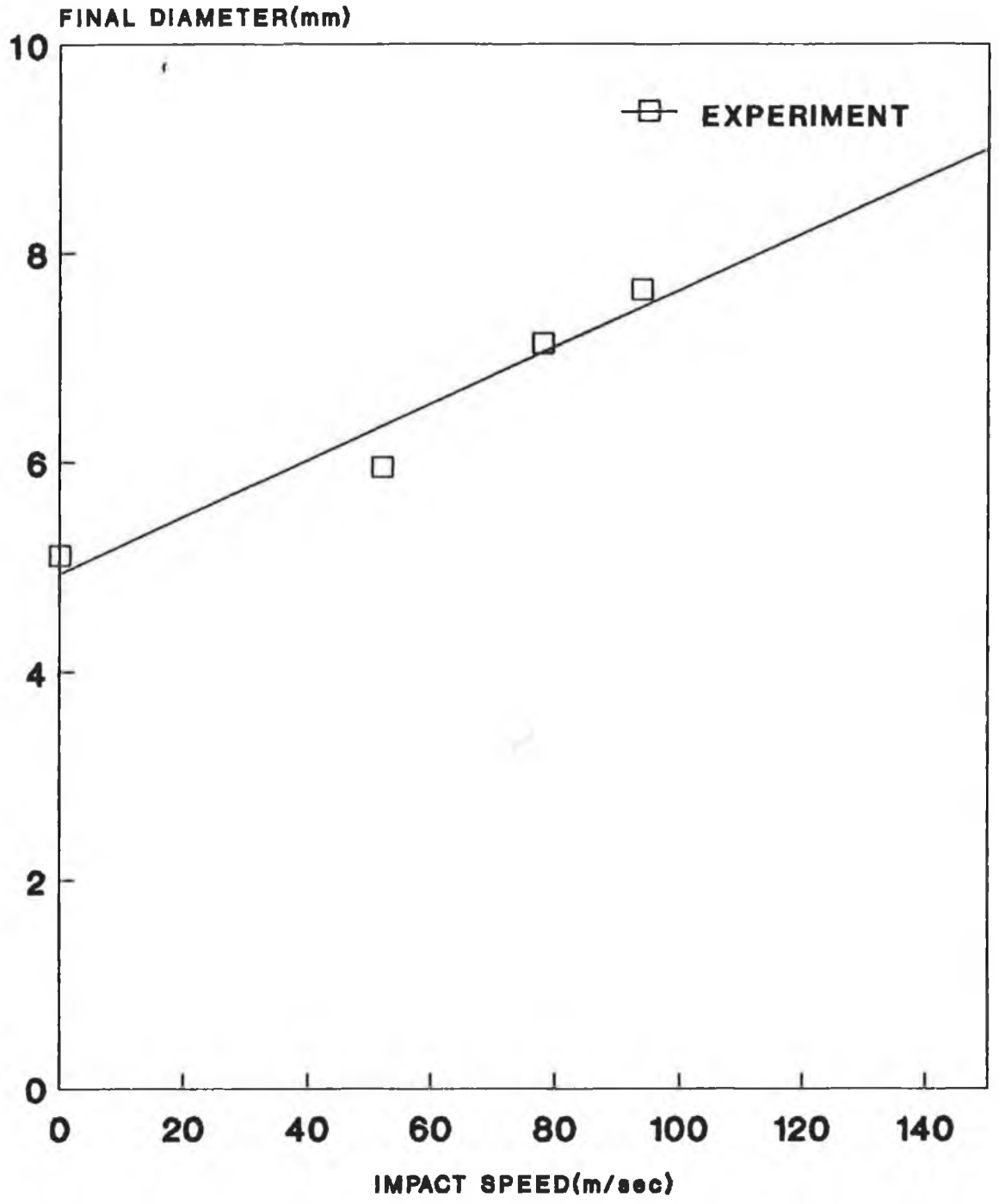

Fig.(3.10)

Variations In the Final Height Of Stainless-Steel With Impact Speed

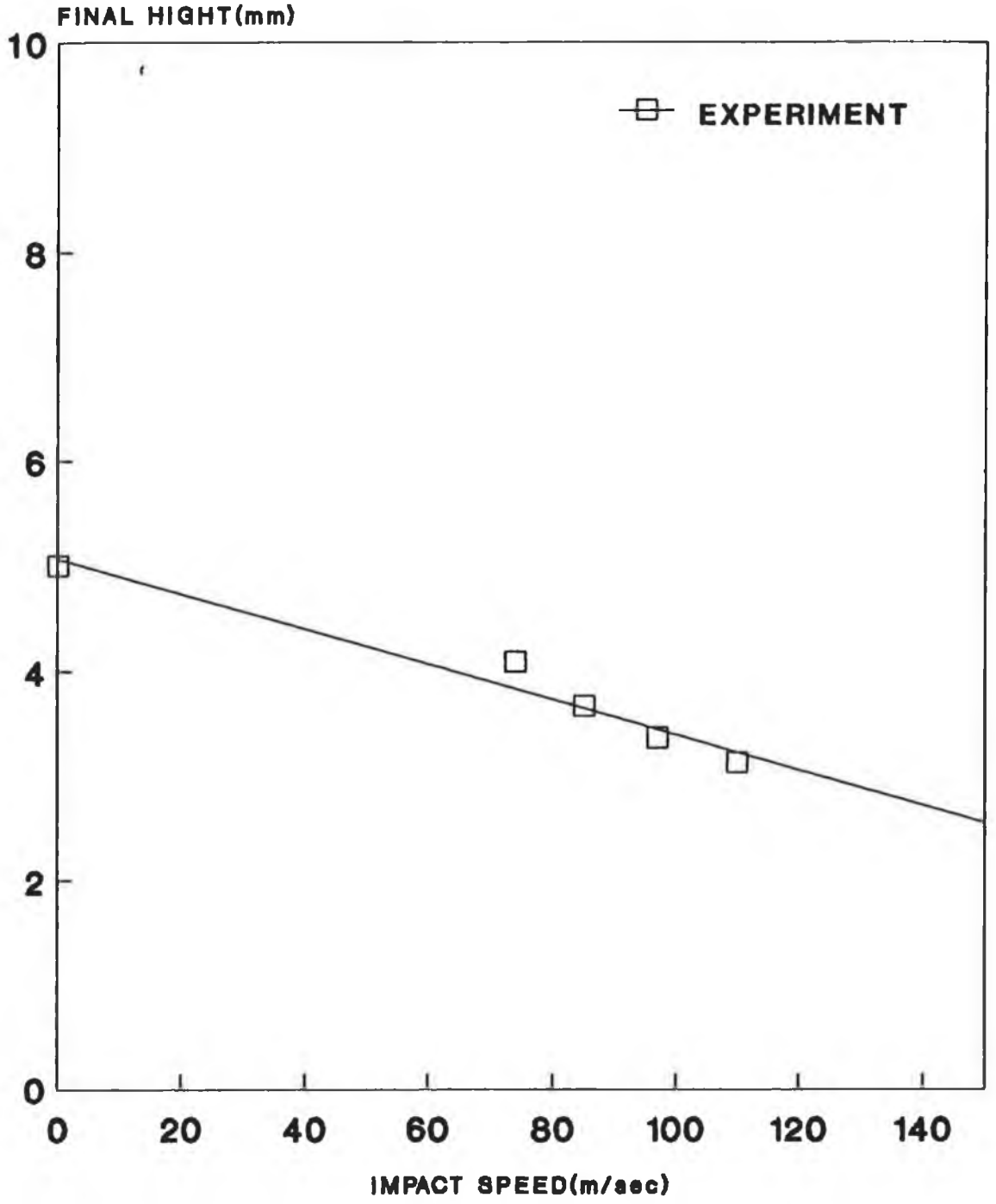

Fig.(3.11)

Variations In the Final Diameter of Stainless-Steel With Impact Speed

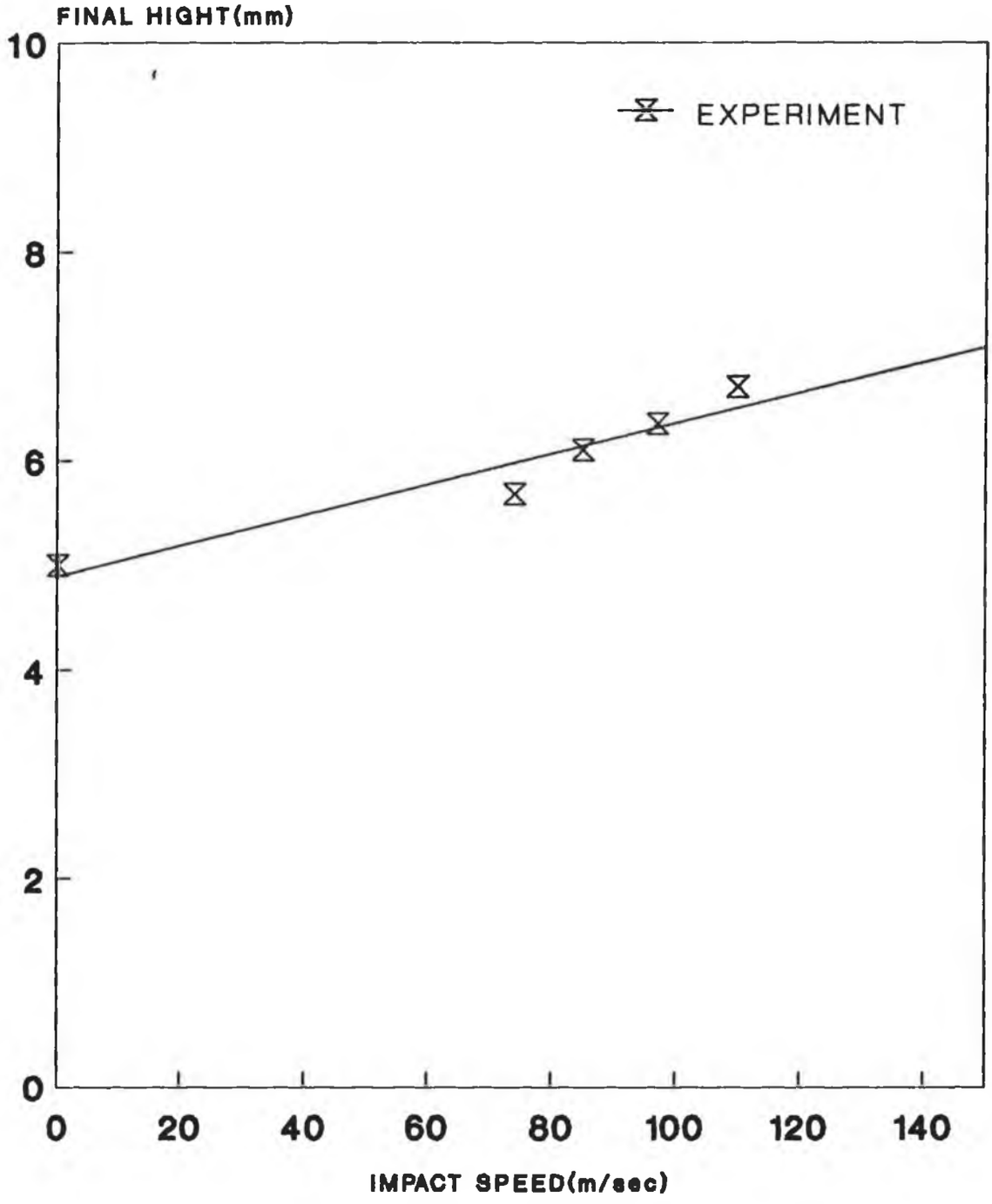

Fig.(3.12)

3.3 HARDNESS TEST

In the present study, only Vicker hardness method was used, due to the very high accuracy of the diamond pyramid form. However inorder to obtain good results the micro-hardness tester **Plate [2.6]**, was isolated from vibration and all the specimens were polished before measuring the hardness in order to find a clear structure. **Plate [3.7]**, shows the specimen used in the hardness test. and **Table [3.3]**, shows the values of the hardness test.

a)Effect of the static deformation on hardness

Copper specimens were deformed statically at different strain levels (four levels of strain were chosen) by using the universal testing machine (INSTRON), and using polythene as the lubricant . To reduce the error, three specimens were used at each strain level and the average of three readings were taken.

The hardness at each strain level was measured at three positions on the polished specimen (side, middle, side) and three specimens of the standard size were used.

Fig.(3.13) shows the variation of hardness value of copper with strain level.

Table (3.3)

NO.	STRAIN LEVEL	HARDNESS VALUE			MEAN
		Corner	Midle	Corner	
1	0.14	116 116	122 135	116 116	120.16
2	0.33	139 125	143 135	135 128	134.26
3	0.91	140 147	160 147	143 143	146.66
4	1.17	160 151	176 160	170 160	162.83

Static Test
Effect of strain level on hardness value

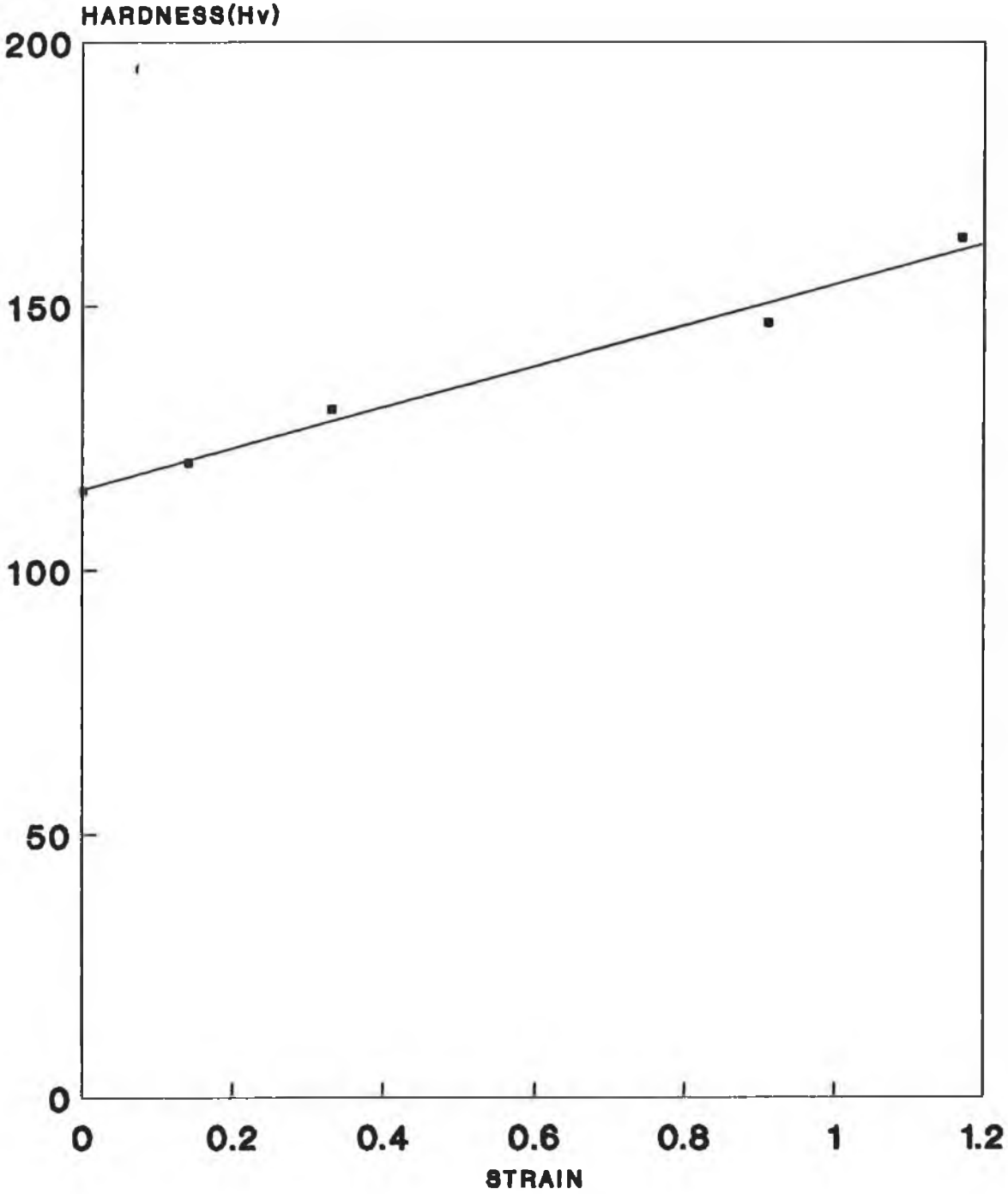

Fig.(3.13)

PLATE(3.7) Shows the Polished Specimens Used to Measure hardness Value for the Copper Specimen.

CHAPTER FOUR

NUMERICAL TECHNIQUE

4.1 Introduction

With the advent of numerical methods in deformation analysis, such as finite difference and finite elements methods **[80,81,82]**, the need for accurate constitutive equations has become more important. In general, a complete material description in-terms of flow stress dependence on temperature, strain, and strain rate is required for these analyses.

Many experimental techniques have been proposed by researchers in the past, to determine stress-strain characteristics of materials at strain rates in excess of 10 per second during deformation. These purely experimental techniques have become more sophisticated and expensive for higher strain rates. In this study the numerical technique used by **Hashmi** and **Thomphson** **[38]**, was modified to incorporate the effect of material inertia, temperature rise during deformation, strain hardening and elastic strain of projectile and anvil.

4.2 FORMULATION

A finite difference numerical technique in conjunction with lumped-mass parameter model was employed to theoretically analyse the deformation of small cylindrical specimens struck by a projectile. A Summary of the important assumptions used in this technique are as follows.

1) The geometry of the actual specimen may be represent with a lumped-mass model, as shown in **Fig.(4.1)** .

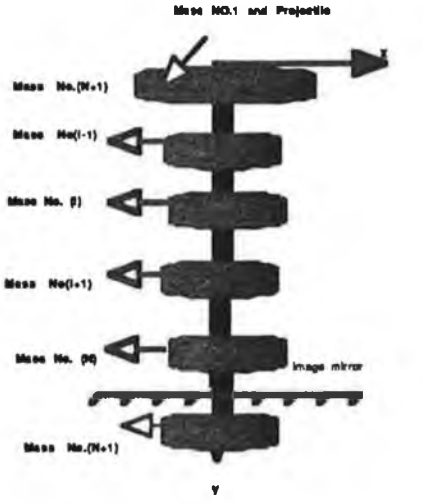

Fig.(4.1) Equivalent Lumped Mass-Model for the Actual Configuration of the Specimen.

This, model simplifies the actual specimen into a mass-link system. The mass of each small element of the specimen is represented by a concentrated disc mass connected to other masses by light links which transmit axial force and strain, the links are assumed to have the same strength properties as that of the actual specimen.

2) The change of density of the specimen during deformation is negligible.

3) The effect of gravity force can be ignored.

4) The impact surface of the projectile and anvil are consider to be rigid body, due to high resistance material"Tool Steel".This assumption is applicable only for case(i), in which the specimen only is represented by lumped mass-model.

5) The deformation is homogenuos, shearing does not take place between the layers of the specimen.

6) Uniform strain occurs in each individual link.

7) Uniform stress distributed along the cross-section of the specimen.

8) Radial expansion of each link is covered by the condition of volume constancy.

The procedure amounts to expressing the dynamic force equilibrium equation for each concentrated mass disc in finite difference form and relating the displacement of each mass disc to the strain in the corresponding link after each time increment. The stress in each link, and hence the axial forces are then determined.

4.2.1 Analysis

The analysis is based on one dimensional axial stress propagation. Using a lagrangian coordinate system with the x-axis vertical to the specimen axis as shown in **Fig.(4.1)**.

Equation of Motion

The general equation of motion for an element of the specimen , soon after impact , can be derived by considering the internal and inertia forces acting on the element and is given by,

$$\partial N/\partial s = M\ddot{u} \qquad (4.1)^1$$

Equation (4.1) may be written in finite-difference form and the resulting equation applies to the lumped masses.**Fig.(4.2)** shows the force acting on the link.

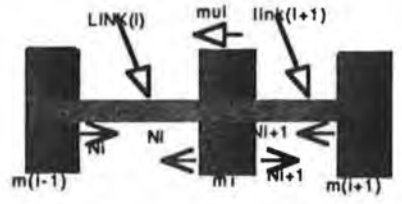

Fig.(4.2) Force Acting on Disc and Lumped Model

The finite-difference equation for the concentrated disc at the I_{th} location of the model is given by,

$$N_{I+1} - N_I - \Delta s_o M.\ddot{u}_{I,j} = 0 \qquad (4.2)$$

---

1 The Equations From (4.1) to (4.13) are According to Reference [38]

Equation (4.2) applies to all the masses in the specimen and gives the instantaneous values of $u_{i,j}$ for any time t_j when coupled with the following relationship between acceleration and displacement in finite difference notation;

$$u_{i,j+1} = \ddot{u}_{i,j} (\delta t)^2 + 2u_{i,j} - u_{i,j-1} \qquad (4.3)$$

The time increment δt is defined by,

$$\delta t = t_{j+1} - t_j \qquad (4.4)$$

Strain and Strain Rate

The difference in displacement of an element between i_{th} and $i+1_{th}$ location may be expressed by,

$$\Delta\Delta s_{i,j+1} = u_{i,j} - u_{i+1,j+1} \qquad (4.5)$$

and the change in length of the link $\delta(\Delta s)_{i,j+1}$ occurring during the time interval δt is given by,

$$\delta(\Delta s)_{i,j+1} = \Delta s_{i,j} + \Delta\Delta s_{i,j+1} \qquad (4.6)$$

Then the strain increment and strain rate occurring in each link during the time interval is given by;

$$\delta\varepsilon_{l,j+1} = \text{Ln}\,[\delta(\Delta s)_{l,j+1}/\Delta s_{l,j+1}] \qquad (4.7)$$

and

$$\dot{\varepsilon}_{l,j}=\delta\varepsilon_{l,j+1}/\delta t \qquad (4.8)$$

Stress and Force

The stress in the element is determined from the strain, strain rate, internal energy and material property. Since the strain and strain rate are constant within the element, the stress is also constant. The stress is obtained by using the appropriate constitutive equation given by,

$$\sigma_{l,j+1}= f(\varepsilon, \dot{\varepsilon}, T) \qquad (4.9)$$

In order to facilitate the calculation of stress which, due to friction and inertia effect, may vary across the cross section of the specimen, it is necessary to idealize the actual cross section to an equivalent cross section model which consists of a number of layers across each of which

the stress is assumed to uniform. The circular cross section of the specimen is assumed to consist of **n** discrete layers of material which can carry normal stresses. These layers are considered to be separated by a material which can not carry any normal stress but has infinite shear rigidity.

In order to describe the elastic-plastic stress state in a layer of the section-model, further idealization is made and each layer is assumed to consist of sublayers, which are assumed to be made up from constituent material with similar elastic-perfect plastic material properties.The number of such sublayers is determined by the number of positive sloped sides in the approximated stress-strain diagram shown in **Fig.(4.3).**

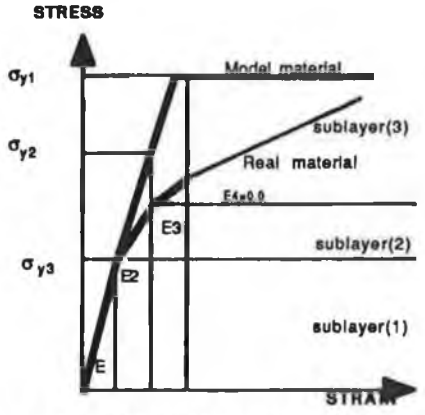

Fig..(4.3) POLYGONAL STRESS-STRAIN CURVE

The yield stress of each of this sub-layers is given by the product of the elastic modulus and the corresponding strain levels of the polygonal stress-strain curve.

$$\sigma_{y_1} = E_1.\varepsilon_1 \quad \sigma_{y_2} = E_2.\varepsilon_2 \quad \sigma_{y_3} = E_3.\varepsilon_3 \qquad (4.10)$$

This idealization permits stress computation and unloading following elastic path.The cross sectional area of each sub-layer is given by;

$$A_{L1} = A(E_1 - E_2)/E_1$$
$$A_{L2} = A(E_2 - E_3)/E_1 \qquad (4.11)$$
$$A_{L3} = A(E_3 - E_4)/E_1$$

where

E_1 Elastic modulus.

A Area of the layer in the link.

L Refers to the sub-layer .

The stress in the link is then simply given by;

$$\sigma_{l,j+1} = (A_{L1} . \sigma_{y_1} + A_{L2} . \sigma_{y_2} + A_{L3} . \sigma_{y_3}) \qquad (4.12)$$

And hence the axial force in link i is given by;

$$N_{l,j+1} = A_{l,j+1} . \sigma_{l,j+1} \qquad (4.13)$$

Time Interval

In the existing form,when using the present numerical technique, the time increment can not be chosen arbitrarily. The value of the time increment should be less than the time needed for the elastic wave to propagate through the length of the link.

At the instant the projectile touches the top surface of the test specimen, an elastic wave will propagate at speed C_e ,given by the following equation;

$$C_e = (E/\rho)^{1/2} \qquad (4.14)^2$$

where

E is elastic modulus.

ρ is density.

The time taken for elastic wave to propagate is given by;

$$\Delta t = (\Delta s_o / C_e) \qquad (4.15)$$

Where

Δs_o Initial link length.

C_e Elastic wave speed.

---

[2] All the Equations used to Calculate the Time Interval are According to Reference [84].

Static Stress-Strain Properties

The static stress-strain behaviour has been determined under uniaxial compression test, to obtain the static characteristics in terms of stress-strain curves. These curves can usually be approximated with a number of straight lines in the plastic region and always one line in the elastic region, In this analysis, two straight lines have been used to represent the plastic region. as shown in Fig.(4.3).

Inertia effect

To enable the stress and strain properties to be determined accurately appropriate for the investigation of the strain rate effect, it can be realized from the early work [57,59], that further corrections are required to separate the behaviour of the material from inertia and friction contributions. These effects are always present although they can be minimized by careful design of the experiment.

It is now well accepted that, during a high speed compression test, in addition to axial particle velocity, the radial and tangential particle velocities of the specimen material may achieve high values. As a result the specimen requires higher stress to deform. For heavier material and larger specimens this stress enhancement can be considerable. For smaller specimens and lighter material, these effect are often demonstrated to be negligible [56].

In this study, when the test specimen is subjected to fast dynamic compression between the rigid surfaces of the projectile and anvil, the inertia force would be present and plastic yielding might be affected. It is thus necessary to make a moderately accurate assessment of their effect, to obtain a better constitutive equation.The analysis developed by **Slater[83]** was used in this study to assess the inertia effect during deformation.

$$\sigma_{ml} = \sigma_l \left[1+(3/16)\rho(V^2/\sigma_l)(r/h)\right] \qquad (4.16)$$

where

- **r** current radius.
- **h** current hight.
- ρ density.
- **V** impact speed.
- σ_l current flow stress[3].

[3] l Refer to the Number of the Link.

friction effect

The radial constraint of the specimen caused by friction at the interface is considered to be a major problem in metal working operations and must be controlled adequately to optimize processing procedures for the economical production of components.

The longitudinal stresses required to deform the material is increased by the radial stress according to Von-Mises yield criteria;

$$\sigma_z - \sigma_r = \sigma_y \qquad (4.17)$$

where

σ_z Longitudinal stress.

σ_r Radial stress.

σ_y Yield stress.

In this study, polythene sheet was used on the two faces of the specimen, and the contact face of the projectile was coated with Petroleum Jelly. It was found that, the deformation is homogenuos, and there was no need to incorporate the friction effect (μ=0.0).

Effect of stress wave

Many theories have been proposed, to study the effect of elastic and plastic waves during the deformation processes[84]. Slater[83] reported that, for velocities in excess of about (300m/sec), elastic and plastic waves may propagate which are able to travel up and down the specimen several times during the deformation. The travel of these waves, can cause variation on the axial force at the upper and lower plates. Since the impact velocities for the tests conducted in this study are in the of range (50-250m/sec). Therefore, the effect of stress waves in the specimen should be insignificant and has not been taken into account in the numerical analysis in any explicit manner.The technique itself accounts implicitly for the stress fronts which propagate up and down the specimen (for rigid projectile and anvil) and also through the projectile , specimen and the anvil (for elastic projectile and anvil).

4.2.2 Condition to Terminate the Simulation of the deformation for a Velocity.

From known initial and final dimensions of the specimen together with the mass and impact velocity of the projectile, the deformation was simulated using finite difference techniques and based on the assumed constitutive equation . To ascertain the end of this deformation , three boundary conditions were suggested;

1) When the projectile rebounds (contact force between the projectile and specimen becomes zero or positive). as shown in **Fig.(4.5a)**.

2) When the remaining kinetic energy at time(t_j) becomes equal or greater than the kinetic energy at time(t_{j+1}). as shown in **Fig.(4.5b)**.

3) When the position of mass No.(2) at time (t_{j+1}) does not change or the direction of movement changes from that at time (t_j).

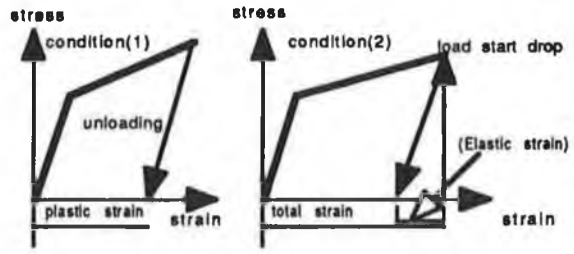

Fig.(4.5) Condition to Terminate the Simulation

The difference between condition(1) and (2) is simply that in (1) the specimen has recovered the elastic strain after deformation, where as in condition (2) the computation is stopped before any elastic recovery takes place. Since the measued final height is obtained after the elastic recovery it is more logical to use condition (1).

4.3 Effect of Elastic Deformation of the Projectile and the Anvil

To study the effect of elastic deformation of the projectile and anvil, due to stress propagation the whole system was represented by lumped mass model as shown in **Fig.(4.4)**.

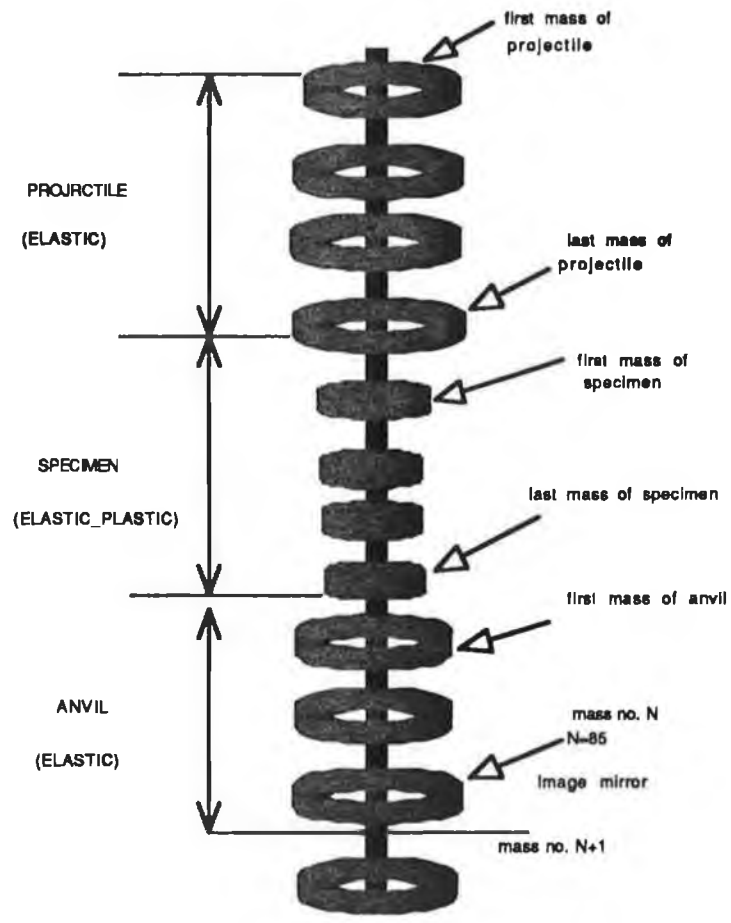

Fig.(4.4)Projectile, Specimen and Anvil in Lumped Mass Model.

The dimension of the projectile is as in the experiment, where the length is four times longer than the specimen length and the diameter is two times bigger than the specimen diameter. It was not found necessary to consider the whole length of the anvil used in the experiment[4],

[4] Different lengths (Number of Masses) of the anvil was tried and no significant effect was obsoerved.

therefore, the anvil is assumed (five times longer than the specimen length), and the diameter (two times bigger than the specimen diameter). The numerical procedure discussed previously has been used to calculate the stress, strain, strain rate and the elastic deformation on the anvil and projectile.

The boundary condition for this new condition is changed, where the projectile and the anvil deforms only elastically due to there high yield stresses, and the specimen deforms both elastically and plastically. The last link of the projectile is in contact with the first mass of the specimen and the last link of the specimen is in contact with the first mass of the anvil.

4.4 CONSTITUTIVE EQUATION

The flow stress of the material is influenced by,

1) Factors unrelated to deformation process, such as chemical composition, metallurgical structure and grain size.

2) Factors related to deformation process, such as temperature, degree of deformation (strain) and rate of deformation (strain rate).

Thus, the flow stress (σ), can be expressed as a function of temperature(T), strain (ε) and strain rate($\dot{\varepsilon}$);

$$\sigma_{i,j+1} = f(\varepsilon, \dot{\varepsilon}, T) \qquad (4.9)$$

The mathematical description of the relationship between the stress,strain and their time derivation is referred to as the constitutive equation.Such constitutive equations are of much current interest, especially in terms of high temperature and high impact speed.

From the time of earliest experimental attempts, various forms of constitutive equations have been proposed to describe the dynamic behaviour of the material, the most commonly used form of the rate dependent theory , was proposed by **Malvern [85] (1951)**. He proposed stress, strain, strain rate law to model the dynamic behaviour of material of the form;

$$\sigma = f(\varepsilon) + a \ln(1+b.\dot{\varepsilon}_p) \qquad (4.18)^5$$

where

$f(\varepsilon)$ is the static stress.

$\dot{\varepsilon}_p$ is the plastic strain rate.

a,b are the physical parameters.

and the most general form of the stress function;

$$E\dot{\varepsilon} = \dot{\sigma} + g(\sigma, \varepsilon) \qquad (4.19)$$

where

$\dot{\sigma}$ The elastic strain rate.

g Strain rate dependency.

Although various number of constitutive equations have been proposed by a number of researchers [86-87], there appears to be no universally accepted single law.

[5] Equation (4.18) and Equation (4.19) are According to Reference[85].

4.4.2 Proposed Equation

In this study, a new constitutive equation has been suggested, with reference to the static stress-strain properties.

$$\sigma_d = K\varepsilon^n [1+ (m\dot{\varepsilon})^p] \qquad (4.20)$$

where

K	Strength coefficient constant.
ε	Natural strain.
n	Strain hardening index.
$\dot{\varepsilon}$	Strain rate [1/sec].
m and p	Material constants.

This equation is chosen due to its simplicity and the availability of relevant data. One of the limitations of this equation is that it does not cater for any change in overal shape of the static stress-strain curve, but simply shifts it vertically with increasing strain rate.

When this equation incorporated in the simulation using the numerical technique on a **PC** computer, this simulation of the deformation allowed the prediction of the material constants **m** and **P**. The first step in determining the constitutive equation is to derive the constants **k** and **n** in the static part. The value of "**k**" is derived from the static stress-strain curve at natural strain equal to unity, and the constant "**n**" is determined by trial and error until close fit of the quasi-static curve was obtained.

Effect of thermal softening on strain hardening

The energy consumed during the plastic deformation is converted into heat, while only a small proportion of that energy is used in distorting the crystal structure of the material.

In this investigation, the temperature rise (ΔT) during deformation was estimated by considering the plastic work done according to **Holzer and Brown[55]** as,

$$\Delta T = {}^{f}/(\rho\, s) \int_{0}^{\varepsilon_f} \sigma\, \delta\varepsilon \qquad (4.21)$$

where **f** is the portion of the work of deformation appearing as heat, ρ is the density, **s** is the specific heat[6]. **Bishop[88]**, reported that the value of (**f**) for steel and copper is 0.865 and 0.92 respectively.

It was thought to be important to include the temperature effect in this study.

The general equation for all the materials was established as.

$$G = (T_O/T)^{\theta} \qquad (4.22a)$$

$$G_1 = (T_O/T)^{\theta_1} \qquad (4.22b)$$

This equation is established from the stress-strain curves at high temperature,and was found to give good agreement with those in **Ref.[34]**, and the values of (θ) and ($\theta 1$) are depended on the material[7].

[6] The Values of ρ and **s** are Given in Table[5.2] in Chapter Five.

[7] The values of θ and θ_1 are Given in Table[5.3] in Chapter Five.

Equation (4.20) is thus modified to incorporate the effect of temperature rise during deformation by introducing the factor "G", so that

$$\sigma_d = K\, G_1 \varepsilon^{nG} [1 + (m\dot{\varepsilon})^p] \qquad (4.23)$$

where

- **G** Thermal softening effect on strain hardening factor .
- **G_1** Thermal softening effect on strength coefficient factor .
- **θ** Material constant.
- **θ_1** Material constant.
- **T** Adiabtic temperature rise (k).
- **T_o** Test temperature (k).

Effect of strain rate on strain hardening

Equation (4.20) has also been modified to incorporate the effect of strain rate on strain hardening, as

$$\sigma_d = K\varepsilon^{n/R}[1+ (m\dot{\varepsilon})^p] \quad (4.24)$$

where

$$R=[\ln(\dot{\varepsilon}/\dot{\varepsilon}_o)+1]^{\beta} \quad (4.25)$$

$\dot{\varepsilon}$ strain rate.

$\dot{\varepsilon}_o$ strain rate constant (1 per second).

β constant (equal to 0.28) [8].

Effect of strain rate and temperature on strain hardening

Equation (4.20), modified to incorporate effects of both the strain rate and the thermal softening on strain hardening then becomes,

$$\sigma_d = KG1\varepsilon^{n\alpha}[1+ (m\dot{\varepsilon})^p] \quad (4.26)$$

where

$$\alpha = (G/R) \quad (4.27)$$

G thermal softening factor.

R strain rate effect on hardening factor.

[8] The Value of β established from Reference [89].

CHAPTER FIVE

THEORETICAL RESULT AND DISCUSSION

Section(A)

Introduction

Having described the steps to calculate strain, strain rate, stress and estimating the inertia corrections, the final stage was to combine these steps to determine the force in each link. The changing area of the specimen is taken into account assuming constant volume, so that the longitudinal strain is related to the area strain. The dynamic true stress is therefore obtained as:

$$\sigma_d = K\varepsilon^n [1 + (m\dot{\varepsilon})^p] \qquad (4.20)^1$$

When equation (4.20) is incorporated into the numerical technique. It provides prediction of the final dimensions of the specimen at a given impact speed and for known values of the strain rate sensitivity constants m and P.

[1] All the Equations are Previously Described in Chapter Four, Also the Sequences of the Equation are According to Chapter Four.

The first step in determining the material constants m and P involves assumption of arbitrary values of these parameters. The final dimensions were then predicted theoretically in terms of final height and final diameter at a given speed. The next step is to fix the value of (m) and change the value of (P) iteratively for a closer agreement between the theoretical and experimental results at a selected velocity. If the agreement is not close then the value of (m) is than changed again and the value of (P) is changed iteratively.This process is repeated until a very close agreement between the theoretical and experimental results is achived. Then the same values of (m and P) were used to predict the final dimension of the specimen at several velocities, if the same agreement were achieved then, these values were accepted as the material strain rate sensitivity constant. The selection of the velocities should cover a large range of strain rate (10^2 - 10^5 per second).

The best fit constants for the material investigated in this work are as following;

Table[5.1]

MATERIAL	m(sec.)	P	n	K(MPa)
MILD-STEEL	0.333	0.0350	0.115	750
COPPER	0.0024	0.0400	0.07	350
STAINLESS-STEEL	0.004	0.0080	0.102	1040

Figs.(5.1)to(5.6) show the experimentally obtained lines (which are the mean of a series result presented in chapter 3) together with lines obtained by changing the value of m and P. These figures also show the variation of final height and diameter for different values of (P). It can be seen from these figures that, increasing the value of (P) will lead to the increase in the predicted final height. Three combinations of (P) at the same value of (m) were used for each material. It is essential to state that these values of P and m give the best matching between the experimental and theoretical result for final height and final diameter against impact speed lines. A better fit than this can not be achieved for say the final height line without worsening the fit for the final diameter line.

Figs.(5.7)and(5.8) show the variation of final height and diameter for different boundary conditions for terminating the simulation of the deformation of mild-steel specimens. These figures show that, no significant variation between the result under the three conditions were found. Finally, no significant effect on the values of **m** and **P** were found when the three condition were used, and the value of **m** and **P** reported here are based on condition (1) (contact force equal to zero).

Variations in the final height of Mild-steel with impact speed

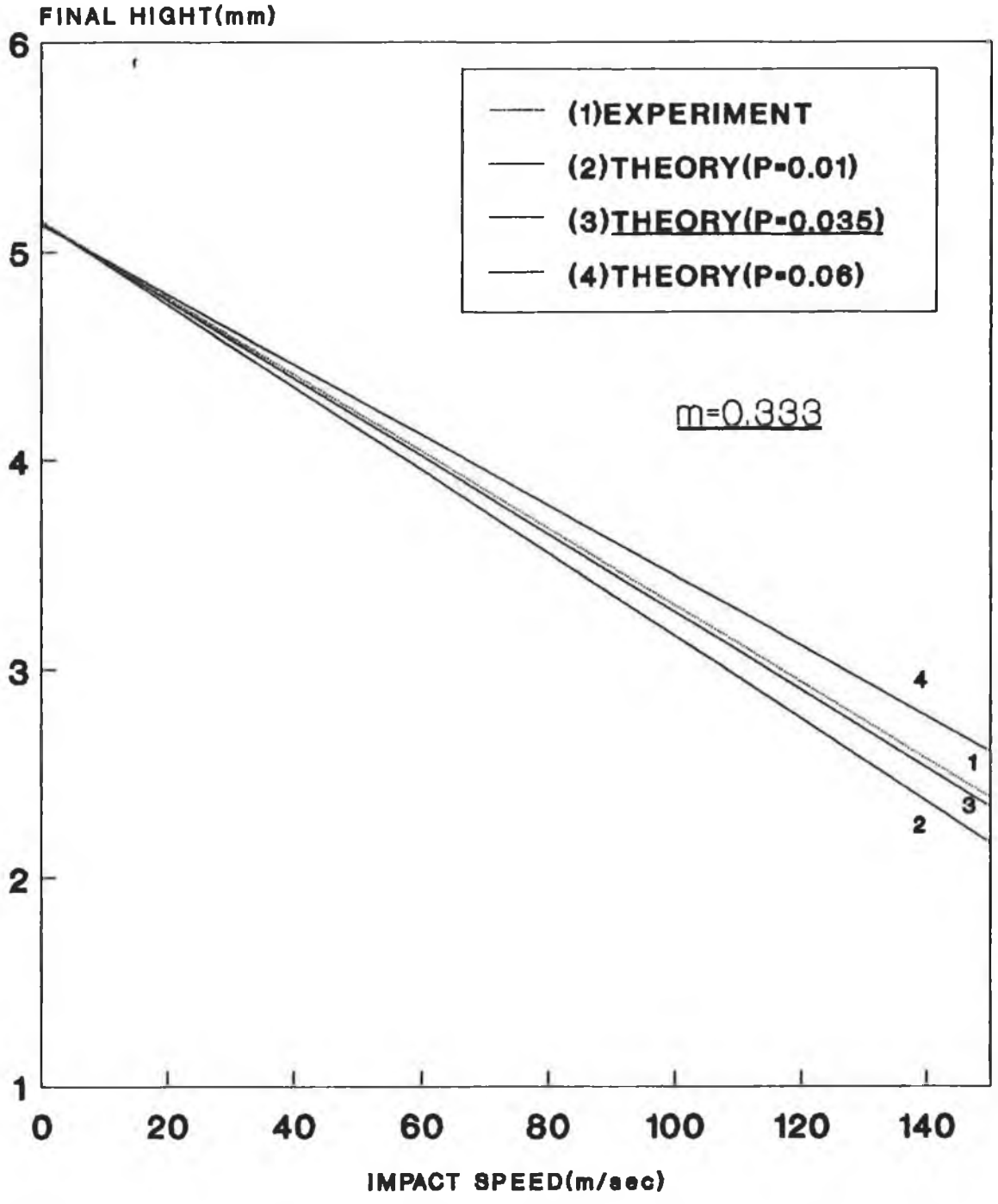

Fig.(5.1)

Variations in the final diameter of Mild-steel with impact speed

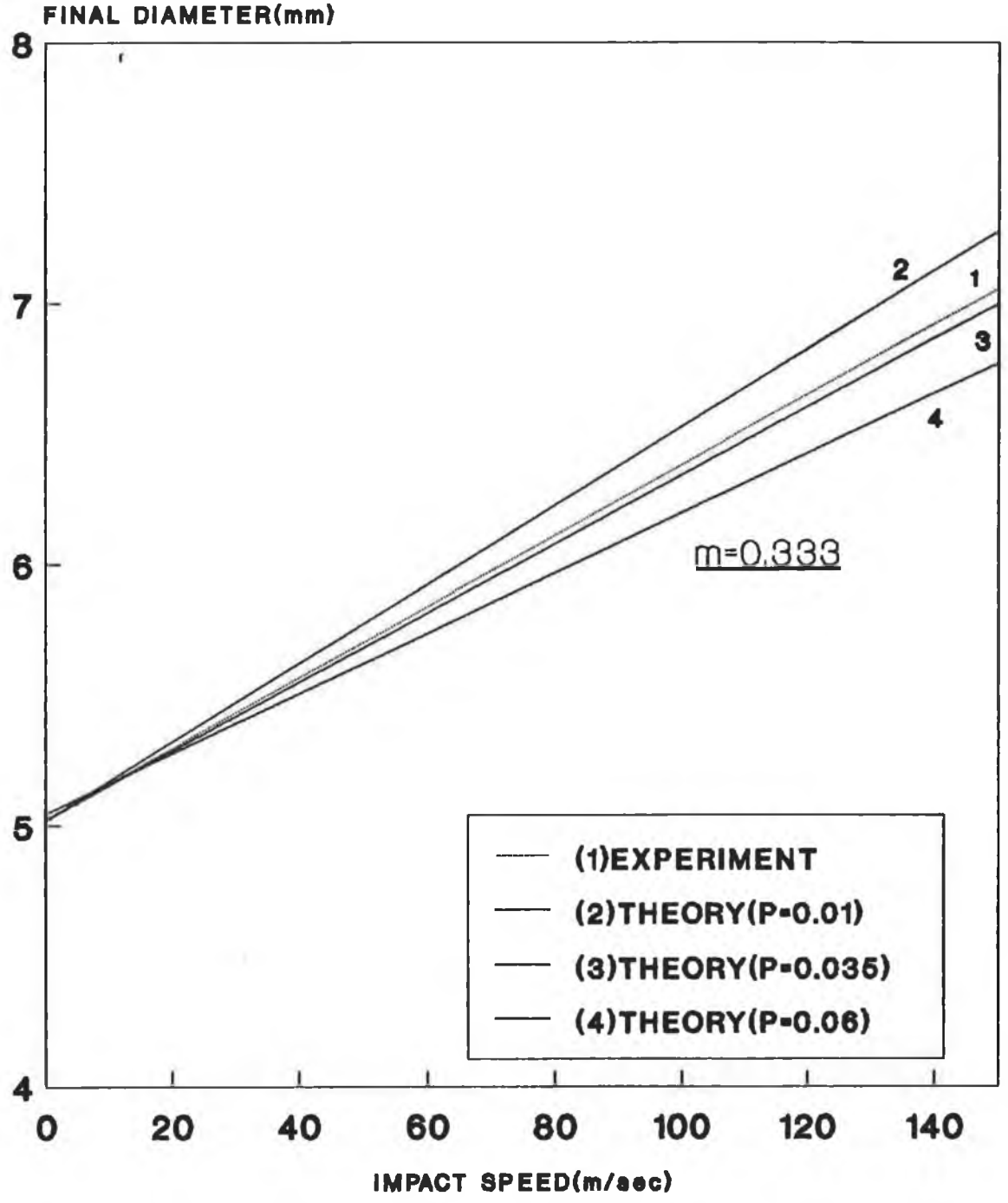

Fig.(5.2)

Variations in the final height of Copper with impact speed

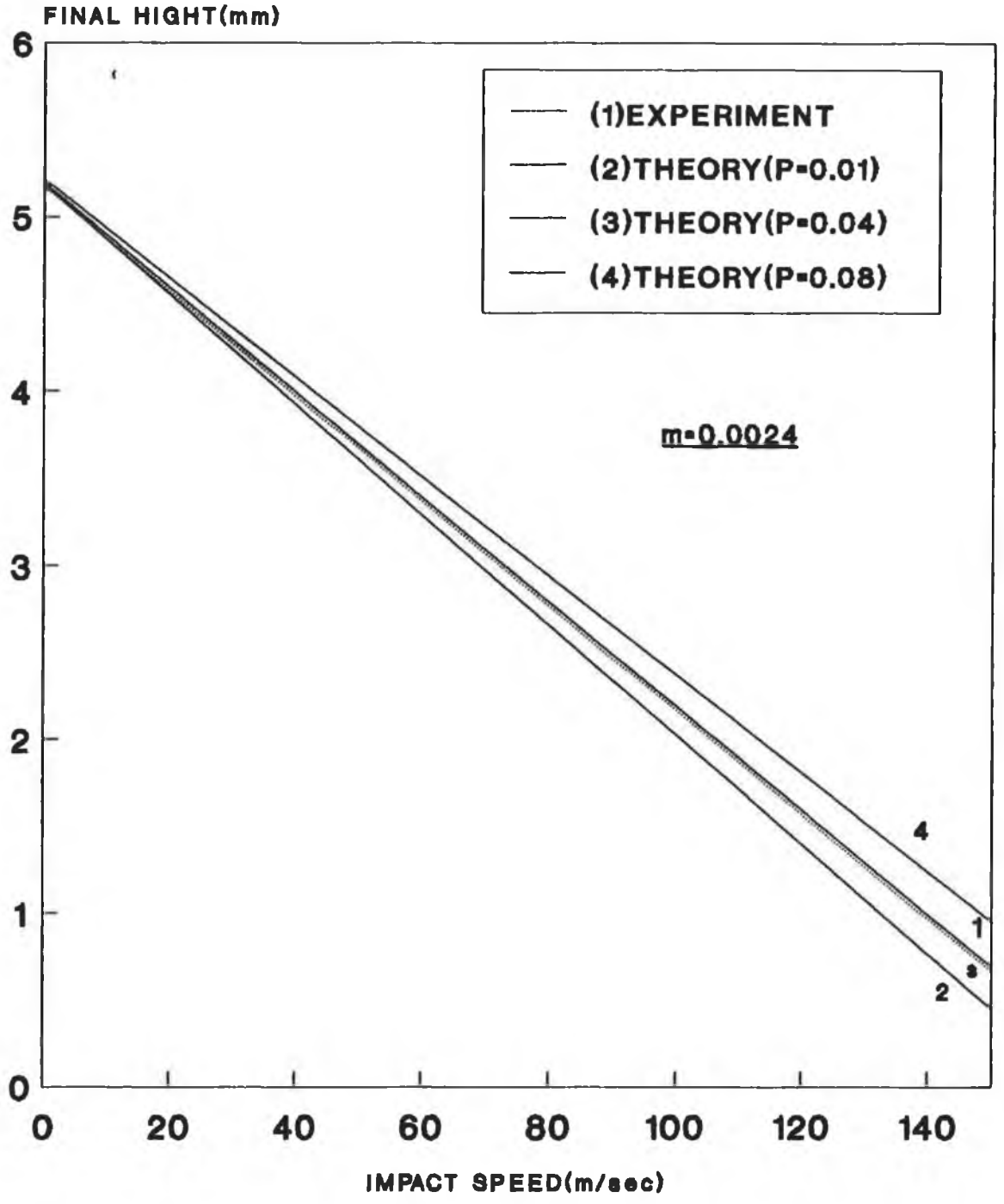

Fig.(5.3)

Variations in the final diameter of Copper with impact speed

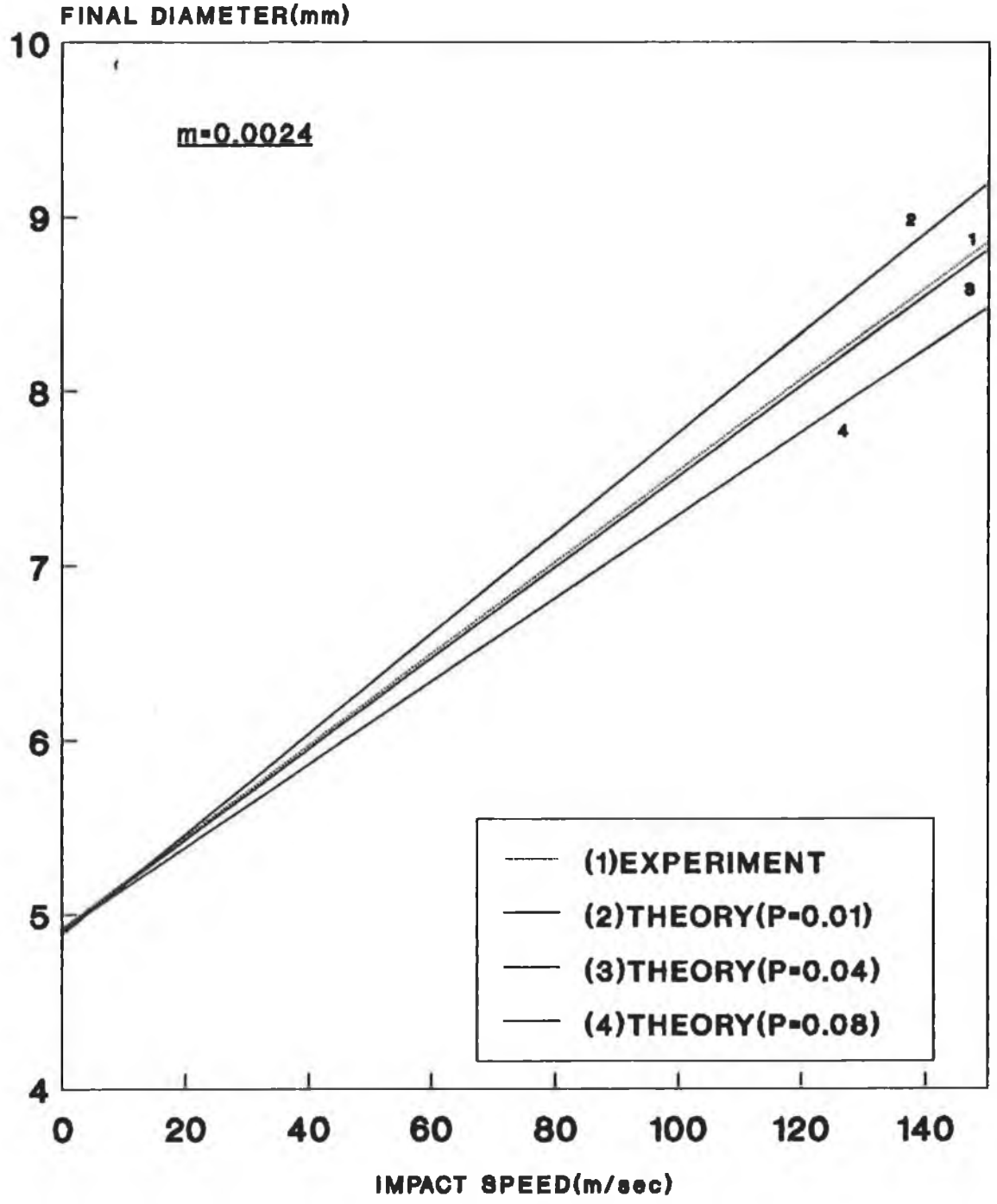

Fig.(5.4)

Variations in the final height of
Stainless steel with impact speed

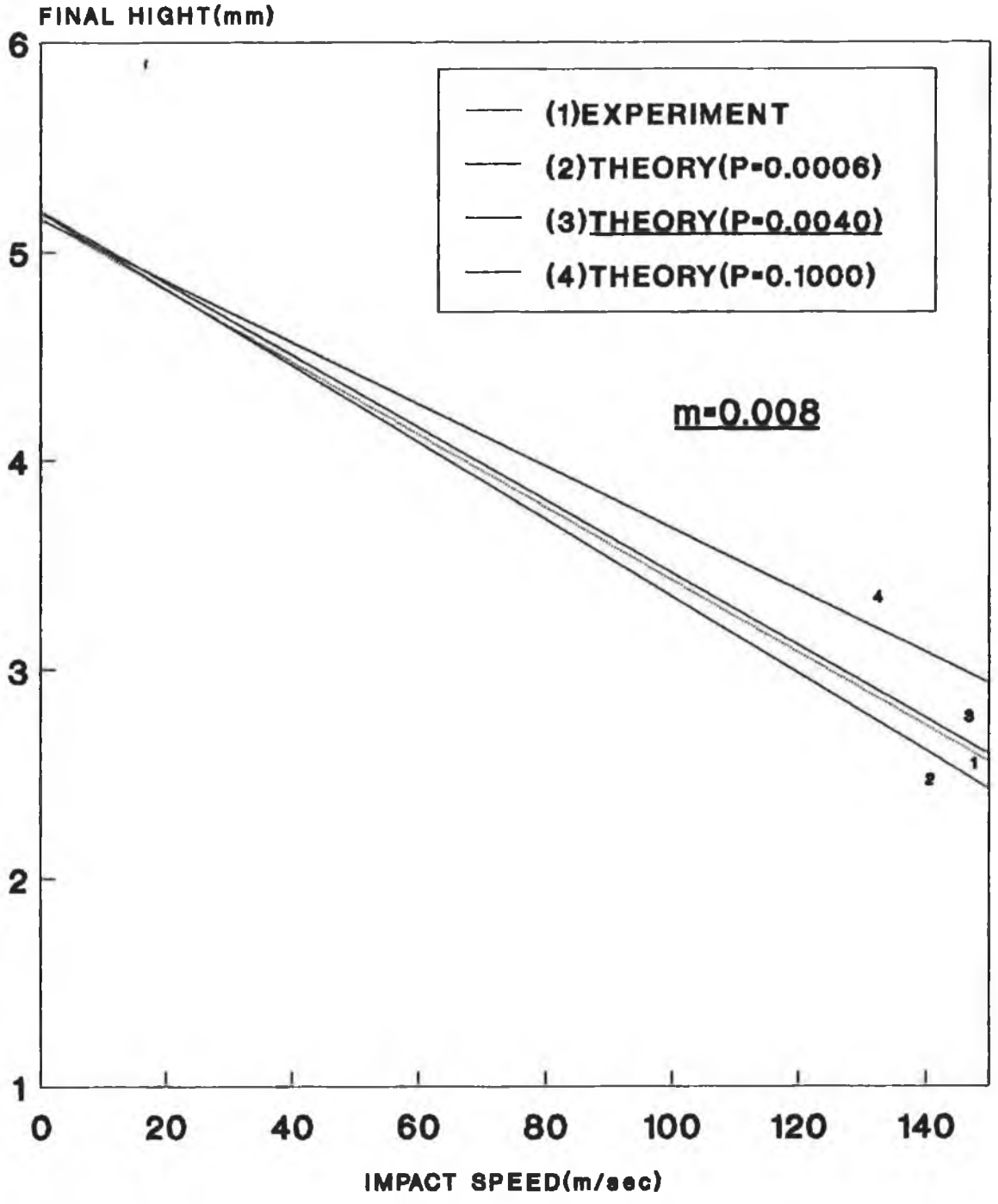

Fig.(5.5)

Variations in the final diameter of Stainless steel with impact speed

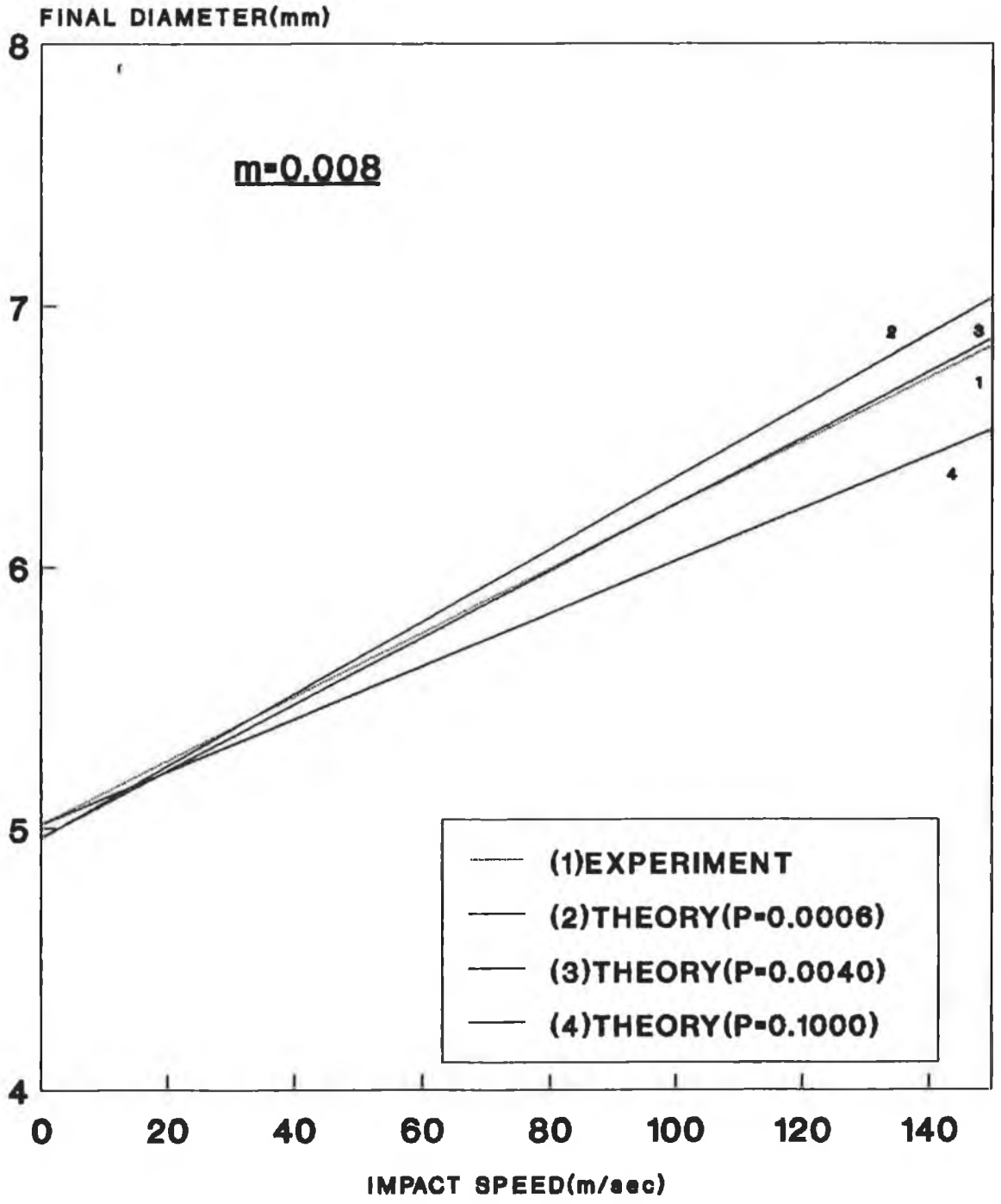

Fig.(5.6)

Variations in the final height of Mild steel with impact Speed and conditions

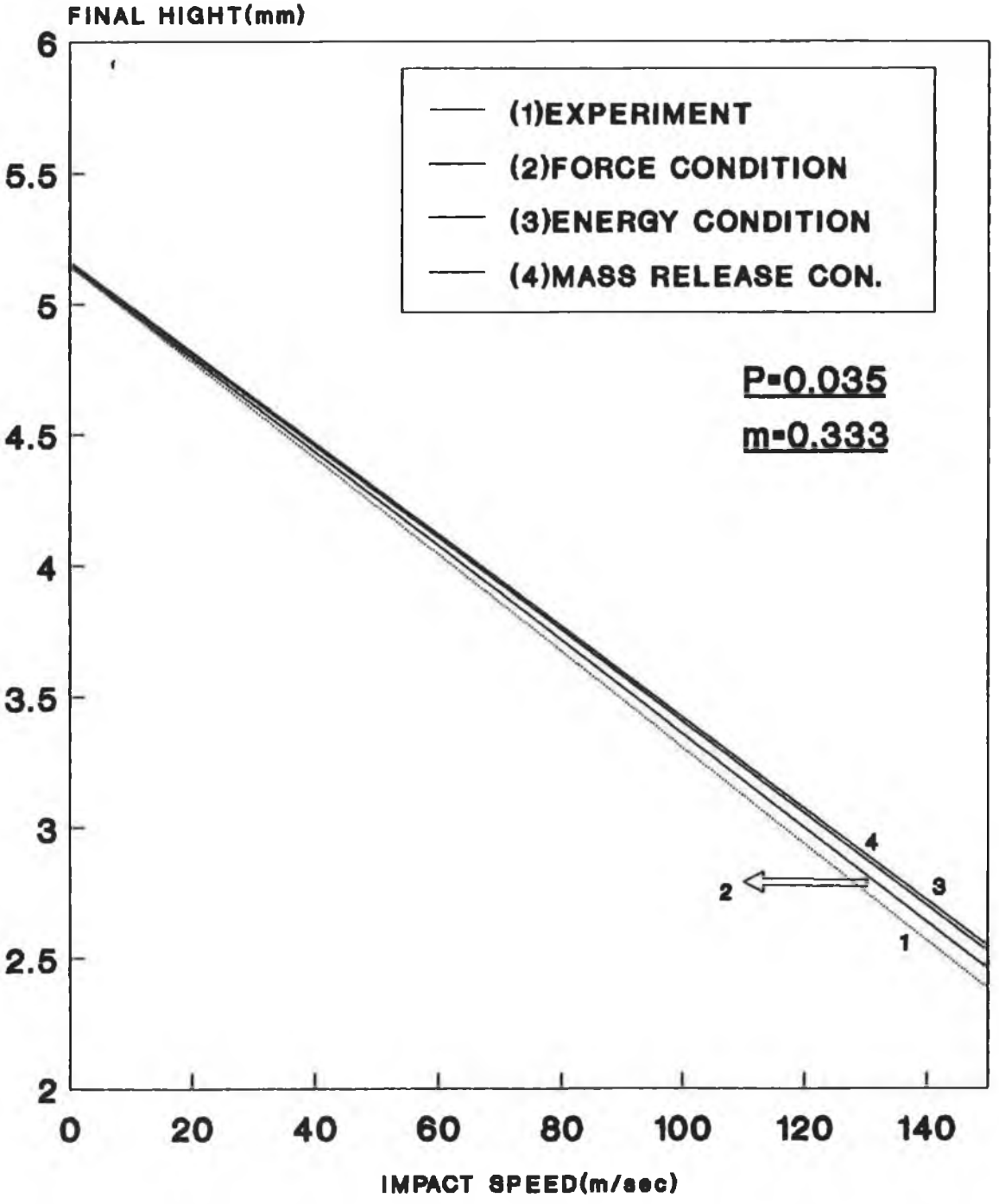

Fig(5.7)

Variations in the final diameter of Mild Steel With impact speed and conditions

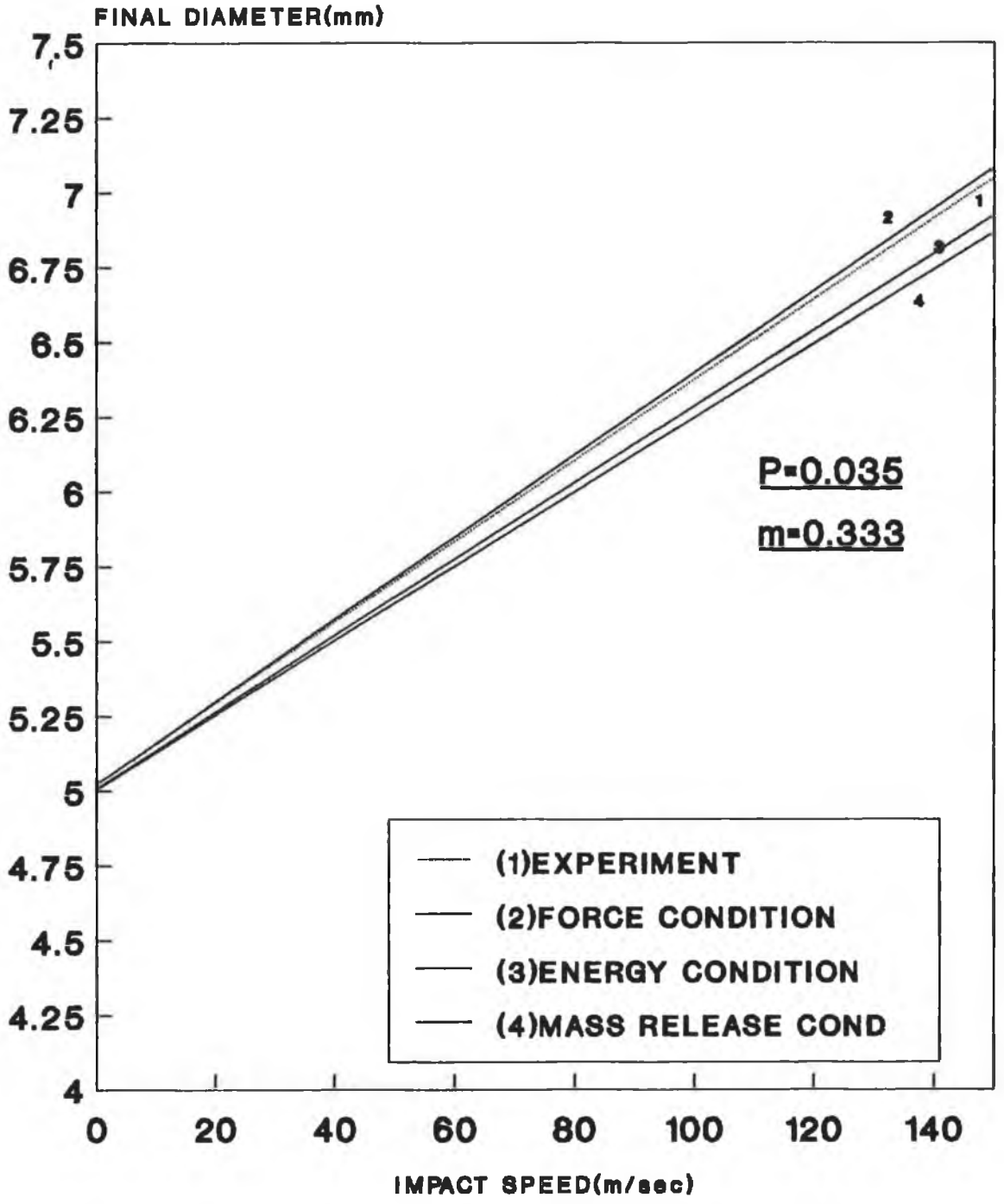

Fig.(5.8)

Determination of stress-strain curves

Knowing the material constants m and P for each material and applying them into the proposed equation(4.20), the true stress-strain curve could be obtained.

Figs.(5.9)to(5.11) show the dynamic stress-strain curves at different strain rates together with the quasi-static curves. The main feature in using equation(4.20) is that, it only moves the curves vertically as strain rate increases and no change in the overall shape of the static curve takes place.

Figs.(5.12)to(5.14) show the relationship between the ratio of dynamic to static flow stress obtained in this work and the strain rate. These figures show the degree of rate sensitivity obtained for all three materials investigated in this study. It can be seen that the ratio for mild steel varies between (2.2-2.44), for copper between(2.1-2.25) and for stainless-steel between (2.-2.1), at strain rate range from (10^2-10^5) per second.

Theoretical Curves
True stress-strain curve of Mild-steel

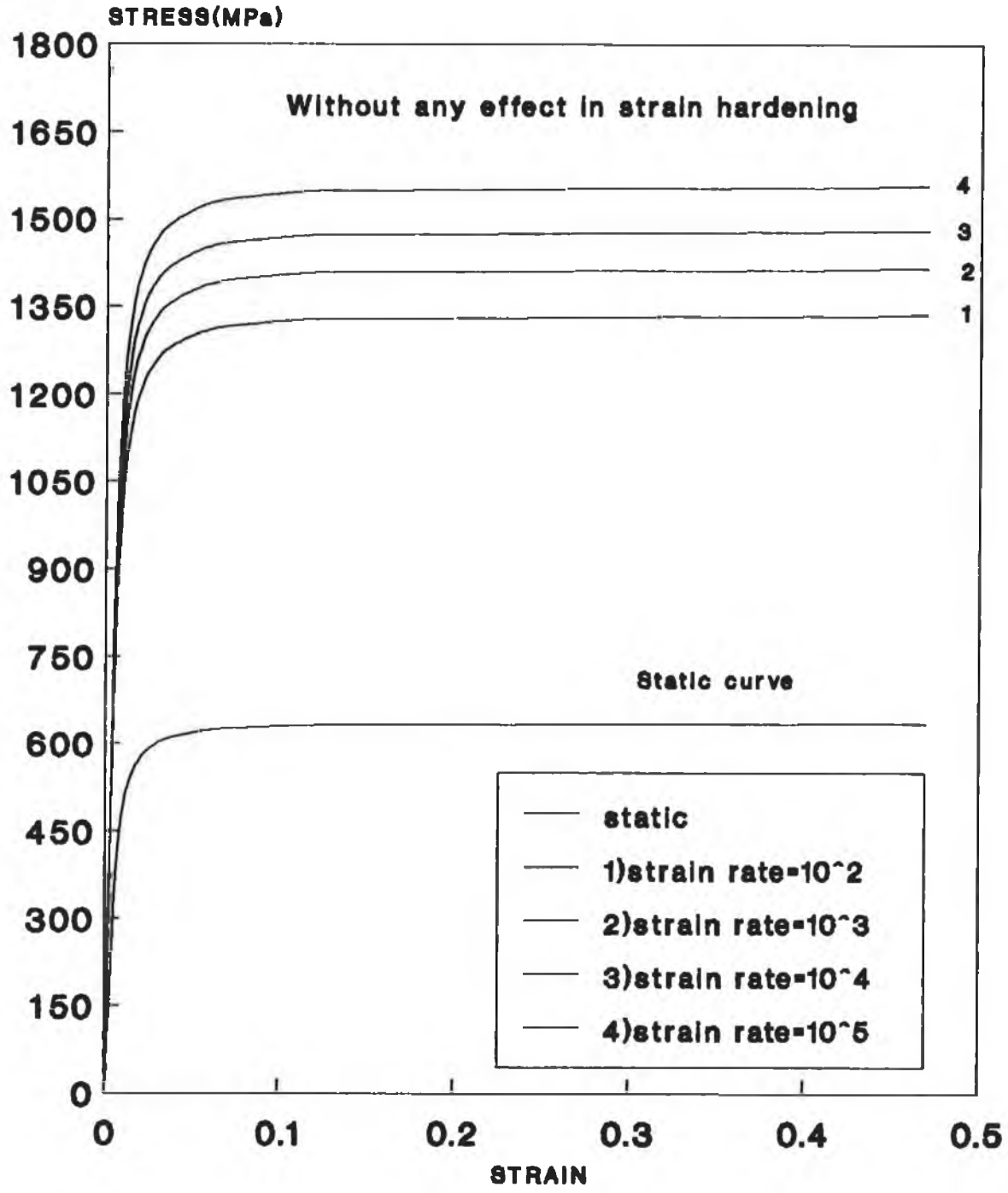

Fig.(5.9)

Theoretical Curves
True stress-strain curve of Copper

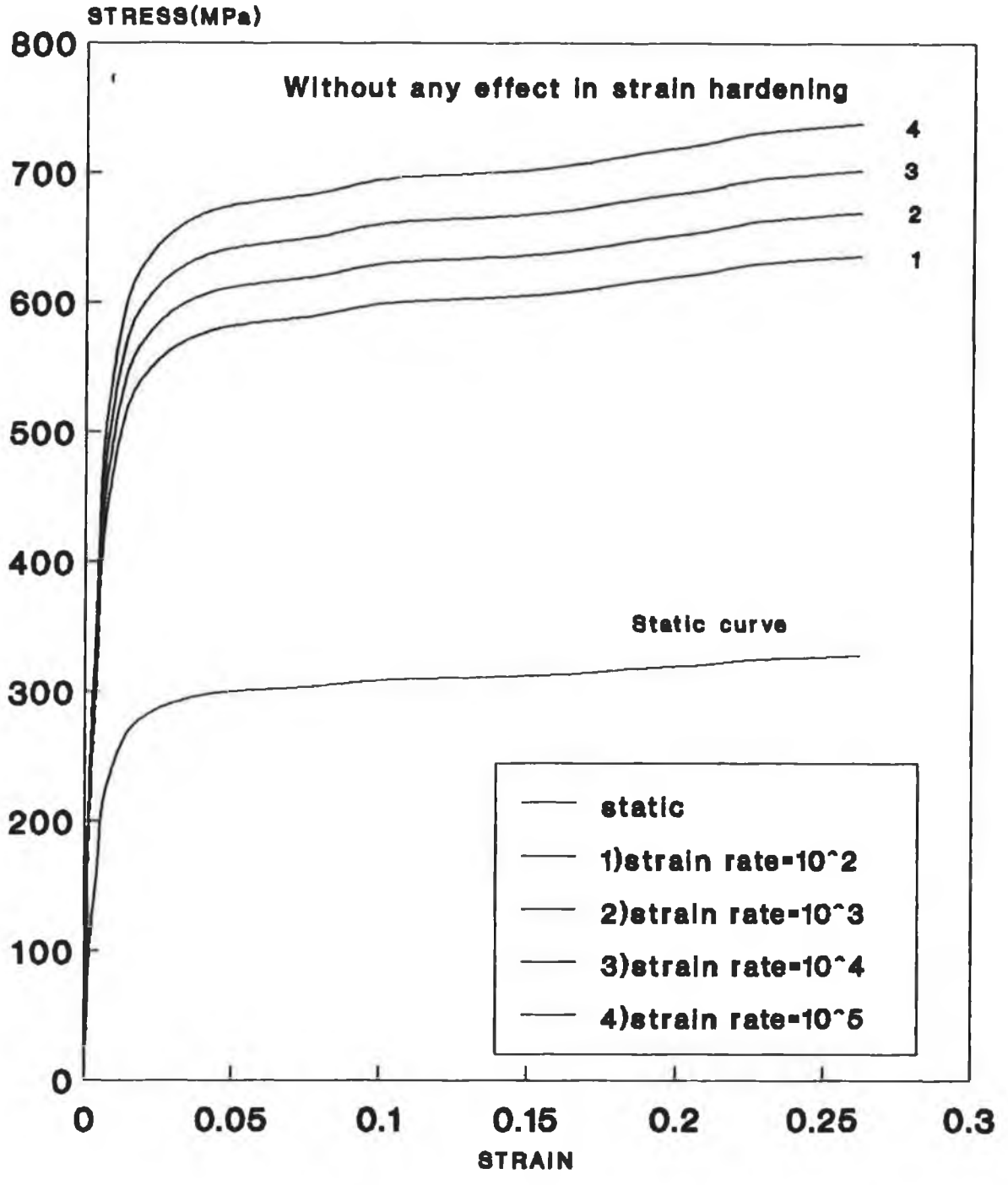

Fig.(5.10)

Theoretical Curves
True strain-stress curve of Stainless-steel (304)

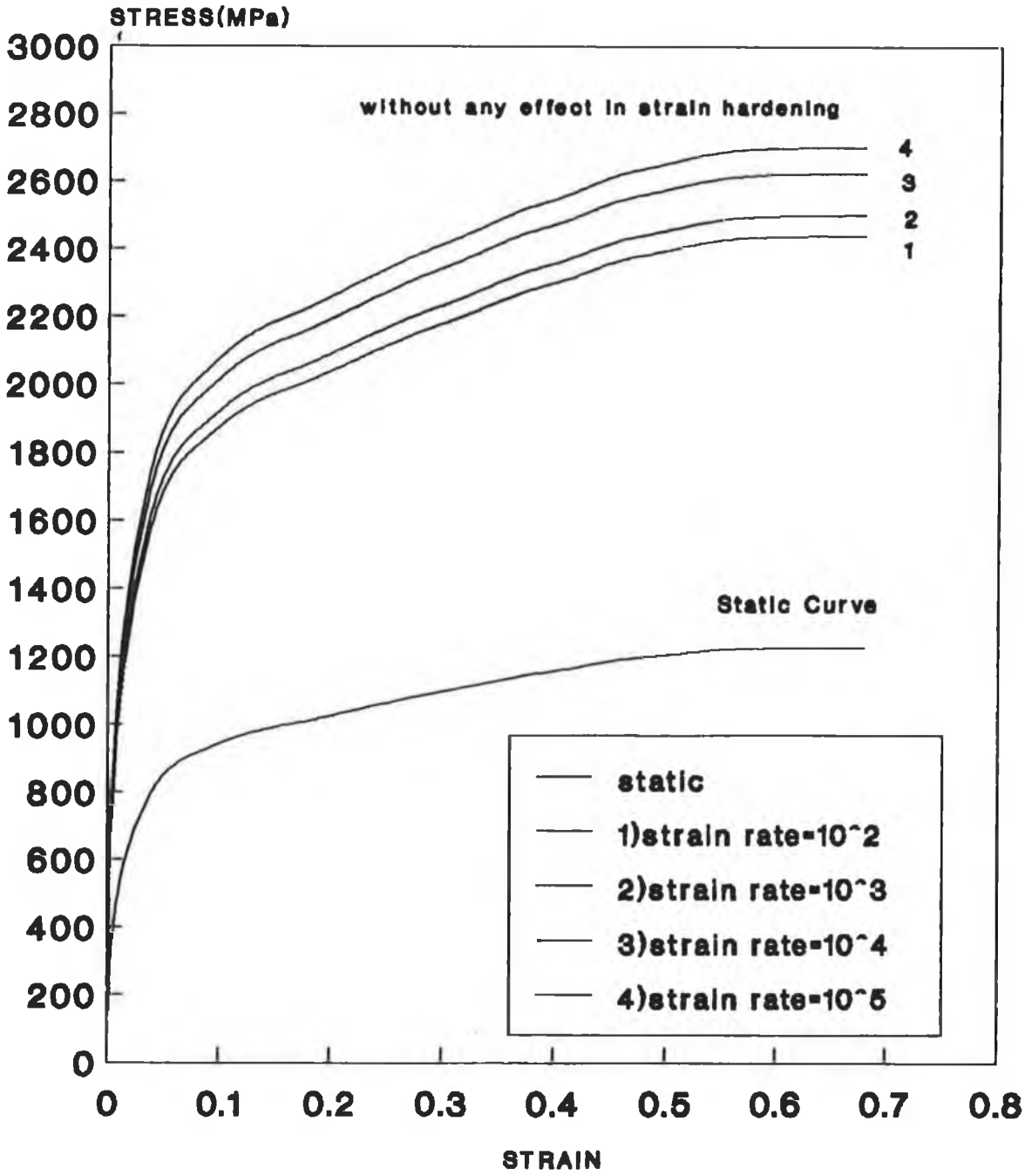

Fig.(5.11)

Theoretical curve
Variation of flow stress ratio with strain rate for Mild steel

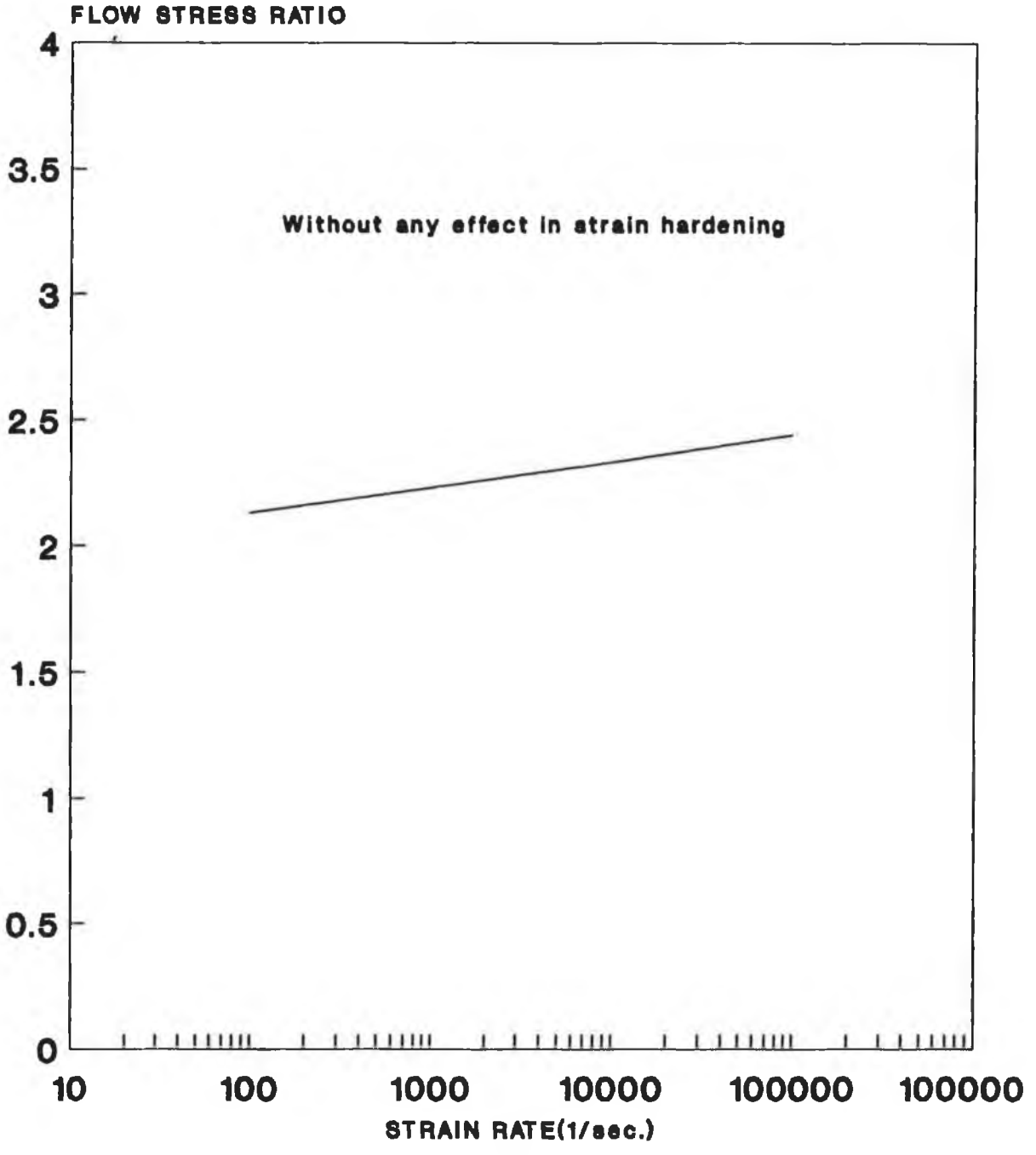

Fig.(5.12)

Theoretical curves
Variation of flow stress ratio with strain rate for Copper

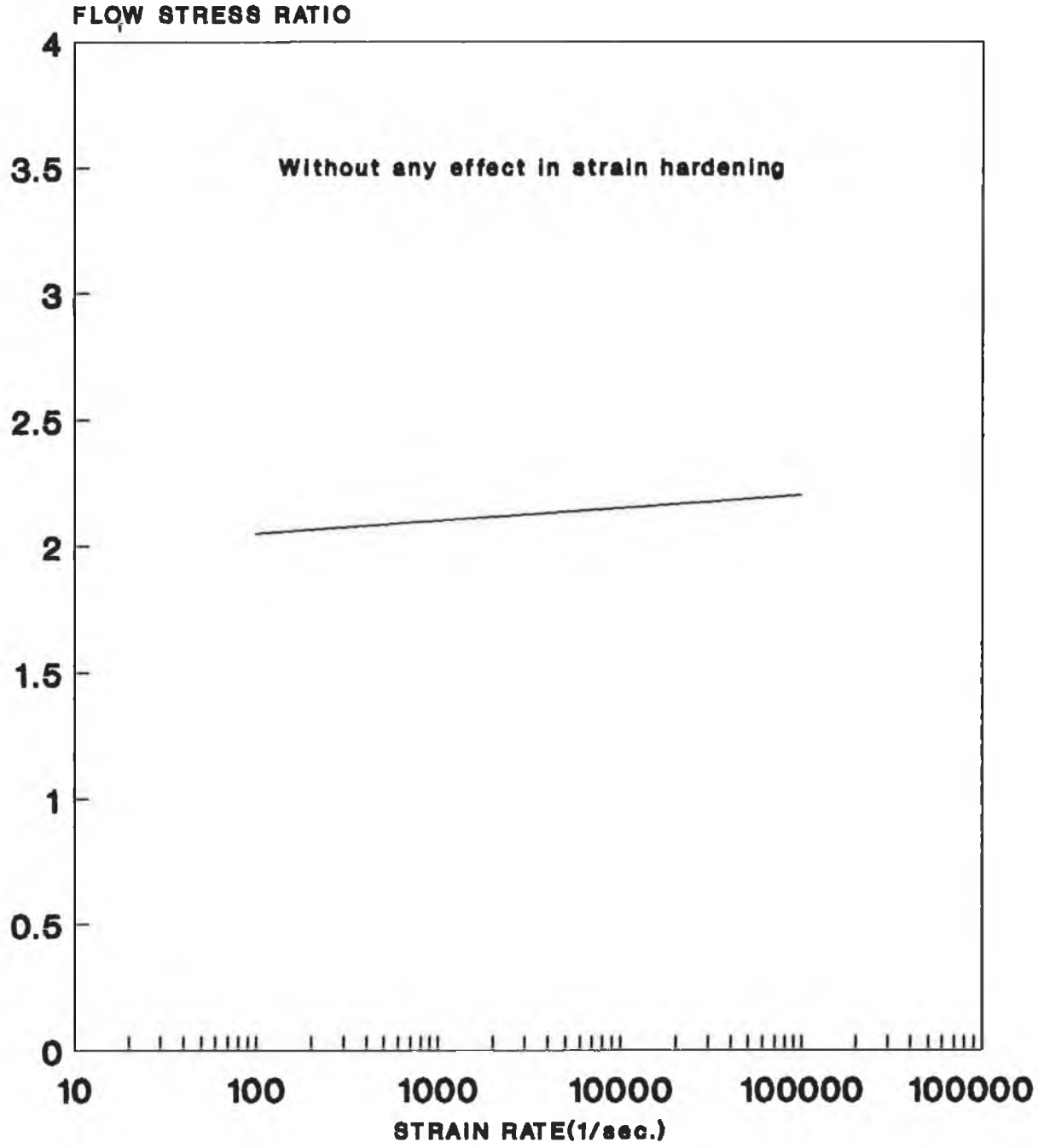

Fig.(5.13)

Theoretical curves
Variation of flow stress ratio with strain rate for Stainless steel(304)

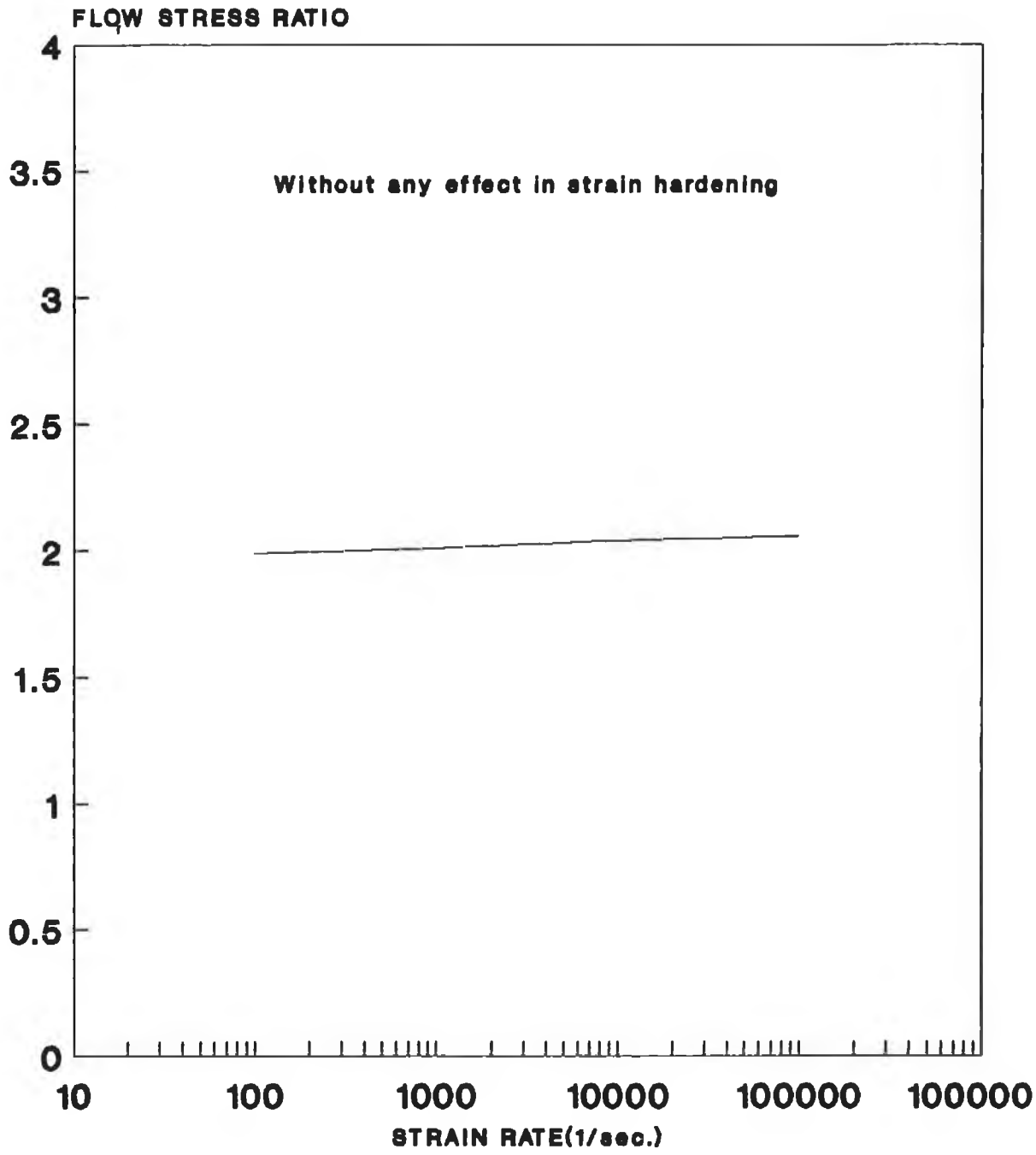

Fig.(5.14)

Modified constitutive equation after catering for temperature rise during deformation:

A considerable rise in the temperature during deformation occurred. This happened due to the impact of the tool steel projectile against the test specimen and the plastic deformation which took place subsequently within a very short period of time.The temperature rise, ΔT, can be estimated by the following equation:

$$\Delta T = \frac{F}{(\rho\ S)} \int_{o}^{\varepsilon_f} \sigma\, \delta\varepsilon \qquad (4.21)$$

where

ε_f Final strain.

f Factor indicating the portion of plastic work transformed into temperature rise.

ρ Density [Kg/m^3].

S Specific heat capacity[J/kg.k].

Bishop[88], reported that the value of **f** for steel and copper is 0.865 and 0.92 respectively.And the value of **S** and ρ are reported in Table(5.2) according to reference **[90]**.

Table[5.2]

Material	Density [kg/m^3]	Specific heat [J/kg.K]
Mild steel	7833	465
Copper	8954	383
Stainless-steel	7933	460

The maximum rise in the temperature was estimated to be, in the case of mild-steel, 483 K at an impact speed of 120 m/sec., for copper 393 K at an impact speed of 78 m/sec., and for stainless-steel 463 K. impact speed of 110 m/sec.

Since, this rise in temperature is well known to have an effect on the material properties(flow stress decreases) and the final shape of the stress-strain curve, therefore, it was thought essential to find a general form of temperature dependent constitutive equation for the three material investigated over the range of up to 673 K.

The dynamic constitutive equation modified to take into account the effect of temperature rise, is as shown below ;

$$\sigma = K G_1 \varepsilon^{nG} [1 + (m\dot{\varepsilon})^p] \qquad (4.23)$$

where

$$G_1=(To/T)^{\theta 1}$$

$$G =(T_o/T)^{\theta}$$

To Reference temperature (273 K)

T Adiabatic temperature rise (K).

θ,θ1 Constants.

The magnitude of θ1,θ were determined based on results from reference [34] and are shown in Table[5.3].

Table[5.3]

Material	θ	θ1
Mild steel	0.300	0.050
Copper	0.500	0.068
Stainless-steel	0.288	0.038

When equation(4.23) was incorporated into the numerical technique, the predicted final height and final diameter against impact velocity lines changed and consequently the material constant m and P were changed for closer agreement between the theory and experiment. The values of m and P for all the three materials determined in this way are shown in the Table [5.4] below.

Table[5.4]

MATERIAL	m(sec.)	P
Mild-steel	0.3330	0.050
Copper	0.0024	0.060
Stainless-steel	0.0040	0.014

Figs.(5.15)to(5.17) show the dynamic stress-strain curves obtained using equation (4.23). It can be seen from these figures that there is a significant change in the shape of the dynamic stress-strain curve in comparison with the static curve.In all cases, the adiabtic stress reaches a maximum and then decreases with increasing strain. This is due to effects of thermal softening and it is more apparent in the case of copper than mild steel and stainless steel as seen from these figures.

Figs.(5.18)to(5.20) give clear picture of the effect of strain rate and strain on the flow stress ratio. It is noticeable that the rate sensitivity of the material varies with strain at constant strain rate, where this sensitivity decreases as the strain increases. The rate sensitivity over strain rate range of 10^2 - 10^5 per second and strain equal to 0.1 were found to be within the range (2.17 to 2.68), (1.76-2.2) and

(2.0-2.127) for mild steel, copper and stainless-steel respectively. At strain equal to 0.7 the ratio of the dynamic to static stress over strain rate range 10^2-10^5 per second varies between (1.9-2.36), (1.66-2.1) and (1.94-2.08) for mild steel, copper and stainless-steel respectively.

Theoretical curves
True stress-strain curves of Mild-steel

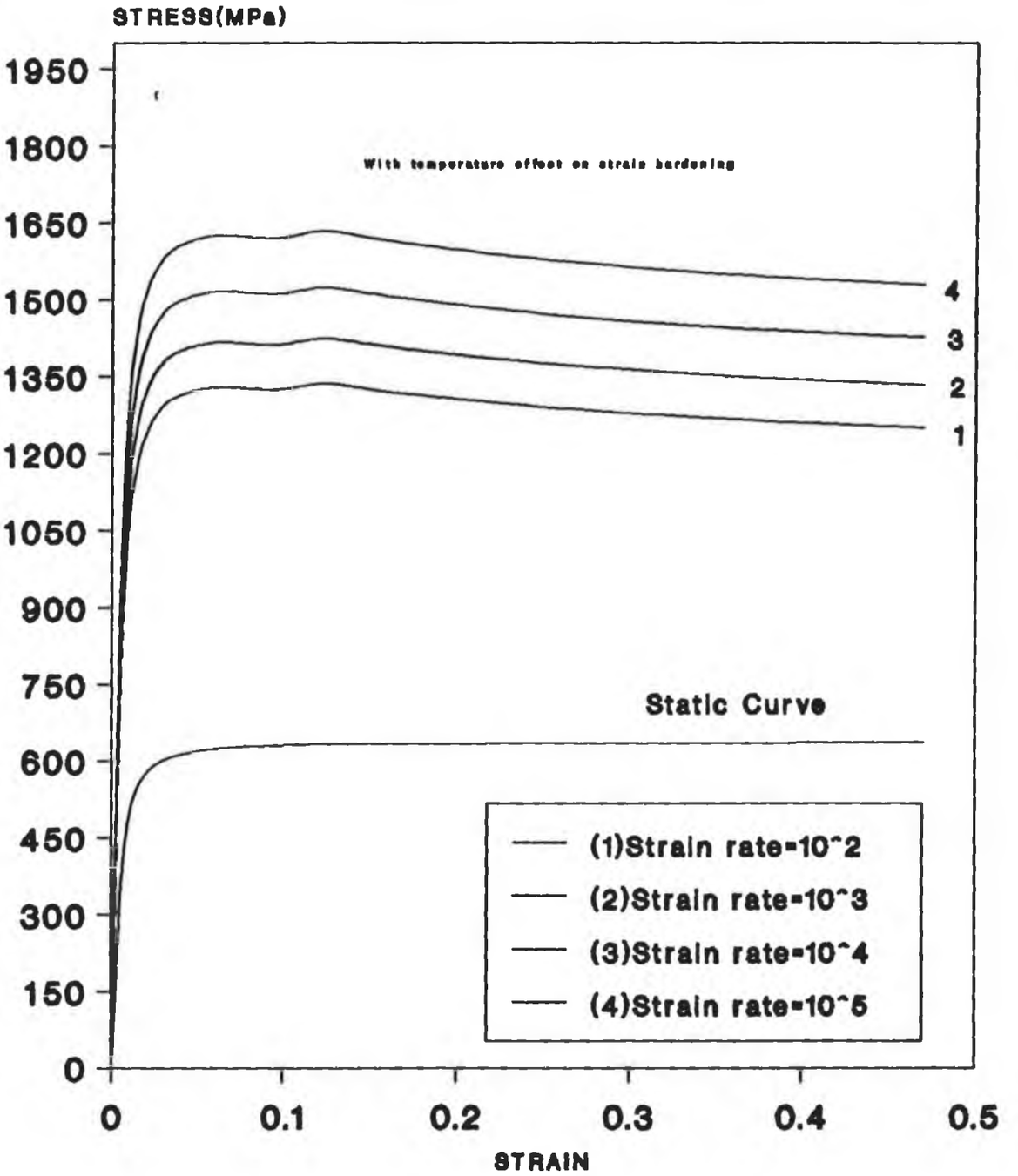

Fig.(5.15)

Theoretical curves
True stress-strain curves of Copper

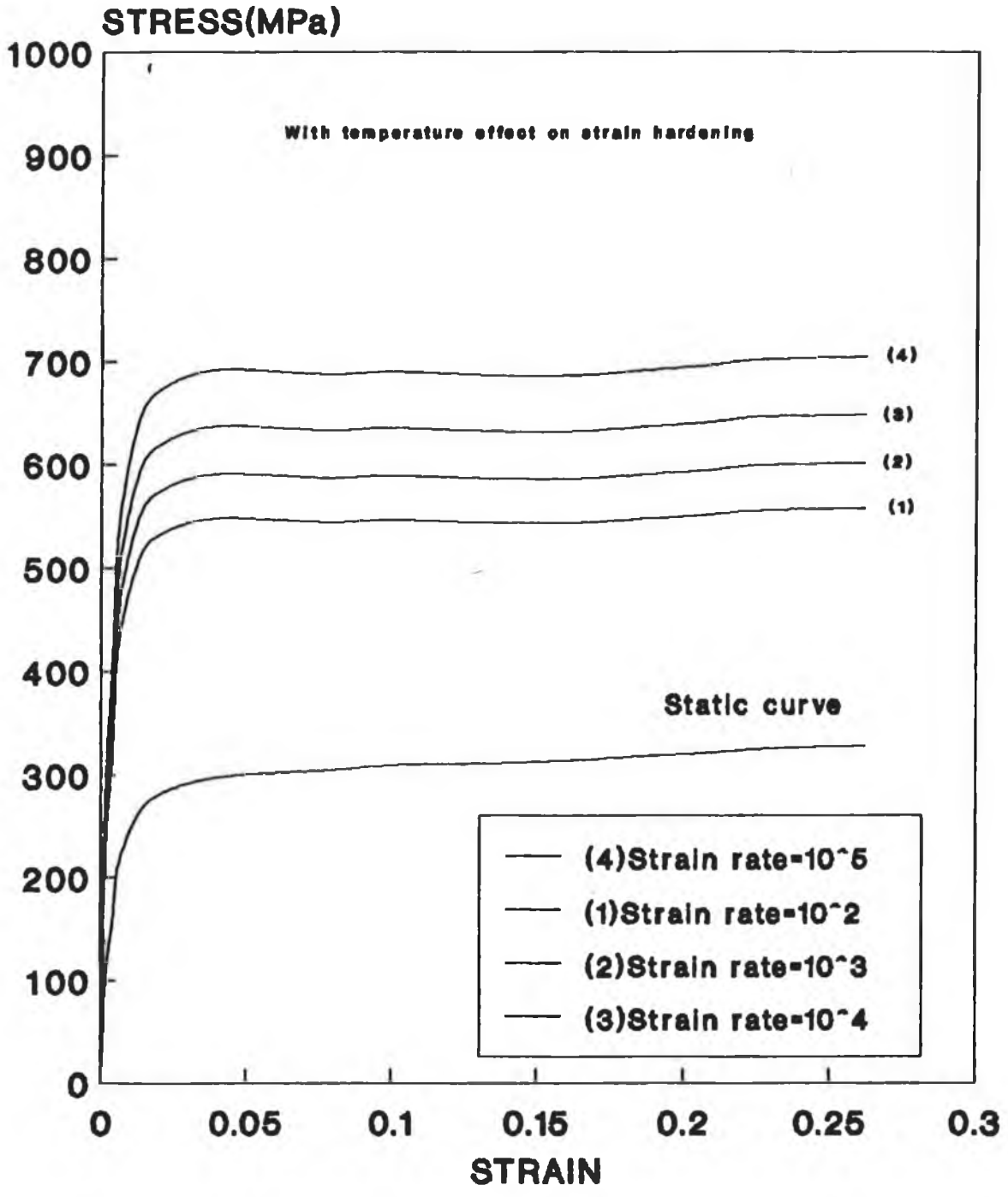

Fig.(5.16)

Theoretical Curves
True strain-stress curves of Stainless-steel (304)

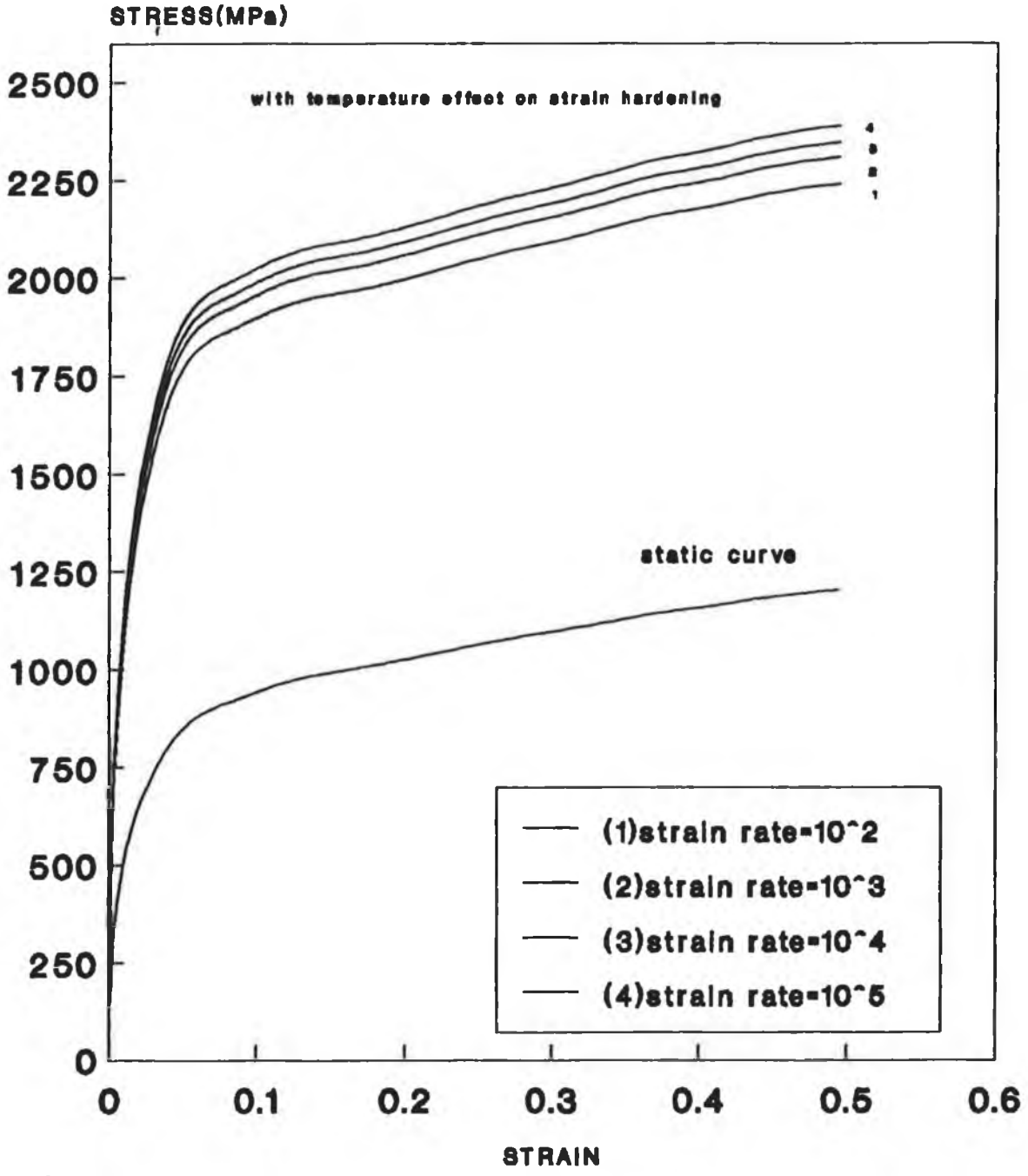

Fig.(5.17)

Theoretical curves
Variation of flow stress ratio with strain rate for Mild steel

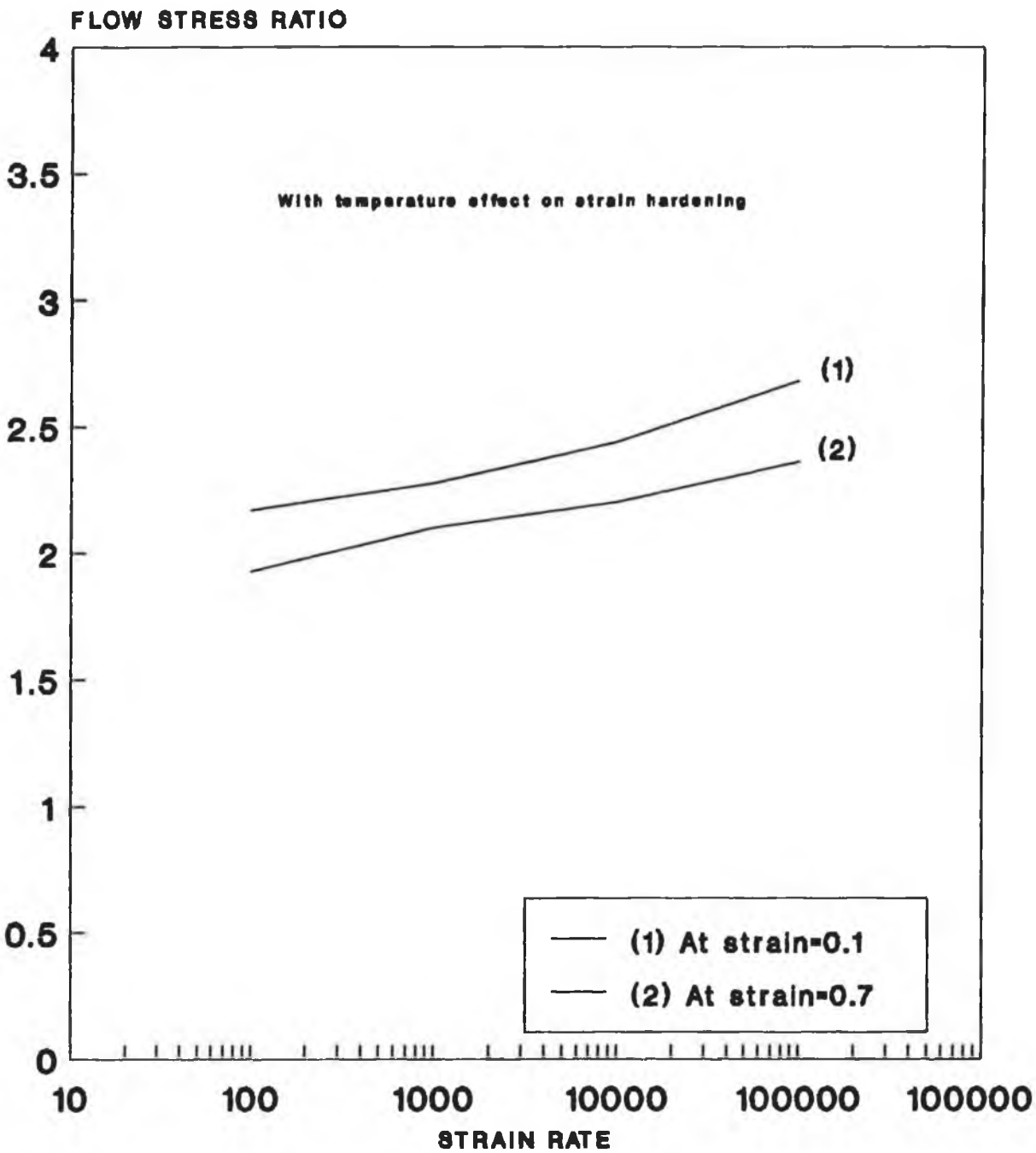

Fig.(5.18)

Theoretical curves
Variation of the flow stress ratio with strain rate for Copper

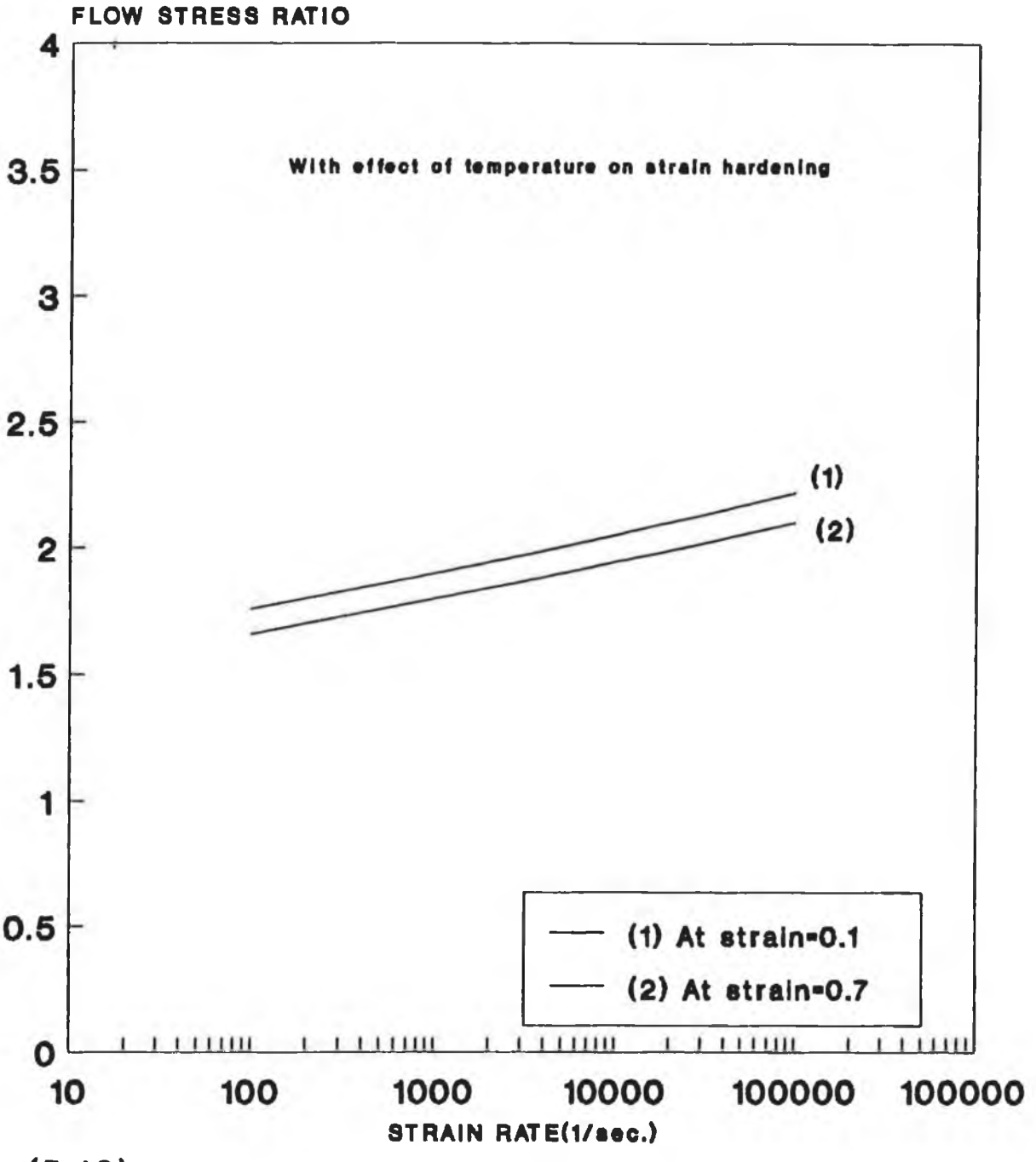

Fig.(5.19)

Theoretical curves
Variation of flow stress ratio with strain rate for Stainless-steel(304)

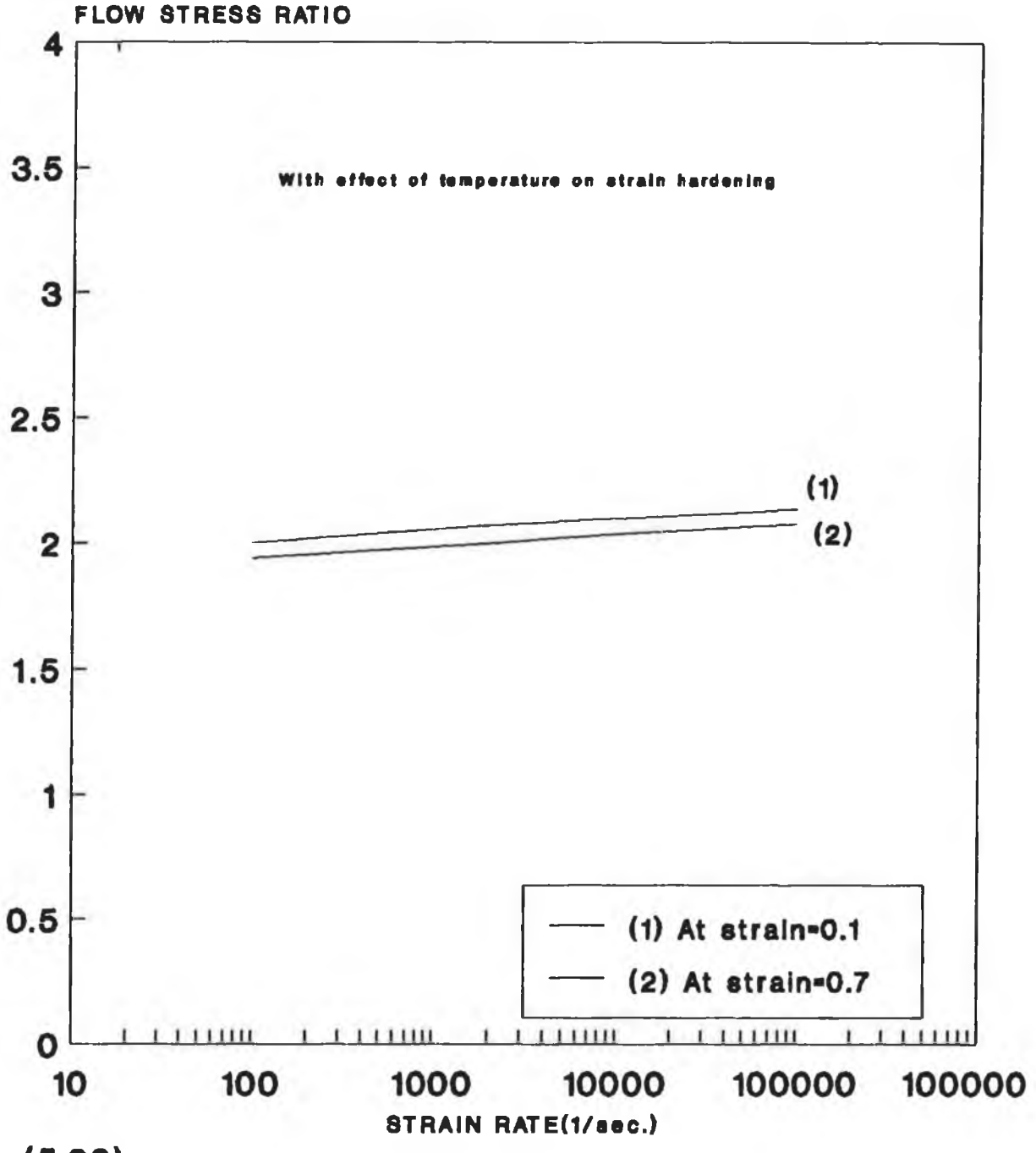

Fig.(5.20)

Effect of strain rate on strain hardening

The effect of strain rate on strain hardening was incorporated in the proposed constitutive equation (4.20), resulting in a new form given as;

$$\sigma_d = K\varepsilon^{n/R}[1+(m\dot{\varepsilon})^p] \qquad (4.24)$$

where

$$R = [\ln(\dot{\varepsilon}/\dot{\varepsilon}_o) + 1]^{\beta} \qquad (4.25)$$

$\dot{\varepsilon}_o$ Constant at 1 per second.

β Constant equal to (0.28), Reference [89].

The above constitutive equation when used to simulate the deformation a new set of values of materials constants were obtained. The resulting constants for all the three materials are presented in Table[5.5] as following;

Table[5.5]

MATERIAL	m (sec.)	P
Mild-steel	0.3330	0.030
Copper	0.0024	0.020
Stainless-steel	0.0040	0.005

Figs.(5.21)to(5.23) illustrate the stress-strain curves given by equation (4.24).The conclusion that can be drawn from these figures is that, the rate sensitivity is a function of strain and strain rate.As the strain increases the strain rate sensitivity decrease at constant strain rate.This phenomena is more clear in the case of mild-steel rather than copper and stainless-steel.These figures also indicate that, as the strain rate increases the material appears to be less resistant to deformation. In other-words, the plastic modulus of the dynamic curve is smaller than that of the static curve, which is an indication of a decrease in strain hardening.

Figs.(5.24)to(5.26) show the effect of strain rate on the flow stress ratio. For strain rate ranging between 10^2 to 10^5 per second and strain equal to **0.1** the ratio varies between (2.39- 2.70), (2.1-2.28) and (2.18-2.26) for mild steel, copper and stainless-steel respectively, for strain equal to **0.7** the ratio varies between (2.14-2.38), (1.98-2.14) and (2.04-2.11) for mild steel, copper and stainless-steel respectively.These figures give a clear indication that, the dynamic flow stress given by equation (4.24) for strain level at 0.1 (strain rate effect on strain hardening) is higher than those given by equation (4.20) (without effect) and equation (4.23) (with temperature effect on strain hardening).

Theoretical curves
True Stress-Strain Curve of Mild-Steel

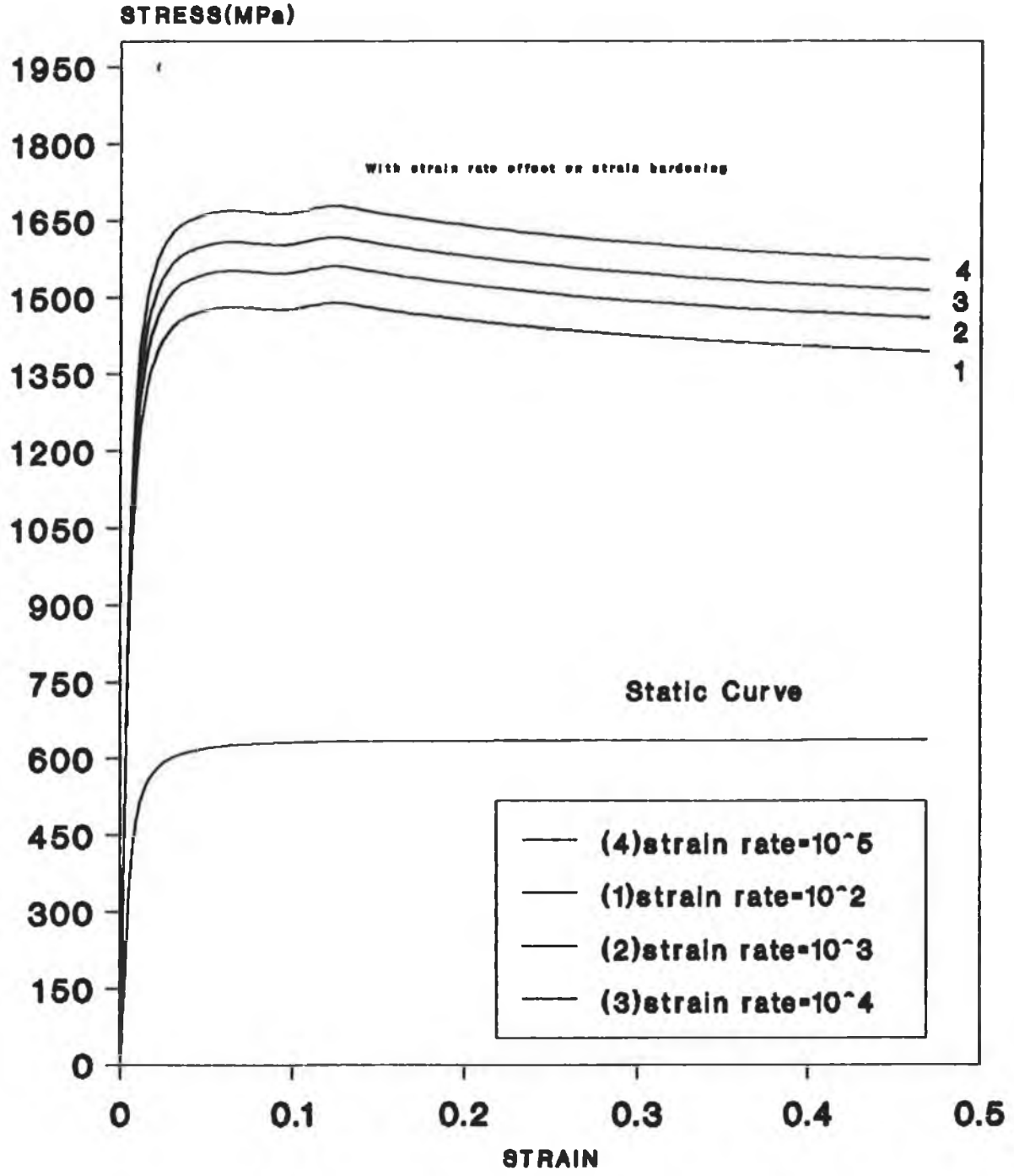

Fig.(5.21)

Theoretical Curves
True stress-strain curve of Copper

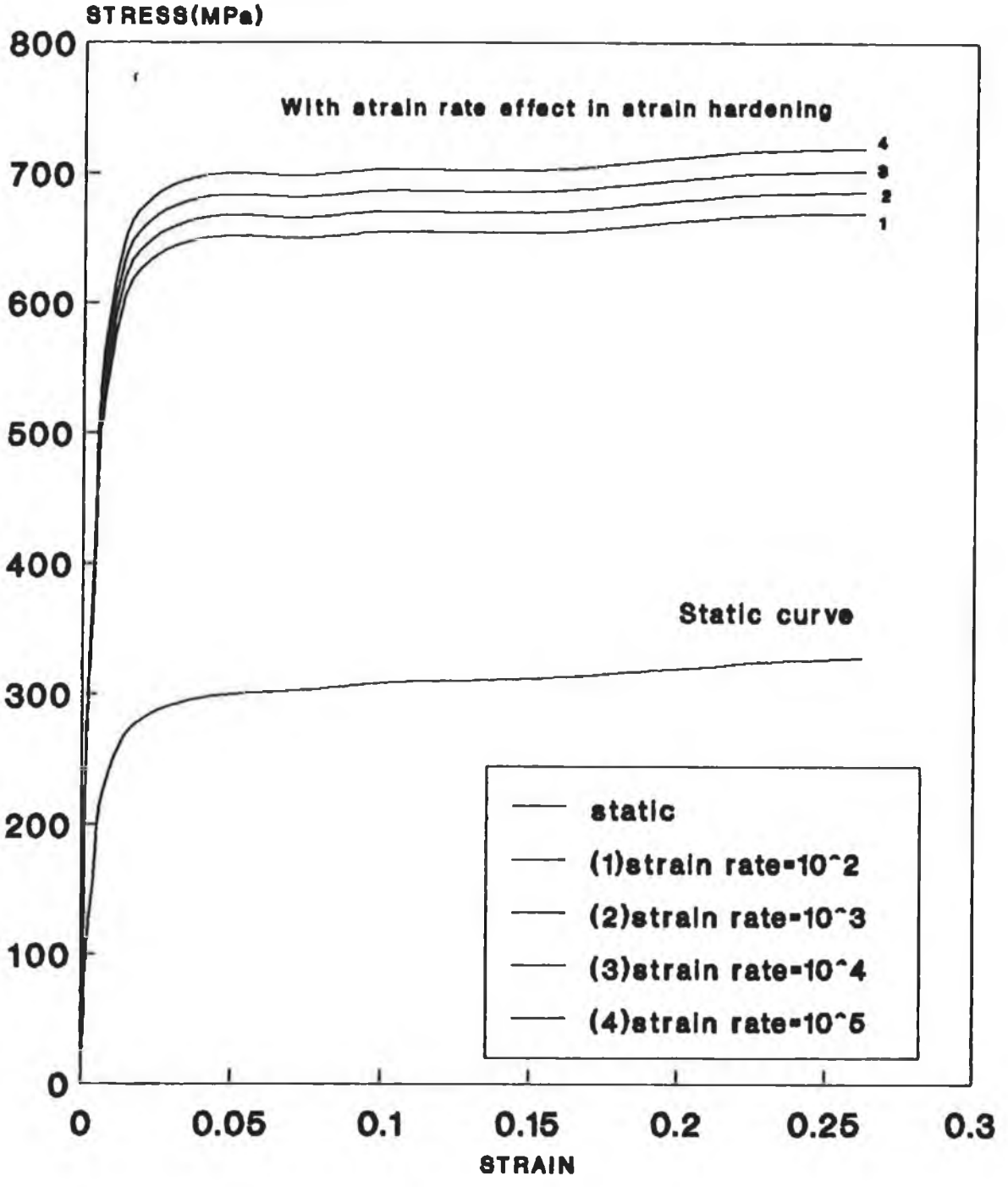

Fig.(5.22)

Theoretical Curves
True strain-stress Curve of Stainless Steel (304)

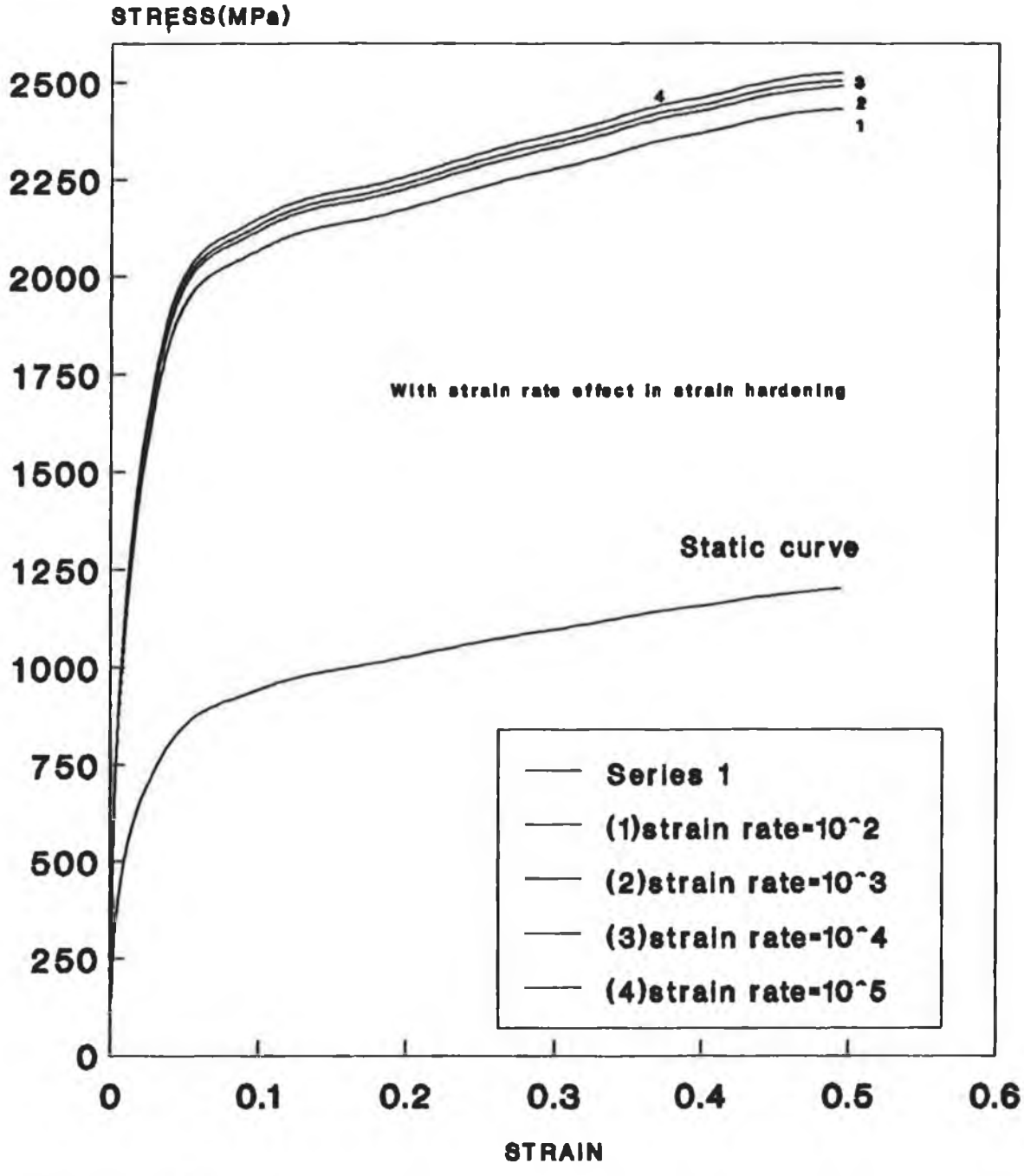

Fig.(5.23)

Theoretical curves
Variation of flow stress ratio with strain rate for Mild steel

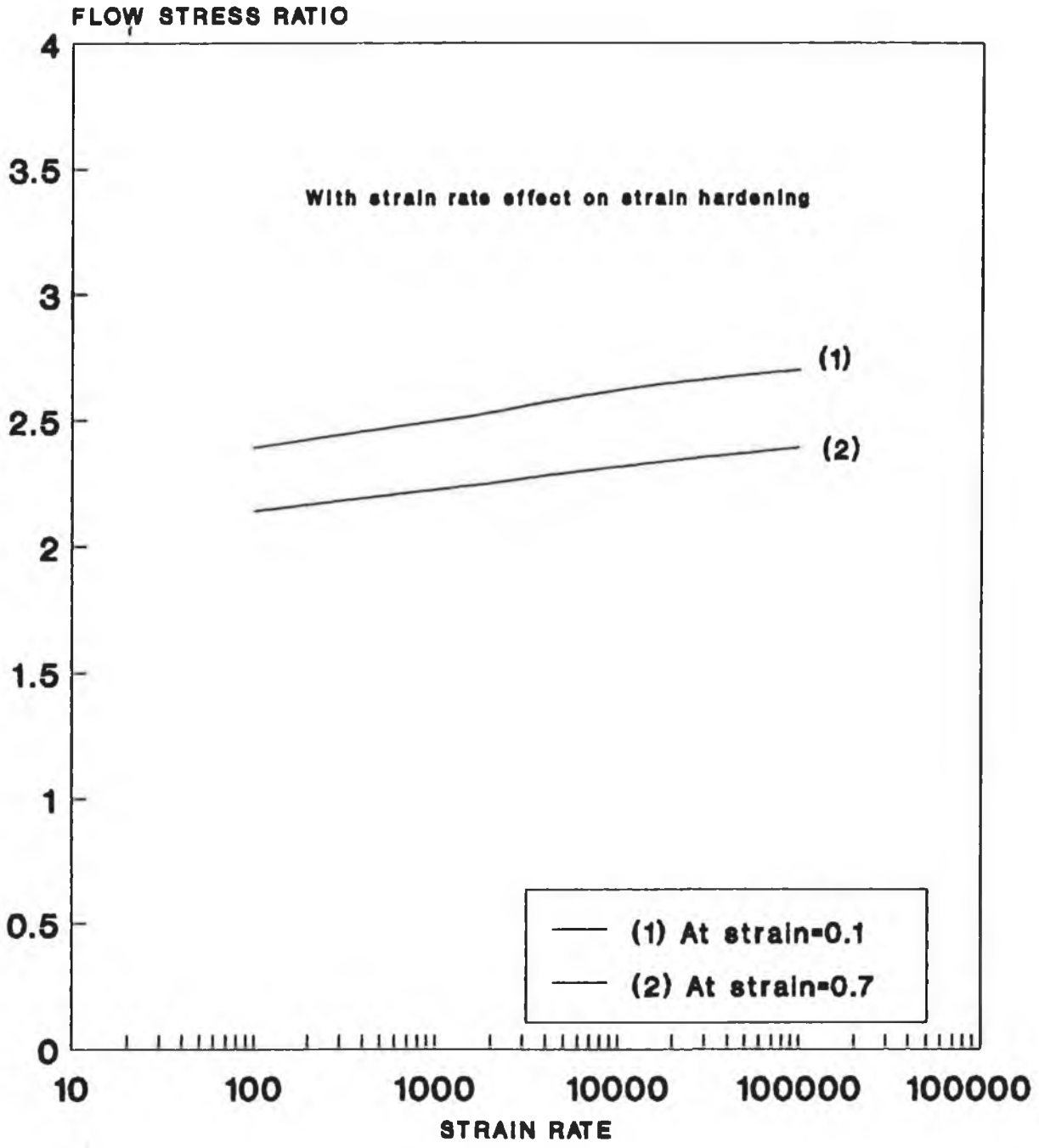

Fig.(5.24)

Theoretical curves
Variation of the flow stress ratio with strain rate for Copper

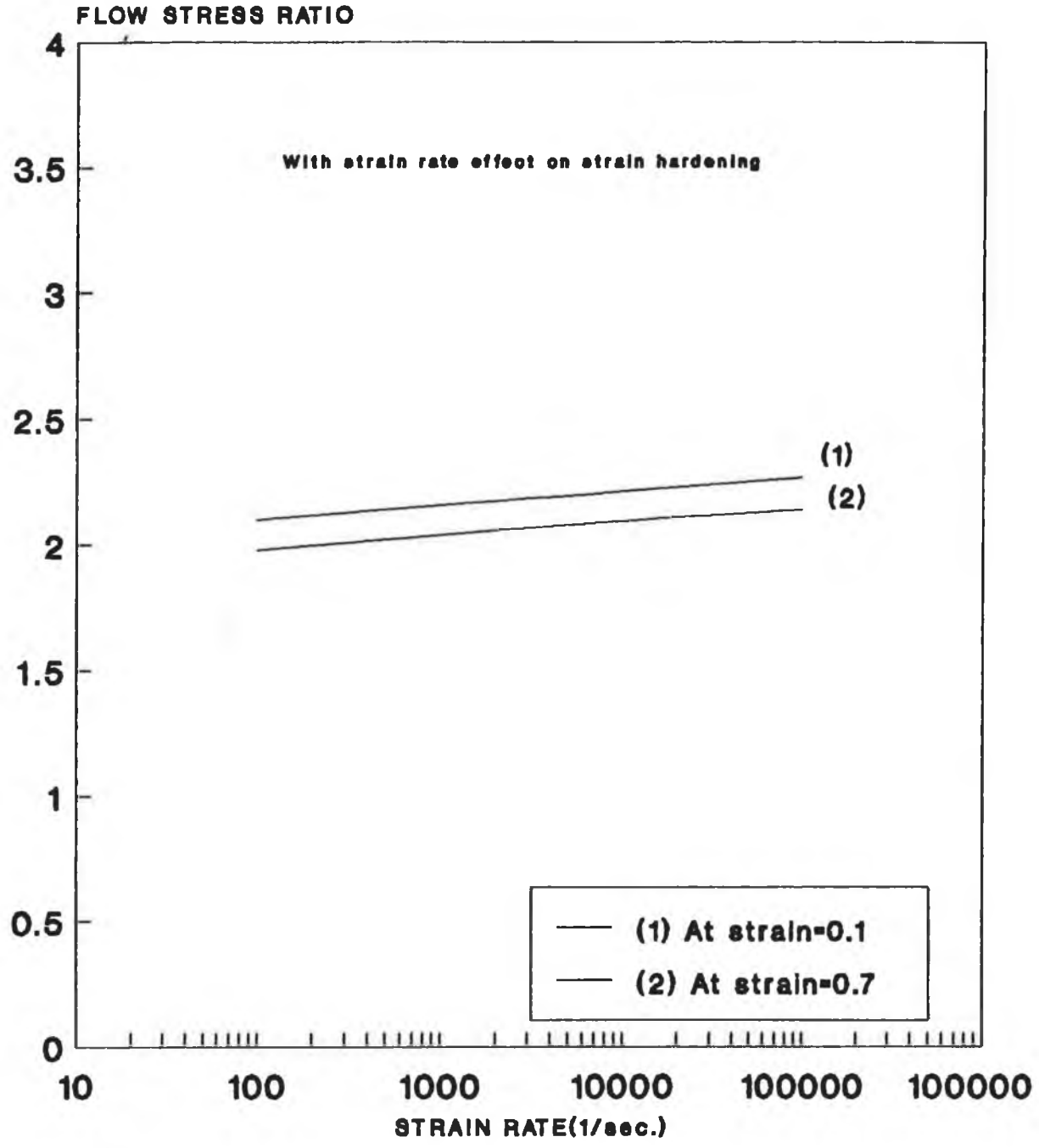

Fig.(5.25)

Theoretical curves
Variation of flow stress ratio with strain rate for Stainless-steel(304)

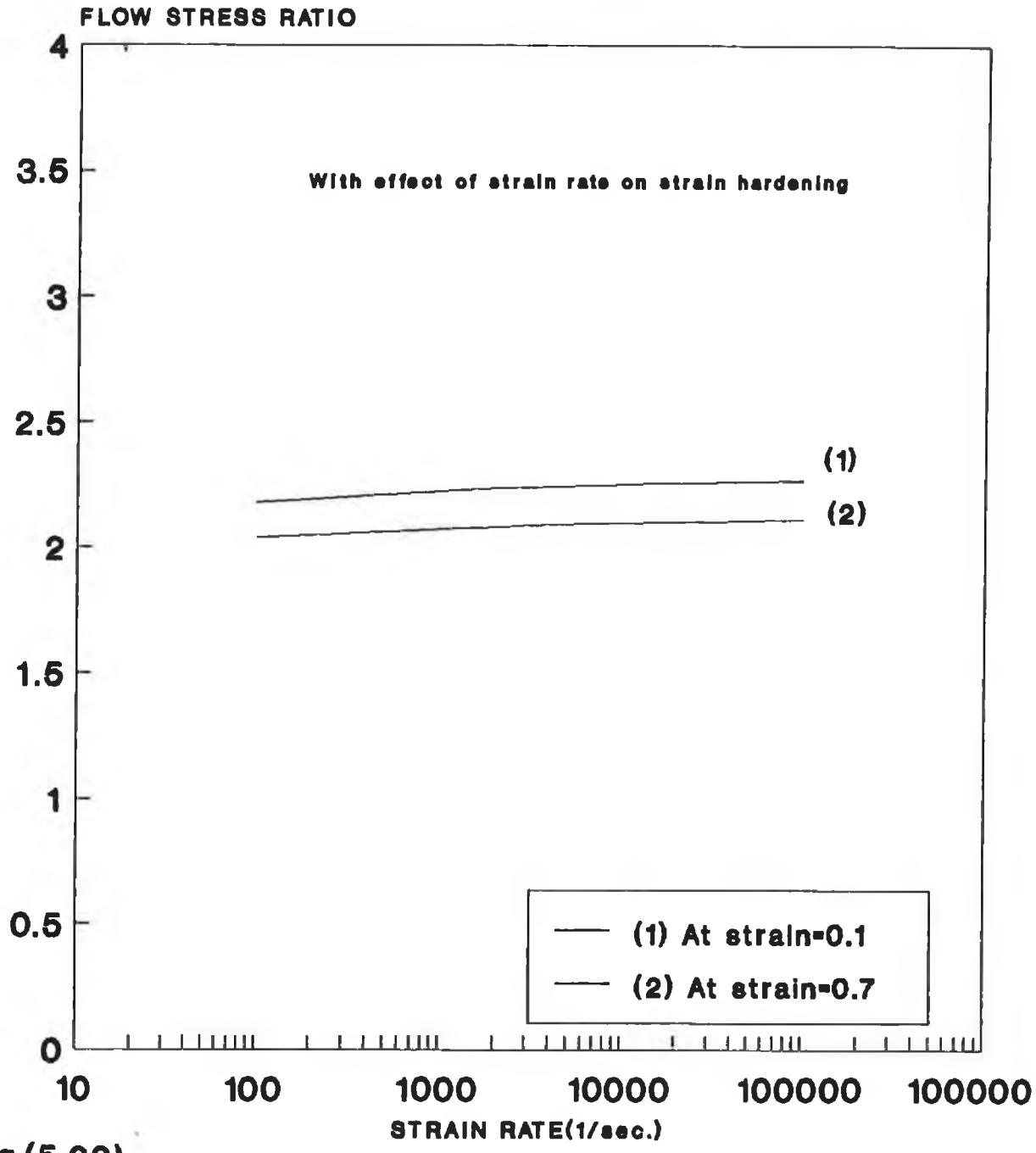

Fig.(5.26)

Effect of strain rate and thermal softening on strain hardening:

It appears from the result obtained so far that the strain rate sensitivity of material are effected by ;

1)Thermal softening factor(G).

2)Strain hardening factor(R).

It is clear from the results obtained using each of the above factors separately that these factors have an effect on the strain rate sensitivity of a material. This could be due to the fact that, when the first factor was incorporated in equation (4.20) the material becomes less sensitive to strain rate. And when the second factor was incorporated in equation (4.20) the material becomes more sensitive to strain rate.It was found that for the both factors the sensitivity varies with strain as strain increase sensitivity decrease at constant strain rate. Therefore, it would be essential to modify the proposed constitutive equation to take into account both effects (G and R).

The new form of the dynamic constitutive equation is given by;

$$\sigma_d = K G_1 \varepsilon^{n\alpha} [1+ (m\dot{\varepsilon})^p] \qquad (4.26)$$

where

$$\alpha = (G/R)$$

When equation(4.26) was incoporated into the numerical technique, new values for the material constant P^2 were obtained for good agreement with the experimental result (in terms of final dimension). The best fit value of the material constants are shown in Table[5.6] as following;

Table[5.6]

MATERIAL	m (sec.)	P
MILD-STEEL	0.3330	0.044
COPPER	0.0024	0.048
STAINLESS-STEEL	0.0040	0.0250

As the material constants m and P were obtained for all the materials investigated , the dynamic stress-strain curves for each material could be determined for strain rate varying between 10^2 to 10^5 per second as shown on Figs.(27) to (29). These figures also show quasi-static curves which can be used for comparison.It is clear that, there is interaction between the two factors (thermal softening and strain rate hardening), where as the thermal softening appears to make the material less sensitive to strain rate (decreases the flow stress) but the other factor appears to increase this sensitivity (increases the flow stress).

---

[2] It was found that no significant change the value of (m) when the effect of strain rate and temperatuer taken into account, and it seems to be that the value of P has significant change than the valur of m.

In the case of copper and mild-steel the effect of strain rate are more clear and the sensitivity increases significantly. It can be seen also that as the strain increases the flow stress decreases.

Fig.(5.30) to (5.32) represents the ratio of flow stress against the strain rate at a given strain.The ratio, at strain rates ranging between 10^2 to 10^5 per second and strain equal to **0.1**, were found to be (2.27-2.68), (1.87 - 2.26) and (2.15 - 2.25) for mild steel, copper and stainless steel respectively. At strain equal to **0.7** the ratio are varies between (1.98-2.35), (1.75-2.1) and (1.94-2.04) for mild steel, copper and stainless-steel respectively.

Theoretical curves
True stress-strain curve of Mild-steel

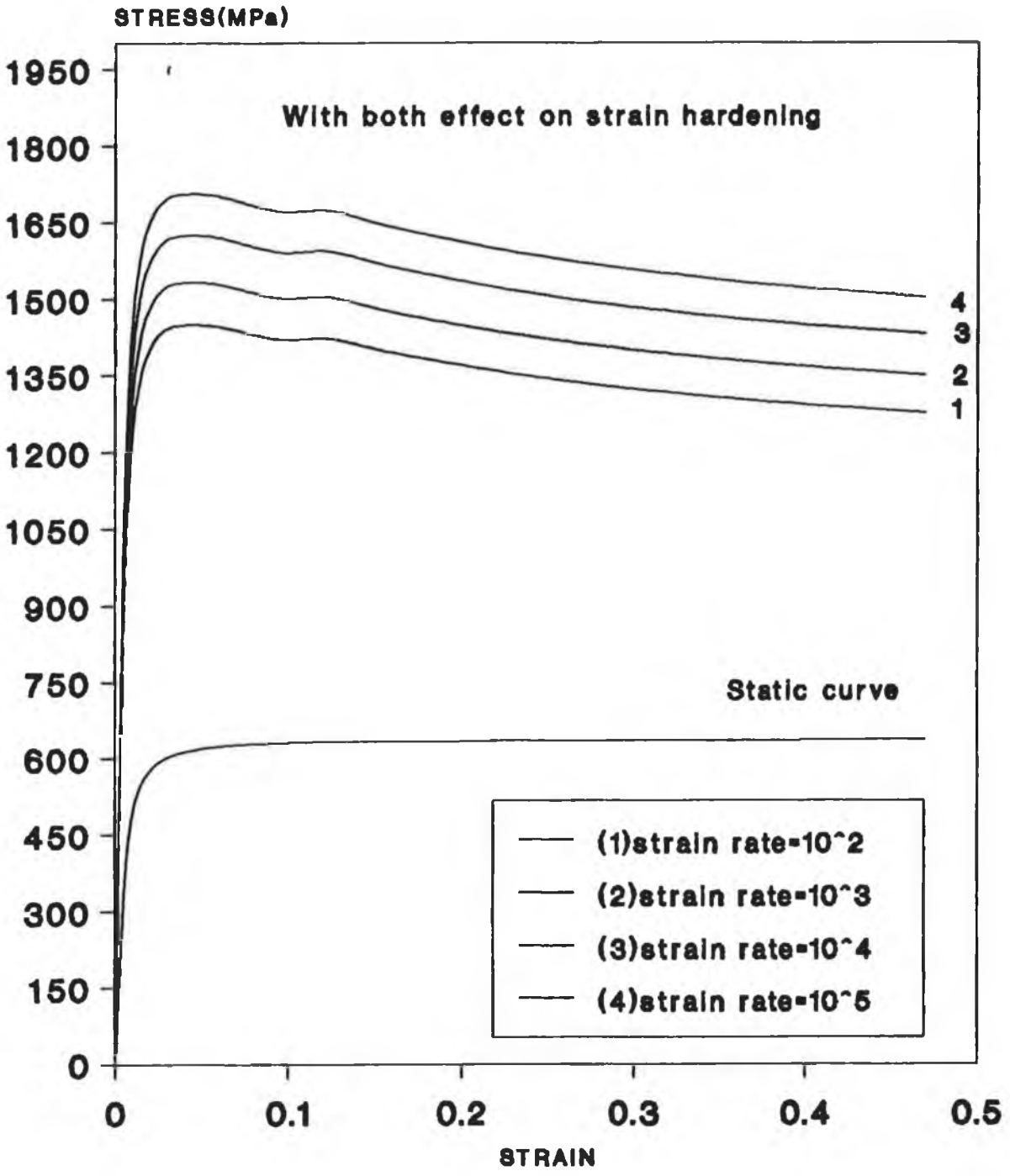

Fig.(5.27)

Theoretical curves
True stress-strain curve of Copper

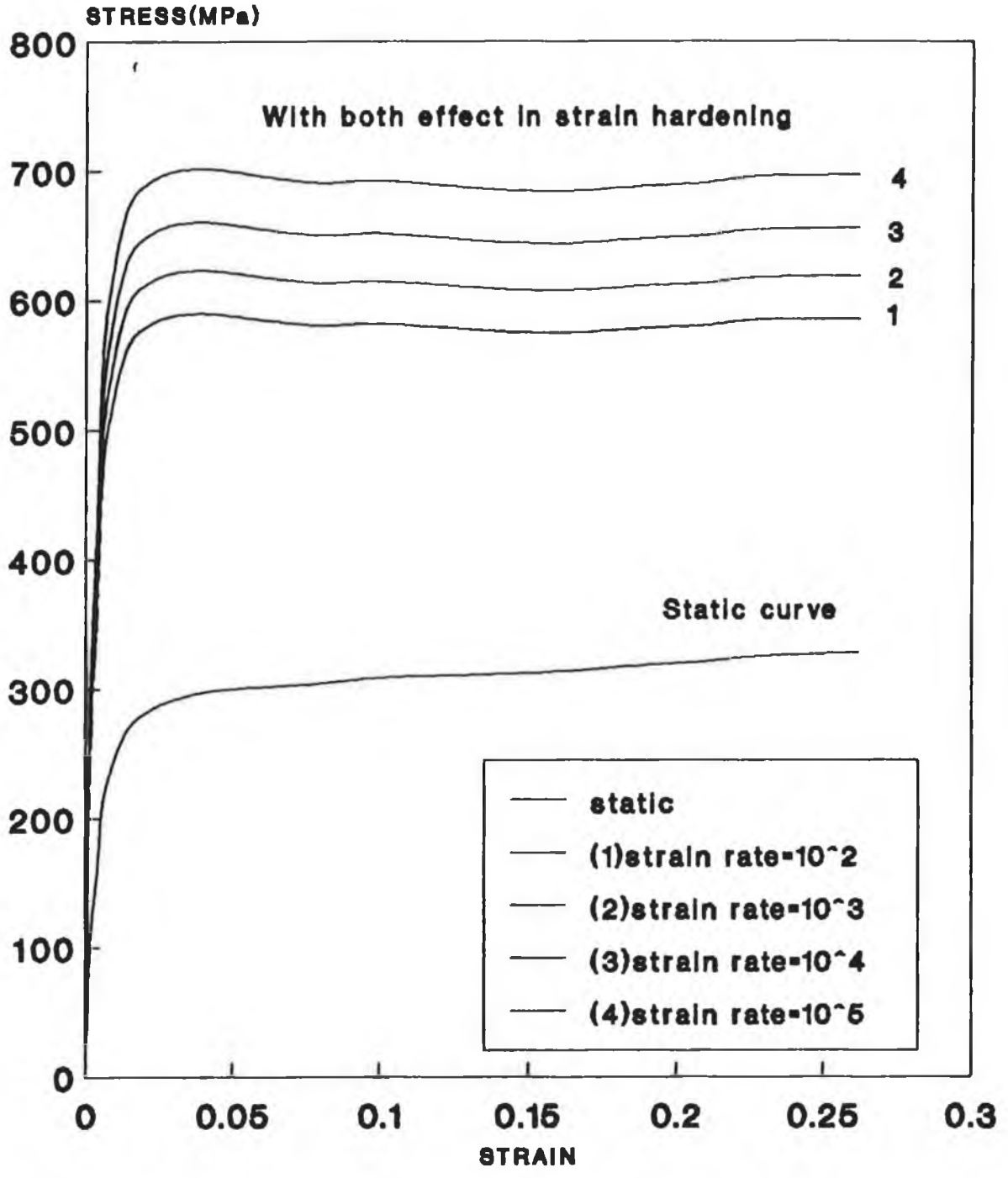

Fig.(5.28)

Theoretical curves
True strain-stress curve of Stainless-steel (304)

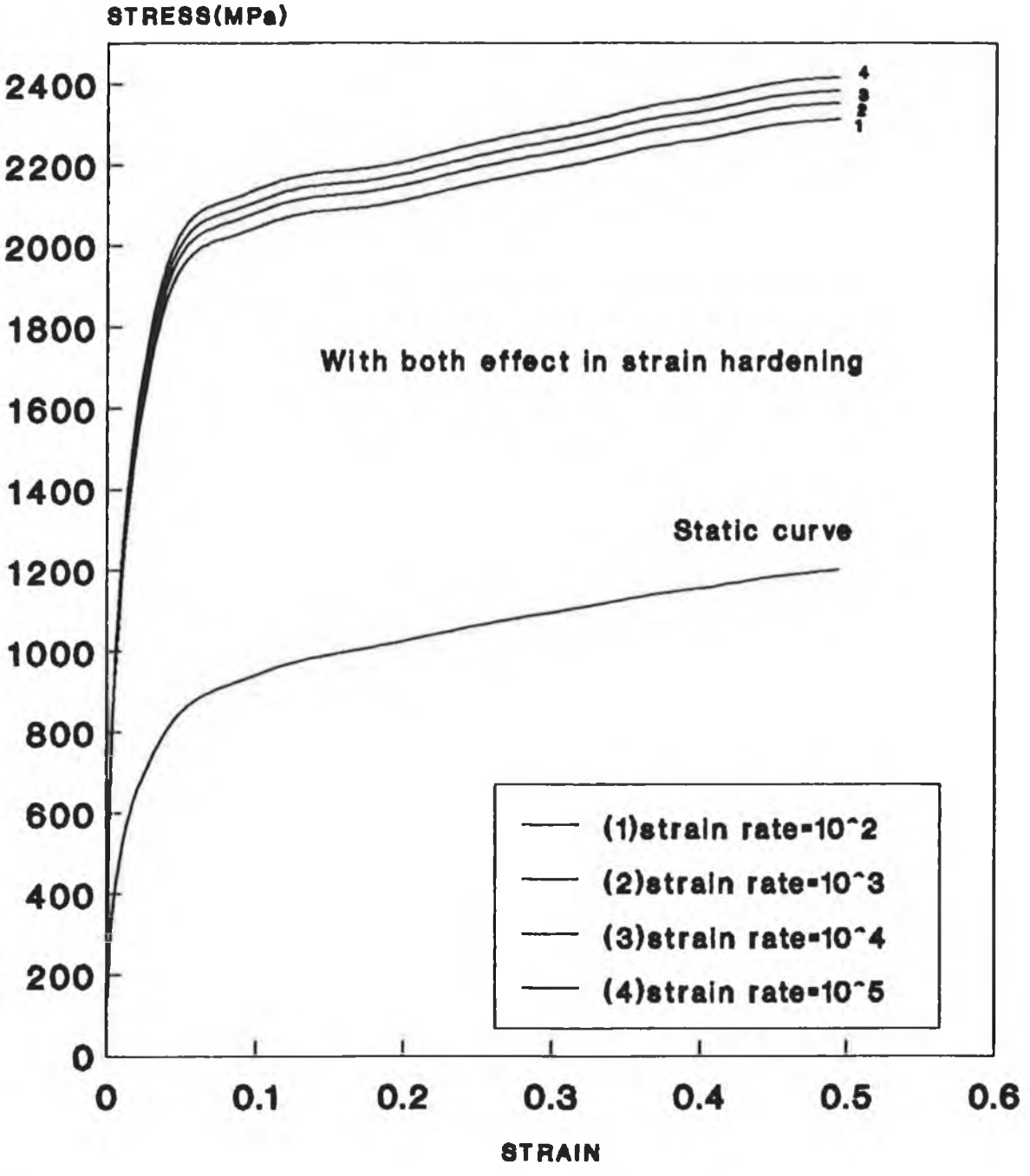

Fig.(5.29)

Theoretical curves
Variation of flow stress ratio with strain rate for Mild steel

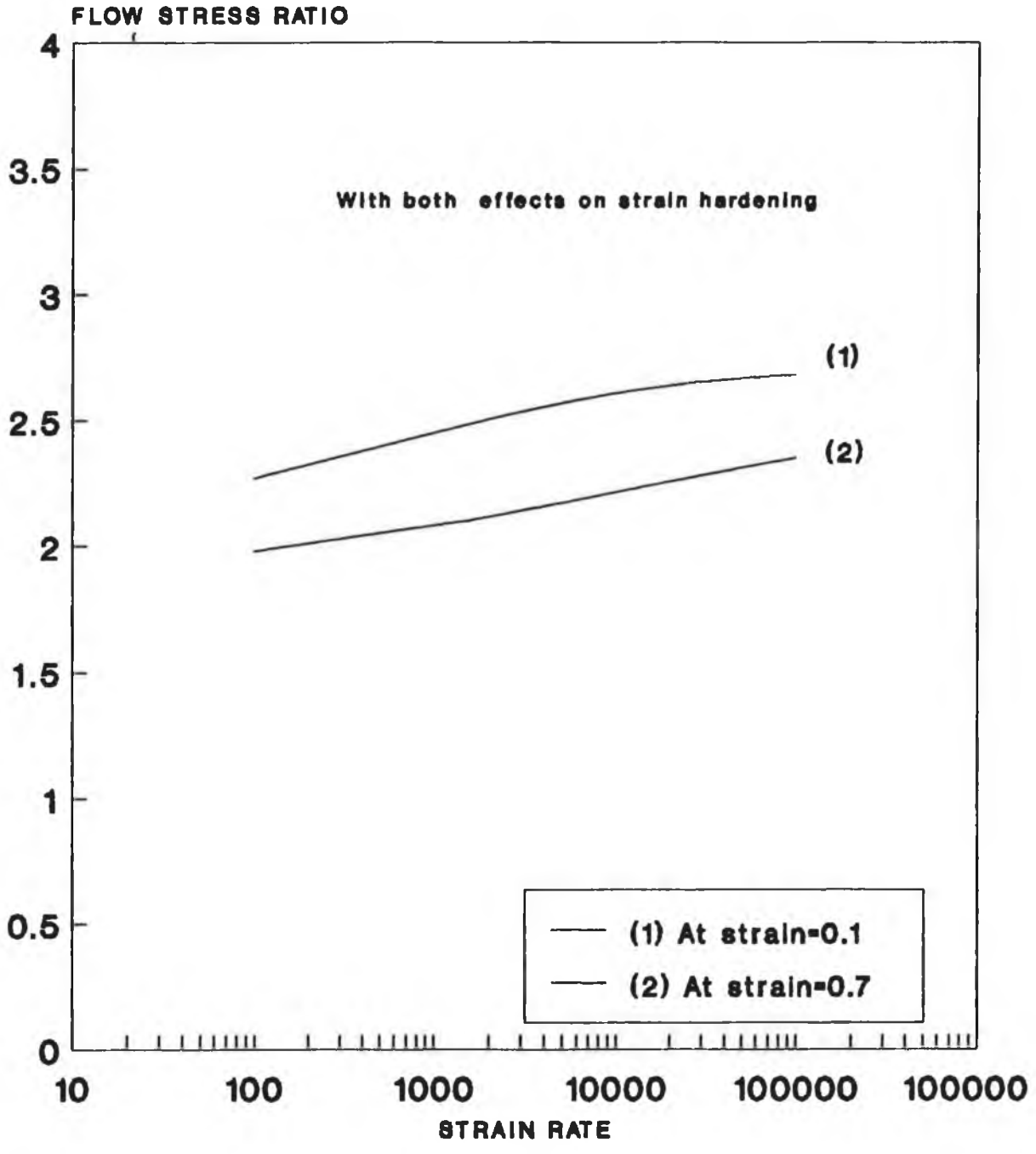

Fig.(5.30)

Theoretical curves
Variation of the flow stress ratio with strain rate for Copper

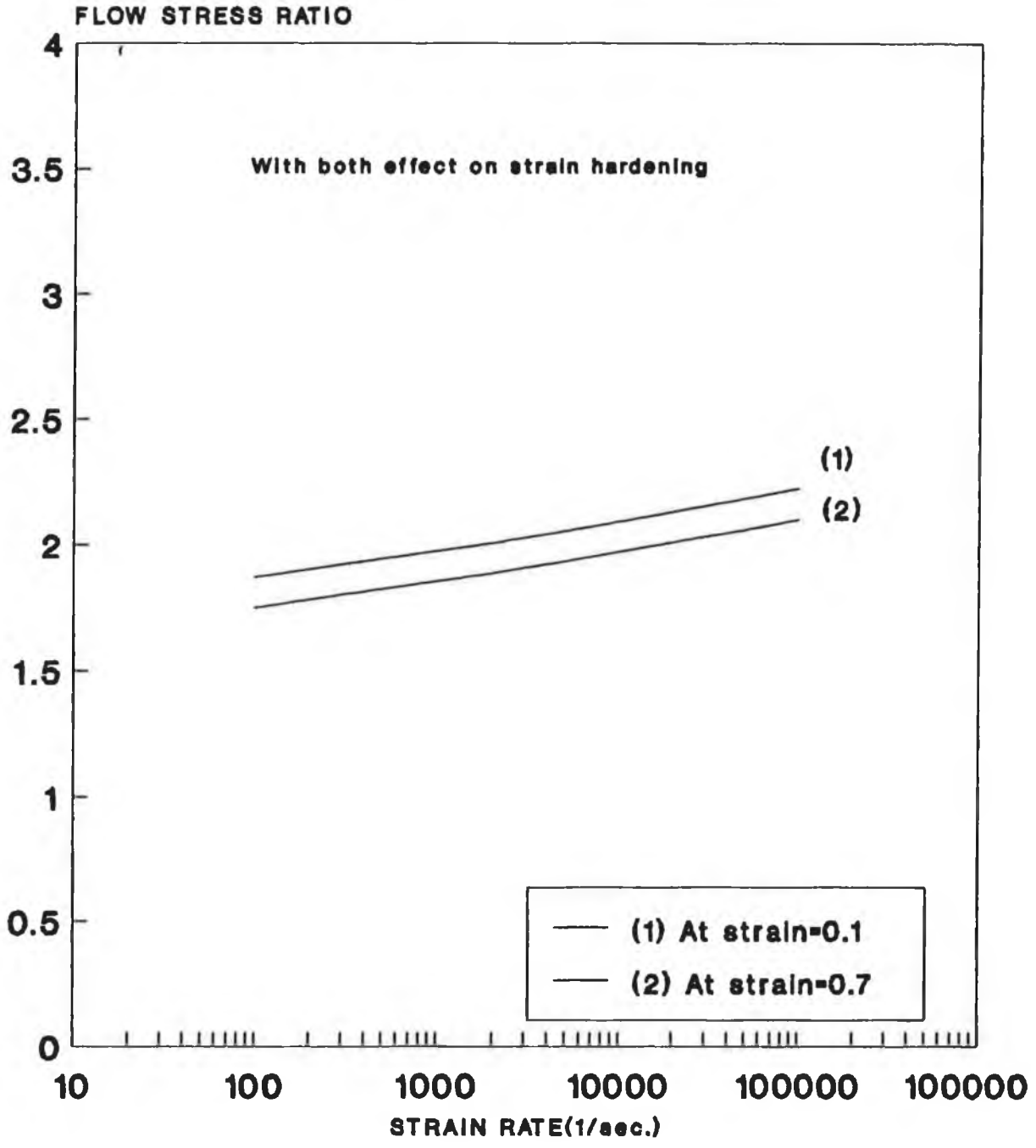

Fig.(5.31)

Theoretical curves
Variation of flow stress ratio with strain rate for Stainless-steel(304)

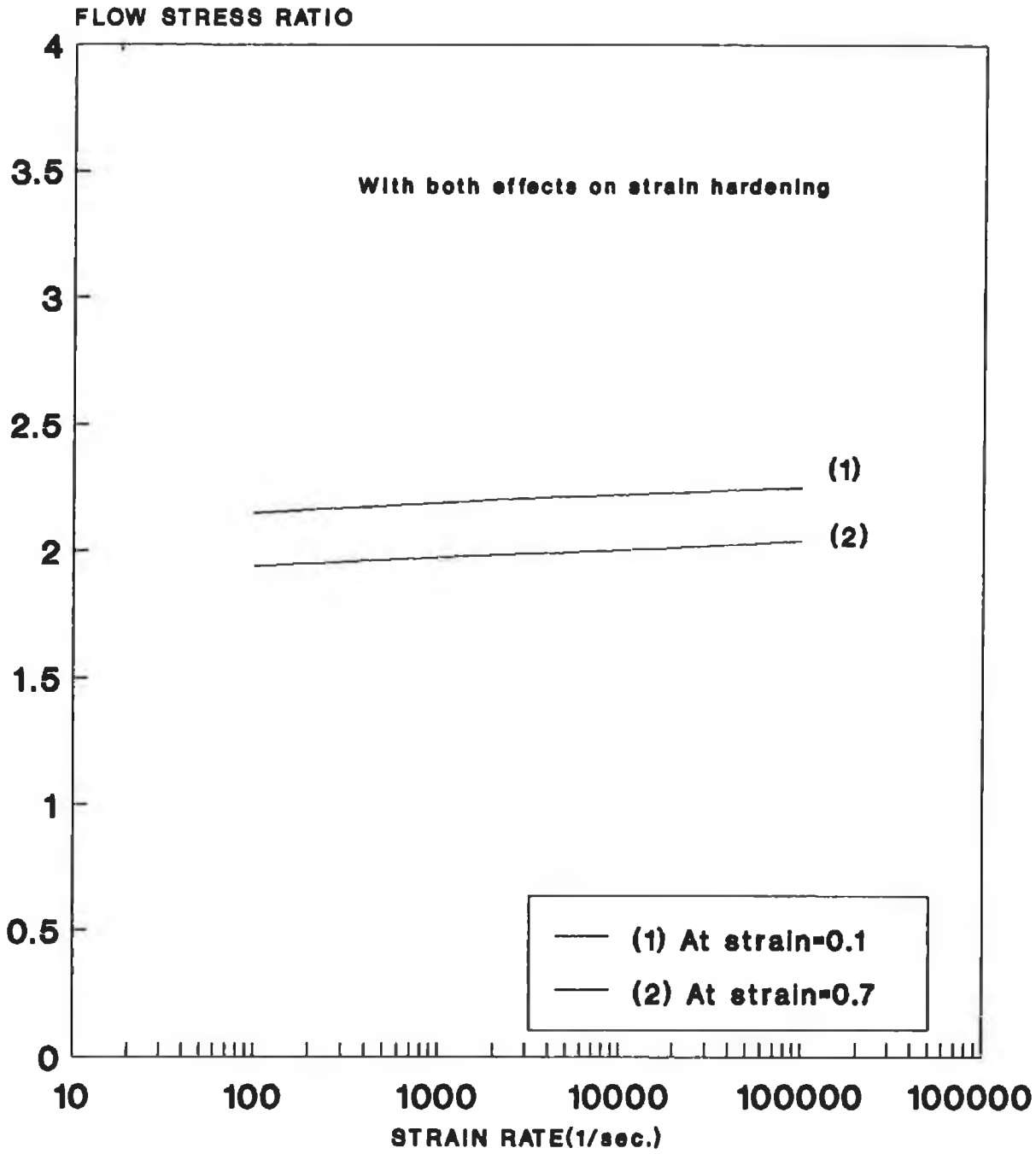

Fig.(5.32)

Effect of elastic deformation of the projectile and the anvil :

In order to study the effect of elastic deformation of the projectile and anvil due to stress wave propagation on the high strain rate constitutive equation, the whole system (projectile, specimen and anvil) was represented by lumped mass model as shown in figur (4.4), and the boundary condition was changed accordingly.The projectile and anvil deformed elastically only, since these were made of much stronger material than that of the specimen.

When the elastic plastic deformation of the combined system was simulated on a PC computer(Appendix BB) in order to provide a new prediction to the material constant (m and P) no significant change on the value of (m and P) was observed and only a small increase in the elastic energy was noticed. More description about the effect of stress wave propagation on the force is given in section B.

Summary of section(A) :

Figs.(33)to(35) show the isothermal and adiabatic stress-strain curves obtained at static and dynamic modes for Mild steel, Copper and Stainless steel respectively. It can be seen that at small strains of up to 0.1, 0.05, 0.2 for mild steel, copper and stainless steel respectively, the two dynamic flow stresses (adiabatic and isothermal) are close together, while as the strain increases the adiabatic dynamic flow stress decreases (due to temperature rise). The strain rate for the dynamic curves in all these three figures is 10^4 per second.

Figs.(36)to(38) show a family of dynamic stress-strain curves obtained using all the proposed equations at a constant strain rate of 10^4 per second. These figures suggest that,

(i) Curve (1) represents the stress-strain relation obtained by equation (4.20).One of the limitation of this equation is that it keeps the same shape as the static curve, but simply shifts it vertically with the strain rate.

(ii) Curve (2) represents equation (4.23) . This curve indicates that, as the strain increases the flow stress obtained is lower than the flow stress obtained by using equation (4.20), and also that the rate sensitivity decreases with the increase in the strain.

(iii) Curve (3) represents equation (4.24).It is clear that the flow stress is higher than those obtained by the other equations. It can be concluded that, as the strain increases the flow stress decreases due to the decrease in the rate sensitivity of the material with strain.

(iv) Curve(4) represents equation(4.26) which takes into account the effect of strain rate and thermal softening on the strain hardening.The result obtained indicates that the flow stress for small strains is greater than the flow stress obtained by Equations 4.20 and 4.23 .

Figs.(39a) to (41a) show the effect of strain rate on the flow stress ratio at a strain of 0.1 according to the four different equations derived for all the three materials.Similar ratio curves are show in figs(39b) to (41b) for strain of 0.7. In all the above figures the curve denoted by (4) is represented the result obtained by using the final version of the dynamic consiitutive equation (4.26).

Figs.(42)to(44) shown the stress ratio at strain 0.1 obtained according to the the final version of the dynamic constitutive equation (4.26) for Mild steel and Copper in compassion with other reported work done in the same field.

Theoretical curves
True stress-strain curves of Mild-steel

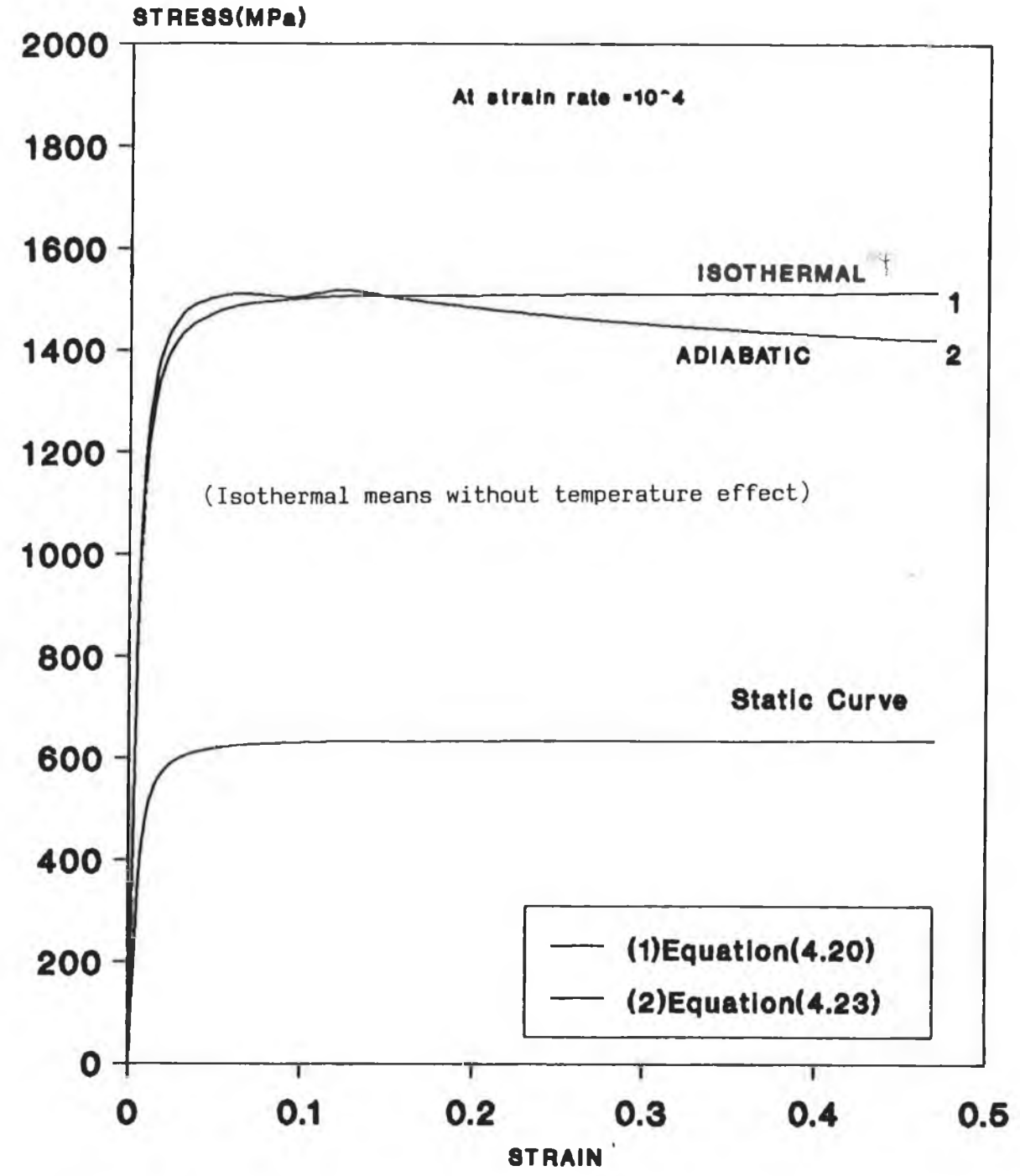

Fig.(5.33)

Theoretical curves
True stress-strain curve of Copper

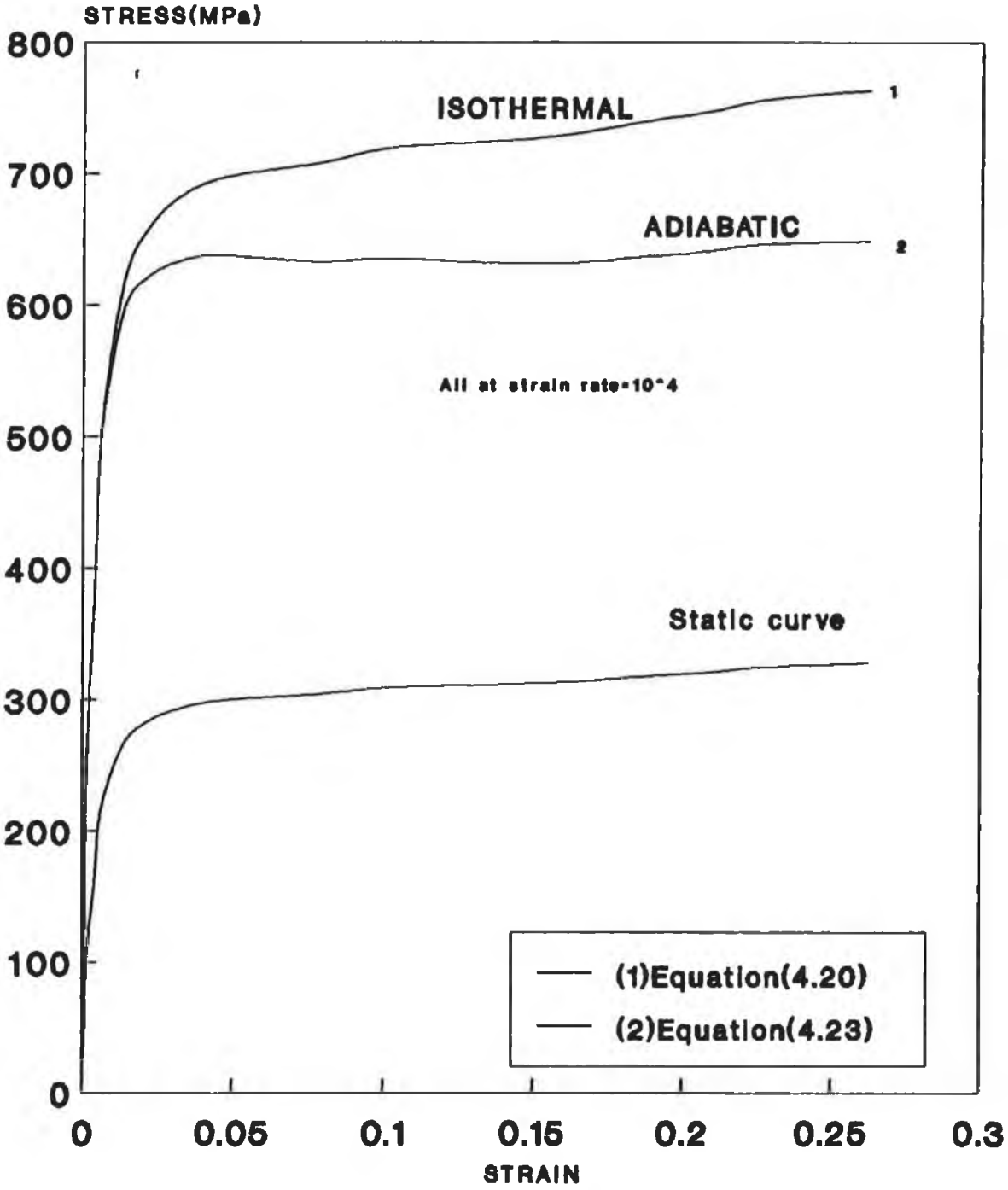

Fig.(5.34)

Theoretical Curves
True strain-stress curves of Stainless-steel (304)

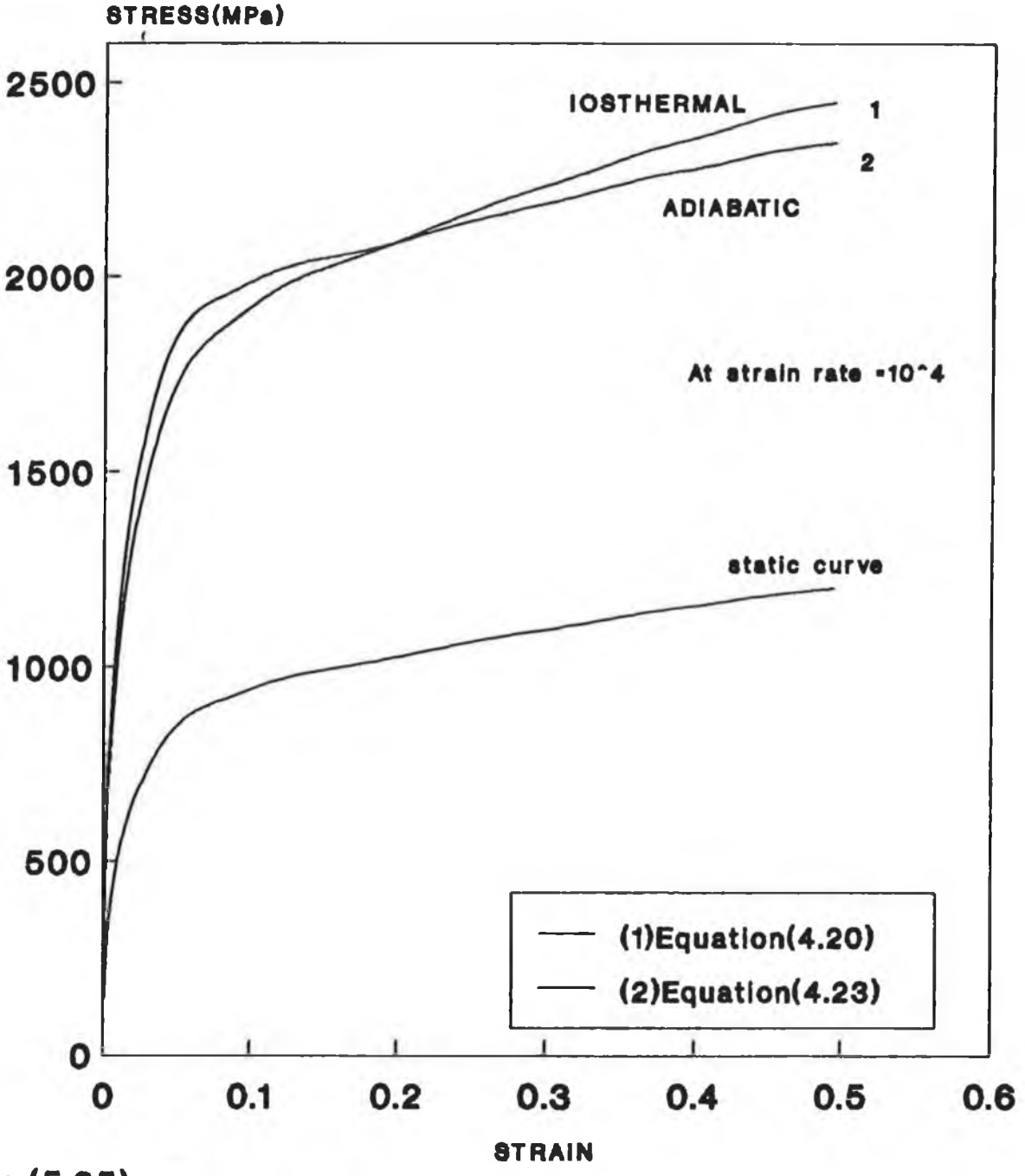

Fig.(5.35)

Theoretical curves
True stress-strain curves of Mild-steel
With Temperature effect

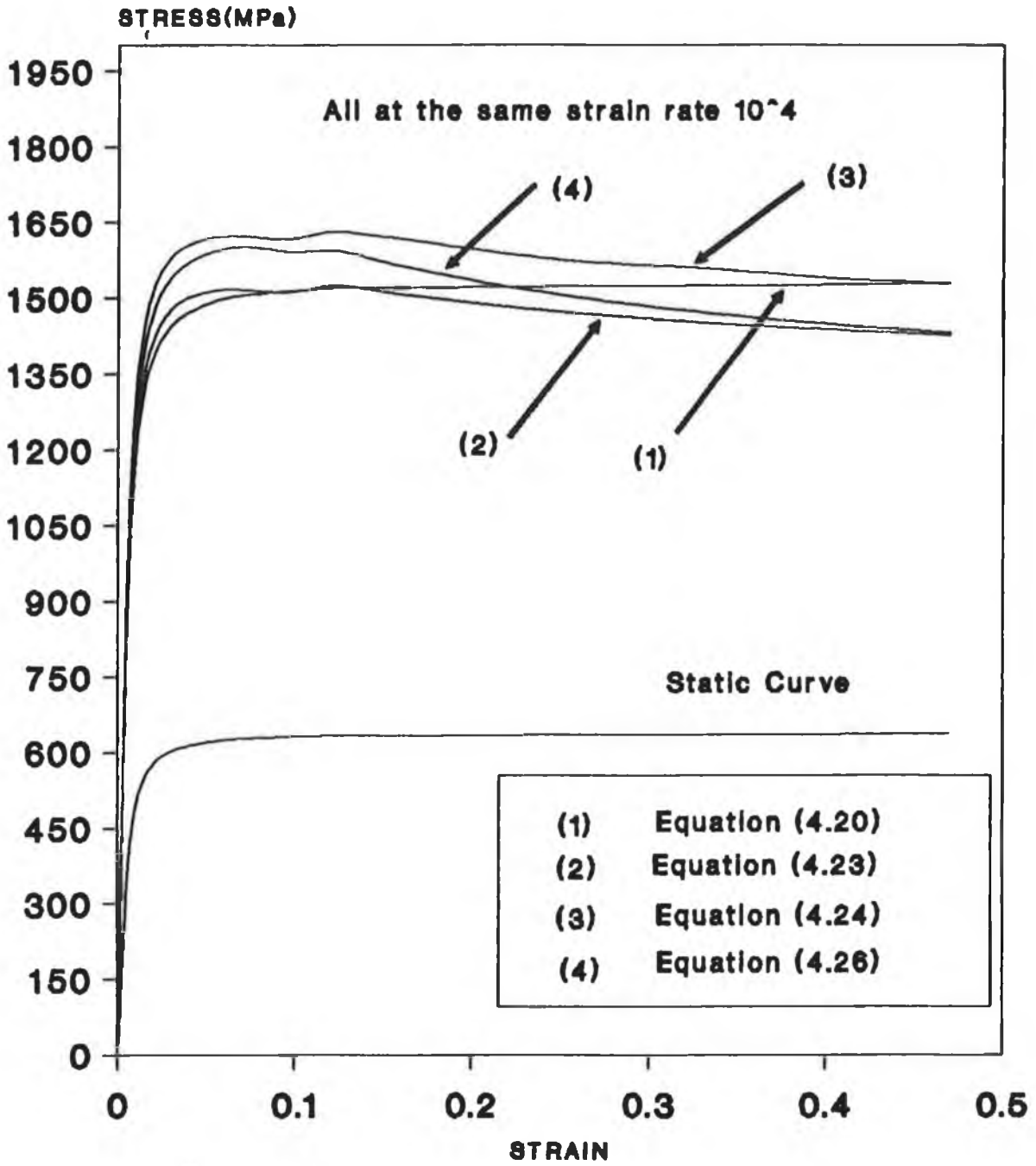

Fig.(5.36)

Theoretical curves
True stress-strain curve of Copper

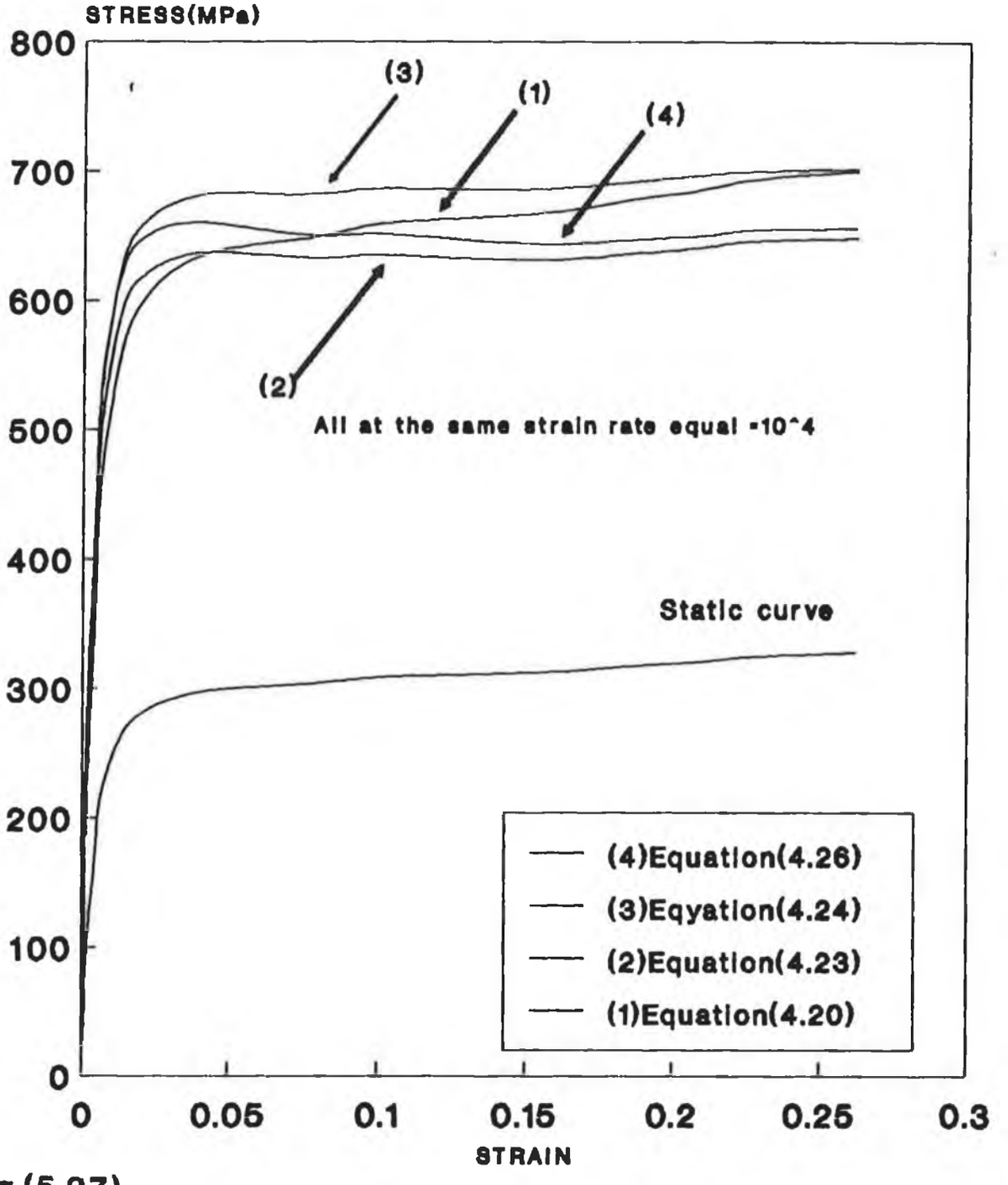

Fig.(5.37)

Theoretical Curves
True strain-stress curves of Stainless-steel (304)

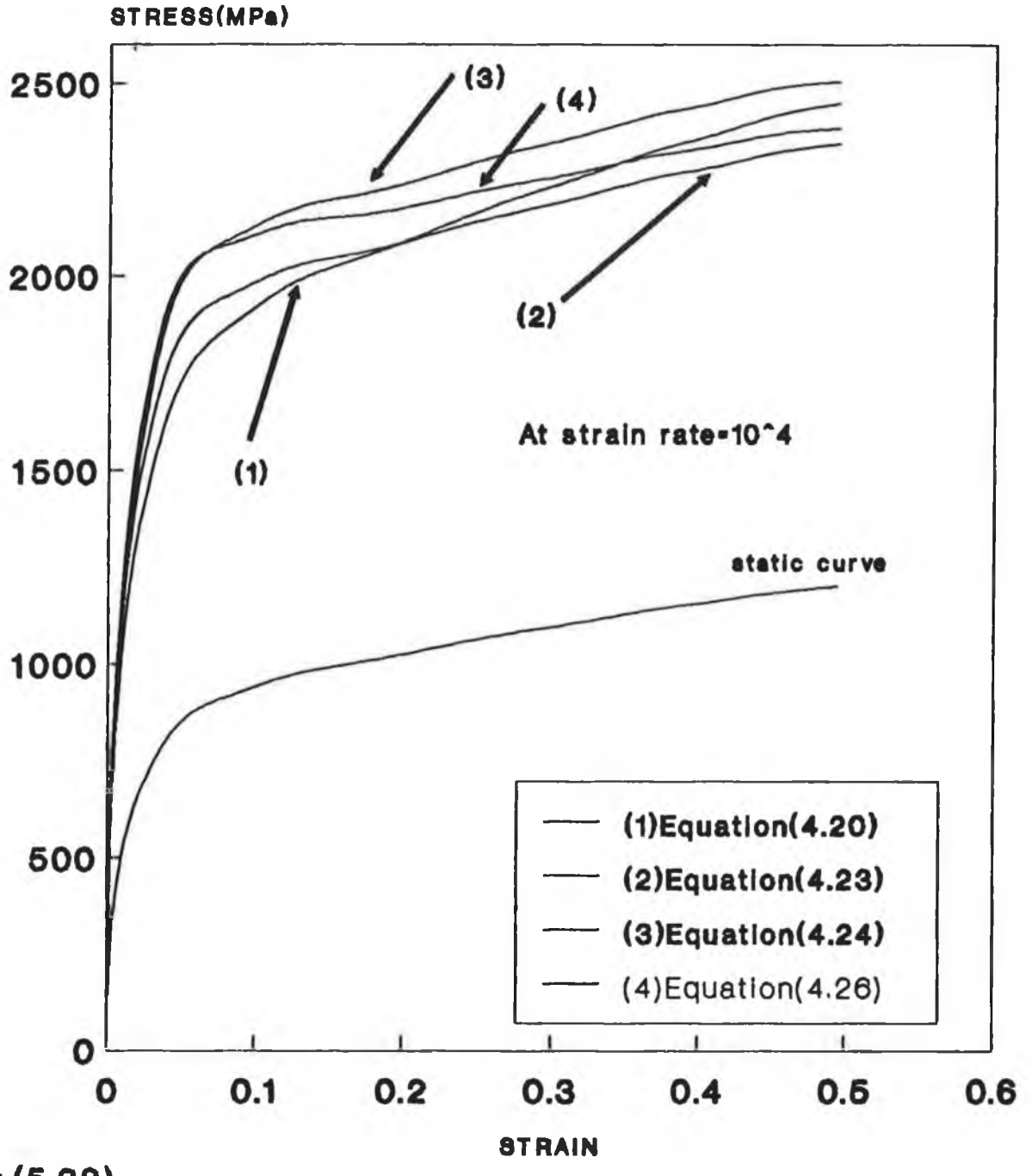

Fig.(5.38)

Theoretical curves
Variation of flow stress ratio with strain rate for Mild steel

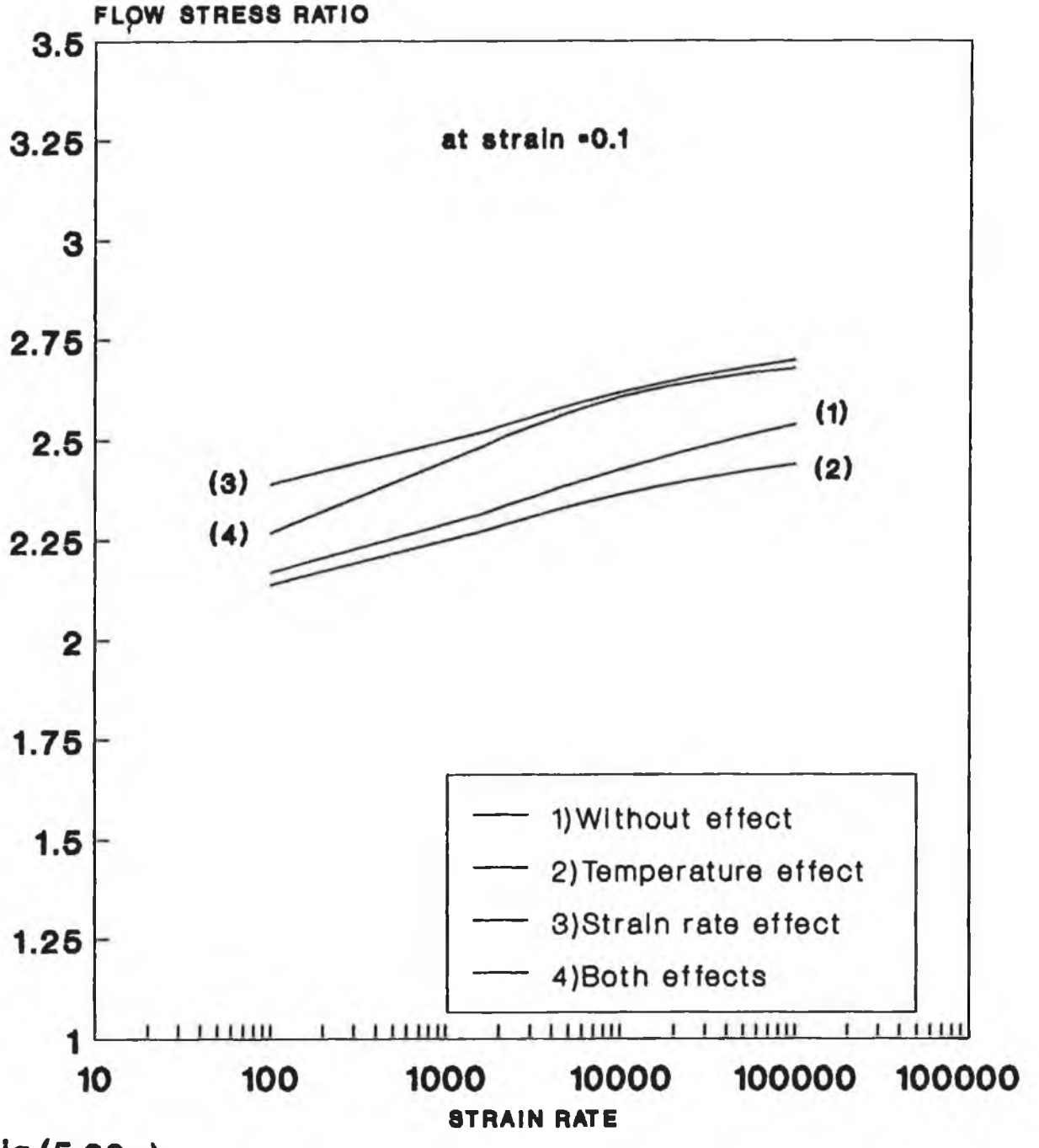

Fig.(5.39a)

Theoretical curves
Variation of flow stress ratio with strain rate for Mild steel

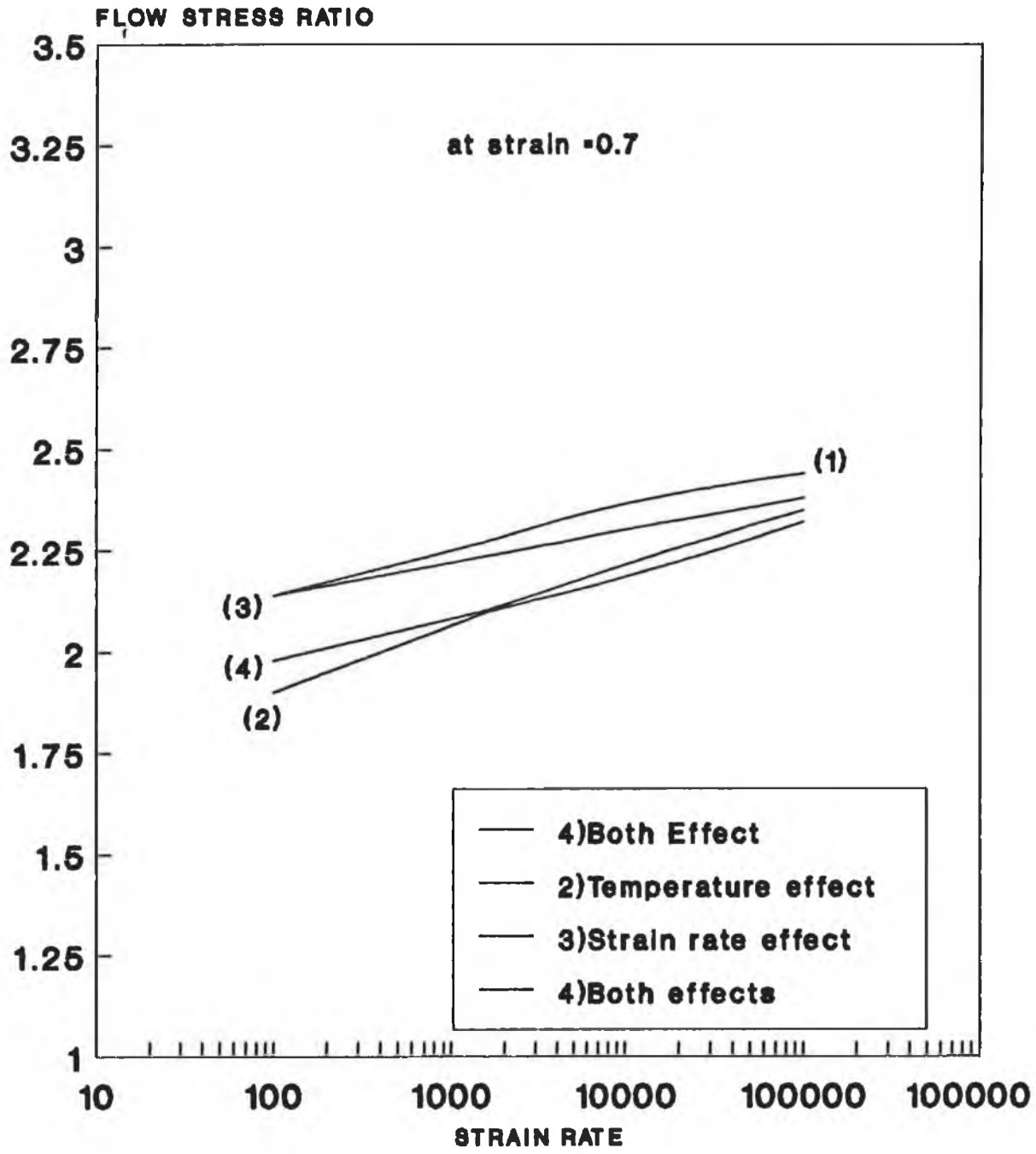

Fig.(5.39b)

Theoretical curves
Variation of flow stress ratio with strain rate for Copper

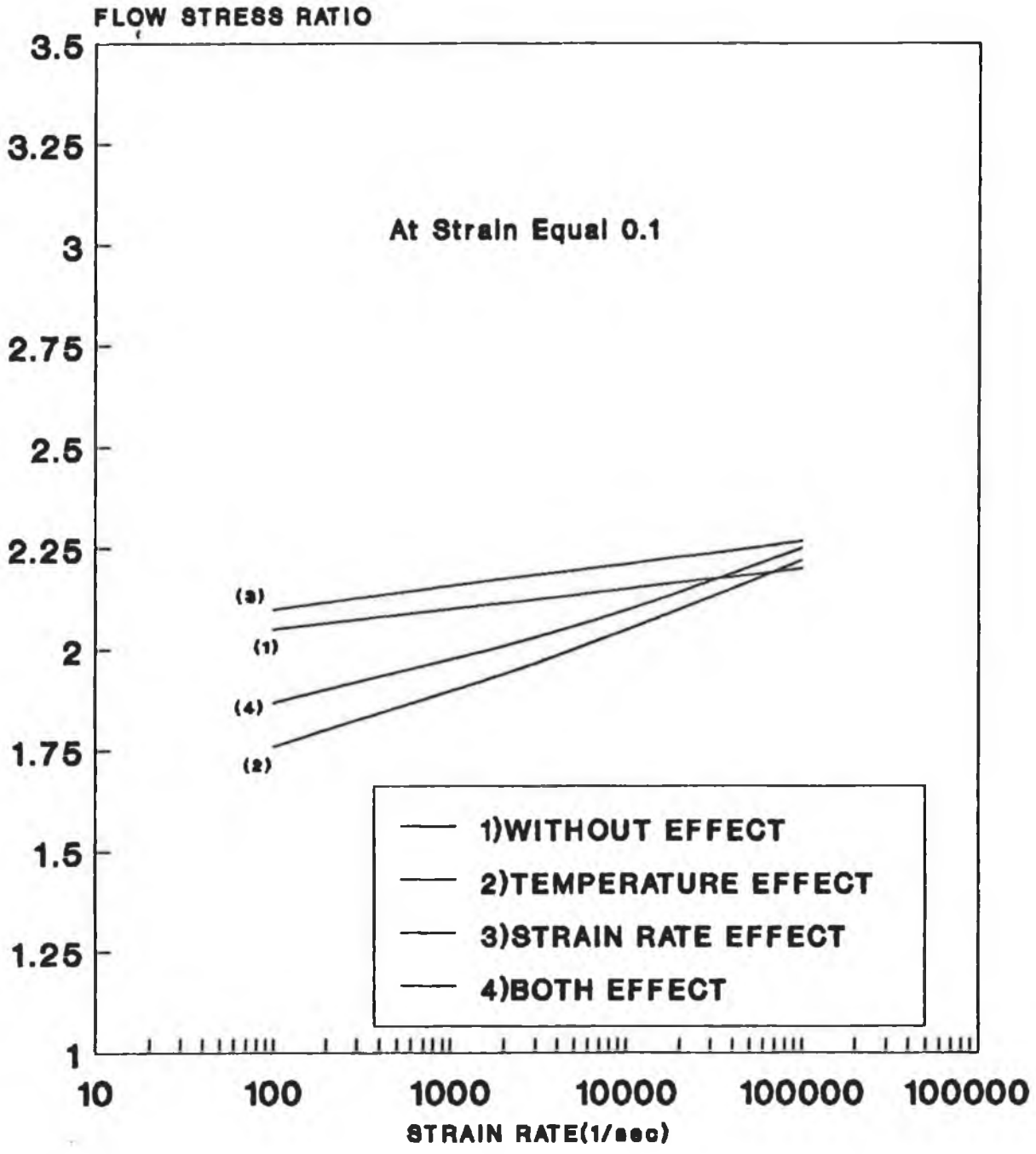

Fig.(5.40a)

Theoretical curves
Variation of flow stress ratio with strain rate for Copper

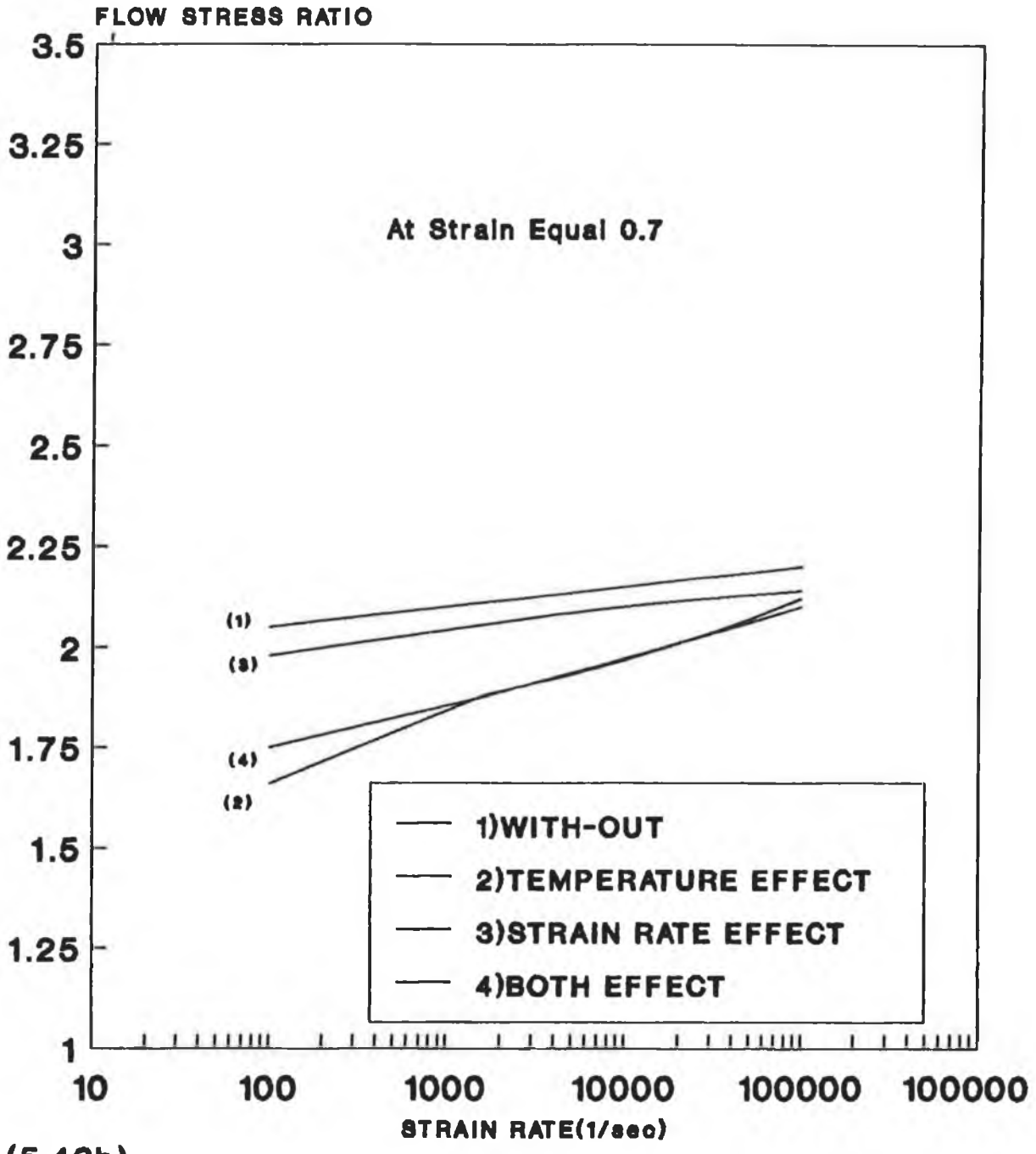

Fig.(5.40b)

Theoretical curves
Variation of flow stress ratio with strain rate for Stainless steel(304)

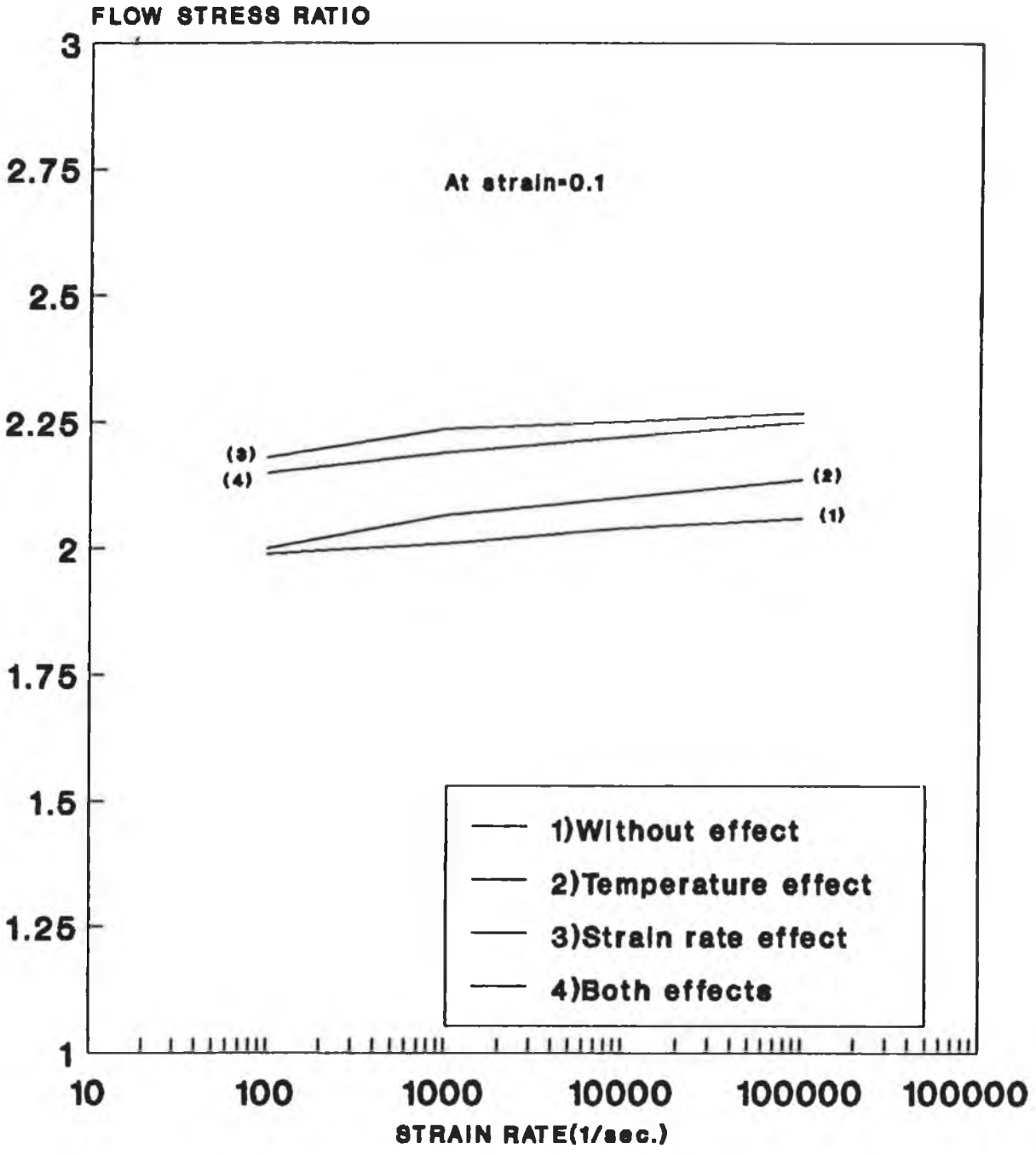

Fig.(5.4 1a)

Theoretical curves
Variation of flow stress ratio with strain rate for Stainless steel(304)

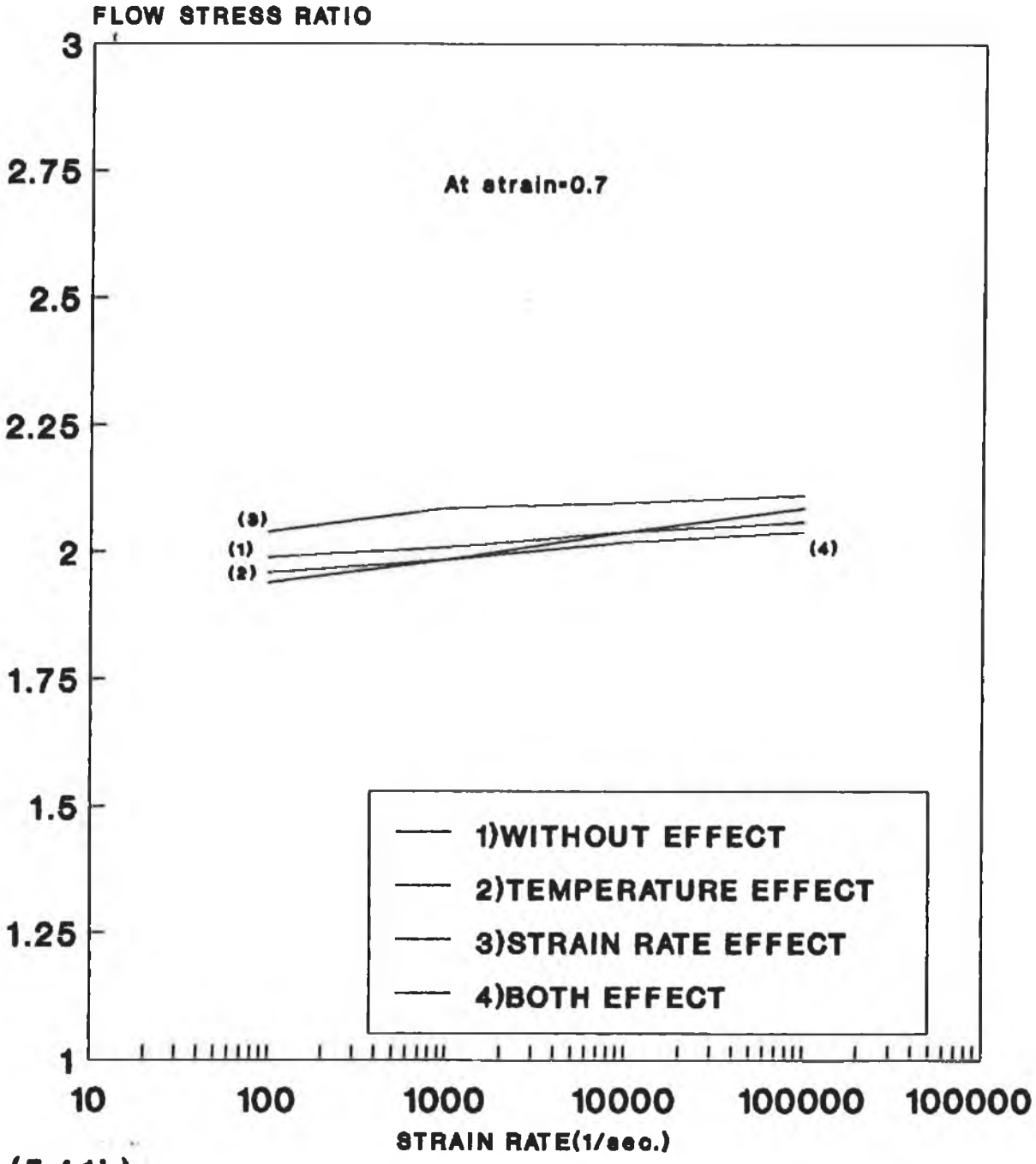

Fig.(5.41b)

Theoretical curves
Comparison of stress ratio versus strain rate curves with similar work done

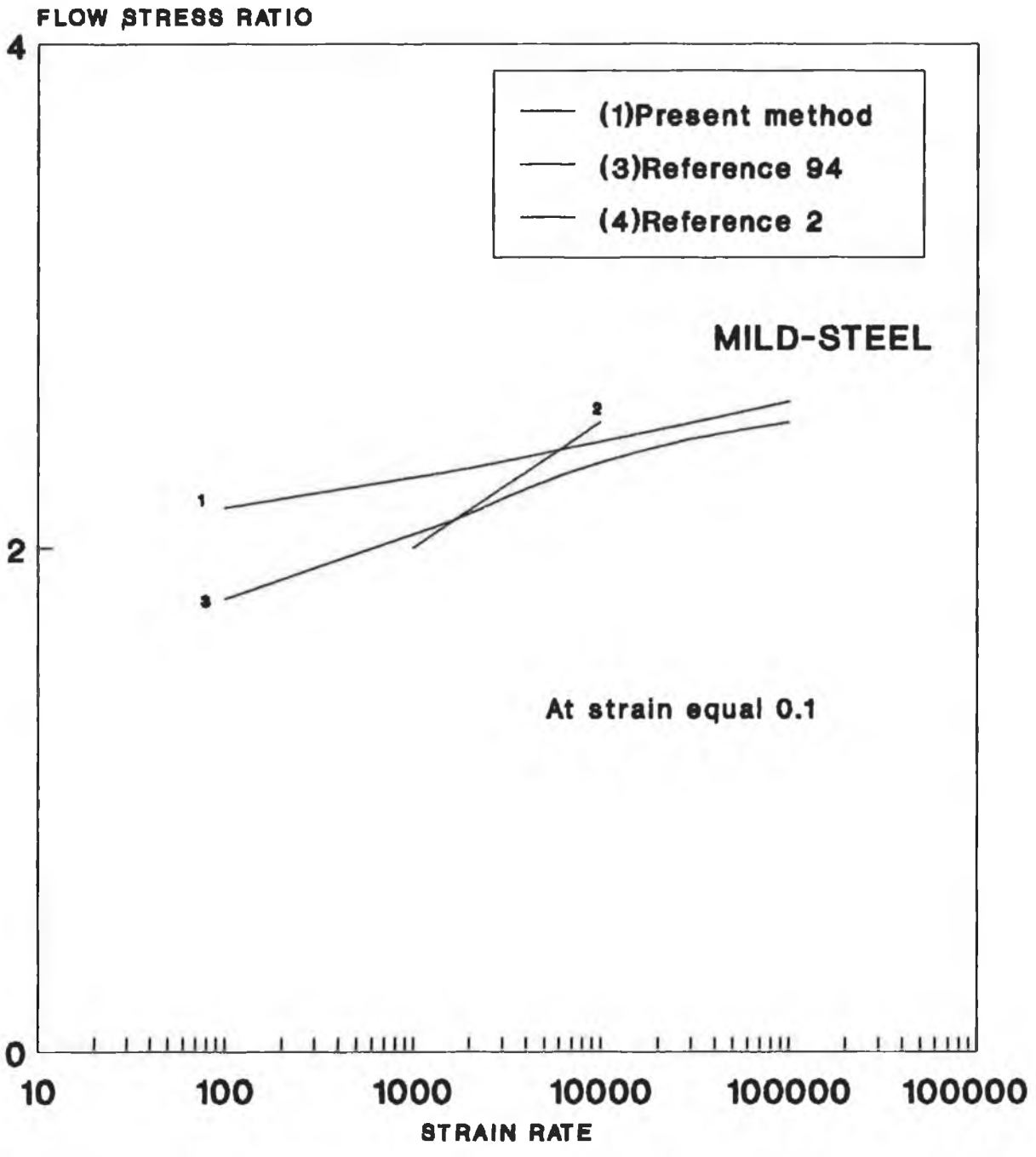

Fig.(5.42)

Theroetical curves
Comparison of stress ratio versus strain rate curves with similar work done.

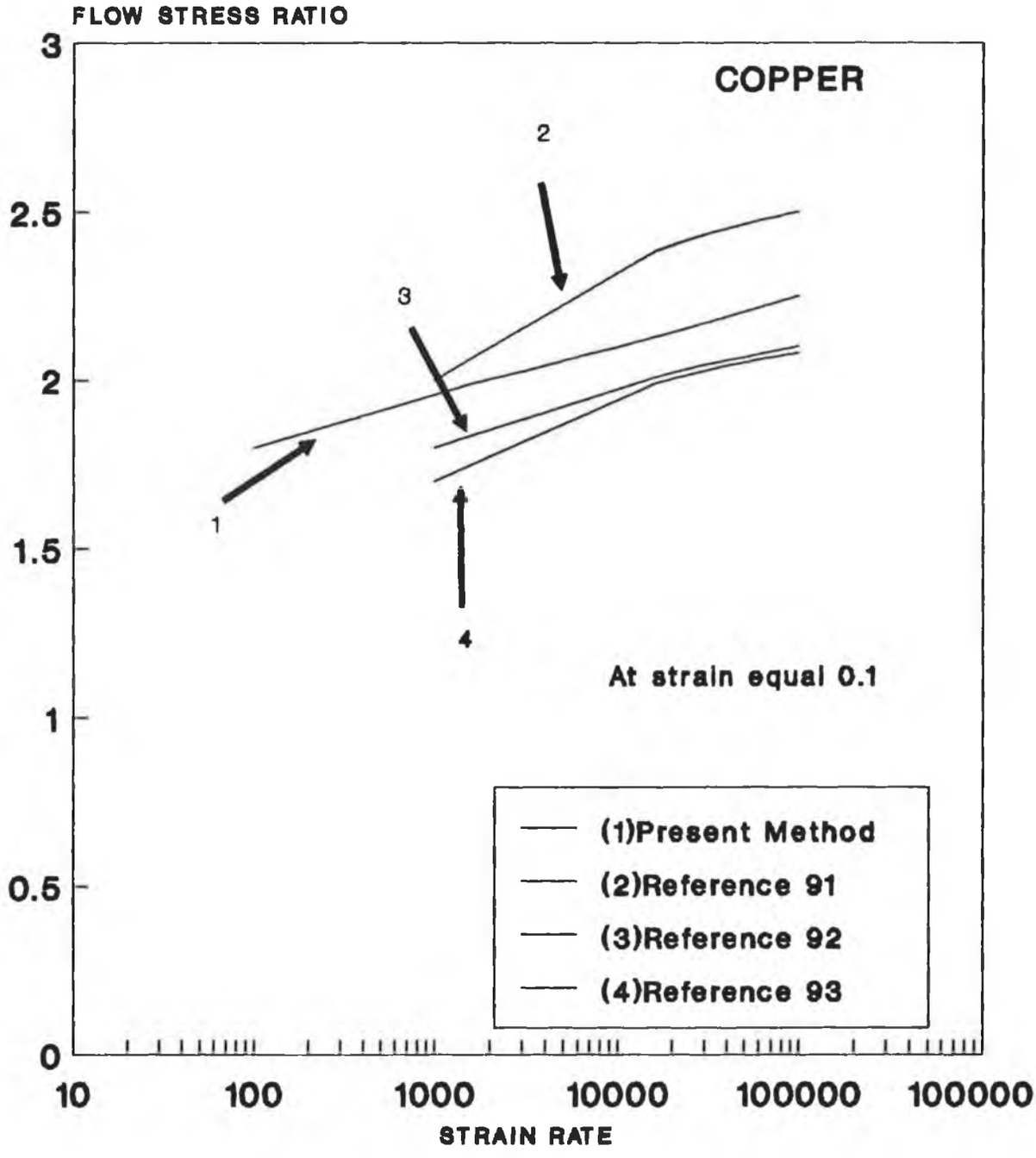

Fig.(5.43)

Section (B)

HISTORY OF THE DEFORMATION

The aim of this section is to give a brief description of the deformation history caused by the impact of the tool steel projectile against the cylindrical test specimen.The deformation was simulated using a PC computer program based on finite difference numerical technique and the proposed constitutive equation (4.26) .The output of the computer program were represented by graphical results in order to describe the deformation behaviour during the impact.

Fig.(5.45) shows the predicated force time-trace for a typical impact test. This figure shows the variation of the force on the contact faces of the projectile and the anvil (upper and lower faces of the specimen) which indicates that during the initial period, up to 5μsec following impact, the force on the upper face is greatest and subsequently the lower force becomes greater than the upper force after 5μsec. The most likely explanation to this is probably the stress wave effect.

Fig.(5.46) shows the variation of the force with the contact time at two different impact speeds.This figure indicate that, the upper and the lower forces become closer as a result of the decreased impact velocity. This may be due to fact that as the velocity decreases the stress wave effect becomes less noticable .

Theoretical curves
Load-time history during deformation of Mild steel specimen

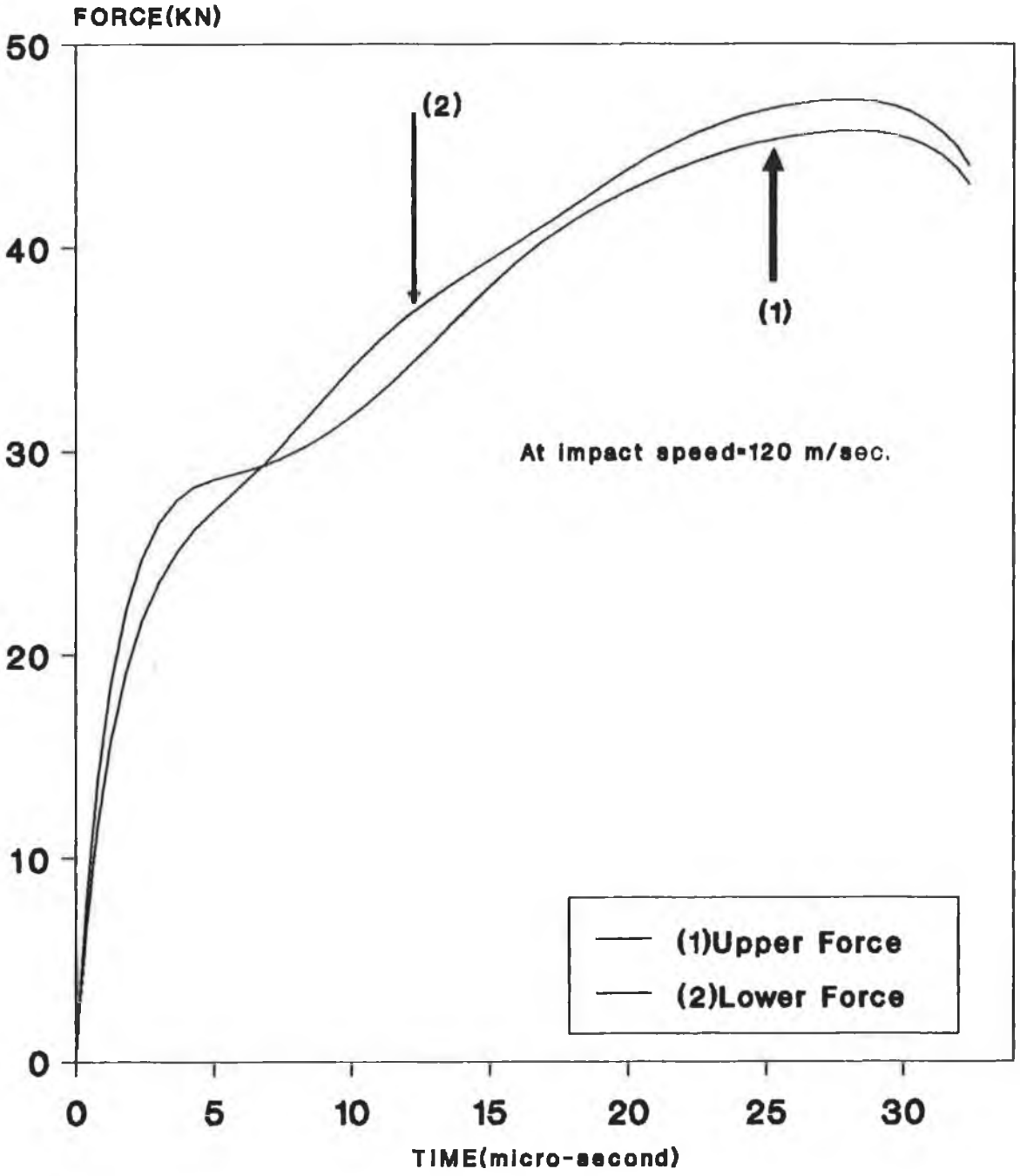

Fig.(5.45)

Theoretical curves
Force-time history during deformation of Mild steel specimen

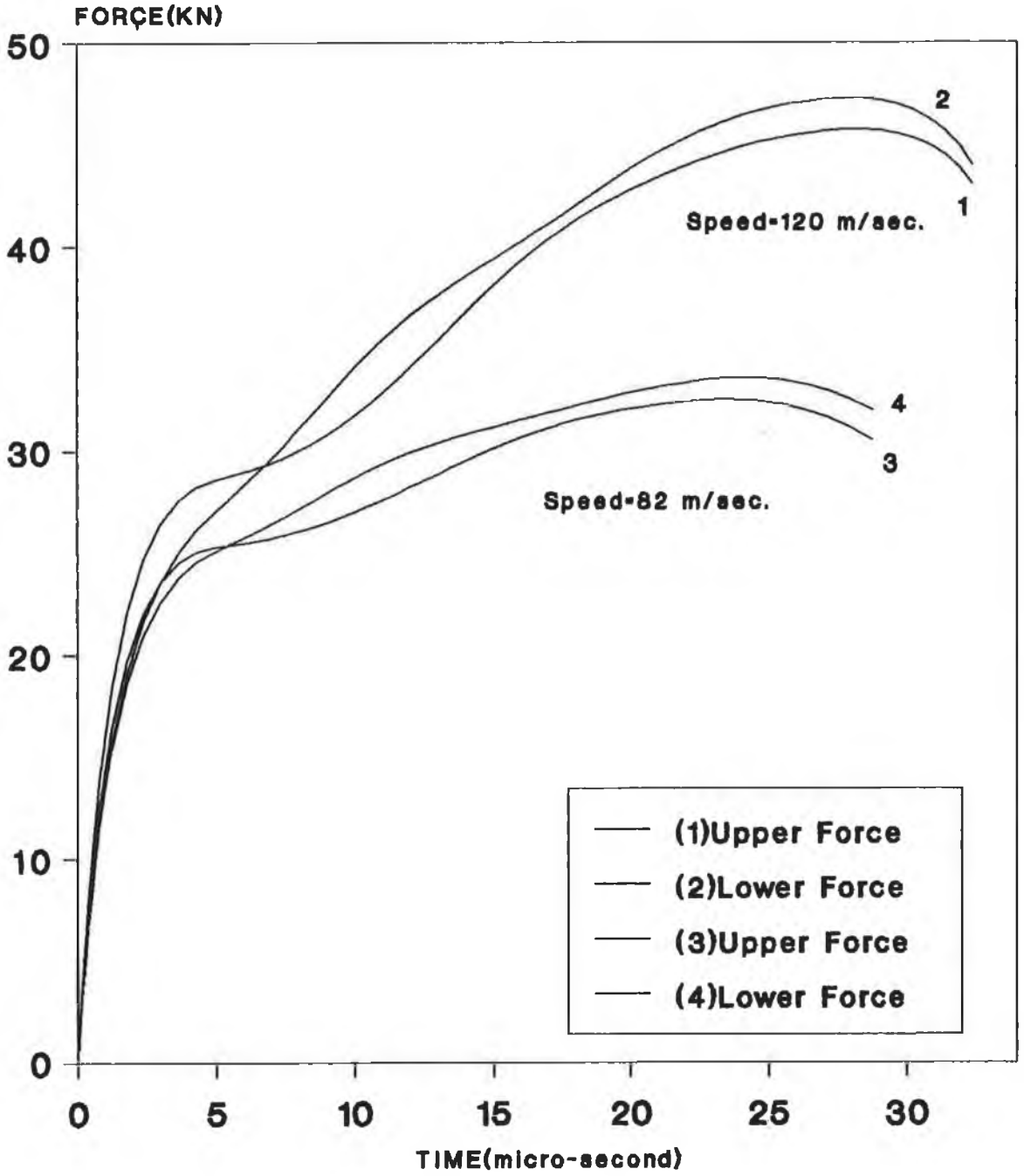

Fig.(5.46)

Fig.(5.47) shows the ratio (upper to lowere force) of the force generated at the projectile and the anvil inerfaces plotted against the specimen deformation. The ratio was found to be high during the initial period following the impact and then dropped in a linear manner to a range of (1.2 to 1.0) for up to 20% of the total deformation. However, subsequently, this percentage ratio varies with a ripple due to the effect of the stress wave while the deformation increases.

Fig.(5.48) shows the variation of force ratio (upper to lower force) against the deformation at two different velocities. It can be seen that the force ratio varies in the same manner as in fig. (47) except that the magniude is smaller during the initial stage for the lower impact speed.

Fig.(5.49) shows the variation of the strain with the contact time for two different impact speed. It is clear that as the contact time increases the strain increases in non-linear manner. This increase in strain depends on the impact speed. It is evident that, most of the deformation of the specimen occurs within the first 26 μsec of the contact time.

Fig.(5.50) shows that, the strain rate increases sharply immediately after impact to a maximum value and then decreases gradually during the later stages of the deformation. The strain rate reaches its maximum value within about 4 μsecond for both impact speeds (82 and 120 m/s).

Theoretical curves
Load ratio-deformation during impact of tool steel onto Mild steel specimen

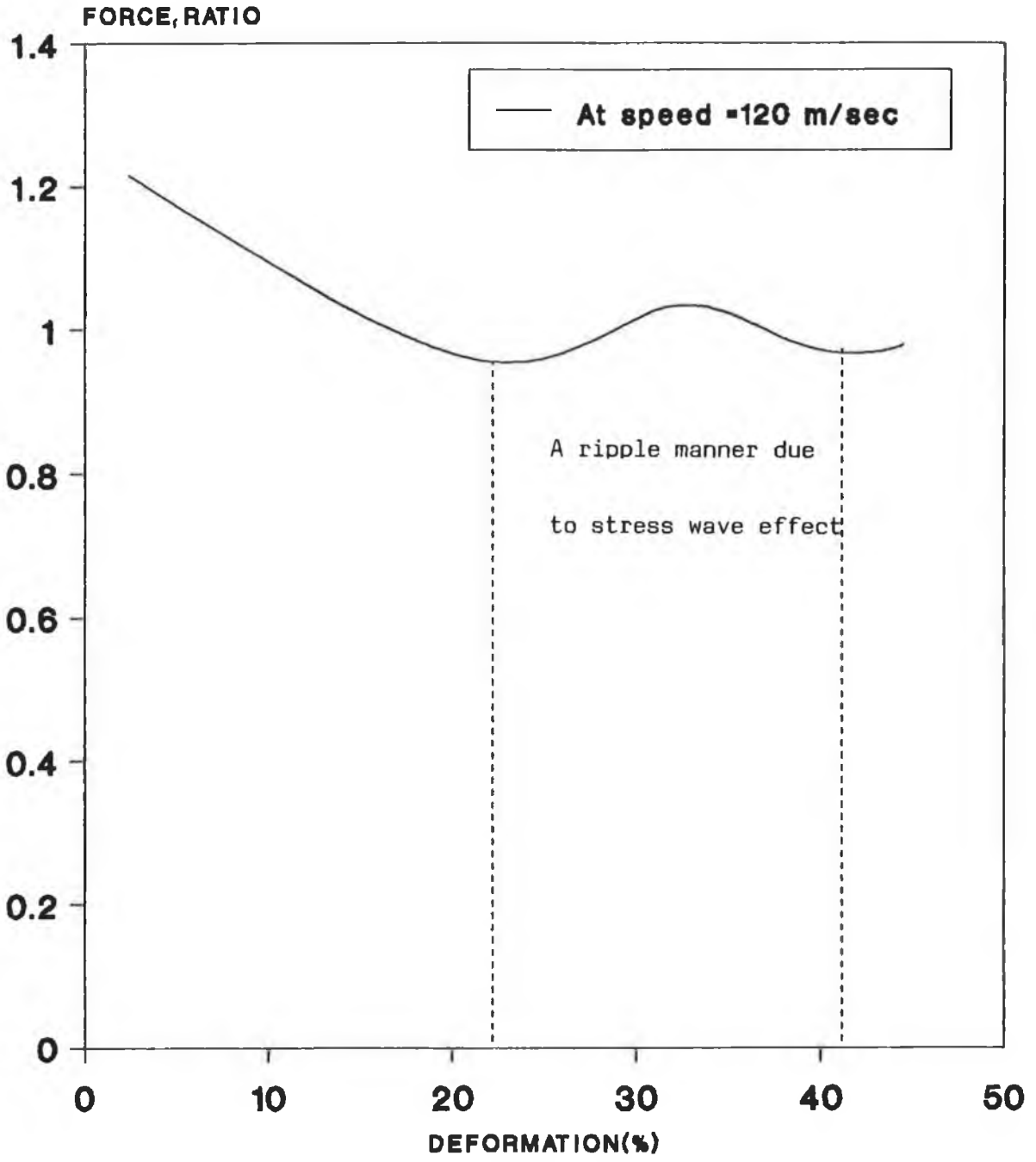

Fig.(5.47)

Theoretical curves
Load ratio-deformation during impact of tool steel onto Mild steel specimen

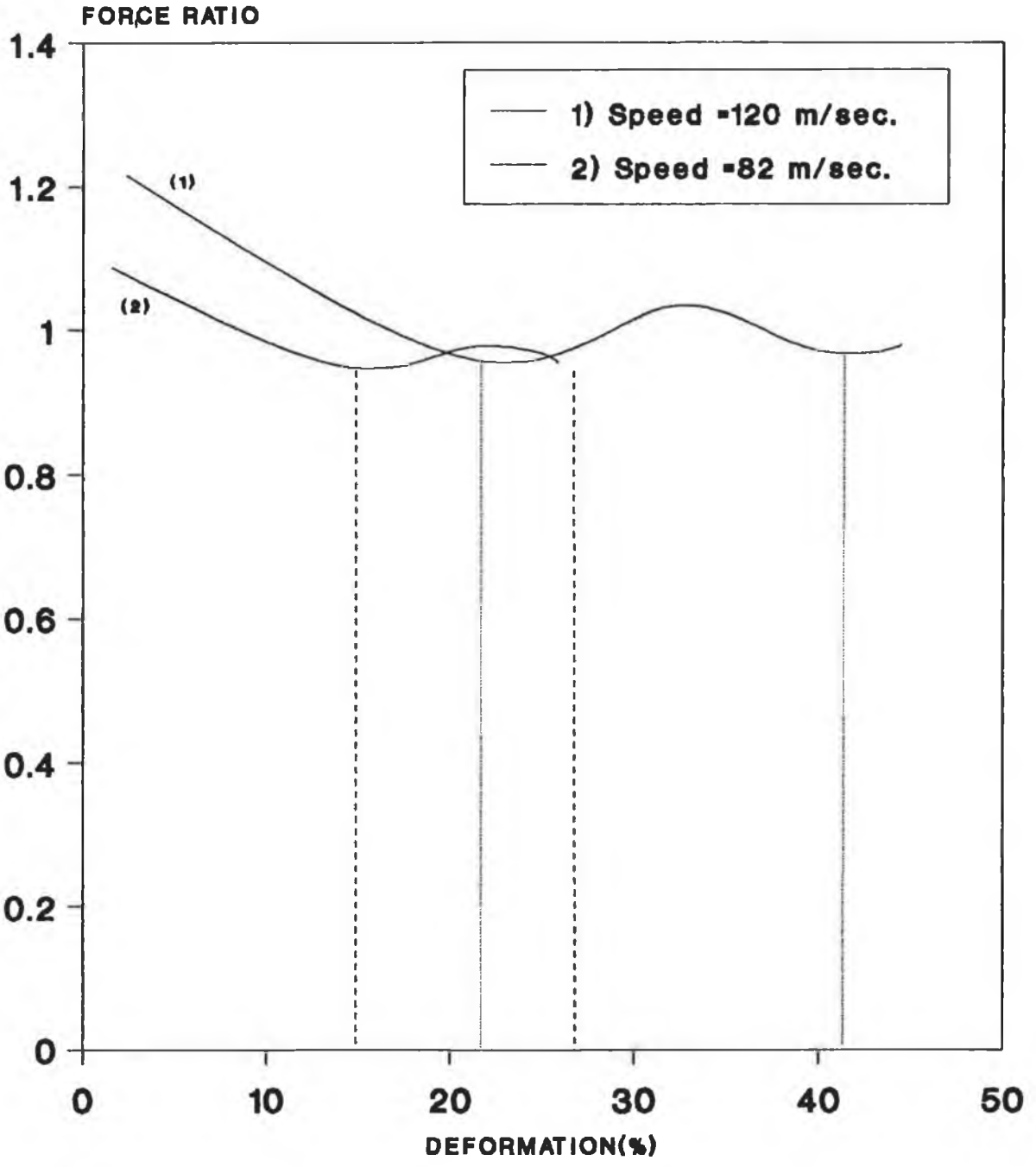

Fig.(5.48)

Theoretical curves
Strain-time history during deformation of Mild steel specimen

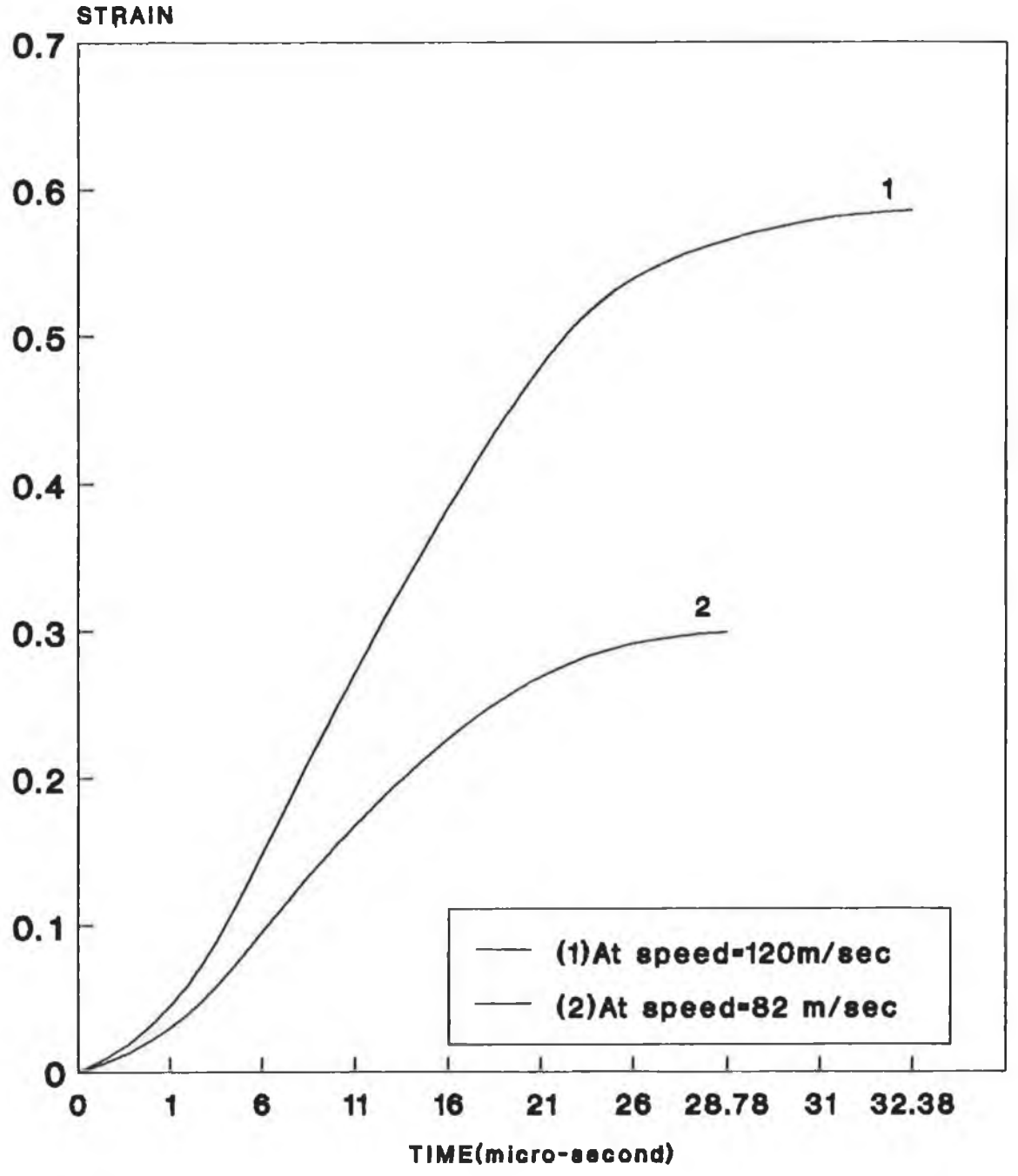

Fig.(5.49)

Theoretical curves
Strain rate-time history during deformation

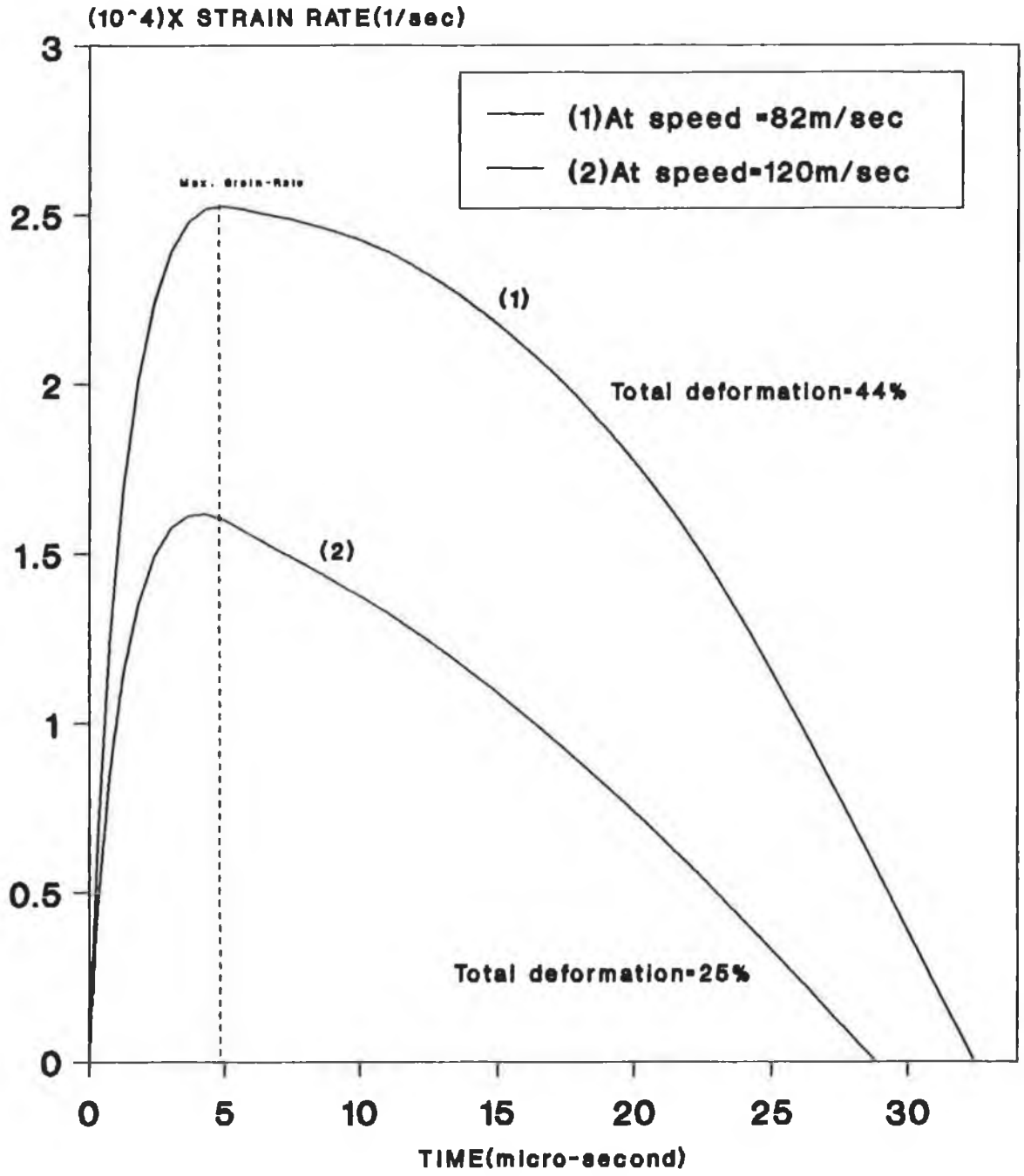

Fig.(5.50)

Fig. (5.51) shows the relationship between the strain rate and strain at two impact velocities. It is evident that the strain rate of about 2.5×10^4 per second is reached for initial strain of about 0.1 for impact speed of 120 m/s . At impact speed of 82 m/s the maximum strain rate reached is about 1.6×10^4 per second by the time the strain reaches 0.08.

Fig. (5.52) shows the variations in the kinetic energy spent with deformation. It is clear from the graph that the higher kinetic energy is used up in an approximantely linear manner with increasing deformation.

Fig. (5.53) shows the variation of the upper force obtained by using equation(4.20) (without any effect on strain hardening) and equation (4.26) (with both effects on strain hardening). It can be seen from this figure that the effect of strain rate is more clear during the initial period(small strain) then as strain increased the effect of thermal softening has becomes more noticable than strain rate.

Fig. (5.54) shows the variation of the upper force with the contact time for all three materials tested. It can be seen that the force acting on the upper face of the specimen was found to be higher for Stainless steel and lower for Copper specimens.

Fig. (5.55) shows the relation between the kinetic energy spent to deform the specimen against the contact time. Results for all the materials plotted in the graph have the same impact speed.

The results obtained show that at the same contact time of (20 μ second) the kinetic energy used up was found to be (86.4%), (78.4%) and (48.6%) for Stainless steel, Mild steel and Copper respectively.

Fig.(5.56) shows the variation of strain with contact time for all three materials at the same impact speed. It is noticeable that a higher strain is obtained for copper than those for mild steel or stainless steel. This is due to fact that copper is a softer material than the other two. Finally it can be seen that for a softer material the contact time increased and the final strain is also increased.

Fig.(5.57) shows the variation of final strain with impact speed for all three materials. It can be seen that the final strain for Copper is grater than in the other to materials for all impact speeds.

Fig.(5.58) shows the relationship between the contact time and impact speed for all three materials. This figure indicates that as the impact speed is increased the contact time increases. It can be seen that for the same impact speed the contact time is longer for Copper and shorter for Stainless steel. This due to the fact that a higher deformation is obtained for Copper than others.

Fig.(5.59) shows the relationship between the maximum temperature rise and impact speed during deformation calculated using equation(4.21). Again the temperature rise in Copper is higher at all impact speeds.

Theotetical curves
Strain rate-strain history during deformation of Mild steel specimen

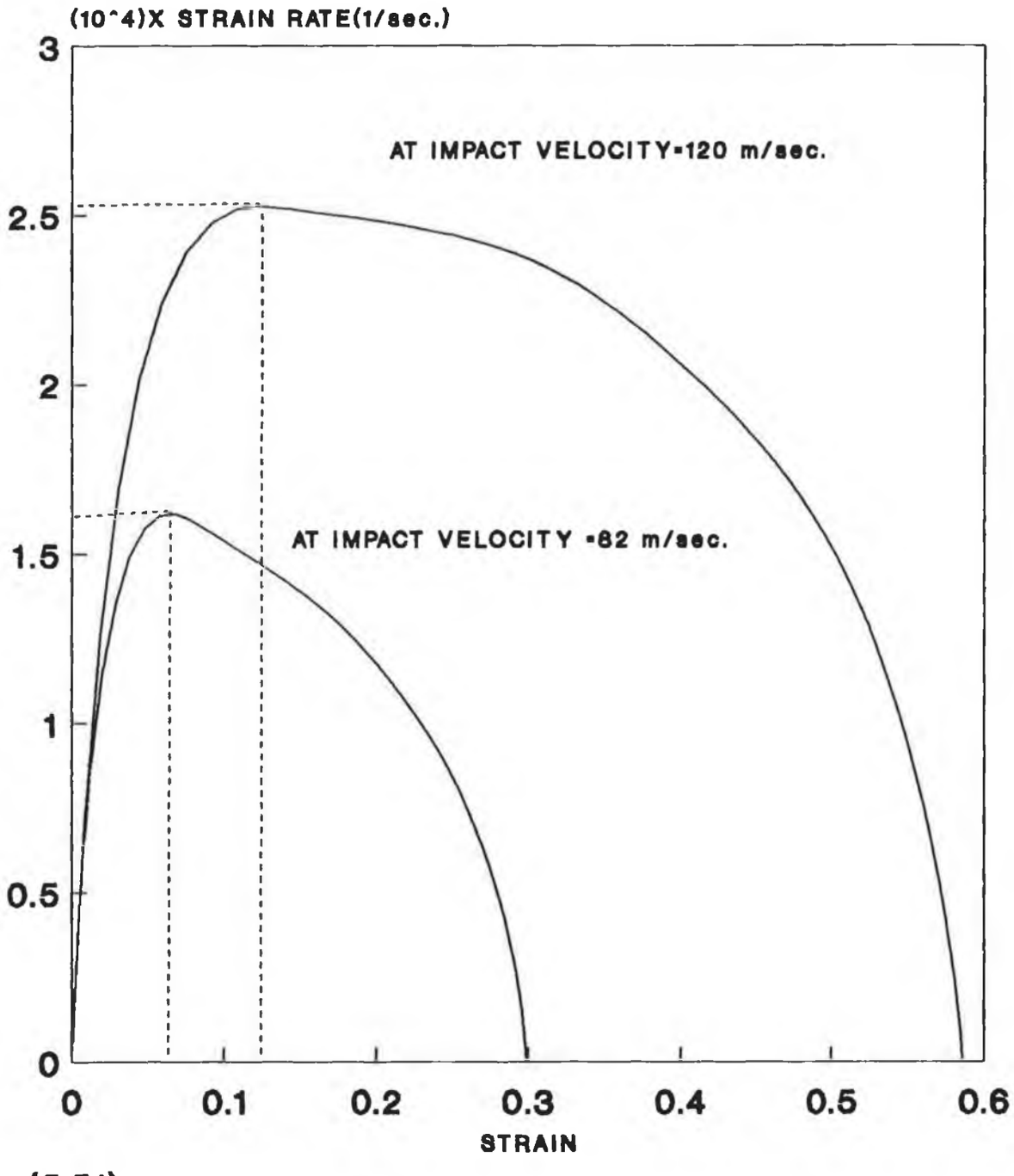

Fig.(5.51)

Theoretical curves
Energy-time history during deformation of Mild steel specimen

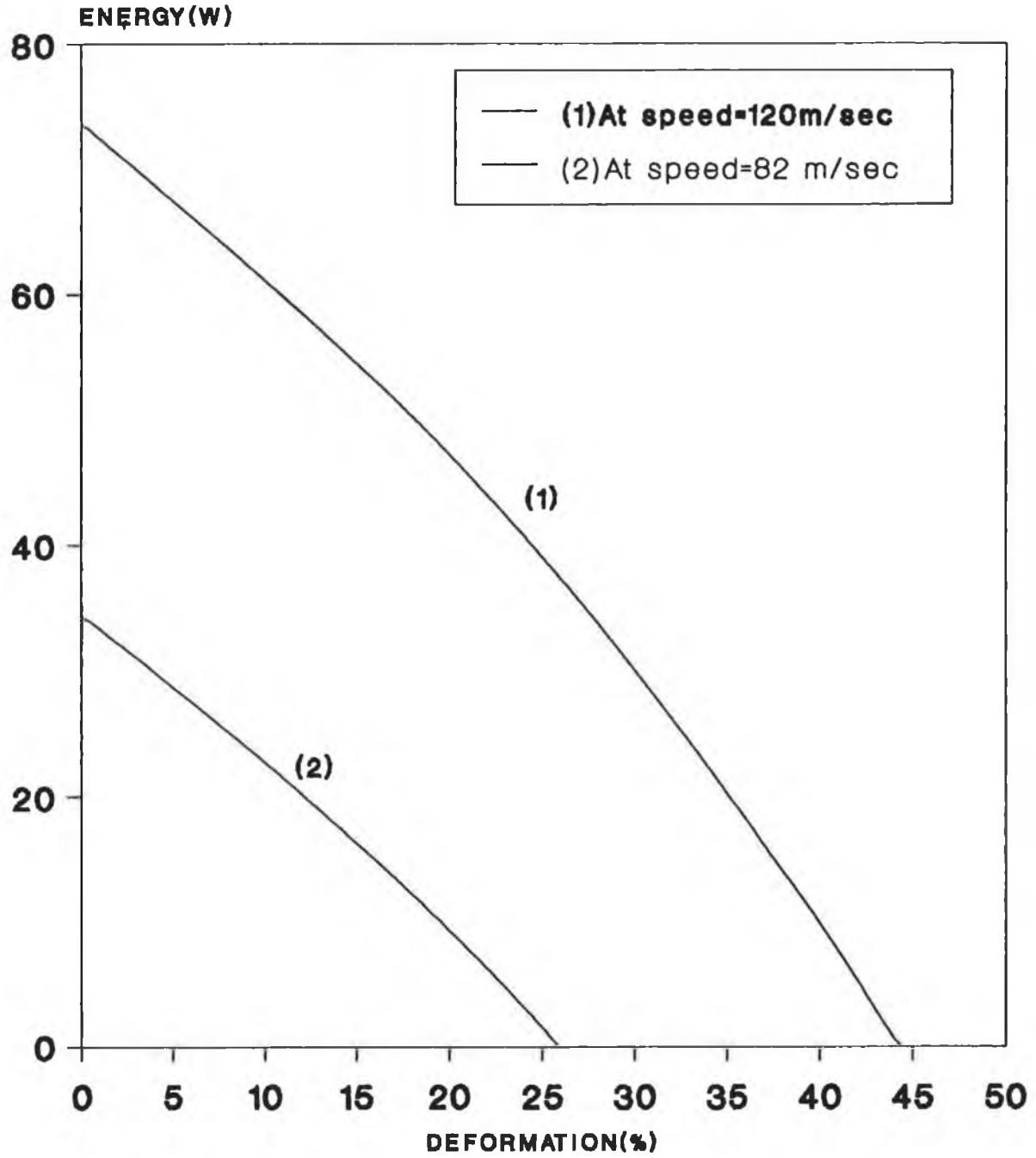

Fig.(5.52)

Theoretical curves
Force-time history during deformation of Mild steel specimen

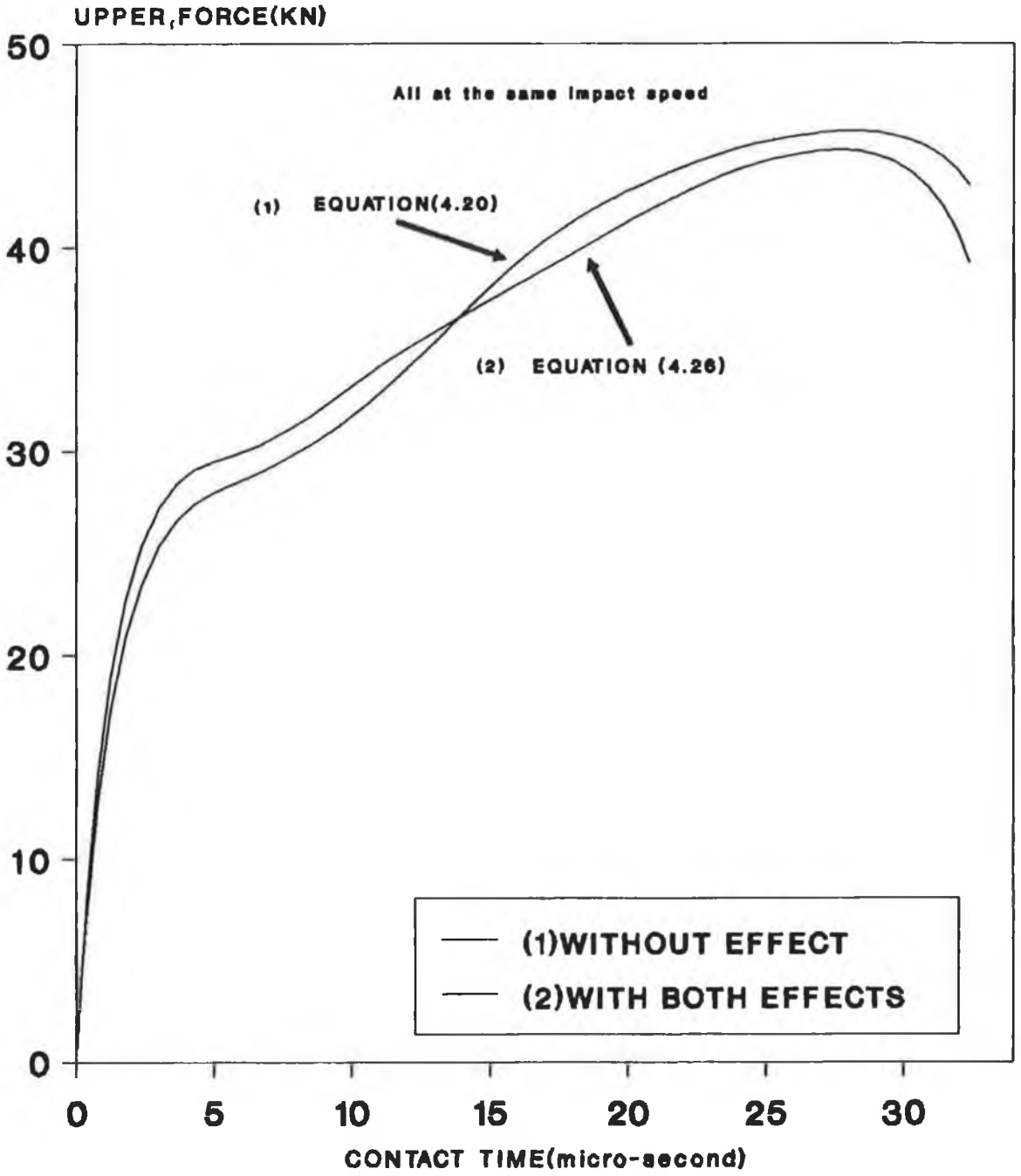

Fig.(5.53)

Theoretical curves
Force-time history during deformation for the three material

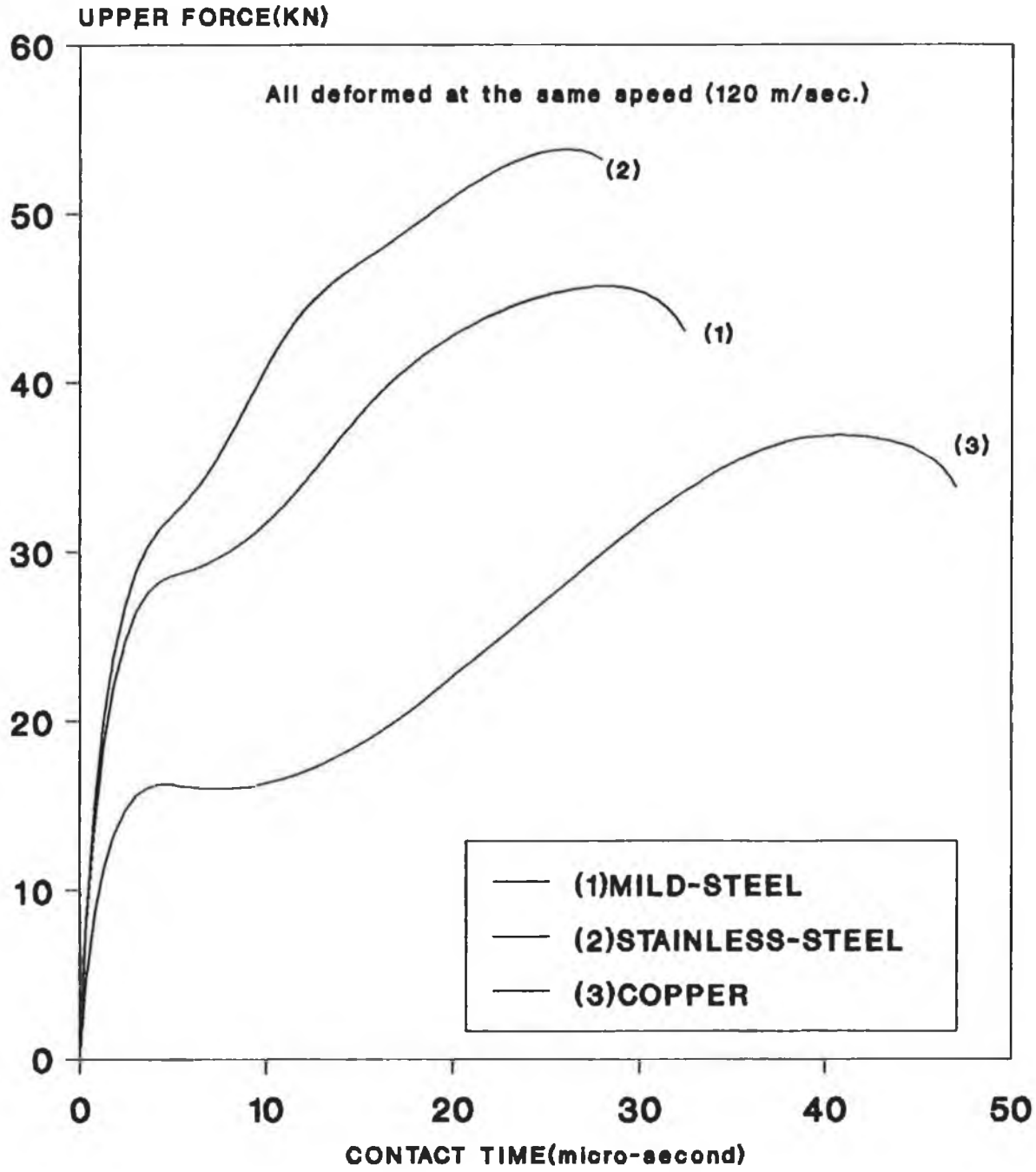

Fig.(5.54)

Theoretical curves
Energy-time history during deformation for the three material

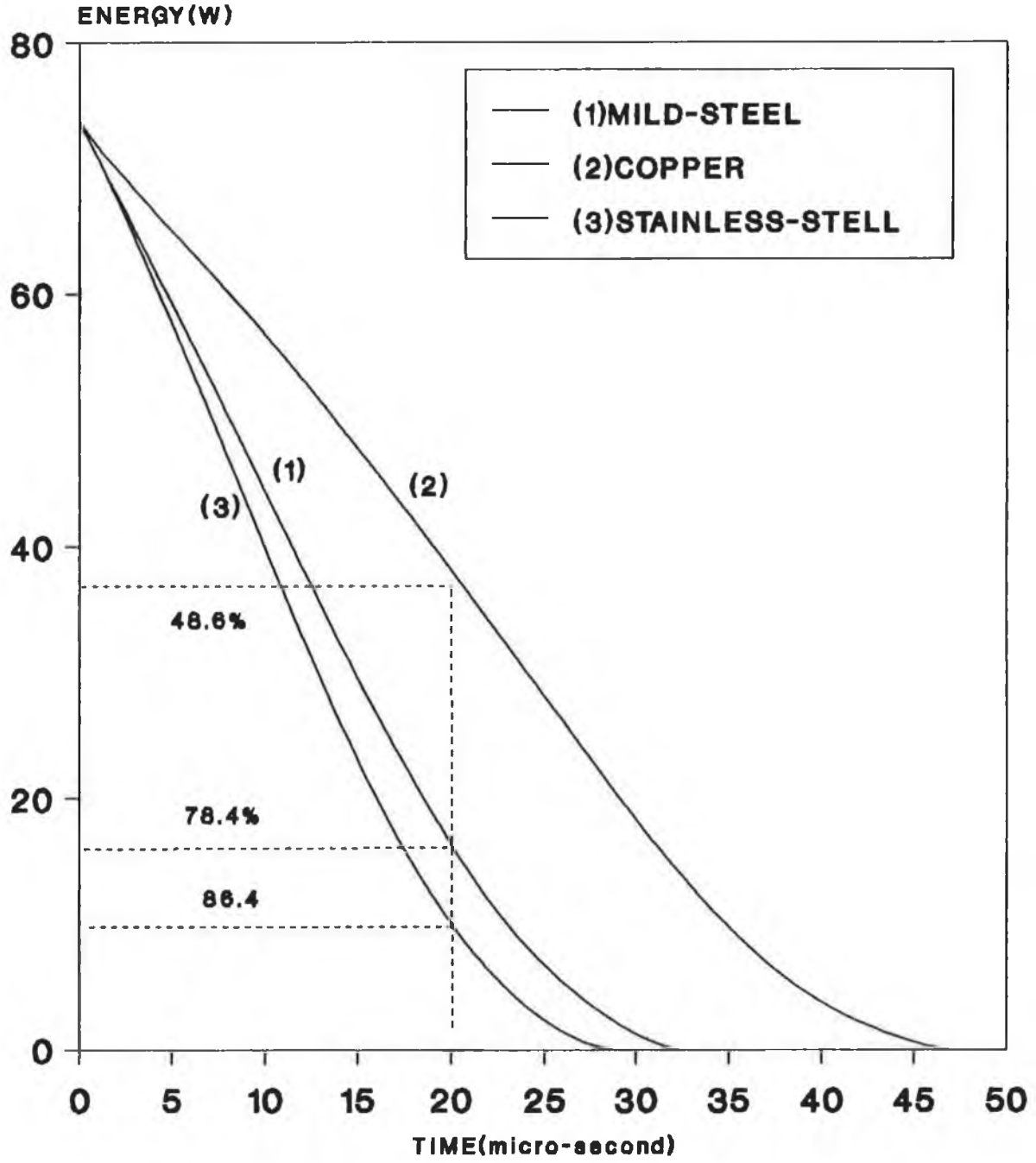

Fig.(5.55)

Theoretical curves
Strain-time history for the three material

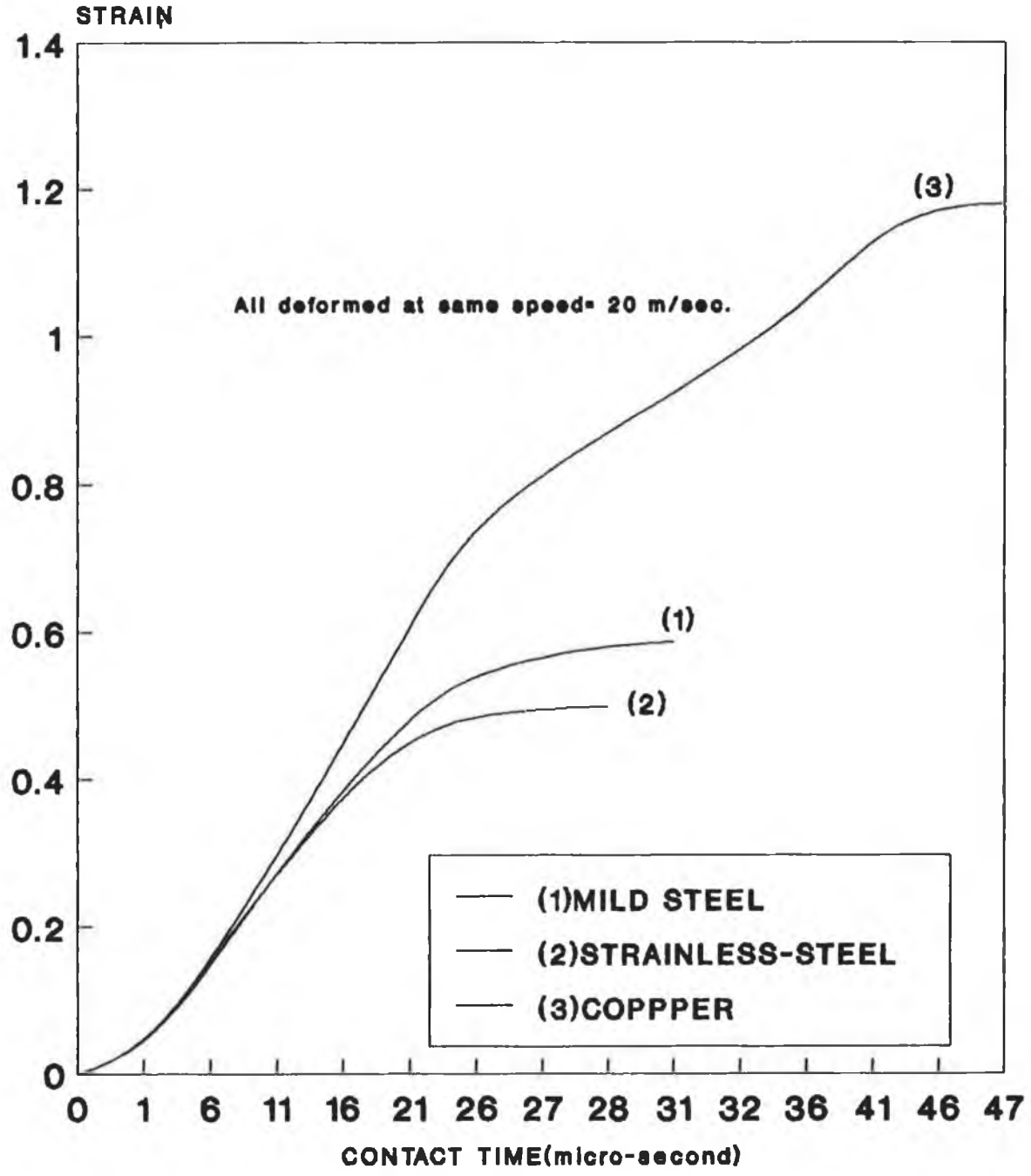

Fig.(5.56)

Theoretical curves
Impact speed and final strain relationship for the three material

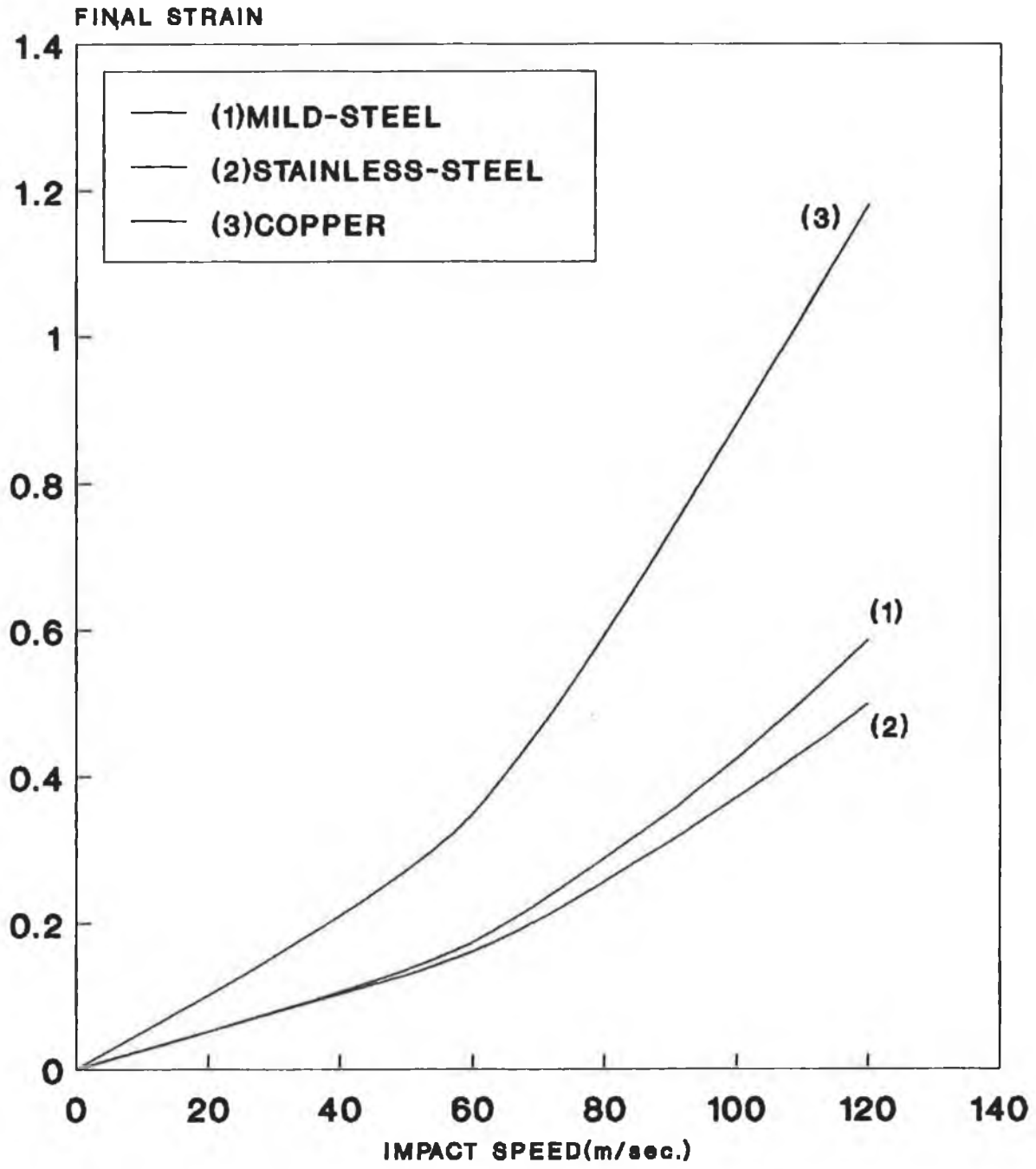

Fig.(5.57)

Theoretical curves
Variation of contact time with impact speed for the three material

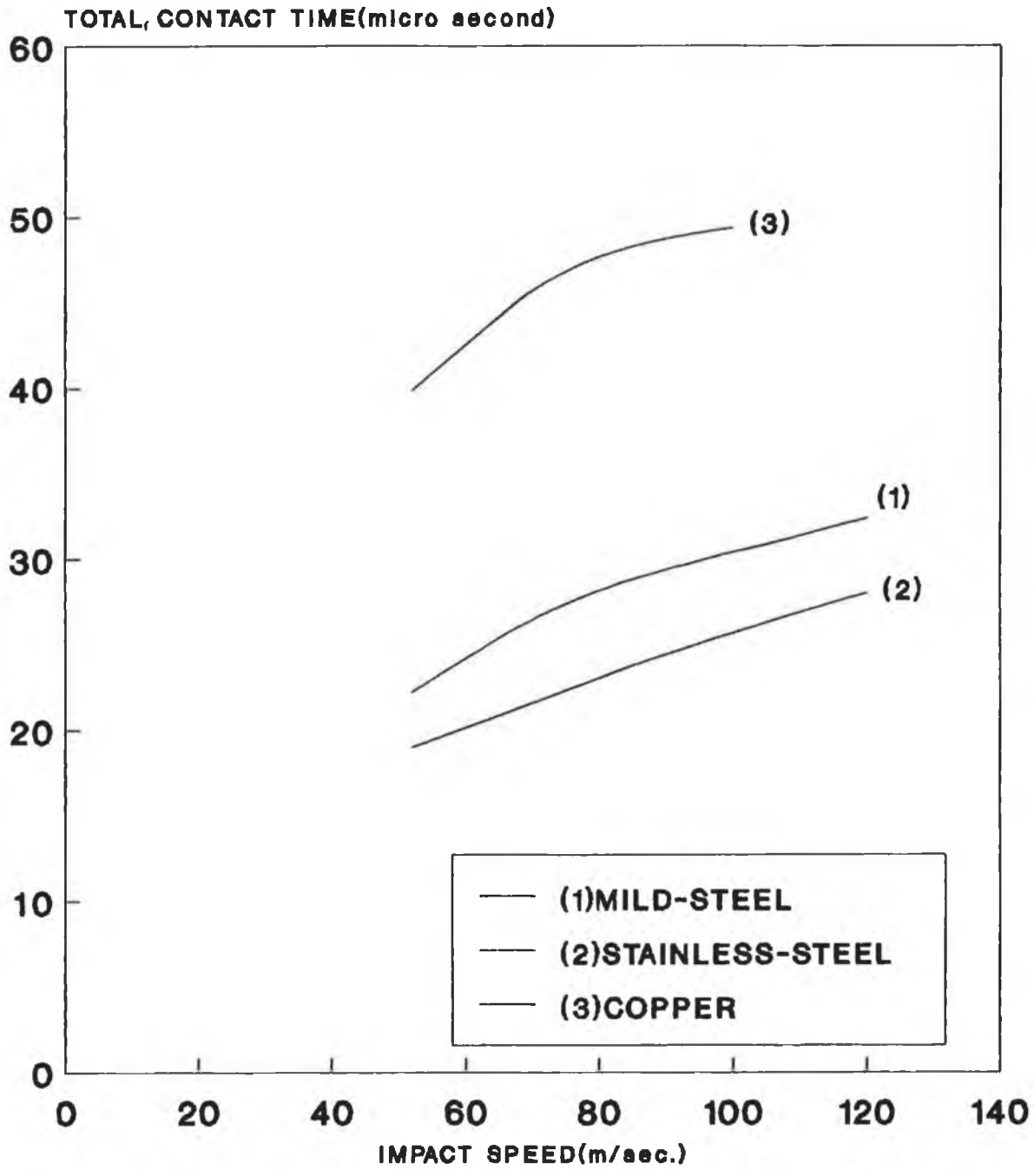

Fig.(5.58)

Theoretical curves
Temperature rise and impact speed relationship for the three material

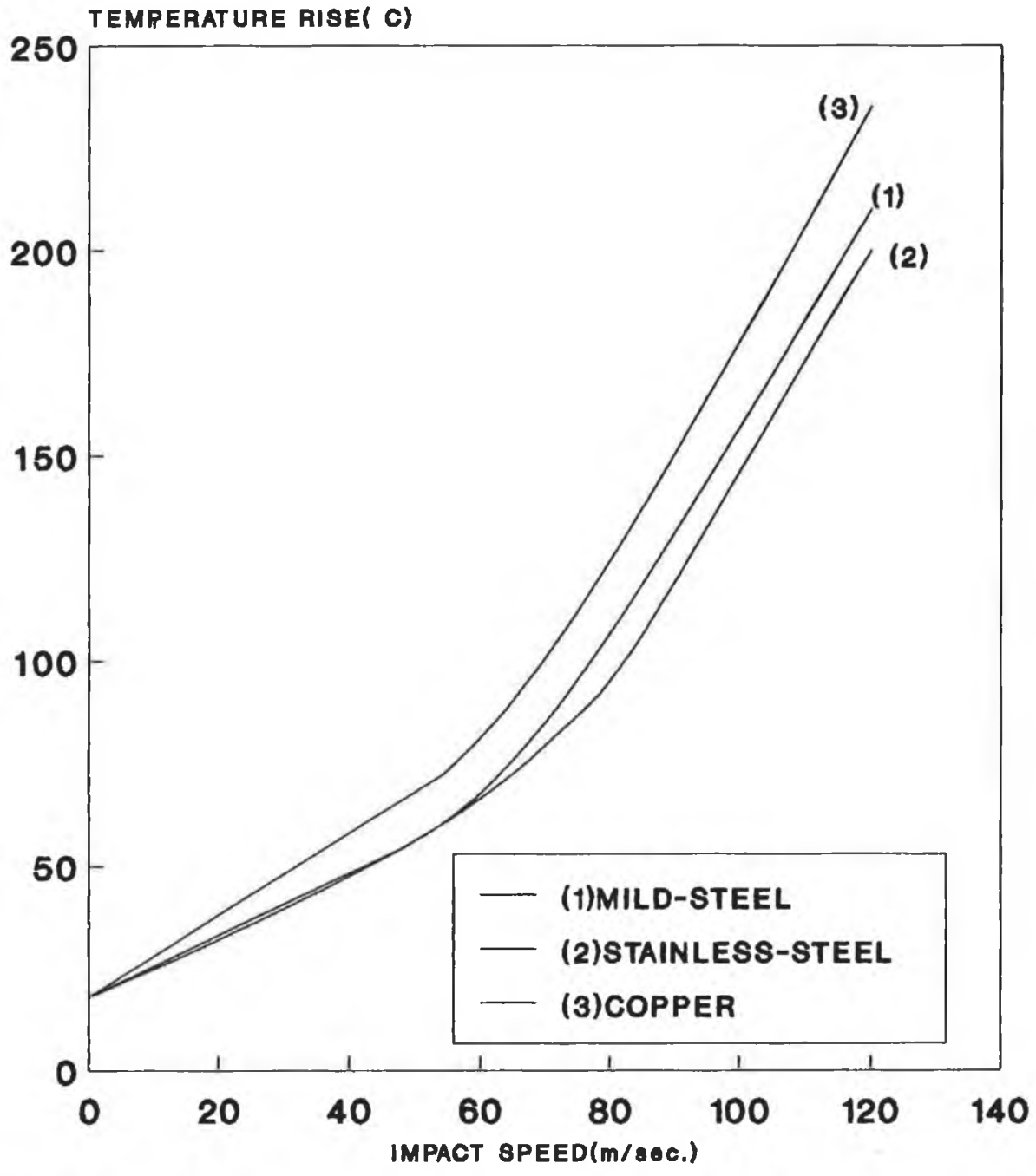

Fig.(5.59)

Fig. (5.60) shows the variation of the force on the projectile and anvil with contact time .It can be seen that during the initial period the force is much higher on the contact mass of the projectile than the contact mass of the anvil. It is evident that the effect of the stress wave on the projectile is more prominent at time (7.5 μsecond) after impact.

Fig. (5.61) shows the variation of the force along the projectile at time 5, 15, 31 μsecond after the impact. It can be seen that the force varies in periodic manner up to distance equal to 75% of the total length of the projectile. As the distance increases the force seems to be varying in a linear manner.

Fig. (5.62) shows the variation of the force along the distance of the anvil bar. It is noticeable that as the distance increases, the force decreases in a periodic manner up to 40% of the total length. The force reaches its maximum just before this length and then starts to decrease in a gradual manner.

Theoretical curves
Load-time history on the contact faces of the projectile and anvil

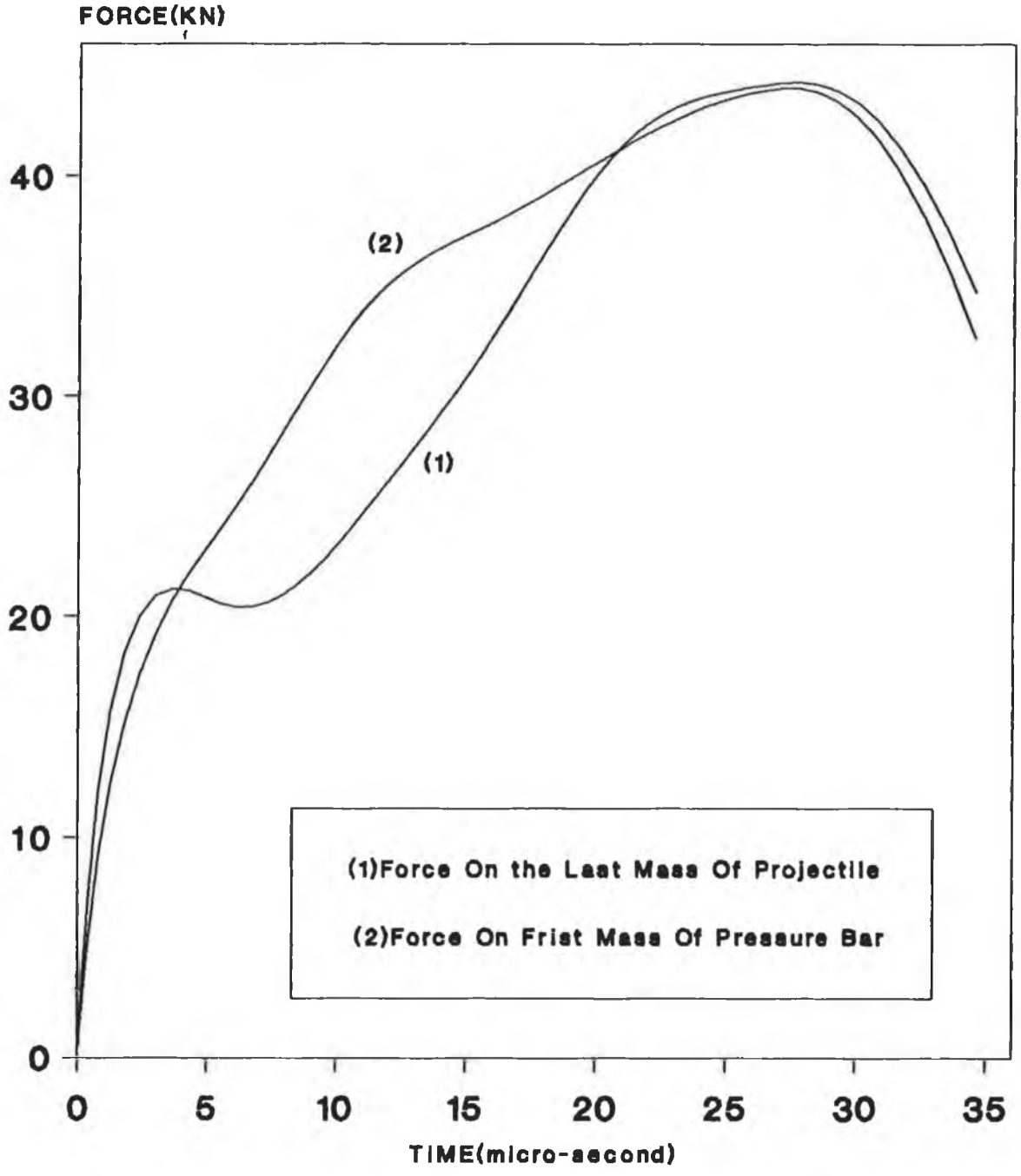

Fig.(5.60)

Theoretical curves
Variation of the force along the projectile distance

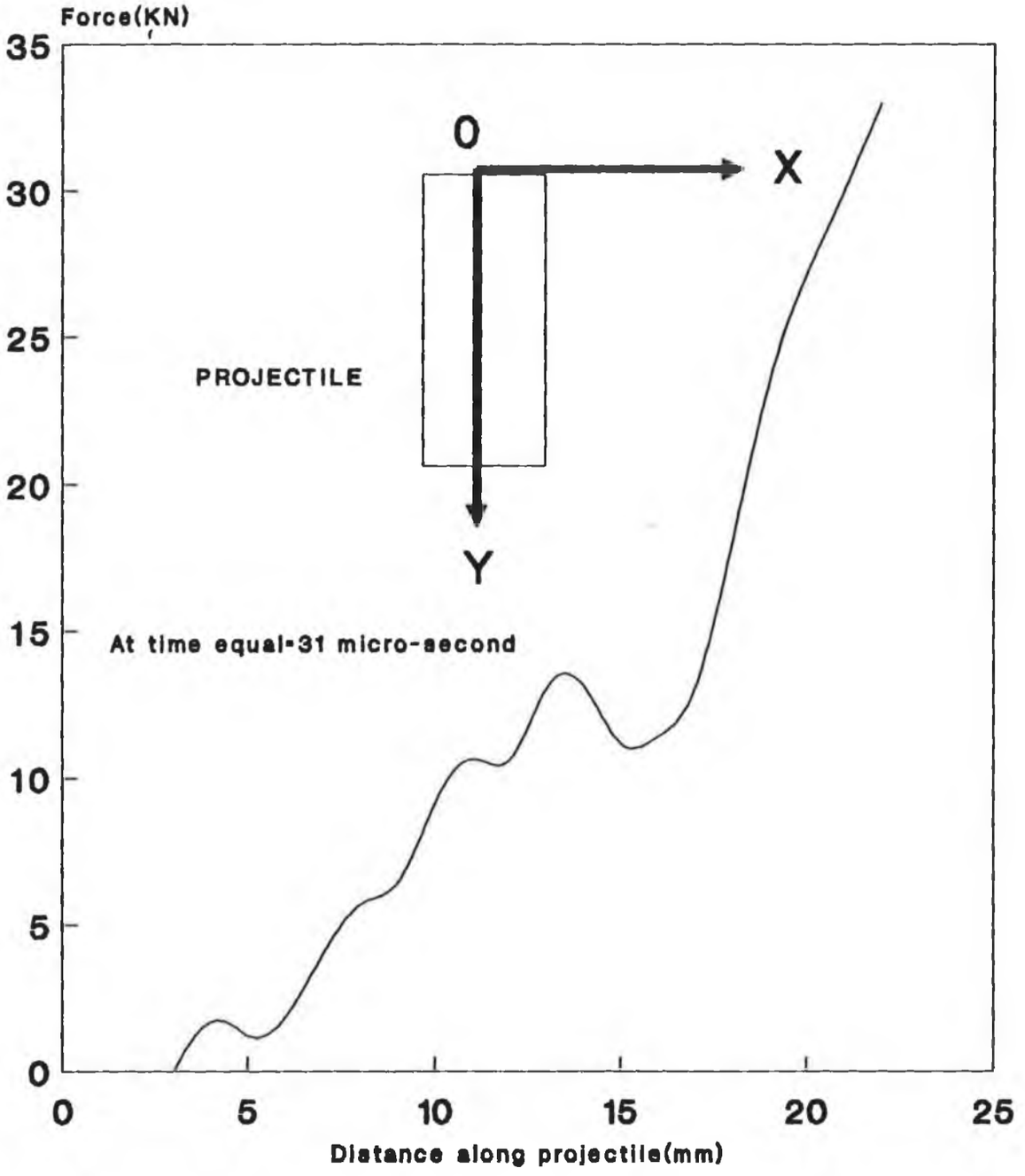

Fig.(5.61)

Theoretical curves
Force Variation along the Pressure Bar

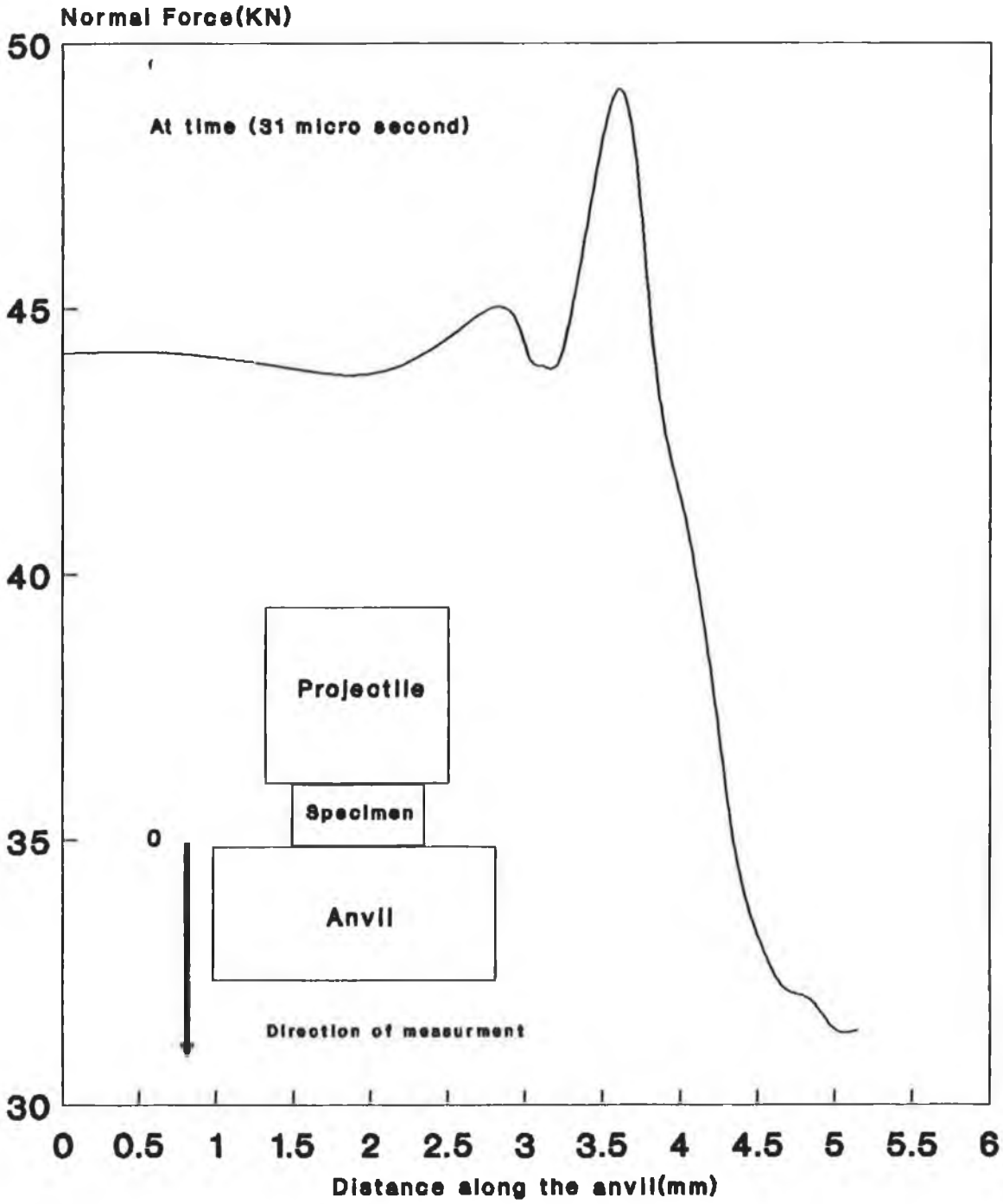

Fig.(5.62)

CHAPTER SIX

Conclusions and Suggestion for Future Work

a) Conclusions

This Project has been undertaken with the objective of establishing a high strain rate constitutive equation for three different materials.The following conclusions can be drawn from the experiments conducted under quasi-static and dynamic compression test and the theoretical work.

(i) Experimental Part

1) The quasi-static stress-strain properties of the three material were obtained experimentally at room temperature, and a suitable equation were established from the literature review for the flow stress for temperatures of up to 400 ℃.

2) A homogeneous deformation was achieved during the impact of a tool steel projectile onto the test specimen, when two layers of Polythene sheet were used in the upper face and the projectile was coated with Petroleum Jelly.

3) The best lubricant was selected, by deforming the specimens at the same strain level with three types of lubricants and barrelling was found to be negligible.

4)The effect of the static deformation and the dynamic deformation on the hardness value had been obtained.

(ii) **Theoretical Analysis**

1) A new form of constitutive equation has been established to give the dynamic properties of the three materials investigated in this study.This equation takes into account the effects of strain, strain hardening, strain rate, temperature rise during deformation and inertia effect.

2) It has been found that as the strain increased the dynamic flow stress decreased, and as the strain rate increased the strain hardening decreased.

3) When the specimen, projectile and anvil were represented by a lumped mass model, there was no indication that this affected the results significantly.

4) The Mild steel and Copper were found to have greater strain rate sensitivity than the Stainless steel over strain rates ranging between 10^2 to 10^5 per second.

5) A comparison of the strain rate sensitivity, in the form of the stress ratio-strain rate relationship for the three material, is made with other researcher's work.

6) The deformation history of the impact of the tool steel projectile onto the test specimen has been represented in graphical form to describe the impact mechanics and to study the effect of stress waves on the force.

7) A computer program has been developed using Fortran 77 and using a finite difference technique to analyse the deformation caused by the impact of the tool steel onto the test specimen.

b) Suggestions for Further Work

1) The dynamic properties of other metallic metals such as [Titanium, Stainless-steel(303 and 316), Brass and Nickel], over a wide range of strain rates and temperature.

2) The effect of specimen size, different aspect ratio to be considered (in conjunction with friction) by increasing the specimen diameter, and also the effect of projectile mass on the material sensitivity constants.

3) The effect of the specimen geometry, where more specimen configurations could be considered.

4) Modify the ballistic test and the numerical technique in such a way as to be capable to studying the dynamic properties of brittle materials such as (Glass and Ceramics).

5) Consider other types of materials as non-metallic material and composite materials (metal-matrix material).

6) Extensive experimental data is needed in order to give a clearer picture of the effects of the dynamic deformation on the structure, hardness value and surface roughness of a specimen.

7) More work needs to be done to develop the computer program to give a prediction of the dynamic fracture of the specimen, and to compare the effectiveness of this program (finite difference technique) with a suitable finite element program.

8) Modify the constitutive equation to incorporate the effect of the static and dynamic strain history.

9) It was assumed in this study that the relationship between the impact speed and final height was linear, a more accurate curve could be used to provide a better results.

10) Although in this study the condition (1) (Force Equal Zero) was used to terminate the program, and no significant variations were found with other two condition (Kinetic Energy and Mass Release). It would be desirable to establish the best fit material constants using the other two conditions to terminate the program, and review the results obtained.

References

1. Morimoto,Y; Seguchi,Y and Yamashita, M " Automatic Analysis of Strain Rate Distribution by High Speed Video Camera and Grid Method using Fourier Transform", Int. Conf. Mech. Prop. at High Rates of Strain, Oxford,1989 pp 165-172.

2. Haque, M and Hashmi, M.S.J., " Stress-strain Properties of Structural Steel at Strain Rate of up to 10^5 per second at Sub- zero, Room and High Temperatures.", Mech Mat,1984, 3, pp 245- 256.

3. Holzer, A., " A Technique for Obtaining Compressive Strength at High Strain Rates using Short Load Cells." , Int J Mech Scl. 1978, 20 , pp 553-560.

4. Wulf, G.L and Richardson, G.T., "The Measurement of Dynamic Stress-Strain Relationships at Very High Strains.", J Phys E: Scl Instrum. 1974, 7, pp167-169.

5. Norman, J ., " Response of Structure to the Dynamic Loading .", Int Conf of High Rates of Strain, 1979, pp 254-275.

6. Hernalsteen, P and Leblois, L.C., " The Use of the Energy Absorber to the Protect Structures Against Impact Loading.", Nuclear Engineering and Design, 1976, 37, pp 373-406.

7. Morris, D.R and Watson, A.J., " Dynamic Properties of Construction Materials using a Large Diameter Kolsky Bar. ", Int.Conf.Mech.Prop. at High Rates of Strain. Oxford, 1989, pp 519- 525.

8. Johnson, W., "Impact Strength of Materials.", Edward Arnold Limited, 1972.

9. Zukas, J; Nicolas, T; Swift, H; Greszczuk, L and Curran, D.,"Impact Dynamics", Wiley-Interscience Publication, New York,1982.

10. Malvern, L.E; Tang, T; Jenkins, D.A and Gong, J,C.,"Dynamic Compressive Strength of Cementitious Materials", **Mat Res Soc Symp Proc. Vol 64**.1986.

11. Fisher, U and Krutzik, N.K., " Dynamic Calculation of Nuclear Plant Structures Due to Natural and Man-made Hazards.", **Int. Conf. of Metal Under Dynamic Loading. China**. 1986, pp 875-881

12. Werkel,H and Waas,G ., " Impact on Nuclear Reactor Building Analysis and Experimental Results.", **Int. Conf. of Metal Under Dynamic Loading. China**. 1986, pp 1008-1013

13. Amos, K.A.," Aerospace Application of Materials at High Strain Rates." **Int Conf. Mech.Prop.Mat.at High Rates of Strain, Oxford**. 1989, pp 543-551.

14. Miles, J.,"An Overview of Application in Nuclear Industry." " **Int Conf. Mech.Prop.Mat.at High Rates of Strain, Oxford**. 1989, pp 489-502.

15. Eisenreich, N and Kugler, W., "An Optical Method to investigate the dynamics of Motion and Deformation in Ballistic." **Proc. of Ballistics** April 1983, pp 439-444.

16. Sturgess, C.E.N., "The Use of Impact Forming Devices to Obtain Dynamic Stress strain Data." **Proc. 11th Int. Mach.Tool Des.Res. Conf**., 1970, pp803.

17. Christopherson, D.G and Parsons, B.,"The Effect of Strain Rate in Strip Rolling." **Proc. of Conf. on Prop. of Materials at High Rates of strain**. 1957, pp 115-121.

18. Coupland, H. and Wilson, D., " The Effect of Speed in Deep Drawing." **Proc. of Conf. on Prop. of Materials at High Rates of strain** ,1957, pp 98.

19. Polak, K.," Theoretical and Technological Aspects of High Strain Rate Forming." Int. Conf. of Metal Under Dynamic Loading. China. 1986 pp 952-956.

20. Hosford, W.F and Caddell, R.M., " Metal Forming Mechanics and Metallurgy." Prentice-Hall. 1983.

21. Pugh, H and Watkins, M.," Some Strain-Rate Effects in Drop-Forging Tests." Proc. of Conf. on Prop. of Materials at High Rates of strain. 1957, pp 122-127.

22. Metzler, H.J., " The Development of a High Energy-Rate Forming Machine For Research." Proc. th Int. Mach.Tool Des.Res. Conf. 1982 pp 43-54.

23. Jones, R.G., "Progress in High Energy Rate Forming." J. Inst. of Metals. 1969, Vol 97. pp257-270.

24. Lippman, H., "On Dynamics of Forging." Proc. 7th Int. Mach.Tool Des.Res. Conf. 1966 pp 43-54.

25. Johnson, G.R., " Dynamic Strength and Ductility Testing Using an Explosive Impulse Technique." Int. Conf. of Metal Under Dynamic Loading. China. 1986 pp 662-669.

26. Al-Tounsi, A., " Effect of Sintering Temperature on the High Strain Rate Property of Iron Powder Compacts." MEng. Thesis Dublin City University 1989.

27. Kolsky, H., " An investigation of the Mechanical Properties of Materials At Very High Rates of Loading." Proc of the Phys Soc Sec B Vol 62 ,1949, pp 676-700.

28. Davies, E. and Hunter, S., "The Dynamic Compression Testing of Solids by the Method of the Split Hopkinson Pressure Bar." J.Mech.Phys. Solids ,1963, Vol 11. pp155-179.

29. Taylor, G.I., " The use of Flat-Ended Projectiles for Determining Dynamic Yield Stress." Part (I) Theoretical Considerations , " **Proc. of Royal . Soc. Ser. A194** , London, 1948 pp289-299.

30. Lee, E and Wolf, H., " Plastic Wave Propagation Effects in High Speed Testing.", **J. Appl. Mech.**, Dec. 1951 pp 379-386.

31. Ting, T and Symonds, P., " Longitudinal Impact on Viscoplastic Rods-Linear Stress-strain Rate Law." **J. Appl. Mech.**, June 1964 pp 199-207.

32. Wiffens, A., " The use of Flat-Ended Projectiles for Determining Dynamic Yield Stress." Part (II) Experimental Considerations , " **Proc. of Royal . Soc. Ser. A194** , London, 1948 pp 300-322.

33. Lee, E.H and Tupper, S.J., "Analysis of plastic Deformation in a Steel Cylinder Striking a Rigid Target." **J of Appl Mechs**, March 1954, pp 63-70.

34. Hawyard, J ; Eaton, D and Johnson, W., "The Mean Dynamic Yield Strength of Copper and Low Carbon Steel at Elevated Temperatures from the Measurements of the Mushrooming of Flat-Ended Projectiles" **Int. J.Mech.Scl**.,1968, **Vol 10**, pp 929-948.

35. Hawyard, J., "A Theory for the Mushrooming of the Flat-Ended Projectiles Impinging on a Flat Rigid Anvil, Using Energy Consideration." **Int. J Mech Scl**, 1969, **Vol 11**, pp 313-333

36. Hutching, I.M and O' Brien, T.J., " Normal Impact of Metal Projectiles Against a Rigid Target At Low Velocities." **Int. J.Mech.Scl**.,1981, **Vol 23**, pp 255-261.

37. Balendra, R and Travis, F.W., "An Examination of the Double-Frustum Phenomenon in the Mushrooming of Cylindrical Projectiles Upon High Speed Impact with a Rigid Anvil." **Int. J.Mech.Scl**., 1971, **Vol 13**, pp 495-505.

38. Hashmi, M.S.J and Thomphson, P.J., " A Numerical Method of Analysis for the Mushrooming of Flat-Ended Projectiles Impinging on a Flat Rigid Anvil." Int. J.Mech.Sci., 1977, Vol. 19. pp 273-283.

39. Hashmi, M.S.J.," Strain Rate Sensitivity of a Mild-Steel At Room Temperature and Strain Rates of up 10^5 per second." J. of Strain Analysis ,1980, Vol 15. pp 201-207.

40. Pope, P.H and Field, J.E., " Determination of Strain in a Dynamic Compression Test." J. Phys.E: Sci. Instrum. , 1984.Vol. 17, pp 817-820.

41. Johson, W and Mellor,P.B.," Engineering PLasticity.", Ellis Horwood Limited, England.

42. Banerjee, J.K., " Barreling of Solid Cylinders Under Axial Compression." J of Eng.Mat.and Tech. Trans. of ASME , 1985, Vol. 107, pp 138-144.

43. Gupta, N.K and Shah, C.B., "Barreling of a Short Cylinder in Compression." Int. J. Mach.Tool Des.Res.,1986, Vol 26. pp 137-146.

44. Depierre, E., " A Method for Determination of Constant and Varying Friction Factors During Ring Compression Tests.", Technical Report AFML TL-72-37.

45. Schey, J.A; Venner, T.R and Takomana., " Shape Changes in the Upsetting of Slender Cylinders." J. of Eng. for Indu. Trans. of the ASME. 1982, Vol.104. pp 79-83.

46. Dean, T.A., " The Influence of Billet Inertia and Die Friction in Forging Processes a Simple Energy Approach." Proc. 11th Int. Mach.Tool Des.Res. Conf. 1970, pp 761-777.

47. Lee, C.H and Altan, T., " Influence of Flow Stress and Friction Upon Metal Flow in Upset Forging of Rings and Cylinders." J. of Eng. for Indu. Trans. of the ASME. AUG. 1972 pp 775-782.

48. Venugopal, P; Venugopal, S and Seetharaman, V., " Influence of Strain Rate and Temperature on the Friction Factor of Commercially Pure Titanium." J.of Mat. Processing Technology. 1990, Vol 22, pp91-97.

49. Hashmi, M.S.J., " Upsetting of Cylindrical Billets Between Flat Platens Having Unequal Frictional Properties.", Int. J. Mach.Tool Des.Res. ,1978, Vol 18. pp 189-196.

50. Osakada, K., " A Mechanism of Lubricant Trapping in Slow Speed Compression.", Int. J.Mech.Sci.. 1977, Vol. 19. pp 413-421.

51. Thomson, P.F and Aung, M., " The Profile of Billets in Upset Forging.", Int J Mach.Tool Des.Res. , 1983, Vol 23, pp 191-199.

52. Male, A.T and Cockcroft, M.G., "A Method for the Determination of the Coefficient of Friction of Metals Under Conditions of Bulk Plastic Deformation.", J of Inst. of Metals , 1964-65, Vol. 93. pp38-45.

53. Sheikh, A.D; Dean, T.A; Das, M.K and Tobias, S.A., "The Effect of Impact Speed and Lubricant in Hot Forging: Part (I), Interface Friction and Die Cavity Pressure.", pp 341-345.

54. Narayanasamy, R; Murthy, R; Viswanatham, K and Chary, G,R "Prediction of the Barreling of Solid Cylinders Under Uniaxial Compressive load", J.of Mech Working Technology. 1988. Vol.16. pp 21-30.

55. Holzer, A.J and Brown, R.H., "Mechanical Behaviour of Metals in Dynamic Compression", Transactions of the ASME .1979.Vol 101. pp 238-246.

56. Haque, M.M., "Stress-Strain Properties and Micro-Structural Change in Metal Deformed at Strain Rates of Up to 10^5 per second.", **PhD Thesis, Sheffield City Polytechnic**, Sheffield, UK, 1983.

57. Gorham, D.A., "Specimen Inertia in High Strain-Rate Compression.", **J.Phy. D: Appl. Phys. Vol. 22**. 1989 pp 1888-1893.

58. Dharan, C and Hauser, F., "Determination of Stress-Strain Characteristics at Very High Strain Rates." **Experimental Mechanics**, Sept. 1970 pp 370-376.

59. Hauser, F.,"Techniques for Measuring Stress-strain Relation at High Strain Rates.", **Experimental Mechanics**, Augt. 1968 pp 394-399.

60. Gunasekera, J.S; Havranek, J and Littlejohn,M.H., "The effect of Specimen Size on Stress-Strain Behavior in Compression." **J.of Eng.Mat.and Tech. Trans. of ASME**. 1982, **Vol 104**. pp 274-279.

61. Lindholm, U.S., "Some Experiments With the Split Hopkinson Pressure Bar.", **J Mech Phys Solids**. 1964 , **Vol 12**, pp 317-335.

62. Albertini, C. and Montagnani, M.,"Testing Techniques Based on the Spilt Hopkinson Bar." **Inst of Phys Conf Ser No 21**. 1974, pp 22-32.

63. Gorham, D.A., "Measurement of Stress-Strain Properties of Strong Metals at Very High Rates of Strain." **Inst. Phys. Conf. Ser. No. 47** , 1979.

64. Yokoyama, T and Kishida, K., "A microcomputer-Based System for the High-Speed Compression Test by the Split Hopkinson Pressure Bar Technique.", **J of Testing and Evaluation Vol. 14**. 1986 pp236-242.

65. Lengyel, B and Mohitpour, M., "Dynamic Stress/Strain Data to Large Strains.", **J. of Inst. of Metals**, **Vol.100**. 1972 , pp1-5.

66. Yew, C.H and Richardson, H.A., "The Strain Rate Effect and the Incremental Plastic Wave in Copper.", **Experimental Mechanics**. Auct. 1969, pp 366-373.

67. Mohitpour, M and Lengyel, B., " A Method of Obtaining Isothermal, Constant High Strain Rate Stress-Strain Data.", **Proc. 16th Int. Mach.Tool Des.Res. Conf.**1975. pp 503-506.

68. Hoge, K.G., " Influence of Strain Rate on Mechanical Properties of 6061-TE Aluminium Under Uniaxial and Biaxial State of Stress." **Experimental Mechanics**. April 1966, pp 204-211.

69. Clark, D and Wood, D., "Impact Properties of Some Metals and Alloys", **Trans. ASME**. 1950, **Vol.42**. pp 45.

70. Alder, J and Phillips, V., "The effect of Strain Rate and temperature on the Resistance of Copper, Aluminium and Steel to Compression", **Inst. of Metals**. 1954, **Vol. 83** , pp80-86.

71. Venugopal, P; Venugopal, S and Seetharaman, V., " Strain Rate and Temperature on the Friction Factor of Commercially Pure Titanium.", **J.of Mat. Processing Technology**. 1990, **Vol. 22**. pp91-97.

72. Serensen, S and Dul'nev, R., "The Effect of Rate of Strain on the Mechanical Characteristics of EI437B Alloy and EI481 Steel at Increases Temperatures", **Industrial Lab** . 1962, **Vol. 28**. pp 896-901.

73. Muller, T., "High Strain Rate Behaviour of Iron and Nickel", **J.Mech.Eng.Sci**. 1972, **Vol.14**. pp161-167.

74. Tanaka, K; Matsuo, T; Kinoshita, M and Maede, T., "Strength of Mild Steel at High Strain Rate", **Bulletin of JSME** , 1966, **VOL.9**. pp21-28.

75. Dean, T.A and Sturgess, C.E.N., "Stress-Strain Characteristics of Various Steels Over a Wide Range of Strain-Rates and Temperatures", **Proc Instn Mech Engrs**. 1973, **Vol 187**. pp523-533.

76. Lindholm, U.S and Yeakely, L.M., "Dynamic Deformation of Single and Polycrystalline Aluminium", J Mech Phys. 1965. Vol 13. pp41-53.

77. Woodward, R.L and Brown, R.H., "Dynamic Stress-Strain Properties of a Steel and a Brass at Strain Rates Up to 10^4 per second", Proc Instn Mech Engrs, 1975, Vol 189. pp107-115.

78. Hashmi, M.S.J; Islam, M.N; Haque, M.M and Sparling, L.G., "High Strain Rate Properties of Material: Design and Development of a test Equipment and Methodology", Int. J. Mach.Tool Des.Res. 1985, Vol 25. pp 39-50.

79. Kalpakjian, S.,"Manufacture Processes for Engineering Materials.", Addison-Weslev. USA, 1985, pp 91.

80. Costantino, C.J., "Finite Element Approach to Stress Wave Problems", J of Eng Mechs Division. 1967, Vol 93. pp 153-176.

81. Bathe, K.J; Ramm, E and Wilson, E., "Finite Element Formulations for Large Deformation Dynamic Analysis", Int J for Num Math In Eng. 1975, Vol 9. pp 353-386.

82. Johnson, G.R., "Analysis of Elastic-Plastic Impact Involving Severe Distortions", J of Appl Mechs Trans ASME. 1976.Vol 43. pp 439-444.

83. Slater, R.A.C., "Engineering Plasticity", Macmillan Press Ltd. London, 1977, pp 155-179.

84. Hashmi, M.S.J.," Dynamic Stress and Strain Propagation Through One Dimensional Elastic-Plastic Solids Materials.", Proc. 20th Int. Mach.Tool Des.Res. Conf.1979, pp 203-209.

85. Malvern, L.E., "The propagation of Longitudinal Waves of Plastic deformation in a Bar of Material Exhibiting a Strain Rate Effect.". J Appl Mech. 1951, Vol 18. pp 203-208.

86. Harding, J., "The Development of Constitutive Relationships for Material Behaviour at High Rates of Strain.", Int.Conf.of High rates of strain, Oxford, 1989, pp 254-275.

87. Johnson, G.R and Cook, W.H., "A Constitutive Model and Data for Metals Subjected to Large Strains, High Strain Rates and High Temperatures", Proc 7th Int Symp on Ballistics, Hague, Netherlands 541-547.

88. Bishop, J.F.W., "An Approximation Method for Determining the Temperatures Reached in Steady Motion Problems of Plane Plastic Strain", Quart J Mech and Applied Math, 1956, Vol 9, pp236-245.

89. Saxena, A and Chatfield,D.A.,"The Effect of Strain Rate on Strain Hardening Exponent.", ASE Paper 760209, 1976.

90. Holman, J.P., "Heat Transfer.", McGra-Hill, 1986.

91. Hashmi,M.S.J and Haque,M.M.,"High Strain Rate Properties of an Aluminium alloy and High purity Copper at Room Temperature.",Int. Conf. of Metal Under Dynamic Loading, China, 1986 pp 637-649.

92. Sundarajan, G and Shewman,P.G.," The Use of Dynamic Impact Experiments in the Determination of Strain Rate Sensitivity of Metals and Alloys." Act Metallurgica, 1983, VOl. 31, pp255.

93. Dowling, A.R; Harding, J and Campble, J.D., "The Dynamic Punching of Metals.", J Inst of Metals, 1970, Vol 98, pp215.

94.Tanaka,K and Nojima.," Dynamic and Static Strength of Steels", Inst. Phys Conf ser 47, pp 166.

APPENDIX AA

```
C=============================================================
C      IMPACT OF RIGID TOOL STEEL PROJECTILE INTO CYLINDRICAL TEST
C                  SPECIMENS PLACED INTO A RIGID ANVIL
C-------------------------------------------------------------
C                          (MAIN PROGRAM)
C-------------------------------------------------------------

  IMPLICIT REAL * 8(A-H,O-Z)

    COMMON /IN/ N,N1,NFL,NSFL,ASFL(4,5,22)
    COMMON /SL/ E(4),SIGMA(4),S,A,SNO(4),EPSIL(4)
    COMMON /OU/ BIGR(22),BIGRO,BIGL,PI
    COMMON /CO/ DELTSO,DELTS(22),V(22),DV(22),DDS(22),DELT
    COMMON /LO/ M,M1,M2,J,TIME,DELTAT
    COMMON /ST/ BIGN(22),SN(4,5,22),C2,C7,C1(22)
    COMMON /RS/ VDOTO,RHO,Hf,SB
    COMMON /EQ/ ELAST,PLAST,CINET,STN(22),STNRT(22)
    COMMON /TM/ SUM8,TO(22)
    COMMON /MC/ P,D
    COMMON /TN/ T(5,22),ARR(5,22),AFL(5,22)
    COMMON /SU/ SUM,SUM1,SUM2,SUM3,SUM4,SUM5

C TO OPEN THE MATERIAL DATA AND RESUILT FILES

        CHARACTER G(8)*7,O(8)*7
         G(1)='MHIT1.DAT'
         O(1)='MHIT1.RES'
         G(2)='MHIT2.DAT'
         O(2)='MHIT2.RES'
         G(3)='MHIT3.DAT'
         O(3)='MHIT3.RES'
         G(4)='CV1.DAT'
         O(4)='CV1.RES'
         G(5)='CV2.DAT'
         O(5)='CV2.RES'
         G(6)='ST1.DAT'
         O(6)='ST1.RES'
         G(7)='ST2.DAT'
         O(7)='ST2.RES'
         G(8)='ST4.DAT'
         O(8)='ST4.RES'

C TO OPEN FILES FOR THE DATA TO INPUT THE DATA FROM SUBROUTINE

        DO 14 IW=1,8

        OPEN(6,FILE=O(IW),STATUS='UNKNOWN')

        DO 2004 D=0.0024,0.0024
```

```
      OPEN(UNIT=1,FILE=G(IW),STATUS='UNKNOWN')

      CALL INDATA

C CALCULATION OF THE SLOPE AND AREA OF EACH LAYER AND SUBLAYER IN THE
C                        SPECIMEN MODEL

  19  IF(NSFL-1)210,11,11
  11  CALL SLOPE
      CALL AREA

C THE TIME INCREMENT SHOULD BE LESS THAN THE TIME NEEDED FOR ELASTIC WAVE
C             TO PROPAGTE THROUGH THE LENGTH OF THE LINK

      CALL WAVE

C TO CHECK OUT THE INPUT DATA FILE BY THE USER

      CALL CHECK

C CALCULATION OF TIME OF STRESS WAVE

      CALL CONST

C THE STATE OF THE SPECIMEN JUST BEFORE IMPACT

      CALL INITAL

C CALCULATION THE KINETIC ENERGY SPENT TO DEFORMING THE TEST
                         SPECIMEN

      CALL ENERGY

      CALL PRINT

      BIGN(1)=0.0


C TO CALCULATE THE MECHANICAL PROPERTIES AT EACH TIME OF DEFORMATION

 120  J=J+1
      QQ=CINET
      QH=V(2)
      DO 92 I=1,N1
      C1(I)=E(1)/DELTS(I)
  92  CONTINUE
```

```
C CONDITION TO TERMINATE THE DEFORMATION WHEN FORCE EQUAL TO ZERO

 128  IF(BIGN(2) .GT. 0)THEN
 131      TIME=DELTAT*FLOAT(J)
          CALL ENERGY
          CALL PRINT
          GOTO 23
      END IF

C BOUNDARY CONDITION OD THE MASS (N1)

 132  DDS(N1)=-2.0*DV(N)
      V(N1)=V(N1)-DV(N)
      DDS(1)=0.0

C STRAIN CALCULATION ON EACH LINK AND THE FINAL STRAIN

      CALL STRAIN

C CONDITION TO TERMINATE THE DEFORMATION WHEN THE ENERGY IS ZERO

      IF(V(2).GT.QH)THEN
          WRITE(6,*)'ELEMENT NO.2 GOES UP'
          TIME=DELTAT*FLOAT(J)
          CALL ENERGY
          CALL PRINT
          GOTO 23
      END IF

C CALCUATION OF TEMPERATURE RISE DEURING DEFORMATION IN EACH ELEMENT

      CALL TEMPER

C STRESS CACULATION ON EACH SUBLAYER AND LAYER AS WELL AS
C  THE TOTAL STRESS ACTING ON THE SPECIMEN AT EACH TIME

      CALL STRESS


C CALCULATION OF THE DISPLACIMENT OF EACH MASS AT EACH TIME

      CALL EQUILI

      CALL ENERGY
```

```
C CONDITION TO TERMINATE THE DEFORMATION WHEN THE ENERGY IS ZERO

      IF(CINET.GT.QQ)THEN
          WRITE(6,*)'ENERGY IS MINIMUM'
          TIME=DELTAT*FLOAT(J)
          CALL ENERGY
          CALL PRINT
          GOTO 23
       END IF

C PRINT OUT THE RESULTE DEPEND ON THE VALUE OF M

      IF(J-M1)120,140,210

140   CALL LOOP

      CALL ENERGY

      CALL PRINT

      IF(J-M)120,23,23
C CHECK THE DIFFERENCE BETWWEN THE CACULATED FINAL DIAMENION WITH THE
C        EXPERIMENTAL FINAL DIMENSION,  ERROR ABOUT 3%  ACCEPTED

 23   ERR=0.03
      IF(SUM-Hf)151,13,151
 151  HIH=(ABS(Hf-SUM)/Hf)
      IF(HIH .LT. ERR)THEN
          WRITE(6,*)D
          GO TO 13
      END IF
2002  CONTINUE
2004  CONTINUE
      CLOSE(UNIT=6)
      CALL INITAL
 14   CONTINUE
 210  END
```

```
SUBROUTINE INDATA
 IMPLICIT REAL * 8 (A-H,O-Z)

  COMMON /IN/ N,N1,NFL,NSFL,ASFL(4,5,22)
  COMMON /SL/ E(4),SIGMA(4),S,A,SNO(4),EPSIL(4)
  COMMON /OU/ BIGR(22),BIGRO,BIGL,PI
  COMMON /LO/ M,M1,M2,J,TIME,DELTAT
  COMMON /RS/ VDOTO,RHO,Hf,SB


     READ(1,1) N,NFL,NSFL,M,M1,M2,BIGRO,RHO,DELTAT,FMU1,FMU2,WP,F,
    .      W,Z,SB,Hf,VDOTO,A,S,BIGL,PI,SIGMA(1),(EPSIL(L),L=1,NSFL)

 1    FORMAT(6(10X,I10/),20(10X,D14.8/))

     RETURN
     CLOSE (UNIT=1,STATUS='KEEP')
     END

SUBROUTINE SLOPE
 IMPLICIT REAL * 8  (A-H,O-Z)

  COMMON /IN/ N,N1,NFL,NSFL,ASFL(4,5,22)
  COMMON /SL/ E(4),SIGMA(4),S,A,SNO(4),EPSIL(4)

     E(1)=SIGMA(1)/EPSIL(1)
     DO 4 L=2,NSFL
     SIGMA(L)=A*(EPSIL(L)**S)
 4    CONTINUE
     IF(NSFL-1)16,16,14
14    DO 15 L=2,NSFL
     E(L)=(SIGMA(L)-SIGMA(L-1))/(EPSIL(L)-EPSIL(L-1))
15    CONTINUE
16    E(NSFL+1)=0.
     RETURN
     END

SUBROUTINE AREA
 IMPLICIT REAL * 8  (A-H,O-Z)

  COMMON /IN/ N,N1,NFL,NSFL,ASFL(4,5,22)
  COMMON /SL/ E(4),SIGMA(4),S,A,SNO(4),EPSIL(4)
  COMMON /OU/ BIGR(22),BIGRO,BIGL,PI
  COMMON /CO/ DELTSO,DELTS(22),V(22),DV(22),DDS(22),DELT
  COMMON /RS/ VDOTO,RHO,Hf,SB
  COMMON /TN/ T(5,22),ARR(5,22),AFL(5,22)
```

```
      N1=N+1
      N2=N
      DELTSO=BIGL/FLOAT(N)
      DELT=DELTSO/2.0
      DO 2 I=1,N1
      BIGR(I)=BIGRO
    2 CONTINUE
      WE=RHO*(BIGRO**2)*PI*DELTSO
      FLONFL=NFL
      DO 3 I=1,N1
      DO 4 K=1,NFL
      T(K,I)=BIGR(I)/FLONFL
      ARR(K,I)=FLOAT(K+K-1)*T(K,I)/2.
      AFL(K,I)=2.0*PI*ARR(K,I)*T(K,I)
    4 CONTINUE
    3 CONTINUE
      DO 17 I=1,N1
      DO 18 K=1,NFL
      DO 19 L=1,NSFL
      ASFL(L,K,I)=AFL(K,I)*(E(L)-E(L+1))/E(1)
   19 CONTINUE
   18 CONTINUE
   17 CONTINUE
      DO 20 L=1,NSFL
      SNO(L)=E(1)*EPSIL(L)
   20 CONTINUE
      RETURN
      END

SUBROUTINE CHECK
  IMPLICIT REAL * 8  (A-H,O-Z)

   COMMON /IN/ N,N1,NFL,NSFL,ASFL(4,5,22)
   COMMON /SL/ E(4),SIGMA(4),S,A,SNO(4),EPSIL(4)
   COMMON /OU/ BIGR(22),BIGRO,BIGL,PI
   COMMON /LO/ M,M1,M2,J,TIME,DELTAT
   COMMON /RS/ VDOTO,RHO,Hf,SB
   COMMON /MC/ P,D

      WRITE(6,31)N,NFL,NSFL,M,BIGRO,RHO,DELTAT,D,P,VDOTO,BIGL,
     . (L,EPSIL(L),SIGMA(L),L=1,NSFL)
   31  FORMAT(5H  N= ,I5,6H NFL= ,I5,7H NSFL= ,I5,5H  M= ,I5/
     . 9H  BIGRO= ,D12.5,7H  RHO= ,D12.5,10H  DELTAT= ,D12.5,
     . 5H  D= ,D12.5/5H  P= ,D12.5,17H          VDOTO= ,D12.5,
     . 8H  BIGL= ,D12.5/39H      L        EPSIL              SIGMA,/,
     . (I5,2D12.5))

      RETURN
      END
```

```
SUBROUTINE INITAL
 IMPLICIT REAL * 8 (A-H,O-Z)

  COMMON /IN/ N,N1,NFL,NSFL,ASFL(4,5,22)
  COMMON /OU/ BIGR(22),BIGRO,BIGL,PI
  COMMON /CO/ DELTSO,DELTS(22),V(22),DV(22),DDS(22),DELT
  COMMON /LO/ M,M1,M2,J,TIME,DELTAT
  COMMON /ST/ BIGN(22),SN(4,5,22),C2,C7,C1(22)
  COMMON /RS/ VDOTO,RHO,Hf,SB
  COMMON /EQ/ ELAST,PLAST,CINET,STN(22),STNRT(22)
  COMMON /TM/ SUM8,TO(22)
  COMMON /TN/ T(5,22),ARR(5,22),AFL(5,22)
  COMMON /SU/ SUM,SUM1,SUM2,SUM3,SUM4,SUM5


     J=0
     TIME=0.0
     DO 50 I=1,N1
     V(I)=DELT*(2*I-1)
     STN(I)=0.0D0
     STNRT(I)=0.0D0
     TO(I)=20.0D0
     DV(I)=0.0
     DELTS(I)=DELTSO
     BIGN(I)=0.
     DDS(I)=0.0D0
     DO 40 K=1,NFL
     DO 39 L=1,NSFL
     SN(L,K,I)=0.0
 39  CONTINUE
 40  CONTINUE
 50  CONTINUE
     SUM=0.0D0
     SUM1=0.0D0
     SUM3=0.0D0
     SUM4=0.0D0
     SUM5=0.0D0
     DV(1)=DELTAT*VDOTO
     RETURN
     END
```

```
SUBROUTINE CONST
  IMPLICIT REAL * 8 (A-H,O-Z)

   COMMON /OU/ BIGR(22),BIGRO,BIGL,PI
   COMMON /CO/ DELTSO,DELTS(22),V(22),DV(22),DDS(22)
   COMMON /LO/ M,M1,M2,J,TIME,DELTAT
   COMMON /ST/ BIGN(22),SN(4,5,22),C2,C7,C1(22)
   COMMON /RS/ VDOTO,RHO,Hf,SB

      C2=DELTAT**2/RHO/BIGRO**2/PI/DELTSO
      C7=DELTAT**2/((RHO*BIGRO**2*PI*DELTSO)+WP)

      RETURN
      END

SUBROUTINE WAVE
  IMPLICIT REAL * 8 (A-H,O-Z)

   COMMON /SL/ E(4),SIGMA(4),S,A,SNO(4)
   COMMON /CO/ DELTSO,DELTS(22),V(22),DV(22),DDS(22),DELT
   COMMON /LO/ M,M1,M2,J,TIME,DELTAT
   COMMON /RS/ VDOTO,RHO,Hf,SB

       Ce=(E(1)/RHO)**0.5
       DELTAT1= DELTSO/Ce
       DELTAT = 0.01*DELTAT1
       RETURN
       END

SUBROUTINE LOOP
  IMPLICIT REAL * 8 (A-H,O-Z)

    COMMON /LO/ M,M1,M2,J,TIME,DELTAT

  140   M1=M1+M2
        IF(M-M1)141,142,142
  141   M1=M
  142   TIME=DELTAT*FLOAT(J)
        RETURN
        END
```

```
SUBROUTINE STRAIN
  IMPLICIT REAL * 8  (A-H,O-Z)

   COMMON /IN/ N,N1,NFL,NSFL,ASFL(4,5,22)
   COMMON /SL/ E(4),SIGMA(4),S,A,SNO(4),EPSIL(4)
   COMMON /OU/ BIGR(22),BIGRO,BIGL,PI
   COMMON /CO/ DELTSO,DELTS(22),V(22),DV(22),DDS(22),DELT
   COMMON /LO/ M,M1,M2,J,TIME,DELTAT
   COMMON /ST/ BIGN(22),SN(4,5,22),C2,C7,C1(22)
   COMMON /RS/ VDOTO,RHO,Hf,SB
   COMMON /EQ/ ELAST,PLAST,CINET,STN(22),STNRT(22)
   COMMON /TN/ T(5,22),ARR(5,22),AFL(5,22)
   COMMON /SU/ SUM,SUM1,SUM2,SUM3,SUM4,SUM5

      SUM=0.0D0
      SUM1=0.0D0
      SUM2=0.0D0
      SUM3=0.0D0
      SUM4=0.0D0
      SUM5=0.0D0
      DO 10 I=2,N
      DDS(I)=DV(I)-DV(I-1)
 10   CONTINUE
      DO 2004 I=2,N1
      SUM1=SUM1+DDS(I)
2004  CONTINUE
      DO 30 I=1,N
      V(I)=V(I)+DV(I)
 30   CONTINUE
      DO 40 I=2,N1
      DELTS(I)=DELTS(I)+DDS(I)
      IF(DELTS(I)-0.01*DELTSO)31,32,32
 31   DELTS(I)=0.01*DELTSO
 32   BIGR(I)=(DELTSO*BIGRO**2/DELTS(I))**0.5
      SUM=SUM+DELTS(I)
      SUM3=SUM3+(2.*BIGR(I))
      STN(I)=LOG(ABS(DELTS(I)/DELTSO))
      SUM4=SUM4+STN(I)
      STNRT(I)=DDS(I)/DELTS(I)/DELTAT
      SUM5=SUM5+STNRT(I)
      FLONFL=NFL
      DO 50 K=1,NFL
      T(K,I)=BIGR(I)/FLONFL
      ARR(K,I)=FLOAT(K+K-1)*T(K,I)/2.
      AFL(K,I)=2.*PI*ARR(K,I)*T(K,I)
      DO 60 L=1,NSFL
      ASFL(L,K,I)=AFL(K,I)*(E(L)-E(L+1))/E(1)
 60   CONTINUE
 50   CONTINUE
```

```
 40   CONTINUE
      SUM3=SUM3/N
      SUM4=SUM4/N
      SUM5=SUM5/N
      RETURN
      END

SUBROUTINE STRESS
 IMPLICIT REAL * 8  (A-H,O-Z)

  COMMON /IN/ N,N1,NFL,NSFL,ASFL(4,5,22)
  COMMON /SL/ E(4),SIGMA(4),S,A,SNO(4),EPSIL(4)
  COMMON /OU/ BIGR(22),BIGRO,BIGL,PI
  COMMON /CO/ DELTSO,DELTS(22),V(22),DV(22),DDS(22),DELT
  COMMON /LO/ M,M1,M2,J,TIME,DELTAT
  COMMON /ST/ BIGN(22),SN(4,5,22),C2,C7,C1(22)
  COMMON /RS/ VDOTO,RHO,Hf,SB
  COMMON /EQ/ ELAST,PLAST,CINET,STN(22),STNRT(22)
  COMMON /TM/ SUM8,TO(22)
  COMMON /MC/ P,D
  COMMON /TN/ T(5,22),ARR(5,22),AFL(5,22)

      SUMS=0.0D0
      DO 100 I=2,N1
      SNDS=C1(I)*DDS(I)
      BIGN(I)=0.
      DO 90 K=1,NFL
      FN=0.0D0
      DO 80 L=1,NSFL
      SN(L,K,I)=SN(L,K,I)+SNDS
      IF(SN(L,K,I)-SNO(L))30,70,11
 11   SNY=SNO(L)*(1.+(ABS(STNRT(I))*D)**P)
      IF(SN(L,K,I)-SNY)70,70,20
 20   SN(L,K,I)=SNY
      GO TO 70
 30   IF(SN(L,K,I)+SNO(L))31,70,70
 31   SNY=SNO(L)*(1.+(ABS(STNRT(I))*D)**P)
      IF (SN(L,K,I)+SNY)40,70,70
 40   SN(L,K,I)=-SNY
 70   FN=FN+SN(L,K,I)*(ASFL(L,K,I))
 80   CONTINUE

C       THE SIGN OF THE SCOND TERM IN THE NEXT EQUATION SHOULD
C     CORROSPOND WITH THE SIGN OF -FN- AND NOT ADDED TO -FN- ,
C     BECAUSE -FN- MIGHT EITHER HAS A NEGATIVE VALUE OR A POSITIVE ONE.
C
C       FN=FN+(PI*ARR(K,I)*T(K,I)*3.*RHO*(DDS(I)/DELTAT)**2*(BIGR(I)**2
C    . -ARR(K,I)**2-(T(K,I)**2/4.))/4./DELTS(I)**2)
C
```

```
C       TO CHANGE THIS THE EQUATION WILL BE DIVIDED TO CALCULATE THE
C       RESULTANT FORCE FROM RADIAL INERTIA AND COMPARE ITS SIGN WITH
C       THE SIGN OF -FN- AND CHANGE ITS SIGN IF NECESSARY THEN ADD IT
C       TO -FN-.

      FRI=(3.*PI*AFL(K,I)*RHO*(DDS(I)/DELTAT)**2*(BIGR(I)**2
     . -ARR(K,I)**2-(T(K,I)**2/4.))/8./DELTS(I)**2)
       FRI=DSIGN(FRI,FN)
       FN=FN+FRI
       IF (I .EQ. 2) THEN
  3    FRC1=(1.+2.*FMU1*(BIGR(I)-ARR(K,I))/SUM)
           FN=FN*FRC1
       ELSE IF (I .EQ. N1) THEN
  4    FRC2=(1.+2.*FMU2*(BIGR(I)-ARR(K,I))/SUM)
           FN=FN*FRC2
       END IF
       BIGN(I)=BIGN(I)+FN
  90   CONTINUE
       STSS(I)=(BIGN(I)/(PI*BIGR(I)**2))
       SUMS=SUMS+STSS(I)
  100  CONTINUE
       SUMS=SUMS/N
       BIGN(1)=0.
       RETURN
5      END

SUBROUTINE EQUILI
  IMPLICIT REAL * 8  (A-H,O-Z)

   COMMON /IN/ N,N1,NFL,NSFL,ASFL(4,5,22)
   COMMON /CO/ DELTSO,DELTS(22),V(22),DV(22),DDS(22),DELT
   COMMON /ST/ BIGN(22),SN(4,5,22),C2,C7,C1(22)

      DO 20 I=1,N
      IF(I .EQ. 1) THEN
        DV(I)=DV(I)+C7*(BIGN(I+1)-BIGN(I))
      ELSE
        DV(I)=DV(I)+C2*(BIGN(I+1)-BIGN(I))
      END IF
  20   CONTINUE
      RETURN
      END
```

```
SUBROUTINE PRINT
  IMPLICIT REAL * 8  (A-H,O-Z)

   COMMON /IN/ N,N1,NFL,NSFL,ASFL(4,5,22)
   COMMON /SL/ E(4),SIGMA(4),S,A,SNO(4),EPSIL(4)
   COMMON /OU/ BIGR(22),BIGRO,BIGL,PI
   COMMON /CO/ DELTSO,DELTS(22),V(22),DV(22),DDS(22),DELT
   COMMON /LO/ M,M1,M2,J,TIME,DELTAT
   COMMON /ST/ BIGN(22),SN(4,5,22),C2,C7,C1(22)
   COMMON /RS/ VDOTO,RHO,Hf,SB
   COMMON /EQ/ ELAST,PLAST,CINET,STN(22),STNRT(22)
   COMMON /TM/ SUM8,TO(22)
   COMMON /MC/ P,D

      WRITE(6,90)J,TIME,CINET,ELAST,PLAST,(I,V(I),DELTS(I),
     .           BIGN(I),STN(I),BIGR(I),STNRT(I),I=1,N1)
90    FORMAT(5H  J= ,I5,6HTIME= ,D12.5,8HKINTIC= ,D12.5,
     . 9HELASTIC= ,D12.5,9HPLASTIC= ,D12.5/
     . 40H   I       V      HIGHT      STRESS
     . 39H   STRAIN      RADIUS       STNRT      /(I4,6D12.5))

        WRITE(6,*)SUM
        WRITE(6,*)SUM3
        WRITE(6,*)SUM4
        WRITE(6,*)SUM5
        WRITE(6,*)SUM8
        WRITE(6,*)SUMS
        RETURN
        END

SUBROUTINE TEMPER
  IMPLICIT REAL * 8(A-H,O-Z)

   COMMON /IN/ N,N1,NFL,NSFL,ASFL(4,5,22)
   COMMON /OU/ BIGR(22),BIGRO,BIGL,PI
   COMMON /CO/ DELTSO,DELTS(22),V(22),DV(22),DDS(22),DELT
   COMMON /ST/ BIGN(22),SN(4,5,22),C2,C7,C1(22)
   COMMON /RS/ VDOTO,RHO,Hf,SB
   COMMON /TM/ SUM8,TO(22)

      SUM8=0.0D0
      DO 24 I=2,N1
      W=(ABS(DDS(I)*BIGN(I))/(PI*(BIGR(I)**2)*DELTS(I)))
      TO(I)=(F*W/(RHO*SB))+TO(I)
      SUM8=SUM8+TO(I)
24      CONTINUE
      SUM8=SUM8/N
      RETURN
      END
```

```
SUBROUTINE ENERGY
 IMPLICIT REAL * 8  (A-H,O-Z)

  COMMON /IN/ N,N1,NFL,NSFL,ASFL(4,5,22)
  COMMON /SL/ E(4),SIGMA(4),S,A,SNO(4)
  COMMON /CO/ DELTSO,DELTS(22),V(22),DV(22),DDS(22),DELT
  COMMON /ST/ BIGN(22),SN(4,5,22),C2,C7,C1(22)
  COMMON /EQ/ ELAST,PLAST,CINET,STN(22),STNRT(22)


      CINET=0.0D0
      DO 10 I=2,N
      CINET=CINET+DV(I)**2
10    CONTINUE
      CINET=CINET/C2/2.
      CINET=CINET+(DV(1)**2/C7/2.0D0)
      ELAST=0.
      IF (J)30,20,30
20    PLAST=0.
      CINETO=CINET
      GO TO 9
30    DO 60 L=1,NSFL
      SUM2=0.
      DO 50 I=1,N
      DO 40 K=1,NFL
      SUM2=SUM2+SN(L,K,I)**2*ASFL(L,K,I)
40    CONTINUE
50    CONTINUE
      ELAST=ELAST+SUM2
60    CONTINUE
      ELAST=ELAST/(E(1)/DELTSO)
      PLAST=CINETO-CINET-ELAST
      RETURN
9     END
```

APPENDIX BB

```
C         BOUNDARY CONDITION OF THE MIRROR MASS

  132  DDS(N1)=-2.0*DV(N)
       V(N1)=V(N1)-DV(N)
       DDS(1)=0.0

       CALL STRAIN

C                ****MASS RELASE CONDITION****
C      IF(V(21).LT.QH)THEN
C        WRITE(6,*)'POSITION OF THE MASS NO. 21 INCREASED'
C            TIME=DELTAT*FLOAT(J)
C            CALL ENERGP
C            CALL ENERGS
C            CALL ENERGA
C            CALL PRINT
C            GOTO 42
C      ENDIF

       CALL TEMPER
       CALL PROESS
       CALL STRESS
       CALL EQUILI
       CALL ENERGP
       CALL ENERGS
       CALL ENERGA

C      ****ENERGY MINIMUM CONDITION****

       IF(CINET.GT.QH)THEN
       WRITE(6,*)'ENERGY IS MINIMUM'
          TIME=DELTAT*FLOAT(J)
           CALL ENERGP
           CALL ENERGS
           CALL ENERGA
           CALL PRINT
           GOTO 42
       END IF

C        **PRINT OUT THE RESULTE DEPEND ON THE VALUE OF M*****
       IF(J-M1)120,140,210
  140   CALL LOOP
       CALL ENERGP
       CALL ENERGS
       CALL ENERGA
       CALL PRINT
```

```
      IF(J-M)120,42,42
   42  ERR=0.03
      IF(SUM-Hf)151,14,151
  151  HIH=(ABS(Hf-SUM)/Hf)
      IF(HIH .LT. ERR)THEN
      WRITE(6,*)D
      GO TO 14
      END IF
      WRITE(6,*)SUM
 2000  CONTINUE
 2004  CONTINUE
   14  WRITE(6,*)SUM
  210  END


      SUBROUTINE INDATA
       IMPLICIT REAL * 8 (A-H,O-Z)

      COMMON /IN/ N,N1,K1,K2,R1,R2,NFL,NSFL,ASFL(4,5,94)
      COMMON/SL/E(4),EA(4),SIGMA(4),S,A,SNO(4),EPSIL(4),EPSILA(4),SIGMAL(4)
      COMMON /OU/ BIGR(94),BIGRO,BIGROA,BIGLA,BIGLP,BIGL,BIGLT,PI
      COMMON /LO/ M,M1,M2,J,TIME,DELTAT
      COMMON /RS/ VDOTO,RHO,Hf,SB,WE,WEA

       READ(1,1) N,NFL,NSFL,M,M1,M2,BIGRO,RHO,DELTAT,FMU1,FMU2,WP,F,
     .      W,Z,SB,Hf,VDOTO,A,S,BIGL,PI,SIGMA(1),(EPSIL(L),L=1,NSFL)
    1  FORMAT(6(10X,I10/),20(10X,D14.8/))
       CLOSE (UNIT=1,STATUS='KEEP')
       RETURN
       END

      SUBROUTINE SLOPE
       IMPLICIT REAL * 8  (A-H,O-Z)

      COMMON /IN/ N,N1,K1,K2,R1,R2,NFL,NSFL,ASFL(4,5,94)
      COMMON/SL/E(4),EA(4),SIGMA(4),S,A,SNO(4),EPSIL(4),EPSILA(4),SIGMAL(4)
       E(1)=SIGMA(1)/EPSIL(1)
       EA(1)=E(1)
       DO 4 L=2,NSFL
       SIGMA(L)=A*(EPSIL(L)**S)
    4  CONTINUE
       IF(NSFL-1)16,16,14
   14  DO 15 L=2,NSFL
       E(L)=(SIGMA(L)-SIGMA(L-1))/(EPSIL(L)-EPSIL(L-1))
   15  CONTINUE
   16  E(NSFL+1)=0.
       EA(2)=0.0D0
```

```
      RETURN
      END

      SUBROUTINE AREA
        IMPLICIT REAL * 8  (A-H,O-Z)
      COMMON /IN/ N,N1,K1,K2,R1,R2,NFL,NSFL,ASFL(4,5,94)
      COMMON  /SL/  E(4),EA(4),SIGMA(4),S,A,SNO(4),EPSIL(4),EPSILA(4),SIGMAL(4)
      COMMON /OU/ BIGR(94),BIGRO,BIGROA,BIGLA,BIGLP,BIGL,BIGLT,PI
      COMMON /CO/ DELTSO,DELTS(94),V(94),DV(94),DDS(94),DELT
      COMMON /LO/ M,M1,M2,J,TIME,DELTAT
      COMMON /ST/ BIGN(94),SN(4,5,94),C2,C7,C1(94)
      COMMON /RS/ VDOTO,RHO,Hf,SB,WE,WEA
      COMMON /EQ/ SNOA(4),STN(94),STNRT(94)
      COMMON /TN/ T(5,94),ARR(5,94),AFL(5,94)

      EPSILA(1)=0.0125
      SIGMAL(1)=EA(1)*EPSILA(1)
      N1=N+1
      K1=20
      K2=21
      R1=26
      R2=25
      BIGROA=4.75E-3
      BIGLA=5.0*BIGL
      BIGLP=4.0*BIGL
      BIGLT=BIGL+BIGLA+BIGLP
      DELTSO=BIGLT/FLOAT(N)
      DELT=DELTSO/2.0
      DO 24 I=K2,R2
        BIGR(I)=BIGRO
24      CONTINUE
      DO 22 I=1,K1
        BIGR(I)=BIGROA
22    CONTINUE
      DO 2 I=R1,N1
        BIGR(I)=BIGROA
2     CONTINUE
      WE=RHO*(BIGRO**2)*PI*DELTSO
      WEA=RHO*(BIGROA**2)*PI*DELTSO
      FLONFL=NFL
      DO 3 I=1,N1
      DO 4 K=1,NFL
      T(K,I)=BIGR(I)/FLONFL
      ARR(K,I)=FLOAT(K+K-1)*T(K,I)/2.
      AFL(K,I)=2.0*PI*ARR(K,I)*T(K,I)
 4    CONTINUE
 3    CONTINUE
      DO 474 I=1,K1
```

```
      DO 484 K=1,NFL
      DO 494 L=1,1
      ASFL(L,K,I)=AFL(K,I)*(EA(L)-EA(L+1))/EA(1)
      SNOA(L)=EA(1)*EPSILA(L)
494    CONTINUE
484    CONTINUE
474    CONTINUE
      DO 17 I=K2,R2
      DO 18 K=1,NFL
      DO 19 L=1,NSFL
      ASFL(L,K,I)=AFL(K,I)*(E(L)-E(L+1))/E(1)
      SNO(L)=E(1)*EPSIL(L)
 19    CONTINUE
 18    CONTINUE
 17    CONTINUE
      DO 47 I=R1,N1
      DO 48 K=1,NFL
      DO 49 L=1,1
      ASFL(L,K,I)=AFL(K,I)*(EA(L)-EA(L+1))/EA(1)
      SNOA(L)=EA(1)*EPSILA(L)
 49    CONTINUE
 48    CONTINUE
 47    CONTINUE
      RETURN
      END

    SUBROUTINE CHECK
      IMPLICIT REAL * 8  (A-H,O-Z)
    COMMON /IN/ N,N1,K1,K2,R1,R2,NFL,NSFL,ASFL(4,5,94)
    COMMON/SL/E(4),EA(4),SIGMA(4),S,A,SNO(4),EPSIL(4),EPSILA(4),SIGMAL(4)
    COMMON /OU/ BIGR(94),BIGRO,BIGROA,BIGLA,BIGLP,BIGL,BIGLT,PI
    COMMON /CO/ DELTSO,DELTS(94),V(94),DV(94),DDS(94),DELT
    COMMON /LO/ M,M1,M2,J,TIME,DELTAT
    COMMON /RS/ VDOTO,RHO,Hf,SB,WE,WEA
    COMMON /MC/ P,D

      WRITE(6,31)N,NFL,NSFL,M,BIGRO,RHO,DELTAT,D,P,VDOTO,BIGL,
    . (L,EPSIL(L),SIGMA(L),L=1,NSFL)
31      FORMAT(5H  N= ,I5,6H NFL= ,I5,7H NSFL= ,I5,5H  M= ,I5/
    .  9H  BIGRO= ,D12.5,7H  RHO= ,D12.5,10H  DELTAT= ,D12.5,/
    .  5H  D= ,D12.5/5H  P= ,D12.5,/
    .  8H  VDOTO= ,D12.5,17H          BIGL= ,D12.5,/
    .  39H    L      EPSIL       SIGMA           /(I5,2D12.5))
      RETURN
      END
```

```
      SUBROUTINE INITAL
        IMPLICIT REAL * 8 (A-H,O-Z)
      COMMON /IN/ N,N1,K1,K2,R1,R2,NFL,NSFL,ASFL(4,5,94)
      COMMON /SL/ E(4),EA(4),SIGMA(4),S,A,SNO(4),EPSIL(4),EPSILA(4),SIGMAL(4)
      COMMON /OU/ BIGR(94),BIGRO,BIGROA,BIGLA,BIGLP,BIGL,BIGLT,PI
      COMMON /CO/ DELTSO,DELTS(94),V(94),DV(94),DDS(94),DELT
      COMMON /LO/ M,M1,M2,J,TIME,DELTAT
      COMMON /ST/ BIGN(94),SN(4,5,94),C2,C7,C1(94)
      COMMON /RS/ VDOTO,RHO,Hf,SB,WE,WEA
      COMMON /EQ/ SNOA(4),STN(94),STNRT(94)
      COMMON /EN/ ELASTP,ELASTS.ELASTA,ELAST,PLAST,CINET
      COMMON /TM/ SUM8,TO(94)
      COMMON /TN/ T(5,94),ARR(5,94),AFL(5,94)
        J=0
        TIME=0.0
        DO 50 I=1,N1
        V(I)=DELT*(2*I-1)
        TO(I)=20.0D0
        DV(I)=0.0
        DELTS(I)=DELTSO
        BIGN(I)=0.
        DDS(I)=0.0D0
50      CONTINUE
        DO 444 I=1,K1
        DO 804 K=1,NFL
        DO 494 L=1,1
        SN(L,K,I)=0.0
494     CONTINUE
804     CONTINUE
444     CONTINUE
        DO 54 I=K2,R2
        DO 40 K=1,NFL
        DO 39 L=1,NSFL
        SN(L,K,I)=0.0
39    CONTINUE
40    CONTINUE
54    CONTINUE
        DO 44 I=R1,N1
        DO 80 K=1,NFL
        DO 49 L=1,1
        SN(L,K,I)=0.0
49    CONTINUE
80    CONTINUE
44    CONTINUE
```

```
      DO 448 I=1,K1
      DV(I)=DELTAT*VDOTO
448    CONTINUE
      RETURN
      END

    SUBROUTINE CONST
      IMPLICIT REAL * 8 (A-H,O-Z)

    COMMON /OU/ BIGR(94),BIGRO,BIGROA,BIGLA,BIGLP,BIGL,BIGLT,PI
    COMMON /CO/ DELTSO,DELTS(94),V(94),DV(94),DDS(94),DELT
    COMMON /LO/ M,M1,M2,J,TIME,DELTAT
    COMMON /RS/ VDOTO,RHO,Hf,SB,WE,WEA

      C2=DELTAT**2/RHO/BIGRO**2/PI/DELTSO
      C4=DELTAT**2/RHO/BIGROA**2/PI/DELTSO
      RETURN
      END

    SUBROUTINE WAVE
      IMPLICIT REAL * 8 (A-H,O-Z)

    COMMON/SL/E(4),EA(4),SIGMA(4),S,A,SNO(4),EPSIL(4),EPSILA(4),SIGMAL(4)
    COMMON /CO/ DELTSO,DELTS(94),V(94),DV(94),DDS(94),DELT
    COMMON /LO/ M,M1,M2,J,TIME,DELTAT
    COMMON /RS/ VDOTO,RHO,Hf,SB,WE,WEA

       Ce=(E(1)/RHO)**0.5
       DELTAT1= DELTSO/Ce
       DELTAT = DELTAT1/M2
       RETURN
       END

    SUBROUTINE LOOP
      IMPLICIT REAL * 8 (A-H,O-Z)

    COMMON /LO/ M,M1,M2,J,TIME,DELTAT

140    M1=M1+M2
      IF(M-M1)141,142,142
141    M1=M
142    TIME=DELTAT*FLOAT(J)
      RETURN
      END
```

```
      SUBROUTINE STRAIN
        IMPLICIT REAL * 8  (A-H,O-Z)

      COMMON /IN/ N,N1,K1,K2,R1,R2,NFL,NSFL,ASFL(4,5,94)
      COMMON /SL/ E(4),EA(4),SIGMA(4),S,A,SNO(4),EPSIL(4),EPSILA(4),SIGMAL(4)
      COMMON /OU/ BIGR(94),BIGRO,BIGROA,BIGLA,BIGLP,BIGL,BIGLT,PI
      COMMON /CO/ DELTSO,DELTS(94),V(94),DV(94),DDS(94),DELT
      COMMON /LO/ M,M1,M2,J,TIME,DELTAT
      COMMON /ST/ BIGN(94),SN(4,5,94),C2,C7,C1(94)
      COMMON /RS/ VDOTO,RHO,Hf,SB,WE,WEA
      COMMON /EQ/ SNOA(4),STN(94),STNRT(94)
      COMMON /MC/ P,D
      COMMON /TN/ T(5,94),ARR(5,94),AFL(5,94)
      COMMON /SU/ SUM,SUM1,SUM2,SUM3,SUM4,SUM5

        SUM=0.0D0
        SUM1=0.0D0
        SUM3=0.0D0
        SUM4=0.0D0
        SUM5=0.0D0
        DO 10 I=2,N
        DDS(I)=DV(I)-DV(I-1)
   10   CONTINUE
        DO 2004 I=2,N1
        SUM1=SUM1+DDS(I)
  2004  CONTINUE
        DO 30 I=1,N
        V(I)=V(I)+DV(I)
   30   CONTINUE
        DO 40 I=1,K1
        DELTS(I)=DELTS(I)+DDS(I)
        IF(DELTS(I)-0.01*DELTSO)31,32,32
   31   DELTS(I)=0.01*DELTSO
   32   DELTS(I)=DELTS(I)+DDS(I)
        BIGR(I)=(DELTSO*BIGROA**2/DELTS(I))**0.5
   40   CONTINUE
        DO 124 I=K2,R2
        DELTS(I)=DELTS(I)+DDS(I)
        SUM=SUM+DELTS(I)
        BIGR(I)=(DELTSO*BIGRO**2/DELTS(I))**0.5
        SUM3=SUM3+(2.*BIGR(I))
  124   CONTINUE
```

```
      DO 244 I=R1,N1
      DELTS(I)=DELTS(I)+DDS(I)
      BIGR(I)=(DELTSO*BIGROA**2/DELTS(I))**0.5
244    CONTINUE
      DO 444 I=1,K1
      FLONFL=NFL
      DO 440 K=1,NFL
      T(K,I)=BIGR(I)/FLONFL
      ARR(K,I)=FLOAT(K+K-1)*T(K,I)/2.
      AFL(K,I)=2.*PI*ARR(K,I)*T(K,I)
      DO 446 L=1,1
      ASFL(L,K,I)=AFL(K,I)*(EA(L)-EA(L+1))/EA(1)
446    CONTINUE
440    CONTINUE
444    CONTINUE
      DO 64 I=K2,R2
      FLONFL=NFL
      DO 50 K=1,NFL
      T(K,I)=BIGR(I)/FLONFL
      ARR(K,I)=FLOAT(K+K-1)*T(K,I)/2.
      AFL(K,I)=2.*PI*ARR(K,I)*T(K,I)
      DO 60 L=1,NSFL
      ASFL(L,K,I)=AFL(K,I)*(E(L)-E(L+1))/E(1)
 60    CONTINUE
 50    CONTINUE
 64    CONTINUE
      DO 644 I=R1,N1
      FLONFL=NFL
      DO 540 K=1,NFL
      T(K,I)=BIGR(I)/FLONFL
      ARR(K,I)=FLOAT(K+K-1)*T(K,I)/2.
      AFL(K,I)=2.*PI*ARR(K,I)*T(K,I)
      DO 640 L=1,1
      ASFL(L,K,I)=AFL(K,I)*(EA(L)-EA(L+1))/EA(1)
640    CONTINUE
540    CONTINUE
644    CONTINUE
      NSFL=3
      SUM3=SUM3/N
      RETURN
      END
```

```
      SUBROUTINE STRESS
        IMPLICIT REAL * 8  (A-H,O-Z)

      COMMON /IN/ N,N1,K1,K2,R1,R2,NFL,NSFL,ASFL(4,5,94)
      COMMON/SL/ E(4),EA(4),SIGMA(4),S,A,SNO(4),EPSIL(4),EPSILA(4),SIGMAL(4)
      COMMON /OU/ BIGR(94),BIGRO,BIGROA,BIGLA,BIGLP,BIGL,BIGLT,PI
      COMMON /CO/ DELTSO,DELTS(94),V(94),DV(94),DDS(94),DELT
      COMMON /LO/ M,M1,M2,J,TIME,DELTAT
      COMMON /ST/ BIGN(94),SN(4,5,94),C2,C7,C1(94)
      COMMON /RS/ VDOTO,RHO,Hf,SB,WE,WEA
      COMMON /EQ/ SNOA(4),STN(94),STNRT(94)
      COMMON /MC/ P,D
      COMMON /SU/ SUM,SUM1,SUM2,SUM3,SUM4,SUM5

        SUMS=0.0D0
        DO 100 I=2,N1
        SNDS=C1(I)*DDS(I)
        BIGN(I)=0.
        DO 90 K=1,NFL
        FN=0.0D0
 54     DO 80 L=1,NSFL
        SN(L,K,I)=SN(L,K,I)+SNDS
        IF(SN(L,K,I)-SNO(L))30,70,11
 11     SNY=(SNO(L)*(1.+(ABS(STNRT(I))*D)**(P)))
        IF(SN(L,K,I)-SNY)70,70,20
 20     SN(L,K,I)=SNY
        GO TO 70
 30     IF(SN(L,K,I)+SNO(L))31,70,70
 31     SNY=(SNO(L)*(1.+(ABS(STNRT(I))*D)**(P)))
        IF (SN(L,K,I)+SNY)40,70,70
 40     SN(L,K,I)=-SNY
 70     FN=FN+SN(L,K,I)*(ASFL(L,K,I))
 80     CONTINUE

C       THE SIGN OF THE SCOND TERM IN THE NEXT EQUATION SHOULD
C      CORROSPOND WITH THE SIGN OF -FN- AND NOT ADDED TO -FN- ,
C      BECAUSE -FN- MIGHT EITHER HAS A NEGATIVE VALUE OR A POSITIVE
ONE.
C
C       FN=FN+(PI*ARR(K,I)*T(K,I)*3.*RHO*(DDS(I)/DELTAT)**2*(BIGR(I)**2
C     . -ARR(K,I)**2-(T(K,I)**2/4.))/4./DELTS(I)**2)
```

APPENDIX BB

```
C
C  ELASTIC-PLASTIC DEFORMATION OF IMP  INING ELASTIC PROJECTILE
C        AGAINST TEST SPECIMEN PLACED INTO ELASTIC ANVIL.
C
C     THIS PROGRAM USED FINITE DIFFERENCE NUMERICAL TECHNIQUE AND
C     LUMPED MASS-MODEL TO SIMULATE THE DEFORMATION AND PREDICT
C      THE MATERIAL CONSTANT IN THE ASSUMED CONSTITUTIVE EQUATION.
C
C                    (MAIN PROGRAM)
C

    IMPLICIT REAL * 8(A-H,O-Z)

     COMMON /IN/ N,N1,K1,K2,R1,R2,NFL,NSFL,ASFL(4,5,94)
     COMMON/SL/ E(4),EA(4),SIGMA(4),S,A,SNO(4),EPSIL(4),EPSILA(4),SIGMAL(4)
     COMMON /OU/ BIGR(94),BIGRO,BIGROA,BIGLA,BIGLP,BIGL,BIGLT,PI
     COMMON /CO/ DELTSO,DELTS(94),V(94),DV(94),DDS(94),DELT
     COMMON /LO/ M,M1,M2,J,TIME,DELTAT
     COMMON /ST/ BIGN(94),SN(4,5,94),C2,C7,C1(94)
     COMMON /RS/ VDOTO,RHO,Hf,SB,WE,WEA
     COMMON /EQ/ SNOA(4),STN(94),STNRT(94)
     COMMON /EN/ ELASTP,ELASTS.ELASTA,ELAST,PLAST,CINET
     COMMON /TM/ SUM8,TO(94)
     COMMON /MC/ P,D
     COMMON /TN/ T(5,94),ARR(5,94),AFL(5,94)
     COMMON /SU/ SUM,SUM1,SUM2,SUM3,SUM4,SUM5



C    TO STORE THE RESULTE ON (OUTPUT) FILE

     DO 2004 D=0.015,0.015
     DO 2000 P=0.045,0.045

        OPEN(6,FILE='PAS44.RES',STATUS='NEW')

     OPEN(UNIT=1,FILE='MALL1.DAT',STATUS='NEW')

C         TO OPEN THE MATERIAL DATA FILE

      CALL INDATA

C         CALCULATION THE SLOPE AND AREA OF EACH LAYER
C               AND SUBLAYER IN THE SPECIMEN
```

```
 22   IF(NSFL-1)210,44,44

 44   CALL SLOPE
      CALL AREA

C          THE TIME INCREMENT SHOULD BE LESS THAN THE TIME
C          NEEDED FOR ELASTIC WAVE TO PROPAGTE THROUGH THE
C                     LENGTH OF THE LINK

      CALL WAVE

C          TO ALLOW THE USER TO CHECK THE INPUT DATA

      CALL CHECK

C          CALCULATION OF OF THE CONSTANT

      CALL CONST

C          THE STATE OF THE SPECIMEN JUST BEFORE IMPACT

      CALL INITAL
      CALL ENERGP
      CALL ENERGS
      CALL ENERGA
      CALL PRINT
      BIGN(1)=0.0

C          TO CALCULATE THE MECHANICAL PROPERTIES AT EACH TIME

 120  J=J+1
      QH=CINET
      DO 92 I=1,N1
      C1(I)=E(1)/DELTS(I)
 92   CONTINUE

C          CONDITION TO TERMINATE THE PROGRAM
C           ******FORCE BECOMES TENSION****

C 128  IF(BIGN(21) .GT. 0)THEN
C 131    TIME=DELTAT*FLOAT(J)
C        CALL ENERGP
C        CALL ENERGS
C        CALL ENERGA
C        CALL PRINT
C        GOTO 42
C      END IF
```

```
C        BOUNDARY CONDITION OF THE MIRROR MASS

 132  DDS(N1)=-2.0*DV(N)
      V(N1)=V(N1)-DV(N)
      DDS(1)=0.0

      CALL STRAIN

C              ****MASS RELASE CONDITION****
C      IF(V(21).LT.QH)THEN
C        WRITE(6,*)'POSITION OF THE MASS NO. 21 INCREASED'
C            TIME=DELTAT*FLOAT(J)
C            CALL ENERGP
C            CALL ENERGS
C            CALL ENERGA
C            CALL PRINT
C            GOTO 42
C      ENDIF

      CALL TEMPER
      CALL PROESS
      CALL STRESS
      CALL EQUILI
      CALL ENERGP
      CALL ENERGS
      CALL ENERGA

C      ****ENERGY MINIMUM CONDITION****

      IF(CINET.GT.QH)THEN
      WRITE(6,*)'ENERGY IS MINIMUM'
         TIME=DELTAT*FLOAT(J)
          CALL ENERGP
          CALL ENERGS
          CALL ENERGA
          CALL PRINT
          GOTO 42
      END IF

C       **PRINT OUT THE RESULTE DEPEND ON THE VALUE OF M*****
      IF(J-M1)120,140,210
 140   CALL LOOP
      CALL ENERGP
      CALL ENERGS
      CALL ENERGA
      CALL PRINT
```

```
      IF(J-M)120,42,42
   42 ERR=0.03
      IF(SUM-Hf)151,14,151
  151 HIH=(ABS(Hf-SUM)/Hf)
      IF(HIH .LT. ERR)THEN
      WRITE(6,*)D
      GO TO 14
      END IF
      WRITE(6,*)SUM
 2000 CONTINUE
 2004 CONTINUE
   14 WRITE(6,*)SUM
  210 END


      SUBROUTINE INDATA
      IMPLICIT REAL * 8 (A-H,O-Z)

      COMMON /IN/ N,N1,K1,K2,R1,R2,NFL,NSFL,ASFL(4,5,94)
      COMMON /SL/ E(4),EA(4),SIGMA(4),S,A,SNO(4),EPSIL(4),EPSILA(4),SIGMAL(4)
      COMMON /OU/ BIGR(94),BIGRO,BIGROA,BIGLA,BIGLP,BIGL,BIGLT,PI
      COMMON /LO/ M,M1,M2,J,TIME,DELTAT
      COMMON /RS/ VDOTO,RHO,Hf,SB,WE,WEA

      READ(1,1) N,NFL,NSFL,M,M1,M2,BIGRO,RHO,DELTAT,FMU1,FMU2,WP,F,
     .     W,Z,SB,Hf,VDOTO,A,S,BIGL,PI,SIGMA(1),(EPSIL(L),L=1,NSFL)
    1 FORMAT(6(10X,I10/),20(10X,D14.8/))
      CLOSE (UNIT=1,STATUS='KEEP')
      RETURN
      END

      SUBROUTINE SLOPE
      IMPLICIT REAL * 8  (A-H,O-Z)

      COMMON /IN/ N,N1,K1,K2,R1,R2,NFL,NSFL,ASFL(4,5,94)
      COMMON /SL/ E(4),EA(4),SIGMA(4),S,A,SNO(4),EPSIL(4),EPSILA(4),SIGMAL(4)
      E(1)=SIGMA(1)/EPSIL(1)
      EA(1)=E(1)
      DO 4 L=2,NSFL
      SIGMA(L)=A*(EPSIL(L)**S)
    4 CONTINUE
      IF(NSFL-1)16,16,14
   14 DO 15 L=2,NSFL
      E(L)=(SIGMA(L)-SIGMA(L-1))/(EPSIL(L)-EPSIL(L-1))
   15 CONTINUE
   16 E(NSFL+1)=0.
      EA(2)=0.0D0
```

```
      RETURN
      END

      SUBROUTINE AREA
        IMPLICIT REAL * 8  (A-H,O-Z)
      COMMON /IN/ N,N1,K1,K2,R1,R2,NFL,NSFL,ASFL(4,5,94)
      COMMON  /SL/  E(4),EA(4),SIGMA(4),S,A,SNO(4),EPSIL(4),EPSILA(4),SIGMAL(4)
      COMMON /OU/ BIGR(94),BIGRO,BIGROA,BIGLA,BIGLP,BIGL,BIGLT,PI
      COMMON /CO/ DELTSO,DELTS(94),V(94),DV(94),DDS(94),DELT
      COMMON /LO/ M,M1,M2,J,TIME,DELTAT
      COMMON /ST/ BIGN(94),SN(4,5,94),C2,C7,C1(94)
      COMMON /RS/ VDOTO,RHO,Hf,SB,WE,WEA
      COMMON /EQ/ SNOA(4),STN(94),STNRT(94)
      COMMON /TN/ T(5,94),ARR(5,94),AFL(5,94)

      EPSILA(1)=0.0125
      SIGMAL(1)=EA(1)*EPSILA(1)
      N1=N+1
      K1=20
      K2=21
      R1=26
      R2=25
      BIGROA=4.75E-3
      BIGLA=5.0*BIGL
      BIGLP=4.0*BIGL
      BIGLT=BIGL+BIGLA+BIGLP
      DELTSO=BIGLT/FLOAT(N)
      DELT=DELTSO/2.0
      DO 24 I=K2,R2
        BIGR(I)=BIGRO
24      CONTINUE
      DO 22 I=1,K1
        BIGR(I)=BIGROA
22    CONTINUE
      DO 2 I=R1,N1
        BIGR(I)=BIGROA
2     CONTINUE
      WE=RHO*(BIGRO**2)*PI*DELTSO
      WEA=RHO*(BIGROA**2)*PI*DELTSO
      FLONFL=NFL
      DO 3 I=1,N1
      DO 4 K=1,NFL
      T(K,I)=BIGR(I)/FLONFL
      ARR(K,I)=FLOAT(K+K-1)*T(K,I)/2.
      AFL(K,I)=2.0*PI*ARR(K,I)*T(K,I)
 4    CONTINUE
 3    CONTINUE
      DO 474 I=1,K1
```

```
      DO 484 K=1,NFL
      DO 494 L=1,1
      ASFL(L,K,I)=AFL(K,I)*(EA(L)-EA(L+1))/EA(1)
      SNOA(L)=EA(1)*EPSILA(L)
494    CONTINUE
484    CONTINUE
474    CONTINUE
      DO 17 I=K2,R2
      DO 18 K=1,NFL
      DO 19 L=1,NSFL
      ASFL(L,K,I)=AFL(K,I)*(E(L)-E(L+1))/E(1)
      SNO(L)=E(1)*EPSIL(L)
 19    CONTINUE
 18    CONTINUE
 17    CONTINUE
      DO 47 I=R1,N1
      DO 48 K=1,NFL
      DO 49 L=1,1
      ASFL(L,K,I)=AFL(K,I)*(EA(L)-EA(L+1))/EA(1)
      SNOA(L)=EA(1)*EPSILA(L)
 49    CONTINUE
 48    CONTINUE
 47    CONTINUE
      RETURN
      END

    SUBROUTINE CHECK
      IMPLICIT REAL * 8  (A-H,O-Z)
    COMMON /IN/ N,N1,K1,K2,R1,R2,NFL,NSFL,ASFL(4,5,94)
    COMMON/SL/E(4),EA(4),SIGMA(4),S,A,SNO(4),EPSIL(4),EPSILA(4),SIGMAL(4)
    COMMON /OU/ BIGR(94),BIGRO,BIGROA,BIGLA,BIGLP,BIGL,BIGLT,PI
    COMMON /CO/ DELTSO,DELTS(94),V(94),DV(94),DDS(94),DELT
    COMMON /LO/ M,M1,M2,J,TIME,DELTAT
    COMMON /RS/ VDOTO,RHO,Hf,SB,WE,WEA
    COMMON /MC/ P,D

      WRITE(6,31)N,NFL,NSFL,M,BIGRO,RHO,DELTAT,D,P,VDOTO,BIGL,
    . (L,EPSIL(L),SIGMA(L),L=1,NSFL)
31     FORMAT(5H  N= ,I5,6H NFL= ,I5,7H NSFL= ,I5,5H  M= ,I5/
    . 9H  BIGRO= ,D12.5,7H  RHO= ,D12.5,10H  DELTAT= ,D12.5,/
    . 5H  D= ,D12.5/5H  P= ,D12.5,/
    . 8H  VDOTO= ,D12.5,17H          BIGL= ,D12.5,/
    . 39H    L      EPSIL        SIGMA           /(I5,2D12.5))
      RETURN
      END
```

```
      SUBROUTINE INITAL
        IMPLICIT REAL * 8 (A-H,O-Z)
      COMMON /IN/ N,N1,K1,K2,R1,R2,NFL,NSFL,ASFL(4,5,94)
      COMMON/SL/ E(4),EA(4),SIGMA(4),S,A,SNO(4),EPSIL(4),EPSILA(4),SIGMAL(4)
      COMMON /OU/ BIGR(94),BIGRO,BIGROA,BIGLA,BIGLP,BIGL,BIGLT,PI
      COMMON /CO/ DELTSO,DELTS(94),V(94),DV(94),DDS(94),DELT
      COMMON /LO/ M,M1,M2,J,TIME,DELTAT
      COMMON /ST/ BIGN(94),SN(4,5,94),C2,C7,C1(94)
      COMMON /RS/ VDOTO,RHO,Hf,SB,WE,WEA
      COMMON /EQ/ SNOA(4),STN(94),STNRT(94)
      COMMON /EN/ ELASTP,ELASTS.ELASTA,ELAST,PLAST,CINET
      COMMON /TM/ SUM8,TO(94)
      COMMON /TN/ T(5,94),ARR(5,94),AFL(5,94)
        J=0
        TIME=0.0
        DO 50 I=1,N1
        V(I)=DELT*(2*I-1)
        TO(I)=20.0D0
        DV(I)=0.0
        DELTS(I)=DELTSO
        BIGN(I)=0.
        DDS(I)=0.0D0
50      CONTINUE
        DO 444 I=1,K1
        DO 804 K=1,NFL
        DO 494 L=1,1
        SN(L,K,I)=0.0
494     CONTINUE
804     CONTINUE
444     CONTINUE
        DO 54 I=K2,R2
        DO 40 K=1,NFL
        DO 39 L=1,NSFL
        SN(L,K,I)=0.0
39    CONTINUE
40    CONTINUE
54    CONTINUE
        DO 44 I=R1,N1
        DO 80 K=1,NFL
        DO 49 L=1,1
        SN(L,K,I)=0.0
49    CONTINUE
80    CONTINUE
44    CONTINUE
```

```
      DO 448 I=1,K1
      DV(I)=DELTAT*VDOTO
448    CONTINUE
      RETURN
      END

    SUBROUTINE CONST
      IMPLICIT REAL * 8 (A-H,O-Z)

    COMMON /OU/ BIGR(94),BIGRO,BIGROA,BIGLA,BIGLP,BIGL,BIGLT,PI
    COMMON /CO/ DELTSO,DELTS(94),V(94),DV(94),DDS(94),DELT
    COMMON /LO/ M,M1,M2,J,TIME,DELTAT
    COMMON /RS/ VDOTO,RHO,Hf,SB,WE,WEA

      C2=DELTAT**2/RHO/BIGRO**2/PI/DELTSO
      C4=DELTAT**2/RHO/BIGROA**2/PI/DELTSO
      RETURN
      END

    SUBROUTINE WAVE
      IMPLICIT REAL * 8 (A-H,O-Z)

    COMMON/SL/E(4),EA(4),SIGMA(4),S,A,SNO(4),EPSIL(4),EPSILA(4),SIGMAL(4)
    COMMON /CO/ DELTSO,DELTS(94),V(94),DV(94),DDS(94),DELT
    COMMON /LO/ M,M1,M2,J,TIME,DELTAT
    COMMON /RS/ VDOTO,RHO,Hf,SB,WE,WEA

       Ce=(E(1)/RHO)**0.5
       DELTAT1= DELTSO/Ce
       DELTAT = DELTAT1/M2
       RETURN
       END

    SUBROUTINE LOOP
      IMPLICIT REAL * 8 (A-H,O-Z)

    COMMON /LO/ M,M1,M2,J,TIME,DELTAT

140    M1=M1+M2
      IF(M-M1)141,142,142
141    M1=M
142    TIME=DELTAT*FLOAT(J)
      RETURN
      END
```

```
      SUBROUTINE STRAIN
        IMPLICIT REAL * 8  (A-H,O-Z)

      COMMON /IN/ N,N1,K1,K2,R1,R2,NFL,NSFL,ASFL(4,5,94)
      COMMON /SL/ E(4),EA(4),SIGMA(4),S,A,SNO(4),EPSIL(4),EPSILA(4),SIGMAL(4)
      COMMON /OU/ BIGR(94),BIGRO,BIGROA,BIGLA,BIGLP,BIGL,BIGLT,PI
      COMMON /CO/ DELTSO,DELTS(94),V(94),DV(94),DDS(94),DELT
      COMMON /LO/ M,M1,M2,J,TIME,DELTAT
      COMMON /ST/ BIGN(94),SN(4,5,94),C2,C7,C1(94)
      COMMON /RS/ VDOTO,RHO,Hf,SB,WE,WEA
      COMMON /EQ/ SNOA(4),STN(94),STNRT(94)
      COMMON /MC/ P,D
      COMMON /TN/ T(5,94),ARR(5,94),AFL(5,94)
      COMMON /SU/ SUM,SUM1,SUM2,SUM3,SUM4,SUM5

        SUM=0.0D0
        SUM1=0.0D0
        SUM3=0.0D0
        SUM4=0.0D0
        SUM5=0.0D0
        DO 10 I=2,N
        DDS(I)=DV(I)-DV(I-1)
   10   CONTINUE
        DO 2004 I=2,N1
        SUM1=SUM1+DDS(I)
  2004  CONTINUE
        DO 30 I=1,N
        V(I)=V(I)+DV(I)
   30   CONTINUE
        DO 40 I=1,K1
        DELTS(I)=DELTS(I)+DDS(I)
        IF(DELTS(I)-0.01*DELTSO)31,32,32
   31   DELTS(I)=0.01*DELTSO
   32   DELTS(I)=DELTS(I)+DDS(I)
        BIGR(I)=(DELTSO*BIGROA**2/DELTS(I))**0.5
   40   CONTINUE
        DO 124 I=K2,R2
        DELTS(I)=DELTS(I)+DDS(I)
        SUM=SUM+DELTS(I)
        BIGR(I)=(DELTSO*BIGRO**2/DELTS(I))**0.5
        SUM3=SUM3+(2.*BIGR(I))
  124   CONTINUE
```

```
      DO 244 I=R1,N1
      DELTS(I)=DELTS(I)+DDS(I)
      BIGR(I)=(DELTSO*BIGROA**2/DELTS(I))**0.5
  244  CONTINUE
      DO 444 I=1,K1
      FLONFL=NFL
      DO 440 K=1,NFL
      T(K,I)=BIGR(I)/FLONFL
      ARR(K,I)=FLOAT(K+K-1)*T(K,I)/2.
      AFL(K,I)=2.*PI*ARR(K,I)*T(K,I)
      DO 446 L=1,1
      ASFL(L,K,I)=AFL(K,I)*(EA(L)-EA(L+1))/EA(1)
  446  CONTINUE
  440  CONTINUE
  444  CONTINUE
      DO 64 I=K2,R2
      FLONFL=NFL
      DO 50 K=1,NFL
      T(K,I)=BIGR(I)/FLONFL
      ARR(K,I)=FLOAT(K+K-1)*T(K,I)/2.
      AFL(K,I)=2.*PI*ARR(K,I)*T(K,I)
      DO 60 L=1,NSFL
      ASFL(L,K,I)=AFL(K,I)*(E(L)-E(L+1))/E(1)
   60  CONTINUE
   50  CONTINUE
   64  CONTINUE
      DO 644 I=R1,N1
      FLONFL=NFL
      DO 540 K=1,NFL
      T(K,I)=BIGR(I)/FLONFL
      ARR(K,I)=FLOAT(K+K-1)*T(K,I)/2.
      AFL(K,I)=2.*PI*ARR(K,I)*T(K,I)
      DO 640 L=1,1
      ASFL(L,K,I)=AFL(K,I)*(EA(L)-EA(L+1))/EA(1)
  640  CONTINUE
  540  CONTINUE
  644  CONTINUE
      NSFL=3
      SUM3=SUM3/N
      RETURN
      END
```

```
      SUBROUTINE STRESS
        IMPLICIT REAL * 8  (A-H,O-Z)

      COMMON /IN/ N,N1,K1,K2,R1,R2,NFL,NSFL,ASFL(4,5,94)
      COMMON /SL/ E(4),EA(4),SIGMA(4),S,A,SNO(4),EPSIL(4),EPSILA(4),SIGMAL(4)
      COMMON /OU/ BIGR(94),BIGRO,BIGROA,BIGLA,BIGLP,BIGL,BIGLT,PI
      COMMON /CO/ DELTSO,DELTS(94),V(94),DV(94),DDS(94),DELT
      COMMON /LO/ M,M1,M2,J,TIME,DELTAT
      COMMON /ST/ BIGN(94),SN(4,5,94),C2,C7,C1(94)
      COMMON /RS/ VDOTO,RHO,Hf,SB,WE,WEA
      COMMON /EQ/ SNOA(4),STN(94),STNRT(94)
      COMMON /MC/ P,D
      COMMON /SU/ SUM,SUM1,SUM2,SUM3,SUM4,SUM5

        SUMS=0.0D0
        DO 100 I=2,N1
        SNDS=C1(I)*DDS(I)
        BIGN(I)=0.
        DO 90 K=1,NFL
        FN=0.0D0
 54     DO 80 L=1,NSFL
        SN(L,K,I)=SN(L,K,I)+SNDS
        IF(SN(L,K,I)-SNO(L))30,70,11
 11     SNY=(SNO(L)*(1.+(ABS(STNRT(I))*D)**(P)))
        IF(SN(L,K,I)-SNY)70,70,20
 20     SN(L,K,I)=SNY
        GO TO 70
 30     IF(SN(L,K,I)+SNO(L))31,70,70
 31     SNY=(SNO(L)*(1.+(ABS(STNRT(I))*D)**(P)))
        IF (SN(L,K,I)+SNY)40,70,70
 40     SN(L,K,I)=-SNY
 70     FN=FN+SN(L,K,I)*(ASFL(L,K,I))
 80     CONTINUE

C       THE SIGN OF THE SCOND TERM IN THE NEXT EQUATION SHOULD
C      CORROSPOND WITH THE SIGN OF -FN- AND NOT ADDED TO -FN- ,
C      BECAUSE -FN- MIGHT EITHER HAS A NEGATIVE VALUE OR A POSITIVE
ONE.
C
C       FN=FN+(PI*ARR(K,I)*T(K,I)*3.*RHO*(DDS(I)/DELTAT)**2*(BIGR(I)**2
C     . -ARR(K,I)**2-(T(K,I)**2/4.))/4./DELTS(I)**2)
```

```
C
C     TO CHANGE THIS THE EQUATION WILL BE DIVIDED TO CALCULATE THE
C       RESULTANT FORCE FROM RADIAL INERTIA AND COMPARE ITS SIGN
WITH
C       THE SIGN OF -FN- AND CHANGE ITS SIGN IF NECESSARY THEN ADD IT
C       TO -FN-.

      FRI=(3.*PI*AFL(K,I)*RHO*(DDS(I)/DELTAT)**2*(BIGR(I)**2
     . -ARR(K,I)**2-(T(K,I)**2/4.))/8./DELTS(I)**2)
      FRI=DSIGN(FRI,FN)
      FN=FN+FRI
      BIGN(I)=BIGN(I)+FN
  90  CONTINUE
 100  CONTINUE
      BIGN(1)=0.
      NSFL=3
      RETURN
5     END

      SUBROUTINE EQUILI
      IMPLICIT REAL * 8  (A-H,O-Z)

      COMMON /IN/ N,N1,K1,K2,R1,R2,NFL,NSFL,ASFL(4,5,94)
      COMMON /CO/ DELTSO,DELTS(94),V(94),DV(94),DDS(94),DELT
      COMMON /ST/ BIGN(94),SN(4,5,94),C2,C7,C1(94)

      DO 20 I=1,N
      IF(I.GE.K2.AND.I.LE.R2)THEN
      DV(I)=DV(I)+C2*(BIGN(I+1)-BIGN(I))
      ELSE
      DV(I)=DV(I)+C4*(BIGN(I+1)-BIGN(I))
      END IF
 20   CONTINUE
      RETURN
      END

      SUBROUTINE PRINT
      IMPLICIT REAL * 8  (A-H,O-Z)

      COMMON /IN/ N,N1,K1,K2,R1,R2,NFL,NSFL,ASFL(4,5,94)
      COMMON/SL/E(4),EA(4),SIGMA(4),S,A,SNO(4),EPSIL(4),EPSILA(4),SIGMAL(4)
      COMMON /OU/ BIGR(94),BIGRO,BIGROA,BIGLA,BIGLP,BIGL,BIGLT,PI
      COMMON /CO/ DELTSO,DELTS(94),V(94),DV(94),DDS(94),DELT
      COMMON /LO/ M,M1,M2,J,TIME,DELTAT
      COMMON /ST/ BIGN(94),SN(4,5,94),C2,C7,C1(94)
      COMMON /RS/ VDOTO,RHO,Hf,SB,WE,WEA
      COMMON /EQ/ SNOA(4),STN(94),STNRT(94)
      COMMON /EN/ ELASTP,ELASTS.ELASTA,ELAST,PLAST,CINET
```

```
      COMMON /TM/ SUM8,TO(94)
      COMMON /MC/ P,D
      COMMON /SU/ SUM,SUM1,SUM2,SUM3,SUM4,SUM5




        WRITE(6,90)J,TIME,CINET,ELAST,PLAST,(I,V(I),DELTS(I),
     1            BIGN(I),STN(I),BIGR(I),STNRT(I),I=1,N1)
   90   FORMAT(5H  J= ,I5,6HTIME= ,D12.5,8HKINTIC= ,D12.5,
     1  9HELASTIC= ,D12.5,9HPLASTIC= ,D12.5/
     2  40H   I       V     HIGHT       FORCE
     3  39H   STRAIN        RADIUS      STNRT     /(I5,6D12.5))

        WRITE(6,*)SUM
        WRITE(6,*)SUM3
        WRITE(6,*)SUM4
        WRITE(6,*)SUM5
        WRITE(6,*)SUM8
        RETURN
        END

      SUBROUTINE TEMPER
        IMPLICIT REAL * 8(A-H,O-Z)
      COMMON /IN/ N,N1,K1,K2,R1,R2,NFL,NSFL,ASFL(4,5,94)
      COMMON /OU/ BIGR(94),BIGRO,BIGROA,BIGLA,BIGLP,BIGL,BIGLT,PI
      COMMON /CO/ DELTSO,DELTS(94),V(94),DV(94),DDS(94),DELT
      COMMON /ST/ BIGN(94),SN(4,5,94),C2,C7,C1(94)
      COMMON /RS/ VDOTO,RHO,Hf,SB,WE,WEA
      COMMON /TM/ SUM8,TO(94)

        SUM8=0.0D0
        DO 24 I=K2,R2
        W=(ABS(DDS(I)*BIGN(I))/(PI*(BIGR(I)**2)*DELTS(I)))
        TO(I)=(F*W/(RHO*SB))+TO(I)
        SUM8=SUM8+TO(I)
   24    CONTINUE
        SUM8=SUM8/5
        RETURN
        END


      SUBROUTINE PROESS
        IMPLICIT REAL * 8  (A-H,O-Z)
      COMMON /IN/ N,N1,K1,K2,R1,R2,NFL,NSFL,ASFL(4,5,94)
      COMMON/SL/E(4),EA(4),SIGMA(4),S,A,SNO(4),EPSIL(4),EPSILA(4),SIGMAL(4)
```

```
      COMMON /OU/ BIGR(94),BIGRO,BIGROA,BIGLA,BIGLP,BIGL,BIGLT,PI
      COMMON /CO/ DELTSO,DELTS(94),V(94),DV(94),DDS(94),DELT
      COMMON /LO/ M,M1,M2,J,TIME,DELTAT
      COMMON /ST/ BIGN(94),SN(4,5,94),C2,C7,C1(94)
      COMMON /RS/ VDOTO,RHO,Hf,SB,WE,WEA
      COMMON /EQ/ SNOA(4),STN(94),STNRT(94)
      COMMON /MC/ P,D
      COMMON /TN/ T(5,94),ARR(5,94),AFL(5,94)
      COMMON /SU/ SUM,SUM1,SUM2,SUM3,SUM4,SUM5

        DO 100 I=1,K1
        SNDS=C1(I)*DDS(I)
        BIGN(I)=0.0D0
        DO 90 K=1,NFL
        FN=0.0D0
 54     DO 80 L=1,1
        SN(L,K,I)=SN(L,K,I)+SNDS
        IF(SN(L,K,I)-SNOA(L))30,70,11
 11     SNY=(SNOA(L)*(1.+(ABS(STNRT(I))*D)**(P)))
        IF(SN(L,K,I)-SNY)70,70,20
 20     SN(L,K,I)=SNY
        GO TO 70
 30     IF(SN(L,K,I)+SNOA(L))31,70,70
 31     SNY=(SNOA(L)*(1.+(ABS(STNRT(I))*D)**(P)))
        IF (SN(L,K,I)+SNY)40,70,70
 40     SN(L,K,I)=-SNY
 70     FN=FN+SN(L,K,I)*(ASFL(L,K,I))
 80     CONTINUE

        FRI=(3.*PI*AFL(K,I)*RHO*(DDS(I)/DELTAT)**2*(BIGR(I)**2
     . -ARR(K,I)**2-(T(K,I)**2/4.))/8./DELTS(I)**2)

         FRI=DSIGN(FRI,FN)

         FN=FN+FRI

         BIGN(I)=BIGN(I)+FN
 90     CONTINUE
 100    CONTINUE

        DO 104 I=R1,N1
          SNDS=C1(I)*DDS(I)
          BIGN(I)=0.0D0
          DO 94 K=1,NFL
          FN=0.0D0
          DO 84 L=1,1
          SN(L,K,I)=SN(L,K,I)+SNDS
          IF(SN(L,K,I)-SNOA(L))34,74,14
```

```
 14      SNY=(SNOA(L)*(1.+(ABS(STNRT(I))*D)**(P)))
         IF(SN(L,K,I)-SNY)74,74,24
 24      SN(L,K,I)=SNY
         GO TO 74
         IF(SN(L,K,I)+SNOA(L))34,74,74
 34      SNY=(SNOA(L)*(1.+(ABS(STNRT(I))*D)**(P)))
         IF (SN(L,K,I)+SNY)44,74,74
 44      SN(L,K,I)=-SNY
 74      FN=FN+SN(L,K,I)*(ASFL(L,K,I))
 84      CONTINUE

         FRI=(3.*PI*AFL(K,I)*RHO*(DDS(I)/DELTAT)**2*(BIGR(I)**2
     .  -ARR(K,I)**2-(T(K,I)**2/4.))/8./DELTS(I)**2)

         FRI=DSIGN(FRI,FN)

         FN=FN+FRI

         BIGN(I)=BIGN(I)+FN
 94      CONTINUE
 104     CONTINUE
       BIGN(1)=0.
       NSFL=3
       RETURN
       END

     SUBROUTINE ENERGP
       IMPLICIT REAL * 8  (A-H,O-Z)
     COMMON /IN/ N,N1,K1,K2,R1,R2,NFL,NSFL,ASFL(4,5,94)
     COMMON/SL/ E(4),EA(4),SIGMA(4),S,A,SNO(4),EPSIL(4),EPSILA(4),SIGMAL(4)
     COMMON /OU/ BIGR(94),BIGRO,BIGROA,BIGLA,BIGLP,BIGL,BIGLT,PI
     COMMON /CO/ DELTSO,DELTS(94),V(94),DV(94),DDS(94),DELT
     COMMON /LO/ M,M1,M2,J,TIME,DELTAT
     COMMON /ST/ BIGN(94),SN(4,5,94),C2,C7,C1(94)
     COMMON /RS/ VDOTO,RHO,Hf,SB,WE,WEA
     COMMON /EN/ ELASTP,ELASTS.ELASTA,ELASTP,PLAST,CINET

       CINET=0.0D0
        DO 10 I=1,K1
        CINET=CINET+(DV(I)**2/C4/2.)
 10     CONTINUE
        ELASTP=0.0D0
        IF (J)30,20,30
 20     PLAST=0.
       CINETO=CINET
        GO TO 4
 30     DO 60 L=1,1
       SUM2=0.
```

```
      DO 50 I=1,K1
      DO 40 K=1,NFL
      SUM2=SUM2+SN(L,K,I)**2*ASFL(L,K,I)
 40   CONTINUE
 50   CONTINUE
         ELASTP=ELASTP+SUM2
 60    CONTINUE
         ELASTP=ELASTP/(EA(1)/DELTSO)
  4    DO 80 I=2,K1
      STN(I)=LOG(ABS(DELTS(I)/DELTSO))
      STNRT(I)=DDS(I)/DELTSO/DELTAT
 80   CONTINUE
      NSFL=3
      RETURN
      END
      SUBROUTINE ENERGS
     IMPLICIT REAL * 8  (A-H,O-Z)
    COMMON /IN/ N,N1,K1,K2,R1,R2,NFL,NSFL,ASFL(4,5,94)
    COMMON/SL/E(4),EA(4),SIGMA(4),S,A,SNO(4),EPSIL(4),EPSILA(4),SIGMAL(4)
    COMMON /OU/ BIGR(94),BIGRO,BIGROA,BIGLA,BIGLP,BIGL,BIGLT,PI
    COMMON /CO/ DELTSO,DELTS(94),V(94),DV(94),DDS(94),DELT
    COMMON /LO/ M,M1,M2,J,TIME,DELTAT
    COMMON /ST/ BIGN(94),SN(4,5,94),C2,C7,C1(94)
    COMMON /EQ/ SNOA(4),STN(94),STNRT(94)
    COMMON /EN/ ELASTP,ELASTS.ELASTA,ELAST,PLAST,CINET
       DO 12 I=K2,R2
       CINET=CINET+(DV(I)**2/C2/2.)
 12    CONTINUE
       ELASTS=0.0D0
       IF (J)32,22,32
 22    PLAST=0.
      CINETO=CINET
       GO TO 4
 32    DO 62 L=1,NSFL
      SUM2=0.
       DO 52 I=K2,R2
       DO 42 K=1,NFL
      SUM2=SUM2+SN(L,K,I)**2*ASFL(L,K,I)
 42    CONTINUE
 52    CONTINUE
       ELASTS=ELASTS+SUM2
 62    CONTINUE
       ELASTS=ELASTS/(E(1)/DELTSO)
  4    DO 80 I=K2,R2
      STN(I)=LOG(ABS(DELTS(I)/DELTSO))
      STNRT(I)=DDS(I)/DELTSO/DELTAT
 80    CONTINUE
      RETURN
```

```
      END

      SUBROUTINE ENERGA
    IMPLICIT REAL * 8  (A-H,O-Z)
    COMMON /IN/ N,N1,K1,K2,R1,R2,NFL,NSFL,ASFL(4,5,94)
    COMMON/SL/E(4),EA(4),SIGMA(4),S,A,SNO(4),EPSIL(4),EPSILA(4),SIGMAL(4)
    COMMON /OU/ BIGR(94),BIGRO,BIGROA,BIGLA,BIGLP,BIGL,BIGLT,PI
    COMMON /CO/ DELTSO,DELTS(94),V(94),DV(94),DDS(94),DELT
    COMMON /LO/ M,M1,M2,J,TIME,DELTAT
    COMMON /ST/ BIGN(94),SN(4,5,94),C2,C7,C1(94)
    COMMON /EQ/ SNOA(4),STN(94),STNRT(94)
    COMMON /EN/ ELASTP,ELASTS.ELASTA,ELAST,PLAST,CINET

   DO 14 I=R1,N1
      CINET=CINET+(DV(I)**2/C4/2.)
 14   CONTINUE
      ELASTA=0.0D0
      ELAST=0.0D0
      IF (J)34,24,34
 24   PLAST=0.
     CINETO=CINET
      GO TO 4
34    DO 64 L=1,1
     SUM2=0.
      DO 54 I=R1,N1
      DO 44 K=1,NFL
     SUM2=SUM2+SN(L,K,I)**2*ASFL(L,K,I)
 44   CONTINUE
 54   CONTINUE
      ELASTA=ELASTA+SUM2
 64   CONTINUE
      ELASTA=ELASTA/(EA(1)/DELTSO)
 4    DO 80 I=R1,N1
     STN(I)=LOG(ABS(DELTS(I)/DELTSO))
     STNRT(I)=DDS(I)/DELTSO/DELTAT
 80   CONTINUE
      ELAST=ELAST+ELASTP+ELASTS+ELASTA
   PLAST=CINETO-CINET-ELAST
      RETURN
   END
```